CARDIFF UNIVERSITY

Regulatory B cells in an experimental model of type 1 diabetes

A thesis submitted in the candidature for the degree of
Doctor of Philosophy by

Larissa Camargo da Rosa

School of Medicine

Division of Infection and Immunity

2017

Declaration

This work has not been submitted in substance for any other degree or award at this or any other university or place of learning, nor is being submitted concurrently in candidature for any degree or other award.
Signed Larissa Camargo da Rosa **Date** 09/01/2017

STATEMENT 1

This thesis is being submitted in partial fulfilment of the requirements for the degree of PhD.

Signed Larissa Camargo da Rosa **Date** 09/01/2017

STATEMENT 2

This thesis is the result of my own independent work/investigation, except where otherwise stated, and the thesis has not been edited by a third party beyond what is permitted by Cardiff University's Policy on the Use of Third Party Editors by Research Degree Students. Other sources are acknowledged by explicit references. The views expressed are my own.

Signed Larissa Camargo da Rosa **Date** 09/01/2017

STATEMENT 3

I hereby give consent for my thesis, if accepted, to be available online in the University's Open Access repository and for inter-library loan, and for the title and summary to be made available to outside organisations.

Signed Larissa Camargo da Rosa **Date** 09/01/2017

STATEMENT 4: PREVIOUSLY APPROVED BAR ON ACCESS

I hereby give consent for my thesis, if accepted, to be available online in the University's Open Access repository and for inter-library loans **after expiry of a bar on access previously approved by the Academic Standards & Quality Committee.**

Signed Larissa Camargo da Rosa **Date** 09/01/2017

Summary

Regulatory B cells, producing IL-10, have been studied in many autoimmune diseases. However, less is known about these cells in Type 1 diabetes (T1D), a disease characterized by the destruction of beta-cells by the immune system, leading to deficient production of insulin. Although B cells play a role in development of T1D, most previous investigations have focused on their pathogenic involvement. B cell depletion has been shown to be protective against diabetes development.

To examine regulatory B cells in T1D, we used Non-Obese Diabetic (NOD) mice and non-diabetes-prone $B6^{g7}$ mice as controls. We compared both strains for the production of cytokines and expression of putative regulatory phenotypes in spleen B cells cultured with various stimulants, at different ages. We observed that NOD mice that were > 35 weeks old and naturally protected against T1D had more IL-10-producing B cells than $B6^{g7}$ and diabetic NOD mice, and this number increased even more on stimulation with lipopolysaccharide (LPS) stimulation. When LPS-stimulated B cells from protected mice were cultured *in vitro* with CD8 T cells and DCs, their potential for suppression of T cell cytotoxic activity was higher than unstimulated B cells and B cells from diabetic mice. This inhibitory effect was associated with higher levels of IL-10.

Lastly, we carried out an investigation where B cells were transiently depleted in transgenic NOD mice expressing human CD20, to enable depletion using a human anti-CD20 monoclonal antibody. We evaluated the effect of depletion and repopulation on regulatory B cells, testing whether the protection afforded by B cell depletion was due to a change in regulatory B cell number or function. B cells with putative regulatory phenotypes were susceptible to depletion and, although the treatment with anti-CD20 reduced the incidence and delayed the onset of diabetes, there was no difference in the IL-10 producing B cell population by the time of full repopulation of B cells. Thus, this protective effect of B cell depletion was unlikely to be due to IL-10-producing B cells.

In conclusion, for the first time, regulatory B cells were extensively studied in NOD mice and we demonstrated that protected NOD mice had higher frequencies of spleen B cells producing IL-10 than diabetic NOD mice. Further investigation is warranted to understand how these IL-10-producing B cells contribute to protection against type 1 diabetes.

Ackowledgements

I would like to thank firstly and mostly my supervisor, Professor Susan Wong, for accepting me as a PhD student in her lab and Diabetes Research team. Thank you for believing in me and for being such an amazing mentor during these past 4 years – the most intense years of learning in my life. I would also like to thank my second supervisor, Doctor James Matthews, for the support.

Thank you to each and every member of the Diabetes Research team. To all the very kind colleagues who were always so thoughtful. Working with you all was an incredible experience: Evy De Leenheer, Joanne Davies, James Pearson, Terri Thayer, Matt Lewis, Stephanie Hannah, Wendy Powell, Danijela Tatovic, Dimitri Kakabadse, Farah Arikat and Ravinder Singh. One special thank you to my "B cell Team" colleague and friend, Joanne Boldison. Thank you for all the help, advice and cups of coffee.

I am also very grateful for all the support from the members of the Post Graduate Centre team, all the staff in CEDS, Tenovus and Henry Wellcome buildings, including everyone at JBIOS. One special thank you to Catherine Naseriyan, for all the help with the flow cytometers and the MSD. Thank you to Doctor Peter Morgan as well, for the guidance with the R software and the statistical advices.

I would like to thank the financial support from Science without Borders/CNPq, for granting me this PhD scholarship; Medical Research Council for funding the project this thesis is a part of and the British Society of Immunology for financial support to present this work in an international conference.

Lastly, I would like to thank my mother, my father, my brother and all my family and friends back home. Living so far for this long was the most challenging thing I have ever done, but knowing how much love and positive thoughts you were all sending me every day made it all worth it. Thank you to the friends I made here in Cardiff too, especially the Science without borders gang 2013/2014. I am sorry for only talking about my thesis for the past months, thank you for being so understanding and caring. I love you all!

Thank you! Diolch! Obrigada!

Abbreviations

Act: Activated cells

AF700: Alexa Fluor 700

APC: Allophycocyanin

BAFF: B-cell activating factor

BB rats: BioBreeding rats

Bcl-6: B cell lymphoma-6

BCR: B cell receptor

Blimp-1: B lymphocyte-induced maturation protein-1

BM: Bone Marrow

Breg: Regulatory B cells

BSA: Bovine serum albumin

BV: Brilliant Violet

CD: Cluster of Differentiation

CFSE: Carboxyfluorescein Succinimidyl Ester

CHS: Contact hypersensitivity

CNS: Central Nervous System

CO_2: Carbon dioxide

CpG: Cytosine-Phosphate-Guanine

CTL: Cytotoxic CD8 T cell

CTLA-4: Cytotoxic T-Lymphocyte-Associated Protein 4

DAB: 3-3’ diaminobenzidine

DCs: Dendritic Cells

d$H_2$0: Deionised water

DMSO: Dimethyl Sulfoxide

DNA: Deoxyribonucleic acid

EAE: Experimental Autoimmune Encephalomyelitis

EDTA: Ethylenediaminetetraacetic Acid

ELISA: Enzyme-Linked Immunosorbent Assay

FACS: Fluorescence-Activated Cell Sorting

FITC: Fluorescein Isothiocyanate

FMO: Fluorescence Minus One

FO: Follicular Zone

g (for centrifuge rotation)**:** G-force

G (for needle thickness)**:** Gauge

g (for weight): grams

GABA: γ-Amino Butyric Acid

GAD: Glutamate Decarboxylase

GC: Germinal Centre

GM-CSF: Granulocyte-Macrophage Colony-Stimulating Factor

h: Hour

hCD20: human CD20

HLA: Human Leucocyte Antigen

HRP-PNA: Horseradish peroxidase – Peanut agglutinin

I.P.: Intraperitoneal

I.V.: Intravenous

IA-2: Insulinoma-Antigen 2

ICAs: Islet Cell Antibodies

ICC: Intracellular cytoplasmic staining

IFN: Interferon

Ig: Immunoglobulin

IGRP: Islet-specific Glucose-6-phosphatase catalytic subunit–Related Protein

IL: Interleukin

IMDM medium: Iscove's Modified Dulbecco's medium

iNKT: invariant NKT cells

JBIOS: Joint Biological Services

L: Litre

LD: Live-Dead Dye

LN: Lymph Nodes

LPS: Lipopolysaccharide

LT α1β2: Lymphotoxin α1β2

mAb: Monoclonal Antibody

MACS: Magnetic-Activated Cell Sorting

MFI: Median of fluorescent intensity

mg: Milligram

MHC: Major Histocompatibility Complex

MIP1-β: Macrophage Inflammatory Protein-1β

mL: Millilitre

MLN: Mesenteric Lymph Node

MØ: Macrophages

MSD: Meso Scale Discovery

MZ: Marginal Zone

NK: Natural killers

No.: Number

NOD: Non-Obese Diabetes

Non-Act: Non-Activated cells

Notch 2: Neurogenic locus notch homolog protein 2

ns: N on-significant

OCT: Optimal Cutting Temperature

PAX-5: Paired box protein 5

PBS: Phosphate-Buffered Saline

PCR: Polymerase Chain Reaction

pDCs: Plasmacytoid Dendritic cells

PE: Phycoerythrin

PerCP Cy5.5: Peridinin-chlorophyll proteins (PerCP)

PI2: Proinsulin 2

PLN: Pancreatic Lymph Node

PLP: Paraformaldehyde Lysine Periodate fixative

PMA: Phorbol 12-myristate 13-acetate

pmol: Picomol

PP: Peyer's patches

RNA: Ribonucleic acid

RPMI medium: Roswell Park Memorial Institute medium

S1PR1: Sphingosine 1-phosphate receptor

SLE: Systematic Lupus Erythematosus

T1: Transitional B cells-1

T1D: Type 1 Diabetes

T2: Transitional B cells-2

Tfh: Follicular T helper cell

TGF: Transforming Growth Factor

Th: T helper cell

TIM-1: T cell Ig and mucin domain-1

TLR: Toll-like Receptor

TNF: Tumour Necrosis Factor

Treg: Regulatory T cell

VNTRs: Variable Number of Tandem Repeats

w.o.: Weeks Old

µg: Microgram

µL: Microliter

Conferences where this work was presented

Title	Conference
"B cell production of IL-10 is gender and strain dependent"	**The British Society for Imunology Annual Congress** 01-04/12/2014 National conference
"**A study of B cell depletion and repopulation of regulatory B cell subsets following anti-human CD20 monoclonal antibody treatment of NOD mice**"	**14th International Congress Immunology of Diabetes Society** 12-16/04/2015 International conference
"**Protected NOD mice present higher percentages of IL-10 producing B cells than diabetic mice**"	**Postgraduate Research Day 2015** 27/11/2015 Won Poster prize – Morning session Local conference
"NOD mice protected from autoimmune diabetes have more IL-10-producing B cells than diabetic mice"	**International Keystone Symposia: B Cells at the Intersection of Innate and Adaptive Immunity** 29/05-02/06 – 2016 International conference

List of Contents

1. Introduction 1

1.1 The origin and development of B cells 1

1.1.1 B-2 cells 1

1.1.2 B-1 cells 3

1.2 B cell functions and intercellular interactions 4

1.2.1 Antibody production 4

1.2.2 Antigen-presenting B cells 7

1.2.3 Cytokine-producing B cells 8

1.3 Tolerance and the role of B cells in autoimmune diseases 14

1.3.1 Central Tolerance for B cells 14

1.3.2 Peripheral Tolerance for B cells 14

1.3.3 Autoreactive B cells and autoimmune diseases 15

1.4 Type 1 diabetes – Experimental models and Immunopathogenesis 16

1.4.1 Epidemiology of Type 1 Diabetes 16

1.4.2 Experimental model: NOD mouse 17

1.4.3 Immunopathogenesis 19

1.5 B cells and Type 1 Diabetes – What is known so far? 24

1.5.1 Islet cell antibodies (ICAs) 24

1.5.2 B cell depletion and type 1 diabetes 25

1.5.3 B cells as APCs 27

1.5.4 B cell infiltrating the pancreas 28

1.5.5 Regulatory B cells and Type 1 Diabetes 29

1.6 Aims and Hypothesis 30

2. Methods 31

2.1 Mice 31

2.2 Mouse strain genotyping 32
2.2.1 PCR genotyping of transgenic mice 32
2.2.2 Blood test for genotyping 34
2.3 Detection of diabetes 35
2.4 Dendritic cells – Culture and stimulation 36
2.5 CD8 T cells from G9Cα-/-.NOD mice and B cells – Enrichment and stimulation 37
2.6 Magnetic-activated cell sorting (MACS) of B cells and CD8 T cells 38
2.7 CFSE (Carboxyfluorescein succinimidyl ester) labelling of cells 38
2.8 Cell interaction experiment set-up for Chapter 4 39
2.9 Cell collection and stimulation 39
2.10 Surface monoclonal antibody staining for flow cytometry 40
2.11 Intracellular cytokine staining for flow cytometry 40
2.12 Meso Scale Discovery assay 41
2.13 B cell depletion protocol 42
2.14 Preparation of tissue and frozen sectioning for Germinal centre staining 42
2.15 Germinal centre staining for histological sections 42
2.16 Data analysis 43
2.17 Reagents 44
3. Cytokine production and the expression of regulatory markers in IL-10-producing B cells in NOD mice 52
3.1 Introduction and Objectives 52
3.1.1 Cytokines 52
3.1.2 B cell surface markers – Regulatory B cell markers 53
3.1.3 Objectives 54
3.2 Evaluation of cytokine production by B cells from NOD mice, compared to a non-diabetic prone mouse strain 55
3.2.1 IL-6-producing B cells 58

3.2.2 TGF-β-producing B cells 63

3.2.3 IL-10-producing B cells 71

3.3 Expression of regulatory B cell subpopulation markers in the IL-10-producing B cells 78

3.3.1 Regulatory markers in unstimulated IL-10–producing B cells 80

3.3.2 Regulatory markers in IL-10–producing B cells stimulated with LPS 80

3.3.3 Regulatory markers in IL-10–producing B cells stimulated with anti-CD40 81

3.3.4 Regulatory markers in IL-10–producing B cells stimulated with CpG 85

3.3.5 Regulatory markers in IL-10–producing B cells stimulated with anti-CD40/ CpG 85

3.3.6 Summary 85

3.4 Discussion 88

4. Effect of B cells on the interaction between antigen-specific CD8 T cells and dendritic cells 94

4.1 Introduction and Objectives 94

4.1.1 Introduction 94

4.1.2 Objectives 96

4.2 Experimental Design 96

4.3 The effect of B cells as bystanders in the activation of CD8 T cells by DCs 99

4.3.1 Proliferation, viable CD8 T cells and activation 99

4.3.2 Markers of cytotoxicity (MIP1-β and CD107a) 105

4.3.3 Secretion of inflammatory cytokines 107

4.3.4 Secretion of IL-12p70 109

4.3.5 Secretion of regulatory cytokines 110

4.3.6 Summary 110

4.4 Discussion 112

5. Effect of depletion and repopulation in regulatory B cell subsets in Type 1 Diabetes 115

5.1 Introduction and Objectives 115
5.1.1 Anti-CD20-mediated B cell depletion in humans 115
5.1.2 Anti-CD20-mediated B cell depletion in mice 116
5.1.3 Objectives 118
5.2 Experimental design 119
5.2.1 B cell depletion protocol 119
5.2.2 B cell markers analysed by flow cytometry 121
5.3 Expression of hCD20 in different populations and organs 123
5.4 Effect of B cell depletion and repopulation in the Spleen 129
5.4.1 Extracellular markers: Total B cells (CD19) 131
5.4.2 Extracellular markers: CD21 and CD23 133
5.4.3 Extracellular markers: CD1d and CD5 134
5.4.4 Extracellular markers: CD24 and CD38 134
5.4.5 Extracellular marker: CD43 136
5.4.6 Immunoglobulin expression: IgD and IgM 136
5.4.7 Extracellular marker: CD138 136
5.4.8 Extracellular marker: Tim-1 137
5.4.9 Summary of effects of anti-hCD20 B cell depletion on cellular subsets *ex vivo* 137
5.4.10 Cytokine production and *in vitro* effects on subsets following anti-hCD20 B cell depletion in spleen B cells 138
5.4.11 Summary for *in vitro* surface markers and intracellular cytokines in B cells from the spleen 147
5.5 Effect of B cell depletion and repopulation in the Lymph Nodes 149
5.5.1 Extracellular markers: Total B cells (CD19) 149
5.5.2 Extracellular markers: CD21 and CD23 149
5.5.3 Extracellular markers: CD5 151
5.5.4 Extracellular markers: CD24 and CD38 151

5.5.5 Extracellular marker: CD43 152
5.5.6 Extracellular marker: IgD and IgM 152
5.5.7 Extracellular marker: CD138 152
5.5.8 Extracellular marker: Tim-1 152
5.5.9 Summary 154
5.6 Effect of B cell depletion and repopulation in the Bone marrow 154
5.6.1 Extracellular markers: Total B cells (CD19) 154
5.6.2 Extracellular markers: CD21 and CD23 154
5.6.3 Extracellular markers: CD5 156
5.6.4 Extracellular markers: CD24 and CD38 156
5.6.5 Extracellular marker: CD43 156
5.6.6 Extracellular markers: IgD and IgM 156
5.6.7 Extracellular marker: CD138 156
5.6.8 Extracellular marker: Tim-1 157
5.6.9 Summary 157
5.7 The effects of B cell depletion and repopulation in older hCD20 NOD mice 159
5.7.1 Incidence of type 1 diabetes 159
5.7.2 Effects of the interaction between CD8 T cells, DCs and B cells from hCD20 mice 159
5.7.3 Interaction between CD8 T cells and B cells from hCD20 mice as APC with G9 peptide as antigen 164
5.7.4 Summary 168
5.8 Discussion 170
6. Discussion 176
7. Appendix 184
8. References 188

List of Figures

Figure 1.1 B cell origin, development and maturation 4
Figure 1.2 The generation of plasma and memory cells from follicular B cells, through germinal centres 8
Figure 1.3 Regulatory B cell functions divided by cytokine 13
Figure 1.4 Theories correlating beta cell mass loss and the beginning of type 1 diabetes clinical signs 22
Figure 1.5 Immunopathogenesis of type 1 diabetes. 23

Figure 2.1: Photograph of genotyping of PI homo mice. 34
Figure 2.2 Flow cytometry plots exemplifying the presence of the markers studied 35

Figure 3.1 Schematic representation of the experimental design for the cytokine production evaluation 57
Figure 3.2 Example of gating of flow cytometric plots used for the cytokine production analysis 58
Figure 3.3 Frequency of IL-6 production by unstimulated B cells, B cells stimulated with LPS or anti-CD40 60
Figure 3.4 Frequency of IL-6-producing B cells stimulated with CpG 61
Figure 3.5 Frequency of IL-6-producing B cells stimulated with anti-CD40 and CpG. 62
Figure 3.6 Frequency of TGF-β production in unstimulated B cells. 64
Figure 3.7 Frequency of TGF-β-producing B cells stimulated with LPS 65
Figure 3.8 Frequency of TGF-β-producing B cells stimulated with anti-CD40 67
Figure 3.9 Frequency of TGF-β-producing B cells stimulated with CpG 68
Figure 3.10 Frequency of TGF-β-producing B cells stimulated with anti-CD40 and CpG 70
Figure 3.11 Frequency of IL-10 production in unstimulated B cells 73
Figure 3.12 Frequency of IL-10-producing B cells stimulated with LPS 74
Figure 3.13 Frequency of IL-10-producing B cells stimulated with anti-CD40 75
Figure 3.14 Frequency of IL-10-producing B cells stimulated with CpG 76

Figure 3.15 Frequency of IL-10-producing B cells stimulated with anti-CD40 and CpG. 77
Figure 3.16 Example of the two possible flow cytometric gating strategies for the cytokine-producing regulatory B cell subpopulation analysis. 79
Figure 3.17 Frequency of regulatory markers expression in unstimulated IL-10-producing B cells 82
Figure 3.18 Frequency of regulatory markers expression in IL-10-producing B cells stimulated with LPS. 83
Figure 3.19 Frequency of regulatory markers expression in IL-10-producing B cells stimulated with anti-CD40. 84
Figure 3.20 Frequency of regulatory markers expression in IL-10-producing B cells stimulated with CpG 86
Figure 3.21 Frequency of regulatory markers expression in IL-10-producing B cells stimulated with anti-CD40 and CpG 87

Figure 4.1 Experimental design for chapter 4 – the effect of B cells, as bystanders, on the activation of CD8 T cells. 98
Figure 4.2 Example of the gating of flow cytometric plots used for the determination of CD8 T cell proliferation (CFSE), activation (CD69), degranulation (CD107a) and percentage of live CD8 T cells 101
Figure 4.3 Decreased antigen-specific CD8 T cell proliferation and percentage of viable cells in the presence of LPS-stimulated NOD B cells 102
Figure 4.4 Activation of CD8 T cells cultured with B cells and DCs (percentage of $CD8^+CD69^+$ T cells) 104
Figure 4.5 Concentration of MIP1-β in the supernatants of B cells cultured with CD8 T cells and DCs and percentage of CD8 T cell degranulation (percentage of $CD8^+CD69^+CD107a^+$) 106
Figure 4.6 Concentration of IFN-γ, TNF-α and IL-6 in the supernatants of B cells cultured with CD8 T cells and DCs 108
Figure 4.7 Concentration of IL-12p70 in the supernatants of B cells cultured with CD8 T cells and DCs 109
Figure 4.8 Concentration of IL-10 in the supernatants of B cells cultured with CD8 T cells and DCs 111

Figure 5.1 Experimental design for the studies of B cell depletion and repopulation in NOD mice expressing human CD20 120
Figure 5.2 Example of flow cytometric plots used for the B cell depletion analysis in the spleen 122
Figure 5.3 Frequency of human CD20 in B cells and their subpopulations 124
Figure 5.4 Frequency of human CD20 in B cells and their subpopulations. 125
Figure 5.5 MFI of human CD20 in B cells and their subpopulations 127
Figure 5.6 MFI of human CD20 in B cells and their subpopulations. 128
Figure 5.7 Visual representation of possible proportional variations in subpopulations after B cell depletion 130
Figure 5.8 Effect of B cell depletion and repopulation in the total number of spleen B cells of young mice. 131
Figure 5.9 Effect of B cell depletion and repopulation in spleen B cells of young mice. 132
Figure 5.10 Effect of B cell depletion and repopulation in spleen B cells of young mice 135
Figure 5.11 Effect of B cell depletion and repopulation *in vitro* in B cells of young mice. 139
Figure 5.12 Effect of B cell depletion and repopulation *in vitro* in B cells of young mice 141
Figure 5.13 Effect of B cell depletion and repopulation *in vitro* in cytokine production by B cells of young mice 143
Figure 5.14 Effect of B cell depletion and repopulation *in vitro* in B cells of young mice 145
Figure 5.15 Effect of B cell depletion and repopulation *in vitro* in B cells of young mice 146
Figure 5.16 Effect of B cell depletion and repopulation *in vitro* in cytokine production by B cells of young mice 148
Figure 5.17 Effect of B cell depletion and repopulation in lymph node B cells of young mice. 150
Figure 5.18 Effect of B cell depletion and repopulation in lymph node B cells of young mice 153

Figure 5.19 Effect of B cell depletion and repopulation in bone marrow B cells of young mice. 155
Figure 5.20 Effect of B cell depletion and repopulation in bone marrow B cells of young mice. 158
Figure 5.21 Incidence of type 1 diabetes in hCD20 NOD mice. 160
Figure 5.22 Effect of stimulated and unstimulated B cells on the activation of CD8 T cells by DCs 162
Figure 5.23 Effect of stimulated and unstimulated B cells on the death of CD8 T cells 163
Figure 5.24 Effect of stimulated and unstimulated B cells on the secretion of cytokines 165
Figure 5.25 Effect of stimulated and unstimulated B cells, acting as APCs, in the proliferation and activation of CD8 T cells 166
Figure 5.26 Expression of costimulatory molecules in stimulated and unstimulated B cells, acting as APCs to CD8 T cells..... 167
Figure 5.27 Effect of stimulated and unstimulated B cells, as APCs, on the secretion of cytokines 169

Figure 6.1 Diagram of the main findings and the possible mechanisms for the suppression seen in chapter 4. 181
Figure 6.2 Diagram illustrating the main findings of chapter 5 and some possible effects of B cell depletion by anti-CD20 treatment. 183

Figure A1 FMO and isotype controls for chapter 3. 184
Figure A2 FMO and isotype controls for chapter 5 185
Figure A3 Percentage of B cells (CD19) double positive for IL-10^{+} and TGF-β^{+} 186
Figure A4 Frequency of regulatory markers expression in TGF-β-producing B cells . 187

List of tables

Table 2.1 Age and blood glucose levels for the diabetic mice included in the studies discussed in this thesis 36
Table 2.2 Reagents 44
Table 2.3 Preparation of solutions cited in the Methods 47
Table 2.4 Antibodies used for flow cytometry 48

Table 3.1 B cell subsets based on the expression of surface markers, in rodents and humans (information from Pillai and Cariappa 2009; Blair et al. 2010) 54
Table 3.2 Division of antibodies in 3 panels for cytokine production evaluation in B cells 56

Table 5.1 Summary of the effect of B cell depletion on the subpopulations studied, in different lymphoid organs 173

1. Introduction

1.1 The origin and development of B cells

The immune system comprises a complex set of cells responsible for defending the individual against exogenous harm. Lymphocytes are competent and specialized cells whose major role is to carry out this function. There are two types of lymphocytes: T and B cells, the latter being the main subject of this study.

The primary function of B cells is to produce antibodies and they are characterized by the expression of immunoglobulins (that include IgM, IgD, IgG, IgA and IgE) on their surface, which, in combination with Igα and Igβ, make up the B cell receptor (BCR). These cells can be generated in two locations: bone marrow (BM) or the fetal liver. They are divided into different subsets based on their origin and their generation throughout life (Hardy 2006). However, studies have shown that a small percentage of B cells also develops from progenitors in the thymus (Perera et al. 2013).

1.1.1 B-2 cells

B-2 cells originate in the bone marrow during the individual's entire life and they are known as conventional B cells. Their precursors are hematopoietic cells that populate the bone marrow during the embryonic phase. B cell development is associated with the BCR rearrangements that generate a very large (capable of recognizing more than $5x10^{13}$ antigens) repertoire of antibodies (Pieper et al. 2013).

B cell progenitors are found in the bone marrow and fetal liver during fetal development (and also in the bone marrow of adult individuals, for renewal). When these cells commit to the B cell lineage, they are called pro-B cells. Pro-B cells do not yet produce immunoglobulins (Ig), but they express CD19 (Nera et al. 2006). This is the stage when recombination of the V(D)J genes generates a variety of μ heavy chains. Once pro-B cells are able to produce Ig polypeptides, they are designated pre-B cells. The combination between μ heavy chain and surrogate light chains comprises the pre-B cell receptor and the first checkpoint for B cell maturation is passed once the cells express functional pre-BCR (Melchers 2005). The molecules Igα and Igβ also appear first in pre-B cells.

As the maturation continues, κ and λ light chains go through VJ combinations, and one of them will bind to the μ heavy chain to form the BCR (Almqvist and Martensson 2012).

Thus, immature B cells with low-affinity self-receptors or receptors for external antigens can differentiate into transitional B cells (designated T1 and T2 B cells) and they home to the spleen where they will become follicular or marginal zone B cells. The strength of BCR signals will determine the fate of these immature B cells once they reach the spleen (Figure 1.1).

B cells showing strong BCR signals to exogenous antigens will become Follicular zone (FO) B cells. In the white pulp of the spleen, they are located in follicles close to the T cell zone, which facilitate communication and the onset of T cell-dependent responses, forming germinal centres and generating plasma cells. FO B cells are short-lived and also known as the recirculating subset, migrating from spleen, to lymph nodes (LNs) and bone marrow (where they can be found around sinusoids) (Allman and Pillai 2008).

On the other hand, B cells with BCRs that signal weakly will become Marginal zone (MZ) B cells, a subpopulation more distinct in rodents than in humans. These cells are located between the red pulp and the follicles in the spleen.

Although the BCR signalling strength is important for distinguishing between FO and MZ B cells, B cells also need other signals to migrate and remain in the marginal zone, such as Notch2 and sphingosine 1-phosphate receptor (S1PR1). S1PR1 is important for migration and retention of B cells in the marginal zone, as sphingosine 1-phosphate is a chemokine found more frequently close to the marginal sinus (Pillai and Cariappa 2009; Ramos-Perez et al. 2015).

Due to their proximity to the blood vessels in the spleen, MZ B cells are responsible for acting against blood-borne pathogens and for T-independent responses. Marginal zone B cells express higher frequencies of Toll-like receptors (TLRs) in comparison to FO B cells. These molecules are related to interaction with microbial fragments and rapid response to pathogens, in contrast to the slower, but more specific response provided by FO B cells (Cerutti et al. 2013). They also express a higher frequency of the CD1d molecule. This MHC-like receptor is responsible for presenting lipid antigens to invariant NKT (iNKT) cells (Chaudhry and Karadimitris 2014).

1.1.2 B-1 cells

B-1 cells were first described at the beginning of the 1980's as B cells expressing high levels of IgM, low levels of IgD and a surface marker that, up until then, was only detected in T cells: Ly-1 (now called CD5). They were identified as a small population in the spleen of all mice studied and they were able to secrete natural antibodies (Hayakawa et al. 1983).

30 years later, more is known about B-1 cell function, origin and development. Although they were discovered in the spleen, these cells are mainly found in the peritoneal and pleural cavity of mice (Hayakawa et al. 1985). The expression of CD5 in murine B-1 cells is important, but not essential. Hence, the B1 cell subtype is then subdivided into B-1a ($CD5^+$ B-1 cells) and B-1b ($CD5^-$ B-1 cells) (Baumgarth 2011).

B-1 cells exert an analogous function to Marginal zone B cells: they constitute the defence against blood-borne pathogens before the adaptive immune response is initiated. The production of natural antibodies comprises mainly the synthesis of IgM. However, differently from immunoglobulins secreted after T cell-dependent mechanisms, their repertoire is restricted, the antibodies are polyreactive and their production is not necessarily dependent on stimulation (Boes et al. 1998).

With such similar functions, the differences between B-1 and marginal zone B cells lies in their origin and how they are renewed throughout the individuals' life.

In fetal liver, the organ where most of the B-1 cells are generated, pre-B cells do not produce/produce low quantities of the enzyme responsible for making their BCR as diverse as the B cells in the bone marrow. The presence or absence of certain growth factors (IL-7 and Notch2, for example) could also be involved in the fate of B cell precursors, favouring B-1 or B-2 B cells (Hardy 2006). In adult mice, while B-2 B cells are constantly renewed by new cells being generated in the bone marrow, B-1 B cells are self-renewable (Hayakawa et al. 1986).

In humans, the expression of CD5 is not as useful for distinguishing B-1 cells, as this marker is expressed by human B-2 cells. After further investigation, some researchers have agreed that, in humans, B-1-like B cells are $CD20^+CD27^+CD43^+CD70^-$, and

among these cells, most of them are also $CD5^{+}$. They have the same main function of producing natural IgM, as seen in mice (Rothstein and Quach 2015).

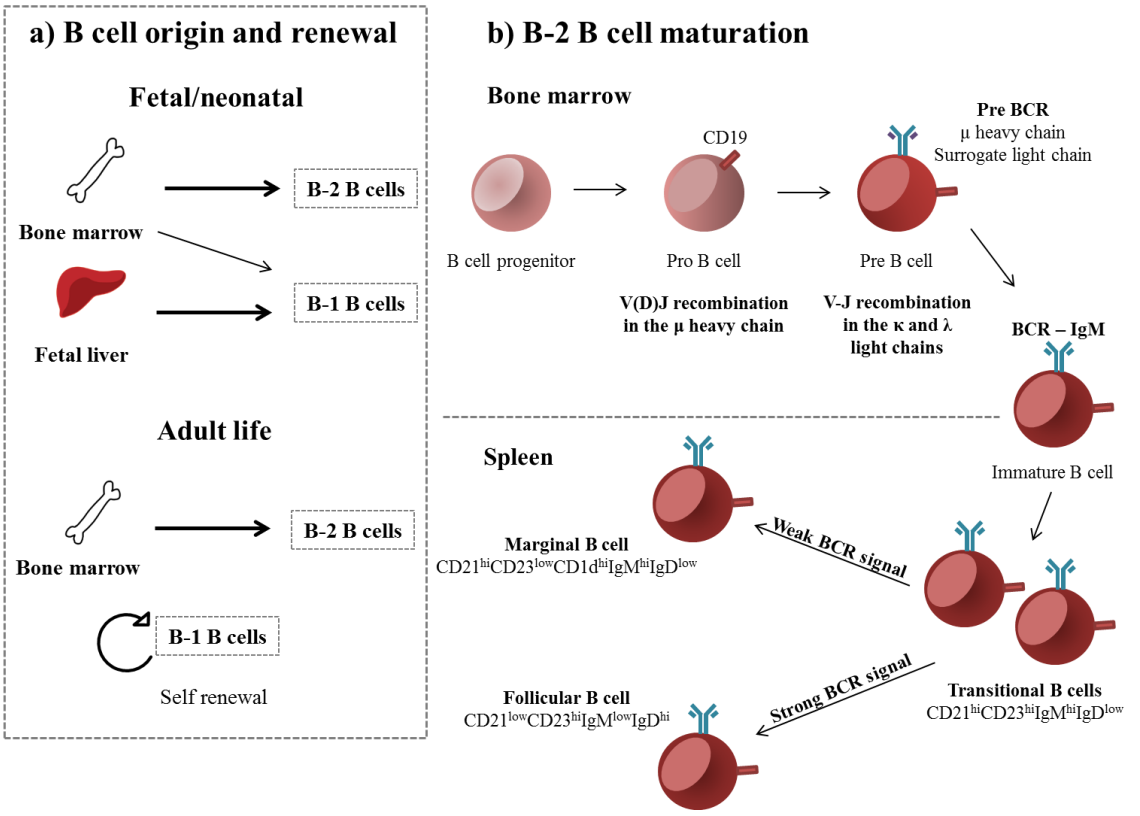

Figure 1.1 B cell origin, development and maturation. B-1 and B-2 B cells have different origins and forms of renewal in adult life (a). B-1 cells are generated mainly during fetal life in the liver, while B-2 cells derive from B cell progenitors in the bone marrow. During adult life, B-1 cells in the peritoneal cavity are self-renewable and do not depend on the new B cells being generated in the bone marrow, unlike the B-2 cells. The process of B cell precursors in the bone marrow becoming B-2 cells in the spleen is illustrated in (b). B cells receive their designations as the B cell receptor is undergoing maturation. When the cells are ready to leave the bone marrow, immature B cells home to the spleen; the strength of their BCR reactivity to exogenous antigens will determine their location in the spleen. Different B-2 cells in the spleen express different surface markers.

1.2 B cell functions and intercellular interactions

1.2.1 Antibody production

As explained previously, producing antibodies against exogenous pathogens is the main function of B cells. Antibodies were discovered to be γ-globulins in 1938, even before the cells responsible for their production were identified (Tiselius and Kabat 1938).

Plasma cells were then described 10 years later as the antibody-secreting cells (Fagraeus 1948).

Although all B cells, by nature, can potentially produce antibodies, plasma cells resulting from T cell-dependent responses are mainly derived from Follicular zone B cells.

The transformation of FO B cells into plasma cells occurs in structures called germinal centres (GCs). Inside the germinal centre, these cells are converted into GC B cells and after going through clonal expansion, somatic hypermutation and affinity maturation, they become high-affinity plasma cells or memory cells (Gatto and Brink 2010).

This process starts when naïve FO B cells circulate through the body and scan for antigens in the lymph nodes, guided by chemokines. Antigens can be found in the LNs and spleen as soluble molecules or can be transported by dendritic cells (DCs); in the spleen, marginal zone B cells can also transport antigens to the follicular area. When B cells encounter their specific antigen, they migrate to the boundary between B and T zones (Okada and Cyster 2006). In this area, B cells are activated by a number of stimuli. These include interactions with activated T cells (called T follicular helper cells – Tfh), binding through the receptor CD40 in B cells and CD40L (CD154) in T cells and by the secretion of cytokines (such as IL-21 and IL-4) by T cells. Activated B cells then start to proliferate and the fast mitosis of these cells pushes the other non-dividing cells aside to form the structures known as germinal centres (Klein and Dalla-Favera 2008).

A transcriptional regulator called Bcl-6 (B cell lymphoma-6) is essential for the establishment of the germinal centres. Bcl-6 is responsible for the regulation of various genes and its role is to make the antigen-engaged B cells commit to functions that are important for the formation of GCs. For example, DNA-damage-induced apoptosis is inhibited as well as differentiation of activated B cells to short-lived plasma cells or memory cells. This transcriptional repressor has also a role in the interaction between B cells and Tfh cells (Kitano et al. 2011). After the germinal centre is established, Bcl-6 is downregulated.

During GC B cell proliferation, two areas become evident: The dark zone, the place where B cells are heavily dividing, and the light zone, where non-proliferating B cells, T cells and follicular DCs are found. During the clonal expansion in the dark zone, B

cells also undergo somatic hypermutation, a process by which the variable region of the B cell receptor gene is rearranged, producing an antibody with the highest affinity possible to the antigen of interest (Brink 2007).

These B cells with rearranged receptors migrate then to the light zone, where the Tfh cells and follicular DCs will select high-affinity antibody-producing B cells. In the light zone, a new step into maturation is accomplished: The chosen B cells have their IgM and IgD substituted for IgG, IgA or IgE, a process called class-switch recombination (Klein and Dalla-Favera 2008). At this stage, the full differentiation of GC B cells into plasmablasts occurs as an outcome of the upregulation of some transcription factors (such as Blimp-1 – B lymphocyte-induced maturation protein-1) and downregulation of others (Bcl-6 and PAX5 – Paired box protein 5). When committed to the plasma cell path, B cells cannot go back to previous stages (Nera et al. 2006).

B cells that do not downregulate PAX5 at this point become memory B cells. In case of a second encounter with the antigen, these memory B cells are many steps ahead of a naïve B cell to become plasma cells, assuring a faster response (Nutt et al. 2015).

A diagram summarising the process of T-dependent generation of plasma cells, through germinal centres, is shown in Figure 1.2.

Along with their class-switched receptor, plasma cells also express $CD138^{+}$ on their membrane, which is important for their identification in assays (Nutt et al. 2015). These antibody- secreting cells can stay in the spleen temporarily or home to the pathogen-infected organ. After the end of the immune response, long-lived plasma cells will be found in the bone marrow, while memory cells tend to remain at the local site of infection (Shapiro-Shelef and Calame 2005).

While the formation of plasma cells through the germinal centre could take several days, T-independent antibody production by Marginal zone and B-1 B cells occurs rapidly after encounter with blood-borne pathogens.

TLRs are very important for the development of T-independent responses. In humans, these receptors are upregulated upon infection and, in mice, they are expressed constitutively in all B cells. However, although murine FO B cells are able to respond to, for example, LPS or CpG stimulation *in vitro* (stimulants for TLR-4 and TLR-9, respectively), only MZ and B-1 B cells differentiate into plasma cells after being

activated via their TLRs (Genestier et al. 2007). Stimulants like LPS can also induce T-cell independent responses through both BCR and TLR activation, acting synergistically to generate class-switched antibodies – mainly IgA in the gut and IgG (Pone et al. 2012).

The mechanisms of antibody-action include: 1) Binding to the pathogen antigen, neutralization and impairment of antigen ligation to the target cell; 2) The constant part of the antibody, called Fc, can induce complement-mediated death following binding of complement and 3) Antibody Fc regions can also bind to Fc receptors in cells like macrophages and Natural Killer cells, causing antibody-dependent cellular cytotoxicity (Chan and Carter 2010). Thus, for their high specificity and mechanisms of action, monoclonal antibodies have been used as treatment for various diseases, including autoimmune diseases; which will be further explained in this chapter and chapter 5.

1.2.2 Antigen-presenting B cells

Lanzavecchia discovered in 1985 that B cells, similarly to dendritic cells and macrophages, were able to present antigens to helper T cells in an MHC-restricted manner. Interestingly, specific B cells had the advantage of being able to capture antigen through their BCR and process them in much lower concentrations than DCs or macrophages (Lanzavecchia 1985).

B cells also express co-stimulatory molecules, such as CD40 (binding to CD40L on T cells), CD80 and CD86 (both binding to CD28 on T cells) and these receptors are upregulated when B cells are activated (Constant 1999).

Studies where mice were genetically modified to be B cell-depleted from birth confirmed the importance of B cells as APCs. When B cells were absent, the activation of CD4 T cells was impaired, but reversed when B cells were transferred back to those mice (Rivera et al. 2001). These studies have also demonstrated the role of B cells as APCs in autoimmune diseases like type 1 diabetes (Serreze et al. 1998) and will be discussed later in this chapter.

During T cell maturation in the thymus, thymic epithelial cells are the main cell type responsible for negative selection of T cells. However studies have shown that APCs, such as DCs and macrophages, but also B cells, could exert this function in the process

of deleting autoreactive T cells as well (Frommer and Waisman 2010; Perera et al. 2013). This role for B cells was demonstrated in both murine models (Frommer and Waisman 2010) and humans (Gies et al. 2017).

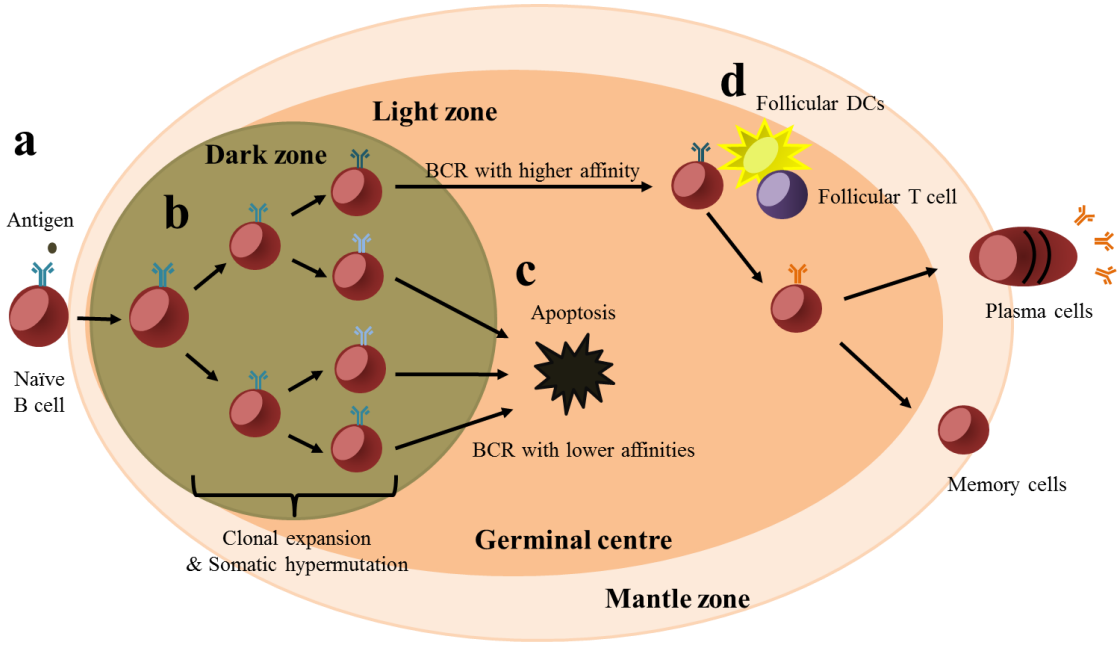

Figure 1.2 The generation of plasma and memory cells from follicular B cells, through germinal centres. When naïve B cells encounter antigens, they travel to the boundary between B and T cell zones and become activated (a). The process of rapid mitosis generates a micro structure called germinal centre, which is divided into two zones: The place where B cells undergo clonal expansion and somatic hypermutation is called the dark zone (b). Somatic hypermutation induces the rearrangement of BCR genes in order to create a new receptor with higher affinity for the antigen. When B cells leave the dark zone, they are tested by Follicular DCs and T cells, in the light zone, for affinity. Those B cells whose BCRs are not advantageous are induced to apoptosis (c). The BCR with the highest affinity is then stimulated to downregulate or upregulate genes which lead to antibody isotype switch (d). These B cells will then become antibody-secreting cells (plasma cells) or memory cells (modified from (Kuppers 2003).

1.2.3 Cytokine-producing B cells

Although the interaction cell-cell between B and T cells (binding through surface markers) has been the main focus so far in this chapter, B cells are also able to produce and secrete cytokines to modulate immune responses.

1.2.3.1 Effector cytokines

In inflammation and infection, B cells can be influenced to produce effector cytokines depending on the microenvironment.

When cultured in the presence of polarized T cells (Th1 or Th2), B cells were induced to polarize. Thus, after being cultured for 3 days in contact with Th1 cells, B cells secreting IFN-γ were detected and designated Be1. On the other hand, a small percentage of B cells cultured with Th2 cells produced IL-4 and were called Be2. IL-6, IL-10 and IL-2-producing B cells were seen among both Be1 and Be2, but these cytokines were produced more by Be2 cells. B cells producing IL-5 were not detected. Most importantly, polarized B cells were also able to polarize naïve T cells in a cytokine-dependent way (Harris et al. 2000).

One subset of B cells produces IFN-α, which is essential for the activation of NK cells and their subsequent secretion of IFN-γ. Although this cytokine was previously considered to be specifically secreted by plasmacytoid DCs, pDC-like B cells produce IFN-α as well, in cases of viral or intracellular bacterial infection (Vinay et al. 2010; Bao et al. 2011)

Cytokines produced by B cells are also responsible for the maturation of other cells and lymphoid structures. For example, in the spleen and lymph nodes, B cells producing lymphotoxin α1β2 (LT α1β2) and TNF, respectively, are necessary for the development of follicular DCs (Shen and Fillatreau 2015). Lymphotoxins secreted by B cells are also associated with the organization and maturation of lymphoid tissues in the gut (such as Peyer's patches) (McDonald et al. 2005).

1.2.3.2 Regulatory cytokines

B cells producing regulatory cytokines are the main subject of this thesis and the most important regulatory cytokine is IL-10.

The concept of B cells producing IL-10 is not new. Although B cells are seen mainly as fundamental components of pro-inflammatory responses, reports indicating that these cells were able to produce IL-10, a suppressive cytokine, date back to the beginning of the 1990's. O'Garra and Howard discussed the presence of murine $CD5^+$ peritoneal and aged splenic B cells able to produce IL-10 when stimulated with LPS. This IL-10 was

able to inhibit macrophage activities and, consequently, T effector cells (O'Garra and Howard 1992).

This function, however, was not fully further explored until 10 years later, when Mizoguchi and colleagues used the term regulatory B cells (Bregs) for the first time to designate a subpopulation of B cells expressing CD1d and able to produce IL-10. These Bregs were able to suppress chronic intestinal inflammation by downregulating pro-inflammatory cytokines, such as IL-1β (Mizoguchi et al. 2002). IL-10 producing B cells became an interesting subject in autoimmune diseases, especially after studies showing that in a mouse model of multiple sclerosis, B cell deficient mice did not recover as usual after the acute phase (remission). This effect was proven to be due to the absence of B cells producing IL-10 (Fillatreau et al. 2002).

Despite their promising role in protection from autoimmune diseases, the first problem in characterizing these regulatory B cells was agreeing on a definite phenotype. Unlike natural regulatory T cells (Tregs) and their expression of Foxp3, at this time, no transcription factor for regulatory B cells has, as yet, been described (Rosser and Mauri 2015). Therefore, regulatory B cells are defined by their ability to produce IL-10 upon stimulation and some phenotypes seem to be more involved in this production.

Following the studies by Mizoguchi, Tedder and colleagues showed that murine B cells expressing $CD1d^{hi}CD5^{+}$ were the main responsible cells for IL-10 production after LPS stimulation for 5 hours (they called these B cells **B10 cells**). They also discovered that mice prone to develop autoimmune diseases had a higher frequency of these B10 cells, compared with C57BL/6 mice (Yanaba et al. 2009). B cells expressing CD1d, as discussed, are mostly found in the marginal zone (Chaudhry and Karadimitris 2014). In experimental autoimmune encephalomyelitis (EAE), transfer of $CD5^{+}$ B10 cells to mice, even after the clinical signs of EAE had appeared, were capable of reducing the disease, while $CD5^{-}$ B cells did not alter disease progression (Yoshizaki et al. 2012).

Furthermore, transitional 2 (T2) B cells ($CD19^{+}CD21^{hi}CD23^{hi}IgM^{hi}$) were also identified as a source for regulatory B cells in a model of collagen-induced arthritis. In this model, the percentage of B cells producing IL-10 decreased during the acute phase and increased again during remission of the disease (Evans et al. 2007). This phenotype is usually seen in regulatory B cells that were previously stimulated *in vitro* with anti-CD40 for 48h, mimicking a T cell interaction. As shown by the low frequency of IL-10-

producing B cells when stimulated with IgM, BCR-dependent stimulation is not necessary for the production of IL-10 (Blair et al. 2009).

One new marker recently associated with the production of IL-10 by B cells is Tim-1 (T cell Ig and mucin domain-1), a molecule commonly expressed by T cells. When detected in B cells, however, Tim-1 was associated with promotion and maintenance of their production of IL-10 (Ding et al. 2011; Xiao et al. 2015). Other B cell phenotypes, including plasmablasts (Matsumoto et al. 2014), were described in mice as being able to produce IL-10 under specific conditions, reviewed by (Rosser and Mauri 2015).

In humans, the expression of $CD24^{hi}CD38^{hi}$ – characteristic of immature B cells – seem to identify the IL-10-producing B cells in the peripheral blood, when cultured and stimulated with anti-CD40. In patients with Systemic Lupus Erythematosus (SLE), regulatory B cells were less suppressive than healthy controls (Blair et al. 2010). The expression of $CD24^{hi}CD27^{hi}$ in human B cells has also been related to IL-10 production (Iwata et al. 2011).

Relating to phenotype heterogeneity and the fact that no transcription factor has yet been discovered, it is believed that regulatory B cells are more of an inducible population than one committed to this fate from the early stages of development. To confirm this theory, Rosser and colleagues demonstrated that the differentiation and optimal function of IL-10 producing B cells in a mouse model of arthritis was dependent on an inflammatory environment containing IL-1β and IL-6 (Rosser et al. 2014). In healthy controls, plasmacytoid DCs are responsible for differentiation of immature B cells into Bregs or IL-10-producing plasmablasts by secreting IFN-α, which acts as a negative feedback for inflammation. However, in cases of patients with SLE, pDCs produce much higher quantities of IFN-α, which induce B cells to differentiate into pathogenic plasma cells instead (Menon et al. 2016).

Although our focus here is on regulatory B cells and autoimmune diseases, it should be noted that IL-10-producing B cells have also been studied in asthma, allergies (as a beneficial factor) and cancer (as an aggravator), in mice and humans (van de Veen et al. 2016).

In addition to IL-10, which has been the main focus when studying Bregs, two other cytokines were described to have roles in the regulatory function of B cells: TGF-β and, more recently, IL-35.

Murine B cells stimulated with LPS were able to induce anergy in CD8 T cells by the expression of TGF-β1 on their surface. When cultured in the presence of these LPS stimulated-B cells (but not B cells stimulated with anti-CD40), CD8 T cells had impaired cytotoxic function and lower production of inflammatory cytokines (Parekh et al. 2003). In human gastric cancer, B cells expressing $CD24^{hi}CD38^{hi}$ were detected in the tumour area. Besides increased IL-10, these B cells also produced TGF-β1 and this cytokine was responsible for the conversion of CD4 T cells into regulatory T cells (Wang et al. 2015).

The ability of LPS-stimulated B cells to induce apoptosis in T cells in a TGF-β-dependent way was also observed in type 1 diabetes (T1D) and will be discussed later in this chapter and chapter 3 (Tian et al. 2001).

More recently, the role of IL-35 produced by B cells was studied. Shen and colleagues demonstrated that upon stimulation with TLR4 and anti-CD40, B cells produced IL-35 (formed by two molecules: EBi3 and p35) and transgenic mice that were B-$p35^{-/-}$ or B-$EBi3^{-/-}$ had more severe cases of EAE, compared to wild type mice. The mechanism of action of IL-35-producing B cells and plasma cells are not fully understood, but it is known that IL-35 can enhance the production of IL-10 (Wang et al. 2014).

A summary of the phenotypes and functions of regulatory B cells is illustrated in Figure 1.3.

Regulatory B cells have been studied in many autoimmune diseases (such as arthritis, EAE and SLE) for the last 15 years. However, less is known about Bregs in the context of type 1 diabetes. What is known so far will be addressed later in the chapter.

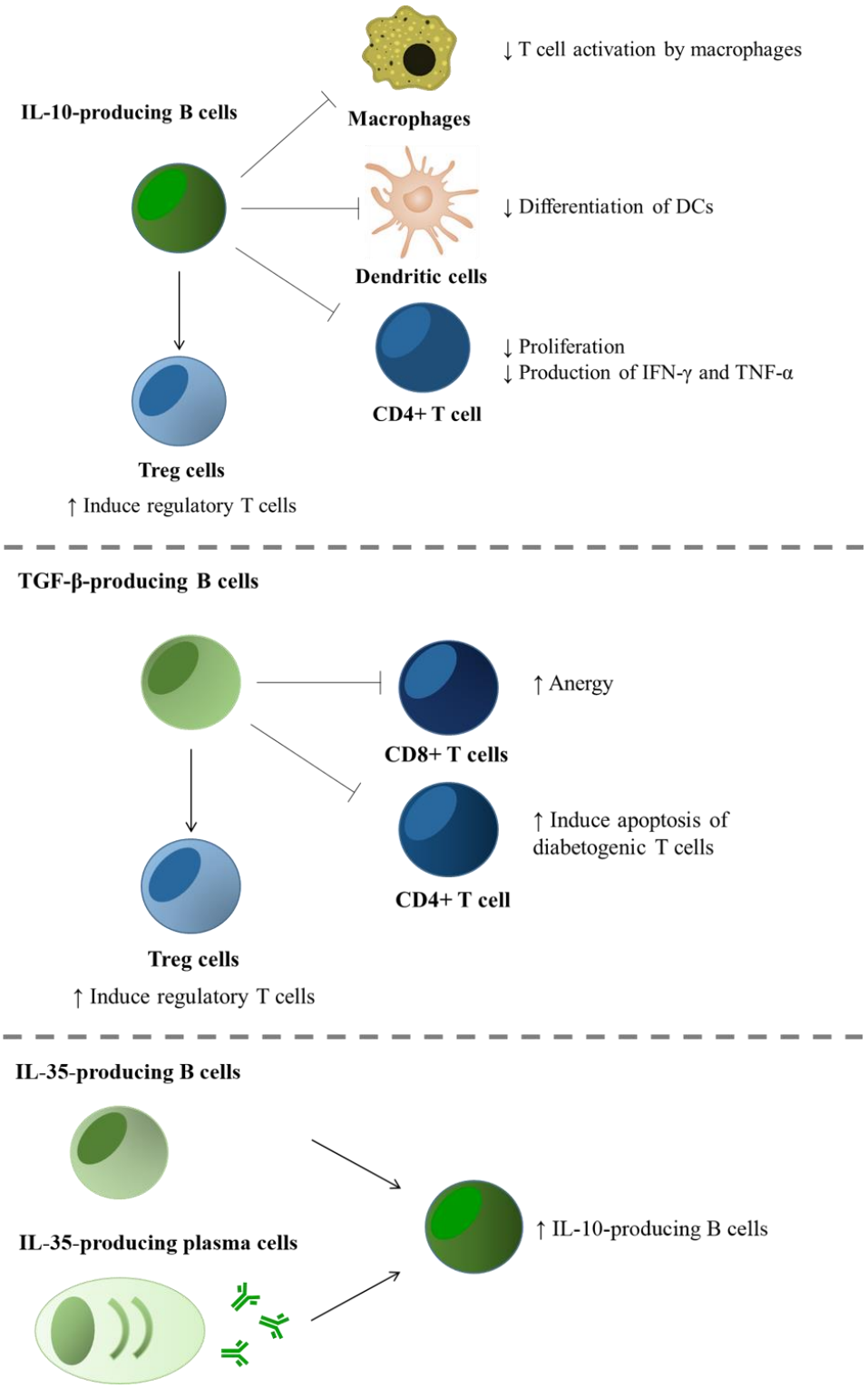

Figure 1.3 Regulatory B cell functions divided by cytokine. Regulatory B cells act differently to suppress inflammatory responses, depending on the cytokine produced. The references for each one of these mechanisms can be found in the text. Forward arrows (→) indicate enhancement and closed arrows (—|) indicate inhibition.

1.3 Tolerance and the role of B cells in autoimmune diseases

1.3.1 Central Tolerance for B cells

B cells undergo gene rearrangements to create an infinite repertoire of B cell receptors/antibodies in the bone marrow. As these combinations are done at random, BCRs with affinity for self-peptides are also generated and mechanisms to avoid autoimmunity are needed (Giltiay et al. 2012).

One study by Wardemann and colleagues estimated that, in healthy donors, 75% of all the immature B cells in the bone marrow were self-reactive. At the first checkpoint for B cell tolerance, these immature BCRs are tested for affinity to self-antigens and around half of these autoreactive B cells are stopped from getting to the circulation (Wardemann et al. 2003).

Central tolerance includes: a) Apoptosis – B cells responding with high affinity to self-antigens are induced to undergo clonal deletion by apoptosis; b) Receptor editing – As an alternative to deletion, B cells can reactivate their machinery for receptor rearrangements in the light chain and create a new, non-autoreactive BCR. It is believed that most B cells in the periphery had their BCR edited before they left the bone marrow; c) Induction of anergy – When the autoantibodies have low affinity for autoantigens, they can be induced to be anergic. This means these B cells can bind, but are unresponsive for their self-antigens. It happens as a consequence of presenting the phenotype IgD^{+}/IgM^{-}, and a lack of co-stimulatory molecules or signalling elements in their activation pathway. However, anergy is reversible and harmless anergic B cells have the potential to become pathogenic and start autoimmune responses (Meffre and Wardemann 2008; Pelanda and Torres 2012; Rosenspire and Chen 2015).

1.3.2 Peripheral Tolerance for B cells

Central tolerance is important, but not sufficient to delete all autoreactive B cells exiting the bone marrow and heading to the spleen and other lymphoid organs. Therefore, mechanisms to delete or suppress these cells in the periphery are also essential.

The second checkpoint for B cell tolerance is administered by regulatory T cells. Patients with a deficiency in their regulatory T cells have more autoreactive B cells in the periphery than healthy controls. Under normal conditions, Treg cells would be able to induce apoptosis of these B cells or downregulate the function of effector T cells that

help autoreactive B cells (Kinnunen et al. 2013). The involvement of Treg cells in B cell peripheral tolerance was observed in mice as well (Ludwig-Portugall et al. 2008). Increased concentration of BAFF (B-cell activating factor), a cytokine responsible for B cell maturation, was also related to the survival of self-reactive B cells in autoimmune diseases like SLE (Meffre and Wardemann 2008).

IgM produced naturally by B-1 B cells has affinity for both self and foreign antigens. Autoreactive natural IgM has a role in binding to apoptotic cell debris, facilitating their phagocytosis. It was demonstrated that a deficiency in natural IgM can lead to autoimmune diseases, such as SLE (Boes et al. 2000).

Mechanisms of central and peripheral tolerance also occur for autoreactive T cells; however, they will not be described in this thesis.

1.3.3 Autoreactive B cells and autoimmune diseases

Central and peripheral tolerance should be sufficient to remove or silence all self-reactive B and T cells. However, when they do not function properly, self-reactive lymphocytes may escape and start an autoimmune disease. The simple existence of autoreactive cells does not characterize autoimmune disease, unless they cause pathology (Salinas et al. 2013). Diseases like SLE, arthritis or Graves' disease are more affected by autoreactive B cells, as autoantibodies are their main trigger.

Nevertheless, self-reactive B cells are not only found in autoimmune diseases that are dependent predominantly on autoantibodies. Studies demonstrated that in NOD mice, an experimental model for type 1 diabetes, central tolerance mechanisms of clonal deletion and receptor editing were not impaired. Hence, the presence of islet autoantibody-producing B cells was due to a problem with peripheral tolerance. Although self-reactive B cells in NOD mice respond similarly to B cells in B6 mice to membrane-bound autoantigens, they are not deleted or kept anergic upon encounter with soluble self-antigens, which constitute an error in the maintenance of the tolerance/autoimmunity homeostasis (Silveira et al. 2004).

In concordance with these findings in mice, insulin-binding B cells with cross reactivity to chromatin and LPS appear to lose their anergic state in pre-diabetic and newly-diagnosed patients with T1D (Smith et al. 2015).

1.4 Type 1 diabetes – Experimental models and Immunopathogenesis

Type 1 diabetes is an autoimmune disease characterized by the destruction of beta cells by the immune system, compromising insulin production. Insulin is responsible for allowing the uptake of glucose by the cells and its partial or total loss causes the main sign of diabetes - hyperglycaemia. Untreated, persistent hyperglycaemia leads to chronic complications such as blindness, nephropathy, neuropathy, accelerated arthrosclerosis, and arteriopathy. To date, type 1 diabetes has no cure and the treatment consists of daily injections of exogenous insulin (Cooke 2009).

1.4.1 Epidemiology of Type 1 Diabetes

According to the World Health Organization, it is estimated that 347 million people in the world have diabetes and autoimmune diabetes accounts for 10% of the cases (World Health Organization 2014). Incidence of T1D is higher in developed countries, with Finland presenting the highest incidence. China, India and Venezuela, on the other hand, have the lowest number of cases per 100,000 people (Atkinson et al. 2014).

T1D occurs as a combination of the effects of both genetic and environmental factors. Autoimmune diabetes has a polygenic pathology and genome-wide association studies have identified more than 40 genes related to the disease (Barrett et al. 2009). Genes associated with the highest risk factors are related to the HLA class II (Human Leucocyte Antigen) region, where alleles can confer susceptibility (DR3/4-DQ8) in Caucasian population or be considered protective (DR7) against type 1 diabetes (Erlich et al. 2008).

The next most important gene region related to diabetes in humans encodes insulin. Polymorphisms in the Variable Number of Tandem Repeats (VNTRs) region, close to the insulin gene, are associated with susceptibility (shorter repeats) or protection (longer repeats) to T1D. The size of the VNTR influences the expression of insulin RNA (Bennett et al. 1995). The majority of other genes linked to susceptibility to type 1 diabetes are related to the immune system (genes for CTLA-4, cytokines and cytokine receptors, for example), reviewed by Van Belle and colleagues (van Belle et al. 2011).

Type 1 diabetes incidence is not consistent, even in homozygous twins and NOD (Non-Obese Diabetic) mice need to be kept in specific pathogen free conditions to develop diabetes. These observations highlight the importance of environmental factors

(Castano and Eisenbarth 1990). Although it is difficult to pin-point their exact contribution, many environmental factors have been studied.

Deficiency in vitamin D intake during fetal development and childhood results in a higher risk of developing T1D. This condition is suggested by the seasonality of this disease and the higher incidence of type 1 diabetes in countries where the exposure to sunlight is compromised (Mohr et al. 2008). Infections may also influence diabetes onset. The role of viruses, bacteria and parasites in the development of type 1 diabetes has been investigated for decades. They could trigger the disease or result in protection, depending on the species (Cooke 2009). In the microorganism field, more recently, there has been an increased interest in the relevance of gut microbiota. Studies in humans and mice demonstrated that variations in the gut microbiota, caused by diet, gender and use of antibiotics, could interfere with the progression of type 1 diabetes (Alkanani et al. 2015; Candon et al. 2015). It is still not fully clear how these alterations lead to susceptibility to T1D. One new study indicated that bacteria from the gut microbiota produce proteins that mimic islet autoantigens, like the Islet-specific Glucose-6-phosphatase catalytic subunit–Related Protein (IGRP), and are able to activate islet autoantigen-specific CD8 T cells and accelerate diabetes in mice (Tai et al. 2016).

1.4.2 Experimental model: NOD mouse

Many of the findings relating to genetics, immunology and pathogenesis of type 1 diabetes have been derived from investigation of animal models, particularly those whose disease develops spontaneously. The main models for Type 1 diabetes are BB (BioBreeding) rats and NOD mice.

NOD mice were developed in Japan, from a cataract-prone strain (JcI-ICR mouse), selecting mice that had spontaneous hyperglycaemia during the inbreeding. This strain starts to develop signs of insulitis (inflammation in the pancreatic islets) by the 4^{th} week of age and the beta cell destruction progresses silently until around the 12^{th} week. When diabetic, mice present with polyuria, glycosuria, hyperglycaemia and loss of weight, as signs of advanced deficiency of insulin (Anderson and Bluestone 2005). It is rare to see new onset of diabetes in NOD mice older than 35 weeks of age.

The incidence of type 1 diabetes in NOD mice is gender-dependent and, in a colony, it varies usually around 60-80% in female mice by the age of 35 weeks and it is always less in male mice (Castano and Eisenbarth 1990; Young et al. 2009). The gender difference is reported to be related to the influence of hormones on the gut microbiota, as germ-free NOD mice and castrated male mice present a similar incidence between males and females. The gut microbiota play a role in the modulation of the immune system (Yurkovetskiy et al. 2013).

The genetic influences on diabetes incidence in the NOD mouse strain, as in humans, are polygenic and more than 40 susceptibility loci have been mapped, although many of them still need to be fully identified (Pearson et al. 2016). The main genes influencing susceptibility to diabetes in NOD mice are located in the H-2 region on chromosome 17 (in NOD mice, it is called H-2^{g7}). One proposed role for the MHC molecule in the pathogenesis of autoimmune diseases can be seen when a polymorphism results in expression of MHC class II molecules (designated I-A^{g7} in NOD mice) that bind weakly to the autoantigen, its presentation in the thymus is not effective and autoreactive T cells escape negative selection (Ridgway et al. 1999).

The polygenic background (although the genes linked to T1D in humans and mice are not exactly the same) and the importance of the genes related to the MHC (HLA in humans), together with the main autoantigens identified in T1D (including insulin and glutamate decarboxylase – GAD) are some of the similarities between the NOD mouse model and humans (Thayer et al. 2010). Furthermore, inflammation can be detected in the islets before the clinical signs of diabetes. NOD mice can also develop other autoimmune diseases, such as sialitis and thyroiditis (Anderson and Bluestone 2005), and humans who develop type 1 diabetes have an increased propensity to other autoimmune diseases.

However, as in any animal model, there are some important differences and limitations: Even though the insulitis in both cases is caused by similar subsets of cells, the infiltration in human pancreas is more sparse and less organized, when compared to the inflammation in murine pancreatic islets, where it is possible to observe an accumulation of cells around the islets; NOD mice do not suffer with ketoacidosis, in contrast to the severe ketoacidosis seen in patients not treated with insulin; while Type 1 diabetes is gender-dependent in NOD mice, showing a striking difference between the

incidence in females and males; in humans, there is no gender-difference in the incidence during childhood and a small bias towards men after puberty (Atkinson and Leiter 1999; Patterson et al. 2009).

1.4.3 Immunopathogenesis

Since Type 1 diabetes has been shown to develop as a result of autoimmunity and with the discovery of insulin autoantibodies in diabetes patients (Palmer et al. 1983), there have been investigations into how T1D develops and progress in humans and mice. The most commonly cited hypothesis for T1D immunopathogenesis was postulated by Eisenbarth in 1986 and updated in 2001 with further modifications (Atkinson and Eisenbarth 2001).

Polymorphisms in genes that are the major risk factors for Type 1 Diabetes predispose individuals to failures on their tolerance mechanisms. As described above, the mutations alter the way insulin is presented in the thymus during negative selection, allowing autoreactive T cells to escape deletion (Ridgway et al. 1999). However, as demonstrated in congenic mice carrying the NOD MHC genes, the polymorphisms are necessary, but not sufficient for diabetes development by themselves (Yui et al. 1996).

Many theories about what triggers diabetes in the pancreas have been investigated. Although immune homeostasis in the pancreatic islets is damaged and the immune system attacks beta cells, leading to its destruction and compromised production of insulin, the role of each cell and what alters this homeostasis is still under investigation.

The association between virus infection and type 1 diabetes has been investigated since the late 1960's-early 1970's. Studies with Coxsackie B virus in mice demonstrated tropism of this virus for beta cells. They infect pancreatic islets, causing lysis of beta cells, infiltration of immune cells and transient hyperglycaemia (Yoon et al. 1978). In humans, this association is mostly based on epidemiological data (Laitinen et al. 2014). Other viruses, such as rubella virus and retroviruses, are also linked to T1D and their mechanisms of action could vary between direct destruction of beta cells or alterations in the immune system (for example, release of autoantigens, upregulation of MHC class I and II, activation of autoantibodies producer B cells and production of pro-inflammatory cytokines) (Jun and Yoon 2003; Richardson et al. 2011).

The importance of immune system cells in the development of type 1 diabetes is incontestable and both CD4 and CD8 T cells play the main roles in beta-cell destruction, which precedes clinical signs of diabetes in humans and rodent models. Murine models naturally deficient in T cells, as NOD.scid and athymic NOD mice, do not develop diabetes. This protection is lost when T cells from diabetic mice are transferred (Christianson et al. 1993; Matsumoto et al. 1993). On this note, one of the most efficient treatments tested so far in clinical trials has been the administration of anti-CD3 monoclonal antibodies to patients, especially newly diagnosed young patients (Daifotis et al. 2013), although the effects are not maintained.

The major role of CD4 T cells is highlighted by the predisposition to T1D lying mainly in the MHC/HLA class II genes. CD4 T cells with affinity for islet autoantigens (such as insulin, GAD and chromogranin A) have been used to investigate the role of these cells in diabetes pathogenesis. Lennon and colleagues demonstrated that the majority of T cells homing to the pancreas are islet-specific and the trafficking is mediated by chemokines (Lennon et al. 2009). These autoreactive CD4 T cells, that escaped deletion in the thymus and are later found in the pancreas, travel from the pancreatic lymph nodes to the pancreas attracted by autoantigens bound to antigen presenting cells (APCs).

One subpopulation of CD4 T cells that is very important for the fate of individuals that are susceptible to type 1 diabetes (and other autoimmune diseases) is the regulatory T cells (Tregs). These cells, with the phenotype $CD4^+CD25^+Foxp3^+$, are key factors for peripheral tolerance, keeping anergic cells in check and suppressing inflammatory responses. Indeed, although the number of Treg cells in healthy controls and patients with T1D is similar, they do not work as effectively in the case of type 1 diabetes and effector T cells are resistant to their suppression (Kuhn et al. 2016; Visperas and Vignali 2016). Indeed, in the islet infiltration of NOD mice, although the number of regulatory T cells was not altered, the expression of CD25 on these Treg cells significantly decreased as infiltration and disease progressed. CD25 is the α-chain of IL-2 receptor, responsible for providing survival signals for the cells (Tang et al. 2008).

In addition to CD4 T cells, studies showed that IFN-γ-producing CD8 T cells, with affinity for the B:15-23 portion of insulin, are present in the islet of 4 week old NOD mice (Wong et al. 1999). Moreover, β2-microglobulin-deficient NOD mice (deficient in

MHC class I molecules) presented no signs of insulitis or diabetes (Serreze et al. 1994; Wicker et al. 1994) and adoptive transfer of these islet-specific CD8 T cell clones, isolated from 7-week old. NOD mice, was sufficient to cause diabetes in irradiated NOD and NOD-SCID mice (Wong et al. 1996). CD8 T cells are responsible for the cytolysis of beta cells, by the release of perforins and granzymes (Amrani et al. 1999; Estella et al. 2006), and also causing death of beta cells through Fas-FasL interactions (Savinov et al. 2003).

Macrophages and DCs are seen circulating in the pancreatic islets of neonatal NOD mice and a higher frequency of these cells by the third, fourth week of life precedes the infiltration of lymphocytes. Temporary depletion on both macrophages and DCs when mice were 8 weeks old delayed the disease and, although by the end of the experiment (35 weeks old) insulitis was present in all NOD mice, treated and non-treated, during the period these cells were depleted in the pancreas, lymphocyte infiltration was reduced and reappeared when macrophages and DCs returned (Nikolic et al. 2005).

One theory proposing that a physiological mechanism is the key to understanding the role of phagocytes in diabetes onset is being investigated. Studies have demonstrated that, as a natural phenomenon that also occurs in mouse strains not prone to diabetes, beta cells transfer vesicles containing insulin and insulin peptides to local macrophages and dendritic cells. Anti-insulin CD4 T cells are then activated when they interact with these APCs (Vomund et al. 2015). This model, however, does not include the role of environmental factors and other cells of the immune system.

The time between pancreatic infiltration and clinical signs varies from one individual to another. In humans, it takes years and in mice it could take months. This time gap suggests that some kind of suppression or regulation is taking place to contain the beta-cell destruction. In the original Eisenbarth proposition for the pathogenesis of diabetes, after the beginning of insulitis there was no turning back in beta cell loss and their mass would only decrease, until there was no beta cells left (Eisenbarth 1986). However, it is believed now that T1D could present relapsing-remitting phases depending on the efficacy of beta-cells to proliferate when attacked, how fast autoantigens are released and how efficient regulatory cells are in the individual (von Herrath et al. 2007). All these factors could delay or accelerate the progression of type 1 diabetes and, in some

cases, regulatory cells may be able to stop destructive beta cell loss before the onset of type 1 diabetes (Figure 1.4).

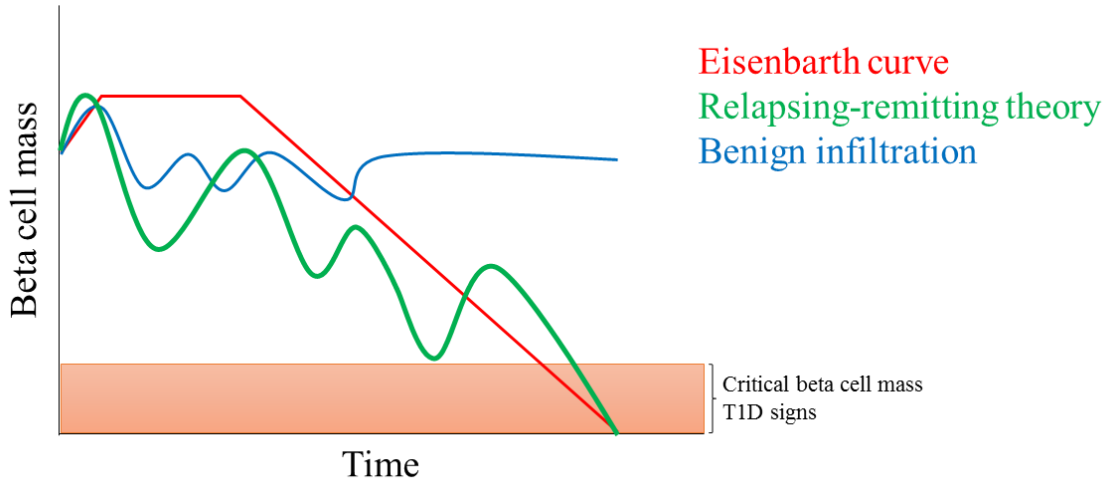

Figure 1.4 Theories correlating beta cell mass loss and the beginning of type 1 diabetes clinical signs. The first theory about how the loss of beta cells correlates with the detection of type 1 diabetes signs was suggested by Eisenbarth in 1986 who postulated that after the beta cell mass started to decrease, there was no way back (red line). However new theories incorporated the idea that regulatory cells balance the damage to the beta cells caused by effector cells, leading to a relapsing-remitting curve (green line). The blue line indicates cases where genetically predisposed individuals present some beta cell mass loss; however, regulatory mechanisms are sufficient to suppress them or an appropriate environmental factor never triggers the disease onset (van Belle et al. 2011).

A diagram explaining the theory for the immunopathogenesis of Type 1 diabetes is shown in Figure 1.5:

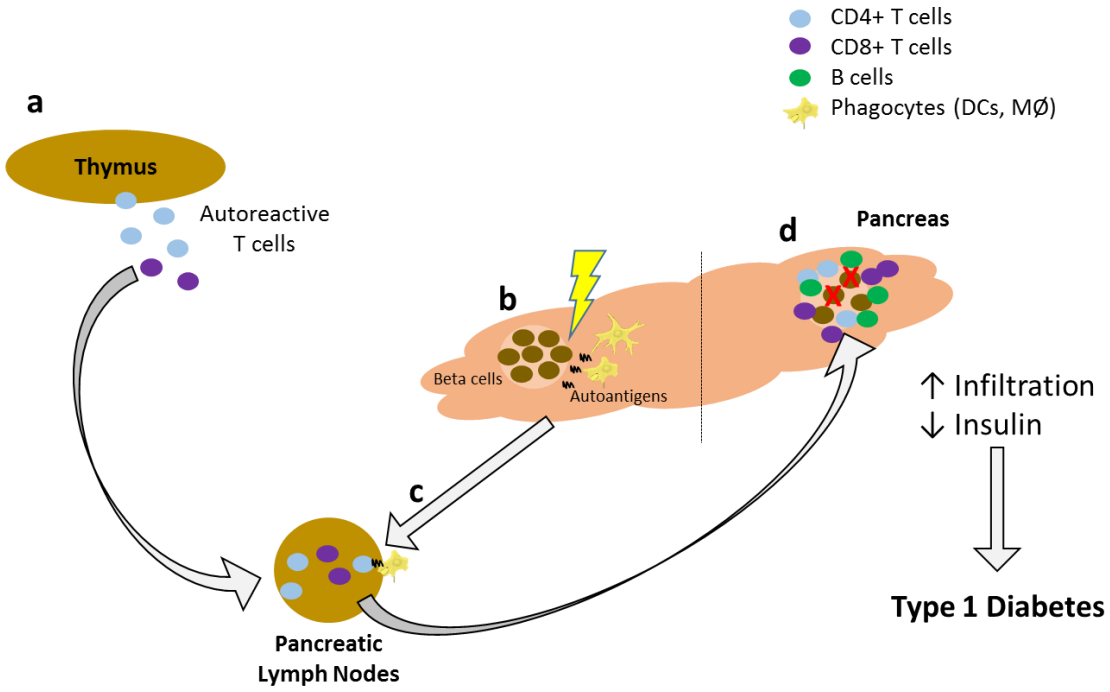

Figure 1.5 Immunopathogenesis of type 1 diabetes. The process that leads to type 1 diabetes begins in the thymus of genetically susceptible individuals (a), where islet-specific autoreactive T cells (purple circles) escape from negative selection. These cells exit the thymus and are found in the pancreatic lymph nodes. Meanwhile, in the pancreas (b), environment factors (like virus infection, for example – here represented by the lightning bolt) may disturb the homeostasis and beta cells, responsible for the production of insulin, start to release self-antigens. These autoantigens are captured by phagocytes (yellow cells) and presented to those autoreactive T cells in the pancreatic lymph nodes (c). Attracted by chemokines, the autoreactive T cells travel to the pancreatic islets and, with the help of B cells (green cells), start to destroy the beta cells (d). As the infiltration progresses, the production of insulin becomes insufficient and the first signs of type 1 diabetes are detected.

Although T cells are believed to be the main cells that actually damage the beta cells, B lymphocytes have multiple functions and influence the onset and progression of Type 1 Diabetes, which will be discussed in the next section.

1.5 B cells and Type 1 Diabetes – What is known so far?

1.5.1 Islet cell antibodies (ICAs)

Although type 1 diabetes is characterized as a disease caused by T cell-mediated beta cell destruction, several other cells of the immune system are involved in this process. The first abnormality associated with B cells in type 1 diabetes was the production of islet cell antibodies (ICAs).

In earlier years when type 1 diabetes was not so clearly defined as an autoimmune disease, ICAs started to be detected in patient blood samples. Palmer and colleagues showed that insulin bound to proteins that were present in the blood of newly-diagnosed patients and those proteins were insulin antibodies. The experiments were performed before the beginning of insulin treatment, so the insulin antibodies were not produced against exogenous insulin (Palmer et al. 1983). GAD, an enzyme responsible for synthesizing γ-Amino Butyric Acid (GABA) from glutamic acid, was first found in the Central Nervous System (CNS) and antibodies against this enzyme were detected in patients with stiff-man syndrome. Interestingly, there was a high incidence of T1D in these patients. In 1990, anti-GAD obtained from patients who had this neurological condition and antibodies against a 64K protein from diabetic patient's sera were tested together. It was demonstrated that they behaved very similarly and both GAD and the 64K protein exhibited the same activity, proving they were the same enzyme, produced not only in the brain, but also in the pancreas and related to type 1 diabetes (Baekkeskov et al. 1990). Insulinoma Antigen-2 (IA-2), designated ICA152 before recognition as the tyrosine phosphatase IA-2, is also found in brain cells as well as in the pancreas. ICA512 was the first membrane protein identified as a target for autoantibodies in type 1 diabetes (Solimena et al. 1996). Recently, another autoantigen has been characterized. Zinc Transporter, ZnT8 – which controls the intracellular concentration of zinc in the insulin granule, was scanned from a list of 300 genes of autoantibodies candidates and showed to be highly expressed in the islets (Wenzlau et al. 2007).

ICAs can be detected in the serum, years before the disease diagnosis, and are still used as a marker for the development of the disease in humans. Even though the production of autoantibodies in type 1 diabetes prediction is well established, the role of autoantibodies in the development of the disease is still uncertain and studies show controversial results. It is proposed that autoantibodies could promote tissue damage or help DCs in antigen presentation and cross presentation to CD4 and CD8 T cells, respectively (Harbers et al. 2007; Silva et al. 2011). However, it is known that they are not themselves pathogenic, at least in mice, as they did not cause disease when antibodies from diabetic mice were transferred to NOD.IgM^{null} (B cell depleted) mice (Serreze et al. 1998).

1.5.2 B cell depletion and type 1 diabetes

Experiments using depletion to study B cell function in type 1 diabetes have been performed by different research groups in many different ways. Noorchashm and colleagues administered μ-chain antibody (anti-IgM) 3 times weekly to NOD mice, initiating the treatment 24h after birth and lasting for 30 weeks. Compared to controls, these mice did not develop insulitis or diabetes. A group of mice received antibody injections for only 8 weeks; in this case, B cell population was reconstituted 10 weeks after the end of treatment, insulitis was detected, but no diabetes was observed. These results showed that B cells are necessary for the development of type 1 diabetes, and although the role of B cells was suggested to be as antigen-presenting cells, autoantibody production as a pathogenic mechanism was not discarded at this point (Noorchashm et al. 1997). For this reason, transgenic NOD mice which only expressed the membrane-bound form of IgM (and therefore did not secrete antibodies) were used to study the effect on diabetes development in the absence of autoantibodies. mIgM transgenic mice had more insulitis and a higher incidence of diabetes compared to the NOD mice completely depleted of B cells. These findings demonstrated that the B cell role in type 1 diabetes is mainly autoantibody-independent (Wong et al. 2004).

Moving from the use of depleting B cells as a mechanism to study the B cell role in disease towards possible treatments, the use of monoclonal antibodies for short-term B cell depletion was first investigated in lymphomas. A chimeric antibody anti-CD20, Rituximab, was efficient when used to treat these B-cell malignancies, and there were

few side effects. There was also interest in this treatment for autoimmune diseases (Johnson and Glennie 2001). In type 1 diabetes, murine studies using rituximab were possible by the generation of transgenic NOD mice expressing human CD20 (Hu et al. 2007). These mice received a cycle of 4 injections of anti-CD20 (2H7 clone) while they were young (4 or 9 weeks old – before hyperglycaemia). In treated mice, diabetes was delayed and the incidence was lower, compared to mice that received control IgG. These findings confirmed the role for B cells in the onset and progression of type 1 diabetes. Moreover, when injected in diabetic mice, 36% of newly-diagnosed mice had decreased blood glucose and sustained this euglycaemia for a long period, although the degree of insulitis was similar to that found in control mice. Because the protection lasted longer than the treatment, the mechanisms proposed for these results involved more than just depletion of pathogenic B cells: increased $CD4^{+}CD25^{+}Foxp3^{+}$ (Treg cells) and less effective macrophages and DCs, for example. Also after repopulation, an increased frequency of transitional B cells was observed in treated mice (Hu et al. 2007).

Anti-CD20 was also tested in a clinical trial. Newly-diagnosed patients with type 1 diabetes received one cycle of the treatment and were followed for one year. Patients receiving rituximab needed less daily insulin administration than controls, presented higher levels of C-peptide (i.e., more insulin being produced) and had reduced levels of glycated haemoglobin. However after one year, the results started to diminish, suggesting that the effects of rituximab were transient (Pescovitz et al. 2009). More detailed studies to understand the mechanisms by which depletion has the protective effect could improve the treatment.

B cell depletion with rituximab does not optimize the mechanisms of central tolerance in treated patients, as shown by Chamberlain and colleagues. After treatment with anti-CD20, the number of new autoreactive B cells repopulating the periphery were similar to non-treated patients (Chamberlain et al. 2016). Thus, the effect of B cell depletion lasting longer than the period when B cells are absent could be due to a correction in the individuals' immune regulatory system. Based on these interesting findings, the effects of B cell depletion and repopulation on regulatory B cells in transgenic NOD mice were investigated in this thesis.

Other antibodies have also been targeted to promote B cell depletion in type 1 diabetes: Treatment with anti-CD22 conjugated with calicheamicin also led to delayed diabetes, decreased insulitis and a reprogramed/more regulatory immune system (Fiorina et al. 2008). Another approach to deplete B cells in NOD mice consisted of eliminating survival signals by neutralizing BLyS/BAFF (B Lymphocyte Stimulator). One dose of this antibody delayed diabetes development, reduced insulitis and decreased the incidence of diabetes during the first weeks; however, by the end of the experiment, the diabetes incidence in treated and control mice was the same (Zekavat et al. 2008).

The results of the depletion experiments, the finding that the production of autoantibodies from islet autoantigen-specific B cells is not important, together with their expression of MHC class II, all suggest that B cells can play an important antigen-presenting role in type 1 diabetes. As APCs, although B cells are not as efficient as dendritic cells, they can bind specifically to soluble autoantigens through their B cell receptor and this antigen specificity means that B cells are potentially very powerful antigen-specific antigen presenting cells. The role of B cells as APCs over other APCs in NOD mice is intensified by the fact that DCs are defective in NOD mice, with impaired development and altered co-stimulatory signals (Vasquez et al. 2004).

1.5.3 B cells as APCs

Insulin-specific B cells, have been shown to be anergic and were able to internalize and process insulin, presenting the antigen to CD4 T cells that were activated *in vitro* (Kendall et al. 2013). Transgenic NOD mice with B cells lacking the I-A^{g7} (NOD-specific) form of MHC class II (other APCs were normal) had decreased incidence of diabetes and had only peri-insulitis but no invasive infiltration. These results showed that although B cells do not participate in the initial priming of T cells by islet autoantigens, they are important for the break in tolerance that leads T cells from benign infiltration to beta-cell destruction (Noorchashm et al. 1999). B cells with APC function are believed to be located in the marginal zone in the spleen. MZ B cells have a superior capacity to activate CD4 T cells (induce proliferation and cytokine secretion) in an antigen-specific manner, when compared to FO B cells. Marginal zone B cells also have higher levels of CD86 than follicular B cells (Attanavanich and Kearney 2004).

1.5.4 B cell infiltrating the pancreas

B cells are found among the cells infiltrating the pancreatic islets, being the most abundant immune cell in the infiltrate of NOD mice (around 48% in 10-week-old mice). These B cells produce TNF-α, similar to macrophages and DCs; islet B cells also had a higher frequency of CD80 and CD86 – co-stimulatory molecules that promote interaction between APCs and T cells (Hussain and Delovitch 2005).

B cells have also been detected infiltrating islets of human patients. They were observed in early periods of insulitis and their number increased four-fold in advanced stages (In't Veld 2014). Their disposition in the islets, analysed by immunohistochemistry, also showed evidence for interaction between B cells and CD8 T cells (Willcox et al. 2009). Variable expression of CD20 in infiltrating B cells (CD20HI and CD20Lo) was also observed and, in general, children diagnosed before 7 years old had more CD20HI B cells; while expression of CD20Lo B cells was found in patients diagnosed after 13 years old. At both ages, in the patients that had high frequencies of infiltrating CD8 T cells. The CD20HI phenotype was also linked to a more aggressive and rapid onset of type 1 diabetes (Leete et al. 2016).

In NOD mice, the interaction between B cells and CD8 T cells was studied in a NOD mouse model of accelerated diabetes (100% incidence by the 15^{th} week of age) where RIP-TNF–α mice were crossed with the NOD-μMT$^{-/-}$ mice (B cell absence from birth). In these new transgenic mice, the disease was delayed. No difference was observed in the number of $CD4^{+}CD25^{+}Foxp3^{+}$ cells in the islet infiltration and pancreatic lymph nodes (PLNs) and this suggested that the effect was not Treg-dependent. However, the delay in the disease was attributed to the interaction between B cells and CD8 T cells, as there was a decreased frequency of these T cells in 8-week-old B-cell depleted mice, when compared to non-depleted mice. B cells are believed to be important also in the second phase of islet infiltration, helping CD8 T cells in their differentiation into cytotoxic cells and providing survival signals to these cells. This was confirmed in the study, as the decrease in the percentage of CD8 T cells in the infiltrate was not observed in 4-6 week old transgenic mice (Brodie et al. 2008). Mariño and colleagues also demonstrated that B cells were responsible for the proliferation and activation of islet specific CD8 T cells in the pancreatic lymph nodes in a MHC class I-dependent manner (Marino et al. 2012).

Besides their help in maintaining CD8 T cells in the pancreatic islets, B cells have also been associated with infiltrating CD4 T cells. The role of B-1 cells in the establishment of destructive insulitis was studied in the DO11 3 RIP-mOVA mouse model, where B cell-depleted mice (by using an anti-CD22-calicheamicin treatment) had decreased incidence of type 1 diabetes. This protective effect was attributed to the lack of $CD19^{+}CD5^{+}$ B cells in the early phases of disease development and when they were absent, T cell infiltration was not observed. The deficiency of B-1 cells did not prevent T cell-priming in the pancreatic lymph nodes, but rather the signals facilitating access of these cells into the islets were not provided. The number of B-1 B cells decreased in the infiltration as the disease progressed and they were substituted by B-2 B cells (Ryan et al. 2010).

1.5.5 Regulatory B cells and Type 1 Diabetes

As discussed previously, cytokine-producing B cells are found among the cells infiltrating the islets, secreting TNF-α and interacting with the T cells. However, observations that B cells were able to suppress responses by producing regulatory cytokines in other autoimmune diseases raised the questions about the association between Bregs and type 1 diabetes.

One of the earliest reports demonstrating the role of regulatory B cells in type 1 diabetes focused on TGF-β-producing B cells. In 2001, Tian and colleagues showed that B cells activated with LPS expressed more FasL, produced higher frequencies of TGF-β than unstimulated B cells and caused apoptosis of diabetogenic T cells, decreasing the incidence of the disease in NOD mice. In this case, the protection was IL-10 independent (Tian et al. 2001).

The role of IL-10-producing B cells in T1D was partially elucidated by Kleffel and colleagues. When compared with diabetic mice, normoglycemic NOD mice (those that reach 35 weeks old with no signs of type 1 diabetes) had lower percentages of B cells infiltrating the pancreas. Moreover, more of these B cells that were seen in the insulitis of protected NOD mice were anergic and produced more IL-10 than the infiltrating B cells in diabetic mice. The comparisons between the spleen B cells of young, protected and diabetic NOD mice did not show any statistically significant difference in the

production of IL-10. However, the B cells were not cultured in the presence of stimulants, such as LPS or anti-CD40 (Kleffel et al. 2014).

Considering what is known about Bregs in other autoimmune diseases and the relatively little knowledge of their role and whether they are defective in the NOD model of type 1 diabetes, a broad study of their phenotype and the differences NOD mice might present while aging was warranted.

1.6 Aims and Hypothesis

Based on the information derived from earlier investigations discussed in this chapter, our hypothesis was that regulatory B cells, especially IL-10-producing B cells, could be impaired in NOD mice, an experimental model to study type 1 diabetes.

Our aims were to investigate the association between regulatory B cells and NODs in the following studies:

1) Compare the ability of B cells to produce inflammatory and regulatory cytokines in NOD and control mice at different ages (Chapter 3);

2) Analyse the expression of regulatory markers in B cells producing IL-10 in protected and diabetic NOD mice (Chapter 3);

3) Study the ability of B cells to regulate immune responses by CD8 T cells and DCs, specific to insulin (Chapter 4);

4) Investigate the importance of regulatory B cells in the protection against type 1 diabetes conferred by B cell depletion (Chapter 5).

2. Methods

Information and details on reagent manufacturers, catalogue numbers and recipes for solutions described in these sections can be found in 2.17 in Tables 2.2-2.4.

2.1 Mice

The following strains of female and/or male mice were used in these studies:

The **NOD/Caj** (Non-Obese Diabetes) is the main murine model used to study type 1 diabetes. This strain was first developed in Japan, while Makino and colleagues worked on the refinement of a cataract-prone strain. NOD mice should be kept in specific pathogen-free environments to ensure high incidence of diabetes in female mice; male NOD mice generally present a lower incidence (Anderson and Bluestone 2005). Our colony has been inbred in Cardiff University for the last 6 years. During the period while these studies were performed (2013-2016), the incidence of diabetes for the female NOD colony varied around 70%.

B6.H-2^{g7} (B6^{g7}) mice were used as a non-diabetes prone control strain. This congenic strain has all the genes from a C57BL/6 mouse, except for the MHC genes (Major Histocompatibility Complex class I and II), which is the NOD MHC H-2^{g7}.

G9Cα-/-.NOD (G9) mice were genetically modified to express the T cell receptor derived from the CD8 T cell clone G9C8, reactive to amino acids 15-23 of the insulin B-chain (Wong et al. 2009).

NOD.MHCII-Ins2 (PI homo) mice have a transgene that encodes proinsulin 2 expressed in antigen presenting cells, as the construct is directed by the MHC Class II promoter I-Eα. This strain does not develop diabetes spontaneously (French et al. 1997).

hCD20/NOD mice were originally developed on the C57BL/6 background (Ahuja et al. 2007) and were backcrossed to the NOD genetic background, more than 10 generations. B cell surface markers, antibody production and diabetes incidence were not affected by the expression of human CD20 (Hu et al. 2007).

Mice were generated and maintained in Joint Biological Services (JBIOS), located in Heath Park – Cardiff University. All animals received water and food *ad libitum* and

were housed in a 12h dark/light cycle and specific pathogen-free conditions in isolators or scantainers. All experiments were conducted according to United Kingdom Home Office guidelines.

2.2 Mouse strain genotyping

2.2.1 PCR genotyping of transgenic mice

Mouse genotyping to confirm the presence of the transgenes were performed by the Diabetes Research Group's technician Joanne Davies, following these protocols:

2.2.1.1 DNA extraction from mouse tissue

Murine tissue obtained from ear coding was collected for DNA extraction at day 1. Each ear sample was added to 250µL of tail digest solution (Table 2.3) and 1µL of pronase. Samples were left overnight in a water bath, pre-heated to 55ºC.

At day 2, samples were removed from the water bath and placed in the fridge, at 4ºC, for 5 minutes. A hundred microliters of saturated salt solution was then added to the samples, which were centrifuged (16200g, 4ºC) for 20 minutes. After centrifugation, the supernatants were collected, transferred to new tubes with 1 µL of RNAase and incubated at 37ºC for 20 minutes. Samples were cooled for 5 minutes in the fridge and 500µL of 100% cold ethanol was added to the samples and vortexed, before centrifugation (20 minutes, 16200g, 4ºC). A hundred percent ethanol was poured off the samples and replaced by 70% cold ethanol. After being centrifuged (20 minutes, 16200g, 4ºC), the tubes were inverted, to remove the excess ethanol and the remaining ethanol was left to evaporate at room temperature for 3 hours. When the samples were dry, 50µL of water for PCR was added to them. DNA samples were stored at 4ºC.

2.2.1.2 PCR protocol and Gel Electrophoresis

A master mix was prepared with 1.5µL 10x PCR buffer, 0.3µL of each primer (20 pmol/µl working solution), 0.6µl dNTP, 0.1µl Taq Polymerase and enough water for PCR to make up to a final volume of 13µl, per sample (for more information on

reagents and how solutions were prepared, please see Tables 2.2 and 2.3). Each 13µl aliquot of the mastermix was then added to one well and 2µl of the DNA extracted from the mouse tissues were added to it. The wells were closed, centrifuged at 300g for 30s and placed in the PCR thermocycler.

The PCR program used was: 1) 94°C for 3 min; 2) 94°C for 1 min; 3) 55°C for 1 min; 4) 72°C for 1 min; 5) Repeat steps 2-4 34 times; 6) 72°C for 5 min and 7) 8°C for 10 min.

One percent agarose gel was prepared, by adding agarose to TAE buffer and boiling the solution in the microwave until the gel powder was dissolved and the solution was clear. After cooling, 5µl of Ethidium bromide was added while stirring for 2 minutes.

The agarose gel was placed in the gel tank, with combs to produce the wells into which the samples were loaded for electrophoresis, and allowed to set for 30 minutes. After setting, the electrophoresis tank was filled with TAE buffer, to cover the agarose gel.

Following completion of the PCR program, 3µl of orange G was added to the samples and 10µl of each sample was loaded into the wells in the agarose gel. A DNA ladder (1000-100bp) was used as a size marker. Gel electrophoresis was performed for 50 minutes at 100V. The gel was then photographed on Gel Doc system. Figure 2.1 shows an example of a PCR gel for NOD.MHCII-Ins2 mice studied.

Primers used for the genotyping of mice cited in this chapter:

NOD.MHCII-Ins2 mice: 5’ CCA CTG CCA AGG TCT GAA GGT CAC C 3’

5’ TTG TTA ATT CTG CCT CAG TCT GCG 3’

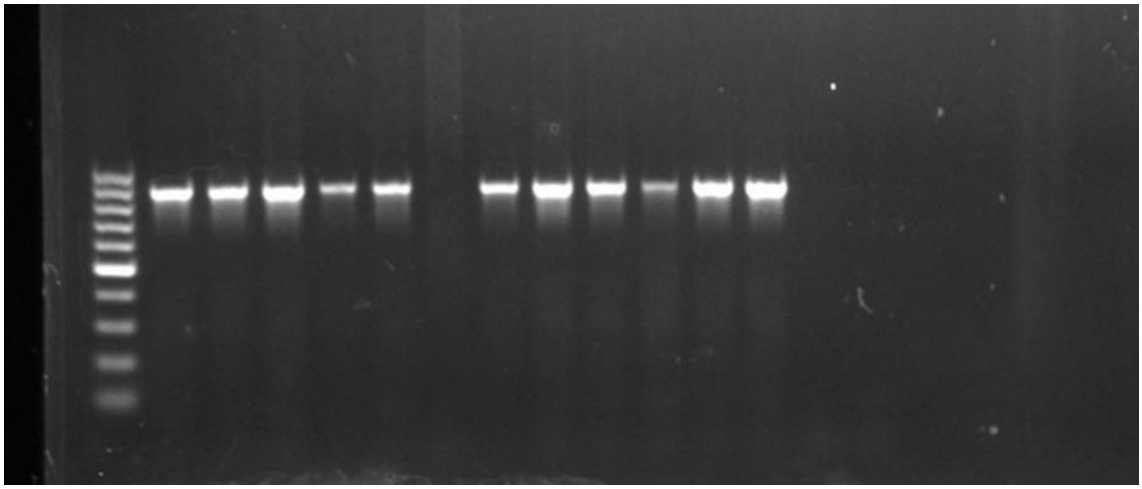

Figure 2.1: Photograph of genotyping of PI homo mice. DNA was extracted from mouse ear tissues and PCRs with primers for the homozygous proinsulin, band size: ~950bp, were performed. After the electrophoresis, the gels were photographed; positive bands are shown as light bars. The first row contains a control 100bp ladder for PCR product band sizes.

2.2.2 Blood test for genotyping

To confirm that every hCD20 NOD mouse expressed human CD20, and the G9Cα-/-.NOD mice were all Vβ6 positive, 50-100 μL of blood were collected from the mouse tail vein into 1ml Blood buffer (Table 2.2) and stained for flow cytometry.

After collection, the samples were centrifuged for 5 minutes (400g, at 4ºC), resuspended and the antibody was added to the cells. Samples were incubated for 30 minutes at 4ºC, and then 1ml of FACS (Fluorescence-Activated Cell Sorting) lysis buffer (diluted 1:10 with dH_20) was added to the cells at room temperature and further incubated for 10 minutes in the dark, to remove erythrocytes. After 10 minutes, the samples were washed with 2ml of FACS buffer and centrifuged (5 minutes, 400g, 4°C) one last time. Cells were then resuspended in 100μL of FACS buffer and analysed by flow cytometry (FACS Canto II) for positivity or negativity. Figure 2.2 presents flow cytometric plots showing samples that were positive for the markers studied.

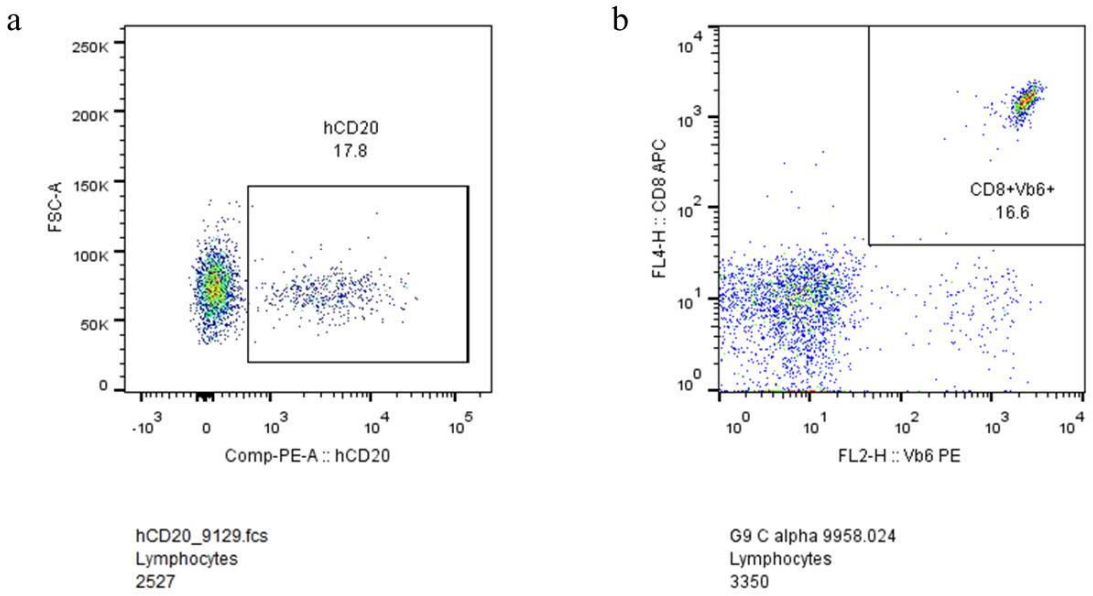

Figure 2.2 Flow cytometry plots exemplifying the presence of the markers studied. 50-100 µL of blood were collected from the tail vein. hCD20 NOD mouse samples were stained with PE human CD20 (a) and samples from G9Cα-/-.NOD mice were stained with APC CD8 and PE Vβ6 (b). After incubation, erythrocytes were lysed and the samples were then ready to be analysed by the flow cytometer. The plots above show positive examples of mice for both strains.

2.3 Detection of diabetes

To diagnose diabetes, NOD mice older than 12 weeks old were tested weekly for glycosuria with Diastix strips (Bayer). If glycosuria was confirmed after two urine positive tests on consecutive weeks, the blood glucose was tested and blood glucose concentration over 13.9mmol/L was diagnostic for diabetes (Wong et al. 2009). Table 2.1 presents the age and last blood glucose level measured in female diabetic NOD mice, which were included in the studies discussed in this thesis.

Table 2.1 Age and blood glucose levels for the diabetic mice included in the studies discussed in this thesis

Age (weeks)	Blood glucose (mmol/L)
Cytokine-production Experiments (Chapter 3)	
24	High (>33)
11.9	29
24	25.8
15.6	21.8
31.0	25.6
19.7	33
22.0	18.3
Functional experiments (Chapter 4)	
16.9	High (>33)
16.9	21.4
13.7	25.8
13.4	21.3
16.6	21.2
17.4	27.1
17.6	15.2
19.4	14.9
18.6	19.4
18.4	19.8
17.9	25.1
14.6	24.5

2.4 Dendritic cells – Culture and stimulation

Dendritic cells (DCs) were obtained from the bone marrow of the posterior legs of experimental mice. The legs were removed and the muscles were cleaned from the bones. They were then placed in 30ml of RPMI complete medium. In a sterile environment, the bones were placed in a Petri dish and, using a 5ml syringe (with a 27G needle), filled with RPMI complete medium. The needle was inserted into the bone marrow cavity and the bone marrow cells were flushed into the Petri dish. After repeating this procedure for all the bones, the suspension was collected from the Petri dish into the 50ml tube, to be centrifuged (10 minutes, 400g, room temperature). The cells were resuspended in 20ml of complete medium, passed through the cell strainer and transferred into a 75cm^3 flask. Cells were incubated in the flask for 2h at 37°C, 5%CO_2. This step aimed to remove macrophages from the cell suspension, which got

attached to the plastic during the incubation, while the immature dendritic cells remained in the suspension.

After incubation, the cell culture was collected into a 50ml tube (avoiding the adherent macrophages) and the cells were counted with Trypan Blue (dilution 1:10), while cells were centrifuged once again (10 minutes, 400g, room temperature). They were then resuspended in RPMI complete medium, to which 1.5ng/ml of GM-CSF was added to a final concentration of $2x10^6$ cells/ml. Cells were then placed in 6-well plates ($5x10^6$ cells/well), with an addition of 4ml of RPMI complete medium + GM-CSF and incubated (37°C, 5%CO_2) for 8 days. Medium changes were performed on day 3 or 4. On day 7, in addition to medium change, DCs received 5µl of 1mg/ml LPS.

2.5 CD8 T cells from G9Cα-/-.NOD mice and B cells – Enrichment and stimulation

Spleens were collected in IMDM complete medium, homogenized and centrifuged at 400g, 4ºC for 5 minutes. The erythrocytes were lysed by the addition of 900µl of deionised water (dH_20) and 100µl of sterile 10X PBS, after quickly flicking the tube to separate the lymphocytes and the debris. To remove dead erythrocytes from the samples, the suspension was passed through a 40µm cell strainer and the cells were centrifuged once again (5 minutes, 400g, 4ºC). After being resuspended in 10ml of medium, cells were counted with Trypan blue, in a 1:10 dilution, and followed to a magnetic sorting (following the manufacturer's instructions – explained below).

After enrichment, B cells were counted with Trypan Blue (1:10 dilution), their concentrations were adjusted to $5x10^6$ cells/ml and cells were then plated in a 6-well plate. Half of the wells were left for 24h without any further stimulation and half of them were stimulated with LPS (5 µg/ml). All plates were incubated (37°C, 5%CO_2) for 24h.

CD8 T cells were counted with Trypan Blue (1:10 dilution). Cells were divided in two portions and half were labelled with CFSE for the proliferation assay. CD8 T cells which were not stained, were centrifuged (5 minutes, 400g, 4ºC), resuspended in IMDM medium and the concentration was adjusted to $4x10^5$ cells/ml.

2.6 Magnetic-activated cell sorting (MACS) of B cells and CD8 T cells

After preparing spleens into cell suspensions, the cells were centrifuged and resuspended in 40µl of MACS buffer (Table 2.2) per 10^7 cells and 10µl of biotinylated antibody beads per 10^7 cells. In both cases (B and CD8 T cells), negative selection kits were used for cell separation. The cells were incubated with the appropriate biotinylated antibody mix for 5 minutes at 2-8ºC and then another 30µl of MACS buffer per 10^7 cells was added, along with 20 µl of Anti-biotin Microbeads per 10^7 cells. Cells were incubated once again for 10 minutes at 2-8ºC.

Before the separation, the magnetic columns were prepared by washing them once with 3ml of MACS buffer. After the incubation with the microbeads, cells were applied to the column, passing through a cell strainer to avoid bubbles. The column was then washed once with 3ml of MACS buffer. The suspension obtained after passing the cells through the column contained the cells of interest.

Purity for B cell sorting: 94-97%. Purity for CD8 T cell sorting: 95%.

2.7 CFSE (Carboxyfluorescein succinimidyl ester) labelling of cells

For proliferation assays, MACs sorted CD8 T cells were labelled with CFSE dye. To prepare the 10mM stock solution, CFSE was diluted in 90µL of the high-quality DMSO (Dimethyl sulfoxide) – as suggested by the manufacturer. Samples were aliquoted in 5µL and stored at -20ºC.

The CD8 T cells were centrifuged after magnetic sorting and resuspended in warm PBS at a concentration of $2x10^6$cells/ml. A sample of the stock solution was diluted in warm PBS to achieve 0.5µM/L – the ideal concentration for G9Cα-/-.NOD mice, as titrated previously in our laboratory (Thayer et al. 2016) – and added to the cells, which were incubated for 15 minutes (37°C, 5%CO_2).

After incubation, cells were centrifuged (5 minutes, 400g, room temperature) and resuspended in warm IMDM medium to wash off any non-attached dye. Cells were incubated again for 30 minutes (37°C, 5%CO_2). Labelled CD8 T cells were then centrifuged for the last time (5 minutes, 400g, room temperature) and resuspended in IMDM medium at a concentration of $4x10^5$ cells/ml.

2.8 Cell interaction experiment set-up for Chapter 4

On day 0, B cells (LPS-stimulated and unstimulated cells) and LPS-stimulated DCs were harvested, centrifuged once (5 minutes, 400g, room temperature) and counted with Trypan Blue (dilution 1:2). The numbers of DCs and B cells were adjusted to $1.6x10^6$ cells/ml and $5.6x10^6$ cells/ml, respectively. The cells were incubated in a 48-well plate, in a proportion of 1:2:7 ($2x10^5$ CD8 T cells; $4x10^5$ DCs; $1.4x10^6$ B cells) and a final volume of 1ml.

For the NOD or $B6^{g7}$ controls, a positive control was achieved by the addition of the nonamer 15-23 peptide from the insulin B-chain (designated G9 peptide) at 1 μg/ml to specified wells.

Experimental cells were set up such that one set was harvested after 1 day, for intracellular cytokine staining. The other set was incubated for 3 days, for analysis of proliferation and surface markers. More details about this experiment set-up are provided in chapter 4.

2.9 Cell collection and stimulation

Pancreatic and mesenteric lymph nodes, Peyer's patches, bone marrow and spleen were collected from NOD, $B6^{g7}$ and hCD20 NOD mice, depending on the investigation.

Lymph nodes and Peyer's patches were placed in Petri dishes containing IMDM and the lymphocytes were released, using needles and forceps. The suspension was divided into FACS tubes, using a cell strainer to avoid collection of debris.

For the B cell depletion experiments, described in chapter 5, bone marrow was collected to study B cells. After taking the posterior legs of hCD20 NOD mice, the bones were cleaned from the muscles and placed in 10ml IMDM medium. In a Petri dish, using a 5ml syringe and a 27G needle, the bone marrow cavity was flushed with media and the bone marrow cells were collected, centrifuged (5 minutes, 400g, 4°C), resuspended in 10ml and passed through a cell strainer.

Spleens were processed as explained in section 2.5 and, after adjusting the cell number, they were ready for surface marker flow cytometric staining. For *in vitro* experiments and analysis of cytokine expression, spleen cells were placed in a 24-well plate and stimulated with: LPS (5 μg/ml), anti-CD40 (5 μg/ml), CpG (0.5 μg/ml) and anti-CD40

with CpG (5 µg/ml and 0.5 µg/ml, respectively) or left unstimulated during incubation (37°C, 5%CO_2) for 24h.

After the stimulation and prior to staining, 10 µL per well of a mix containing monensin (1:1500), Phorbol 12-myristate 13-acetate – PMA (50ng/ml) and ionomycin (500ng/ml) were added to the cells, to activate and prevent cells from releasing the cytokines.

Three hours after the addition of monensin, PMA and ionomycin the cells were harvested and transferred to FACS tubes.

2.10 Surface monoclonal antibody staining for flow cytometry

Cells were harvested and transferred to FACS tubes for antibody staining. 2ml of FACS buffer were added into the FACS tubes containing the cells and then, centrifuged once (5 minutes, 400g, 4°C). Fc receptors were blocked with TruStain diluted in FACS buffer (1:12.5). The cells were incubated for 5-10 minutes at 4ºC and then 50 µl of a master mix containing the determined antibodies for each panel was added to each sample (see Table 2.3) and incubated for 30 minutes at 4ºC. Following this, cells were washed in FACS buffer and then resuspended and stored in 100µl FACS buffer at 4ºC until they were analysed in the cytometer.

Initially, the samples were analysed in an 8-colour-FACS Canto II (BD Biosciences). However, the facility was upgraded with a 16-colour-LSR Fortessa (BD Biosciences) and this then increased the number of fluorochromes that could be analysed simultaneously.

2.11 Intracellular cytokine staining for flow cytometry

For intracellular cytokine staining, the cells were resuspended, vortexed and 200µl of fixation/permeabilisation buffer were added to each sample and incubated for 20 minutes at 4ºC and then washed with 1ml of Fixation/Permeabilisation Buffer (diluted 1:10 in dH_2O). After centrifugation, TruStain was added once again (1:5). 25 µl of each sample was transferred to a new tube for the intracellular cytokine or isotype control staining and cells were kept on ice. Then another master mix, containing the antibodies against the cytokines or the isotype controls, was added to each tube. Cells were

incubated for 30 minutes at 4ºC. After incubation, cells were washed with Fixation/Permeabilisation buffer and centrifuged for the last time. Then they were resuspended in 200µl of FACS buffer and stored at 4ºC to be analysed in a flow cytometer.

For CD107a staining, in chapter 4, the antibody was added to the cell culture half an hour before monensin was added to the wells. As explained, monensin was then left for 3h before harvesting.

2.12 Meso Scale Discovery assay

The cytokines released in the culture supernatants were measured by the Meso Scale Discovery (MSD) assay, according to the manufacturer's (Meso Scale Diagnostics, LLC.) instructions. This multiplex technique followed the same concept of ELISAs (Enzyme-Linked Immunosorbent Assay); however, it allowed the simultaneous measurement of 5-10 cytokines in the same sample.

The cytokines evaluated for these studies were: IFN-γ, IL-6, IL-10, IL-12p and TNF-α, and the plates came pre-coated with the capture antibodies. At room temperature, 50µL of each sample (diluted 1:2 in Diluent 41) was added to the wells. For the standard curve, the highest concentration was prepared by the dilution of lyophilized Calibrator in 1000µL of Diluent 41 (a solution containing serum, blockers and preservatives). The next 6 points were obtained by a 4-fold dilution and the last well was filled with Diluent 41 alone (blank well). The plates were, then, sealed with the adhesive plate seal. Samples and standard curves were incubated for 2h at room temperature, with continuous shaking.

After 2h, the plates were washed 3 times with 150µL/well of Wash Buffer (provided by the kit as a 20X solution, to be diluted in deionized water). To prepare the detection antibody mix, 60µL of each antibody used in the assay was added to Diluent 45 (the final volume for each plate was 3000µL). Plates were sealed again and incubated for 2h at room temperature, while shaking. After incubation, the plates were washed a further 3 times.

For the detection in the MSD instrument (MSD Sector Imager 6000), 150µL of Read Buffer (4X stock solution, to be diluted in deionized water as 2X working solution)

were added to every well. There was no incubation prior to detection and the software used to analyse the plates was MSD Workbench, 2006.

2.13 B cell depletion protocol

Human CD20 NOD mice, received one cycle of treatment with anti-hCD20 antibody (clone 2H7) or control IgG2b antibody (clone MPC-11) when they were 6-8 weeks old.

One cycle consisted of 4 injections, with a 3-day-interval between them: the first injection was intravenous, delivering 500µg of antibody diluted in 200µl of saline. The next 3 injections were via the intraperitoneal route and delivered 200µg of antibody diluted in 200µl of saline.

2.14 Preparation of tissue and frozen sectioning for Germinal centre staining

For the preparation of histological slides, spleens from hCD20 mice were collected during experiments. Spleens did not require fixation, so they were collected in media or PBS. To freeze the organs, a bath of isopentane (2-methyl-butane) was prepared and placed over a tray of dry ice. The organs were placed in a mould, with a thin layer of OCT compound applied on the bottom of the mould. After placing the pancreas or spleen, the mould was filled with OCT and transferred to the isopentane bath, to freeze. Moulds were stored at -80ºC until being sectioned in a cryostat machine. Each slide had three 5µm spleen sections and was stored at -20ºC, until use.

2.15 Germinal centre staining for histological sections

Slides stored at -20ºC were left at room temperature for 10 minutes to defrost. A circle was drawn around the sections with PAP pen, a film-like water repellent to contain the liquids over the sections during staining.

Sections were fixed in cold acetone for 20 minutes and incubated for 20 minutes subsequently in PBS, for hydration. After this period, 1ml of PBS/H_20_2 (0.5ml of 30% H_20_2/100ml PBS) was added over the sections for 10 minutes to inhibit endogenous peroxidase. Slides were then washed with PBS once. To block non-specific reactions, 1ml of PBS + 3% BSA was added for 30 minutes. Samples were washed with PBS, 3% BSA and 0.1% Tween 20.

The slides were then divided in two groups: Half of the slides were stained with biotinylated B220 (B cells) and the other half with biotinylated Thy 1.2 (T cells). The slides were incubated with the antibodies for one hour and, after this period, washed three times with PBS/BSA/Tween.

B cells and T cells inside germinal centres are activated and, for this reason, express L-galactose residues on their surface. These residues bind to peanut agglutinin, a reagent that was labelled with horseradish peroxidase and added to the slides concomitantly with streptavidin + alkaline phosphatase. The mix was left incubating for 1h and the sections were then washed with PBS/BSA/Tween.

For the development of the colours (B and T cells in blue and PNA+ cells in brown), alkaline phosphatase substrate (1:1 solution of nitroblue tetrazolium and 5-brom-4-chloro-3-indolyl phosphate) and DAB (3-3' diaminobenzidine – prepared according to the manufacturer's instruction) were added to the slides, consecutively, and left for 20 minutes. Sections were checked regularly under the microscope for the optimal staining. When ready, the slides were washed one last time with PBS and immuno-mount was used to seal the slides.

* One of the initial aims of chapter 5 was to determine how the generation of germinal centres in the spleen would be affected by B cell depletion and repopulation. However, on staining the spleen sections for immunohistochemistry, no germinal centres were detected even in the spleen of control hCD20 NOD mice. Therefore, images of the slides for the different time points after depletion are not shown in this thesis.

2.16 Data analysis

Flow cytometry percentages were obtained by analysis on FlowJo V10 (Tree Star). Data analysis was performed using GraphPad Prism 4.02 and R 3.2.0.

Parametric data was analysed with t-test or one-way ANOVA, followed by Tukey Honest Significant Difference, carried out post-hoc. Graphs present the data as means and standard error of the mean (SEM). When non-parametric, the data was analysed by Mann-Whitney test or Kruskal-Wallis test, followed by Dunn Test and corrected with Bonferroni test. In these cases, graphs present the data as medians.

The significance level adopted was $p < 0.05$.

2.17 Reagents

Table 2.2 Reagents

Reagent	Dilution/ Concentration	Supplier	Catalogue nº
0.5µg/ml CpG (ODN 1826 sequence: 5'-TCCATGACGTTCCTGACGTT-3')			
10x PCR buffer		Sigma	P2192
2-MercaptoEthanol	55mM	Gibco	31350-010
30% H_2O_2		Sigma	216763
Absolute Ethanol		Sigma	E7023
Acetic acid		Sigma	320099
Acetone		Fisher scientific	A18-4
Agarose powder	1%	AGTC Bioproducts	AGD1
Alkaline phosphatase substrate		Sigma	AB0300
Anti-CD40 monoclonal antibody (Clone FGK45)	5µg/ml	Bio X-cell	BE0016-2
Anti-human CD20 Clone 2H7	Stock concentration: 9.99mg/ml	BioXCell	Produced as requested
B cell MACS Isolation kit		Miltenyi Biotec	130-090-86
Bovine Serum Albumin (BSA)	0.5%	Fisher Scientific	BP1600-100
$CD8a^+$ T cell MACS Isolation kit		Miltenyi Biotec	130-104-075
CFSE – Vybrant® CFDA SE Cell Tracer	1 kit	Invitrogen	V12883
Cytofix/Cytoperm Fixation/Permeabilization Solution Kit		BD Biosciences	554714
DAB kit		Vector	SK4100

dNTP set, containing dATP, dCTP, dGTP and dTTP	5mM working solution	Fisher Bioreagents	10234683
EDTA	0.5M	Ambion	AM9261
Ethidium bromide		Sigma	E-2515
FACS lysing buffer for blood samples	10x concentrated	BD Biosciences	349202
Fetal Bovine Serum	5%	Sigma	F7524
GeneRuler™ 100 bp DNA ladder, 100-1000 bp	0.5µg/µl	Fisher Bioreagents	11873953
GM-CSF (Granulocyte-macrophage colony-stimulating factor) Derived from X63-GM-CSF cells			
HRP-PNA		EY Laboratories	H-2301-2
IMDM (Iscove's Modified Dulbecco's Medium)		Gibco	12440-053
Insulin B chain 15-23 peptide [G9 peptide – LYLVCGERG]	5mg/ml	GL Biochem (Shanghai)	068592
Insulin-Transferrin-Selenium	0.1%	Gibco	41400-045
Ionomycin calcium salt from *Streptomyces conglobatus*	500ng/ml	Sigma	I0634
Isopentane		Fisher scientific	P/1030/21
L-Glutamine	1%	Gibco	25030-081
LPS from *Escherichia coli* 026:B6	5µg/ml	Sigma	L2654
Monensin	1:1500	Sigma	M5273
Mouse IgG2b Isotype control Clone MPC-11	Stock concentration: 11.68mg/ml	BioXCell	BE0086
MSD Multi-spot Assay System	1 V-plex kit	MSD	K15048D-1
OCT compound		Cell Path	KMA-0100-00A
Orange G		Sigma	O-3756
Pap pen		Vector	H-4000

PBS tablets	1 tablet/100ml dH_2O	Thermo Scientific	BR0014G
Penicillin-Streptomycin	1%	Gibco	15070-063
PMA	50ng/ml	Sigma	P8139
Pronase (from *Streptomyces griseus*)	1g Pronase dissolved in 4.4ml water for PCR	Sigma	P6911
RNAase		Sigma	R4642
RPMI-1640 (Roswell Park Memorial Institute Medium)		Gibco	31870-025
Sodium Azide	0.1%	BDH Laboratory Supplies	30111
Sodium chloride		Acrós organic	327300010
Sodium dodecyl sulfate	10%	Sigma	11667289001
Sterile PBS		Sigma	D8662
Streptavidin-alkaline phosphatase		Southern Biotech	7100-04
Taq DNA Polymerase from *Thermus aquaticus*	5U/µl	Sigma	D1806
Tris base	pH 8.0	Fisher Bioreagents	BP152
TruStain fcX (anti-mouse CD16/32) Antibody	1:12.5 (Extracellular)	Biolegend	101320
Trypan Blue Stain		Thermo Scientific	SV30084.01
Tween 20		Thermo Scientific	85114
VectaMount Permanent Mounting Medium		Vector	H5000
Water, molecular biology grade, Rnase, Dnase and Protease free		Fisher Bioreagents	10192813

Table 2.3 Preparation of solutions cited in the Methods

Solution	Volume/Concentration
50x TAE buffer	121g Tris base, 50ml 0.5M EDTA pH 8.0, 25ml Acetic Acid. Make up to 500ml with distilled water. For use, dilute it to 1x with dH_20. Stored at room temperature.
Blood buffer	PBS, 0.5% BSA; 4% 0.1M EDTA and 0.2% Sodium Azide. Stored at 4ºC
FACS buffer	PBS; 0.5% BSA and 0.1 % Sodium Azide. Stored at 4ºC
IMDM complete medium	IMDM medium; 1% Glutamine; 1% Penicillin-Streptomycin; 5% Fetal Bovine Serum; 55mM 2-MercaptoEthanol and 0.1% Insulin-Transferrin-Selenium. Stored at 4ºC
MACS buffer	PBS, 5% BSA and 2mM EDTA. Stored at 4ºC
RPMI complete medium	RPMI medium; 1% Glutamine; 1% Penicillin-Streptomycin; 5% Fetal Bovine Serum and 55mM 2-MercaptoEthanol. Stored at 4ºC
Saturated salt solution	Sodium chloride has a solubility of 35.7 grams in 100ml of cold dH_20
Tail digest buffer	5% 1M Tris pH 8; 4% 0.5M EDTA; 20% Sodium dodecyl sulfate; dH_2O

Table 2.4 Antibodies used for flow cytometry

Antibody	Fluorochrome	Dilution	Supplier	Catalogue no.	Clone
B220	Biotin	1:200	Biolegend	103204	RA3-6B2
CD107	PeCy7	1:200	Biolegend	121620	1D4B
CD11b	APC	1:200	Biolegend	101212	M1/70
CD11b	BV650	1:400	Biolegend	101239	M1/70
CD11c	PerCP Cy5.5	1:400	eBioscience	45-0114-82	N418
CD11c	BV650	1:400	Biolegend	117339	N418
CD138	BV510	1:100	Biolegend	142521	281-2
CD19	APC e780	1:800	eBioscience	47-0193-80	eBio1D3
CD19	AF700	1:100	Biolegend	115528	6D5
CD1d	PE	1:400	BD Biosciences	553846	1B1
CD1d	FITC	1:100	Biolegend	123507	1B1
CD1d	APC	1:200	Biolegend	123512	1B1
CD1d	BV510	1:200	BD Biosciences	563189	1B1
CD21	FITC	1:400	eBioscience	11-0212-81	eBio4E3
CD21	PE CF594	1:1000	BD Biosciences	563959	7G6
CD23	PE	1:800	eBioscience	12-0232-81	B3B4
CD23	PeCy7	1:200	eBioscience	25-0232-81	B3B4
CD23	BV711	1:800	BD Biosciences	563987	B3B4
CD24	BV421	1:800	Biolegend	101825	M1/69
CD24	FITC	1:400	BD Biosciences	553261	M1/69
CD24	BV650	1:400	BD Biosciences	563545	M1/69
CD25	PE	1:200	BD Biosciences	533866	PC61
CD27	APC	1:200	eBioscience	17-0271-81	LG7F9
CD27	PeCy7	1:400	Biolegend	124216	LG.3A10
CD279	BV786	1:200	Biolegend	135225	29F.1A12

CD3	PerCP Cy 5.5	1:200	BD Biosciences	551163	145-2C11
CD3	PE	1:100	Biolegend	100307	145-2C11
CD3	AF700	1:100	Biolegend	100216	17A2
CD3	FITC	1:100	Biolegend	100306	145-2C11
CD3	BV786	1:100	BD Biosciences	564379	145-2C11
CD3	BV605	1:100	Biolegend	100351	145-2C11
CD38	PeCy7	1:800	Biolegend	102717	90
CD38	FITC	1:200	Biolegend	102705	90
CD4	BV421	1:800	Biolegend	100443	GK1.5
CD4	BV650	1:400	Biolegend	100555	RM4-5
CD4	FITC	1:400	BD Biosciences	553729	GK1.5
CD40	PE CF594	1:400	BD Biosciences	562847	3/23
CD43	FITC	1:400	eBioscience	11-0431-82	eBioR2/60
CD43	AF700	1:200	BD Biosciences	565532	S7
CD44	PerCP Cy5.5	1:1600	eBiosciences	45-0441-82	IM7
CD5	FITC	1:200	eBioscience	11-0051-82	53-7.3
CD5	PeCy7	1:200	eBioscience	25-0051-81	53-7.3
CD5	BV421	1:100	Biolegend	100617	53-7.3
CD5	AF700	1:200	BD Biosciences	565505	53-7.3
CD62L	PeCy7	1:800	Biolegend	104417	MEL-14
CD69	BV786	1:200	BD Biosciences	564683	H1.2F3
CD8	PE CF594	1:800	Biolegend	100762	53-6.7
CD8	APC e780	1:200	eBiosciences	47-0081-82	53-6.7
CD80	BV650	1:100	BD Biosciences	563687	16-10A1
CD86	PeCy7	1:200	Biolegend	105116	PO3
CTLA-4	BV421	1:200	Biolegend	106311	UC10-4B9
Fas-L	PeCy7	1:100	eBiosciences	25-5911-82	MFL3
Foxp3	eF660	1:200	eBiosciences	50-5773-82	FJK-16s

Human CD20	PE	1:50	Biolegend	302306	2H7
IFN-γ	BV711	1:100	Biolegend	505835	XMG1.2
IgD	APC	1:800	eBioscience	17-5993-80	11-26c
IgD	PE	1:400	eBioscience	12-5993-83	11-26c
IgD	BV786	1:200	BD Biosciences	563618	11-26c.2a
IgM	BV421	1:200	Biolegend	406517	RMM-1
IgM	PerCP Cy5.5	1:200	Biolegend	406512	RMM-1
IgM	BV650	1:400	BD Biosciences	564027	R6-60.2
IL-10	PerCP Cy 5.5	1:200	eBioscience	45-7101-80	JES5-16E3
IL-10	APC	1:200	BD Biosciences	554468	JES5-16E3
IL-6	APC	1:200	Biolegend	504507	MP5-20F3
IL-6	PerCP efluor710	1:200	eBioscience	46-7061-80	MP5-20F3
Live/Dead dye	eF506	1:500	eBioscience	65-0866-14	
Live/Dead dye	APC e780	1:500	eBioscience	65-0865-14	
Live/Dead dye	BV605	1:500	Invitrogen	L-34959	
MHC I ($H\text{-}2D^b$)	PE	1:1000	Biolegend	111507	KH95
MHC II $I\text{-}A^k$ ($A\beta^k$)	FITC	1:400	Biolegend	109905	10-3.6
MHC II $I\text{-}A^k$ ($A\beta^k$)	PE	1:400	Biolegend	109908	10-3.6
Mouse IgG1, κ Isotype Control	BV421	1:200	Biolegend	400157	MOPC-21
Rat IgG1, κ Isotype Control	APC	1:200	Biolegend	400411	RTK2071

Rat IgG1, κ Isotype Control	BV711	1:100	Biolegend	400441	RTK2071
Rat IgG2b, κ Isotype Control	PerCP Cy5.5	1:200	eBioscience	45-4031-80	eB149/10H5
TCR Vβ6	PE	1:1000	Biolegend	140004	RR4-7
TGF-β	BV421	1:200	Biolegend	141407	TW7-16B4
Thy 1.2	Biotin	1:50	Biolegend	140314	53-2.1
TIM-1	PE	1:200	Biolegend	119505	RMT1-4

3. Cytokine production and the expression of regulatory markers in IL-10-producing B cells in NOD mice

3.1 Introduction and Objectives

3.1.1 Cytokines

Although B cells have a major function as antibody producers, they also exert a role as APCs (antigen presenting cells). In addition, they communicate with T cells and produce cytokines.

Cytokines are proteins secreted mainly by leukocytes as a way to establish communication between cells (Akdis et al. 2016). Studies have shown that they were able, for example, to polarize lymphocytes to differentiate into the various subpopulations of effector cells, such as Th1, Th2, Th17, Be1, Be2 (Harris et al. 2000).

Cytokines can modulate immune responses as well and, therefore, they are also categorised into pro- and anti-inflammatory and their balance is vital for the maintenance of a healthy individual.

The pro-inflammatory cytokine examined in this study, IL-6, is mainly produced by B cells and is important in germinal centres, as enhancers of antibody production. IL-6 is also important in the maintenance of Th17 cells (Bao and Cao 2014).

TGF-β is a regulatory cytokine secreted not only by leukocytes, but also fibroblasts and epithelial cells. TGF-β is very important as a mechanism of action for regulatory T cells and it is also important for the differentiation of Th17 cells, along with IL-6 (Gutcher et al. 2011).

IL-10 is considered the most important regulatory cytokine due to its powerful suppressive effects. When binding to IL-10R in APCs, for example, IL-10 reduces the expression of MHC II and co-stimulatory molecules and, in T and B cells, decreases the secretion of proinflammatory cytokines (Hofmann et al. 2012).

The importance of IL-10-producing B cells and TGF-β-producing B cells in autoimmune diseases and what is known so far about their relevance in type 1 diabetes have already been discussed in chapter 1. This chapter aims to further this investigation.

3.1.2 B cell surface markers – Regulatory B cell markers

As explained in chapter 1, regulatory B cells are not yet determined by one unified phenotype and they are currently characterized by the production of regulatory cytokines, such as IL-10, TGF-β and IL-35. A number of surface markers, however, are associated with the enhanced production of these cytokines by B cells.

As a summary, Table 3.1 presents the phenotypes for the different levels of maturation and subsets of B cells in rodents and humans (Pillai and Cariappa 2009; Blair et al. 2010). Regulatory B cells described in the literature commonly exhibit T2 and Marginal zone (MZ) phenotypes. In addition to markers that distinguish T2 and MZ B cells, regulatory B cells in rodents are also characterized by the markers CD1d and CD5. Yanaba and colleagues described this phenotype for the first time and they observed that $CD19^{+}CD1d^{hi}CD5^{+}$ spleen B cells comprised most of the IL-10-producing B cells and these cells were able to inhibit ear swelling after adoptive transfer (Yanaba et al. 2008).

In humans, immature B cells expressing high levels of CD24 and CD38 are also linked with IL-10 production (Blair et al. 2010).

Table 3.1 B cell subsets based on the expression of surface markers, in rodents and humans (information from (Pillai and Cariappa 2009; Blair et al. 2010)

	Level of maturation/Subsets	B cell Phenotype
Rodents	Immature B cells (T2)	$CD19^{+}IgD^{-}IgM^{+}CD21^{high}CD23^{+}$
	Mature Marginal B cells	$CD19^{+}IgD^{low}IgM^{hi}CD21^{hi}CD23^{-}CD1d^{hi}$
	Mature Follicular B cells	$CD19^{+}IgD^{hi}IgM^{low}CD21^{int}CD23^{+}$
Humans	Immature B cells	$CD19^{+}CD24^{hi}CD38^{hi}$ ($IgM^{hi}IgD^{hi}CD5^{+}CD20^{+}CD27^{-}CD1d^{hi}$)
	Mature B cells	$CD19^{+}CD24^{int}CD38^{int}$ ($IgM^{int}IgD^{+}CD5^{-}CD20^{+}CD27^{-}CD1d^{+}$)
	Memory Cells	$CD19^{+}CD24^{hi}CD38^{-}$ (IgM^{+} or IgM^{-} IgD^{+} or IgD^{-} $CD5^{-}$ $CD20^{+}CD27^{+}CD1d^{+}$)

3.1.3 Objectives

In depth studies about regulatory B cells in Type 1 Diabetes are still limited. Our general hypothesis was that B cells in the NOD mice are deficient in regulatory functions, which could be one of the factors leading to spontaneous development of autoimmune diabetes.

Therefore the first aim was to study cytokine production in $CD19^{+}$ B cells in the non-obese diabetic (NOD) mouse model, discussed in detail previously, in Chapter 1, specifically comparing age and gender with a mouse strain that is not prone to diabetes. The second aim of this chapter was to evaluate the variance of the regulatory markers in IL-10-producing B cells in male and female NOD and $B6^{g7}$ mice. We focused on 30-35 weeks old (w.o.) and diabetic mice, as these were the groups showing the most interesting results for cytokine-producing B cells.

3.2 Evaluation of cytokine production by B cells from NOD mice, compared to a non-diabetic prone mouse strain

The aim of this first study was to evaluate the cytokine production by the whole B cell population after a 24h cell culture. For this analysis, NOD splenic B cells, from male and female mice, were compared to a strain that does not develop autoimmune diabetes ($B6^{g7}$). Congenic $B6^{g7}$ mice share the same genetic background with C57BL/6 mice, with one exception: the MHC, $H\text{-}2^{g7}$, is derived from NOD mice. This strain does not develop type 1 diabetes.

The time points for the investigations were chosen, based on the natural history of type 1 diabetes for this mouse model: young (5-8-week-old) NOD mice, which had just passed the first checkpoint in the pathway to the development of autoimmune diabetes and started to develop infiltration of lymphocytes in their pancreatic islets (insulitis), though there was no sign of hyperglycaemia. Intermediate (13-17-week-old) is the age when NOD mice reach the second checkpoint and begin to develop diabetes; NOD mice that were tested positive for glycosuria for two consecutive weeks and blood glucose over 13.9mmol/L were diagnosed with type 1 diabetes and constituted the diabetic group (see Table 2.1, Chapter 2 for blood glucose levels). These mice have a severe destruction of pancreatic islets and almost no production of insulin; another group of NOD mice > 35 weeks of age with no signs of diabetes were considered to be protected from the disease [The checkpoints of type 1 diabetes in NOD mice were reviewed in (Andre et al. 1996)].

For this set of experiments, spleens were collected and processed into a single cell suspension (Section 2.5) and $2x10^6$ cells were cultured for 24h with different stimulants: Lipopolysaccharide (LPS) activates cells through Toll-like Receptor (TLR) 4 and is the main stimulant described in the literature to enrich for IL-10-producing B cells (Yanaba et al. 2009); CpG are oligonucleotides, non-methylated DNA common in bacteria, which act via TLR-9 and have previously been studied for their ability to induce B cells to produce IL-10 (Mion et al. 2014). Here, CpG was studied alone or associated with anti-CD40 (anti-CD40); CD40 is a co-stimulatory receptor in B cells, activated by CD40L, which is found on T cells, and can enhance the production of cytokines (Mauri et al. 2003). Spleen cells were also cultured with no addition of stimulant (unstimulated). All cells in culture received PMA, ionomycin and monensin 3h prior to the staining: the first two to boost cell activation and the latter to avoid cytokine release

into the supernatant. The choice of the stimulants was based on previous B cell studies and the concentrations were chosen after preliminary titration experiments, performed previously in the lab. To study both inflammatory and anti-inflammatory effects, the cytokines selected were IL-6 (inflammatory) and IL-10, TGF-β (both regulatory).

The putative regulatory subsets were divided into panels, as described in Table 3.2.

Each group displayed in the graphs in chapter 3 consisted of 5-10 mice pooled of at least two independent observations (two repetitions).

Table 3.2 Division of antibodies in 3 panels for cytokine production evaluation in B cells

Panel 1	Panel 2	Panel 3
Live-Dead Dye (LD): eF506	Live-Dead Dye (LD): eF506	Live-Dead Dye (LD): eF506
CD3: PE	CD3: PE	CD3: PE
CD19: APC e780	CD19: APC e780	CD19: APC e780
IL-10 PerCP Cy5.5	IL-10 PerCP Cy5.5	IL-10 PerCP Cy5.5
TGF-β: BV421	TGF-β: BV421	TGF-β: BV421
IL-6: APC	IL-6: APC	IL-6: APC
CD21: FITC	CD1d: FITC	CD24: FITC
CD23: PeCy7	CD5: PeCy7	CD38: PeCy7

Figure 3.1 provides a schematic view of the complex and layered set of data presented next, to clarify the groups and conditions used.

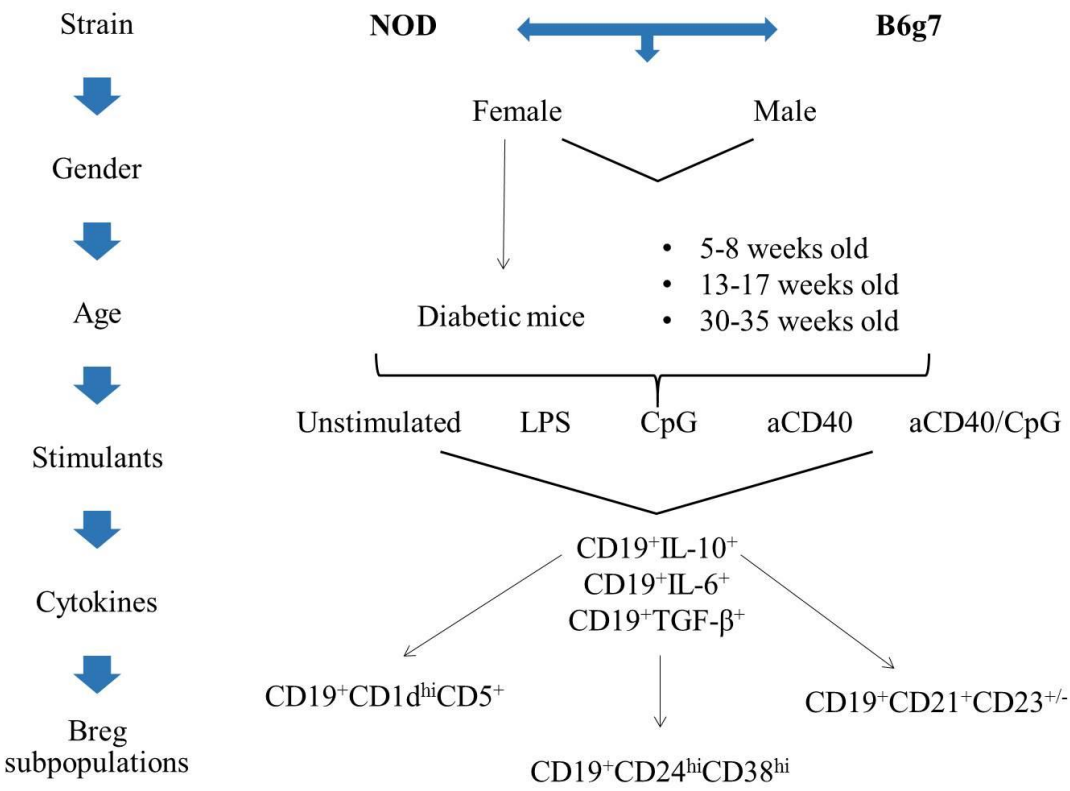

Figure 3.1 Schematic representation of the experimental design for the cytokine production evaluation. NOD mice were compared to a non-diabetes prone mouse strain called $B6^{g7}$. Variations in B cells with gender were also evaluated, as well as the influence of the age of the mice, considering the kinetics of the disease in NOD mice. Spleen cells were cultured for 24h with different stimulants and examined for IL-10, TGF-β and IL-6 production by CD19 positive cells. Finally, the contribution of regulatory B cell subsets to cytokine production by the whole B cell population was investigated.

The gating strategy for this section is illustrated in Figure 3.2. The production of cytokines was determined as the percentage of $CD19^+$ B cell population that was also positive for intracellular IL-6, TGF-β or IL-10 (Figure 3.2e). As the cytokines were present in the three panels (Table 3.2), each individual point shown in the graphs were calculated as an average of these 3 technical replicates.

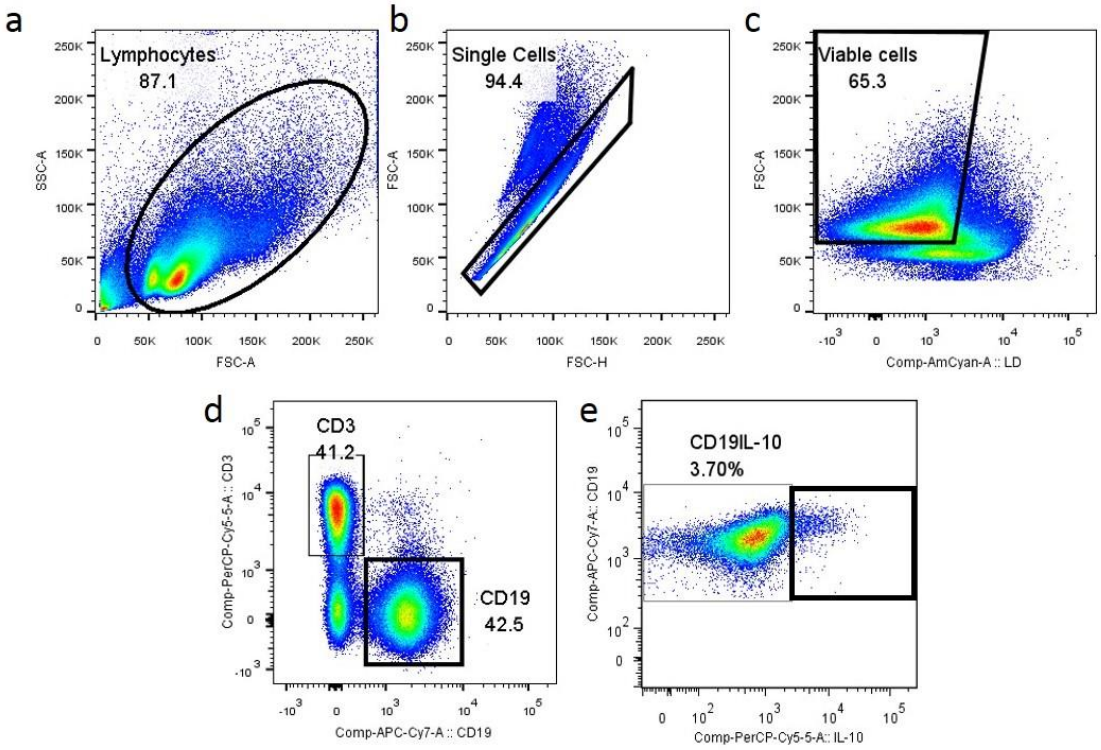

Figure 3.2 Example of gating of flow cytometric plots used for the cytokine production analysis. Spleens from NOD and B6^{g7} mice were collected, erythrocytes were lysed, cells were counted and left in culture with or without stimulants for 24h. Surface markers and intracellular cytokines were examined by flow cytometry. All analysis presented in this and the next chapters proceeded, as follows: (a) determination of lymphocytes by size and granulation, (b) exclusion of doublets and (c) exclusion of dead cells, which were positive for the live/dead dye, and (d) finally discrimination between T cells (CD3) and B cells (CD19). For every sample, 30,000 CD19^{+} cells were acquired. In (e) one example of how the IL-10-producing-B cells were gated can be observed. TGF-β and IL-6 followed this same analysis and the gates were established based on isotype controls – Figure A1, in the appendix.

3.2.1 IL-6-producing B cells

3.2.1.1 Unstimulated, LPS and anti-CD40-stimulated B cells

IL-6 was the pro-inflammatory cytokine examined in this study. However the percentage of IL-6-producing B cells was very low or undetectable in all groups for unstimulated cell cultures (Figures 3.3a and b) and when cells were stimulated with LPS (Figures 3.3 c and d) and anti-CD40 (Figures 3.3 e and f).

3.2.1.2 CpG-stimulated B cells

Stimulation with CpG activated B cells to produce IL-6. Female mice, both NOD and $B6^{g7}$, had increasing percentages of IL-6-producing B cells over time (NOD mice: young 9.4%; intermediate 12%; protected 15.5% and diabetic 19.3%. $B6^{g7}$ mice: young 14.9%; intermediate 23.6% and 30-35 w.o. 17.6%), as observed in Figure 3.4a. B cells from male mice behaved differently when compared between themselves or with female mice. The production of IL-6 by B cells from NOD male mice showed a significant increase from young to intermediate groups, 11.6% to 19.3% respectively, and returned to 12.6% in older NOD mice (Figure 3.4b). On the other hand, the frequency of $CD19^{+}IL\text{-}6^{+}$ cells significantly decreased in male $B6^{g7}$ mice over time (24.5% in young mice to 8.4% in 30-35 week old mice).

3.2.1.3 anti-CD40/CpG-stimulated B cells

The combination of CpG and anti-CD40 produced an interesting synergistic effect in the stimulation of B cells to produce IL-6. Although anti-CD40 alone did not induce $CD19^{+}IL\text{-}6^{+}$ cells, when added in culture with CpG, IL-6-producing B cells were increased compared to CpG alone, a result not seen for the anti-inflammatory cytokines (described next).

In both female mouse strains (Figure 3.5a), the frequency of IL-6 producing B cells increased with age (NOD young: 16.4%; NOD protected: 32% and diabetic: 35%) although the percentages were higher in female $B6^{g7}$ mice (young: 34%; 30-35 week old: 46.5%). The percentage of $CD19^{+}IL\text{-}6^{+}$ cells in young male mice was significantly higher in $B6^{g7}$ mice, when compared to NOD mice (29% versus 19%, respectively), this observation was reversed when mice were 30-35 weeks old and the frequency of IL-6 producing B cells in male NOD mice (31%) was higher than the frequency in male $B6^{g7}$ mice (22.9%), as illustrated in Figure 3.5b.

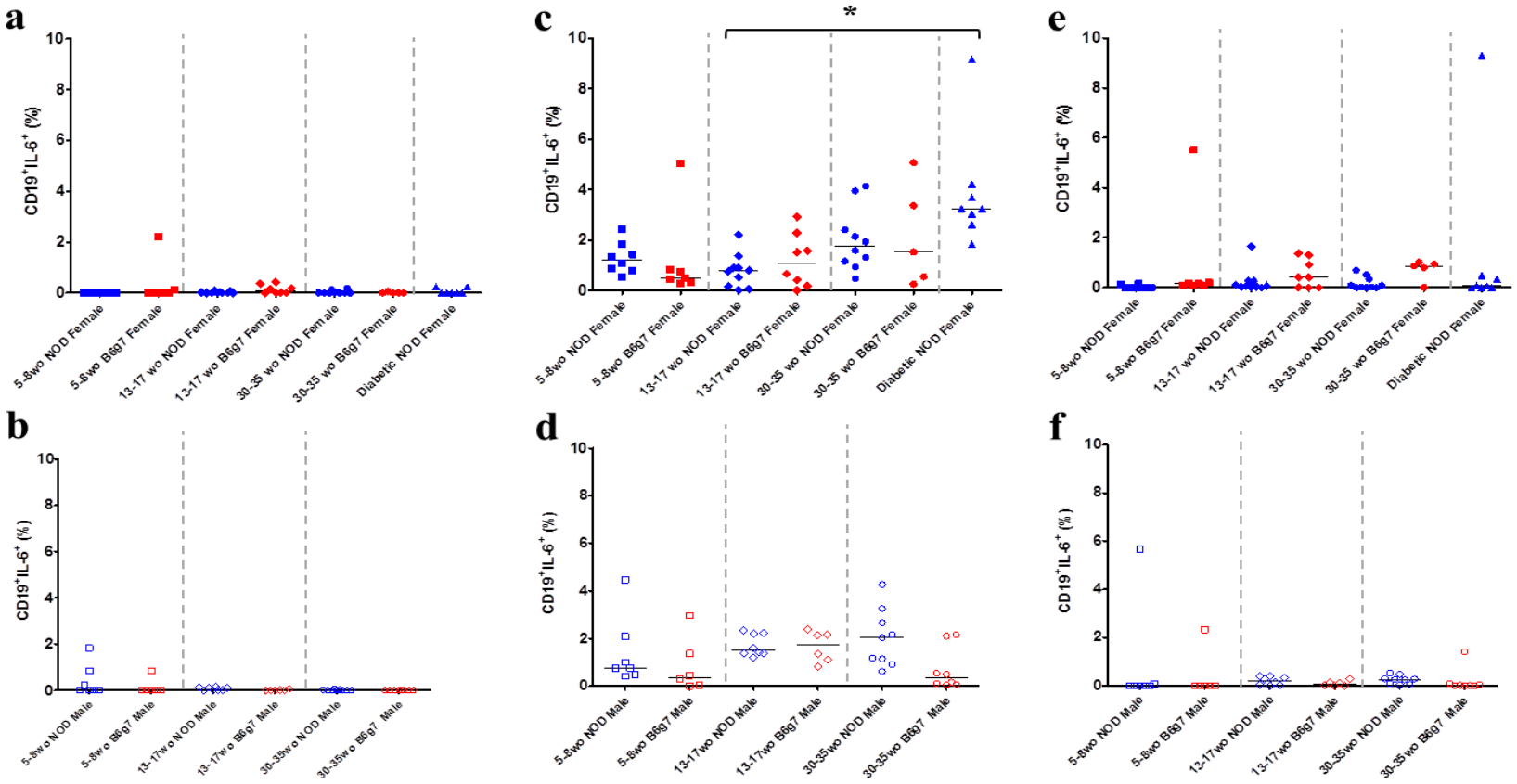

Figure 3.3 Frequency of IL-6 production by unstimulated B cells, B cells stimulated with LPS or anti-CD40. Spleens from male and female NOD and B6g7 mice were collected, erythrocytes were lysed and removed and spleen cells were cultured for 24h with no stimulants or LPS or anti-CD40; PMA, ionomycin and monensin were added for the last 3 hours and then cells were stained for extracellular markers and intracellular IL-6. Samples were examined by flow cytometry and tested with Kruskal-Wallis, followed by Dunn's post hoc test and Bonferroni correction. Filled symbols represent female mice of both strains (a, c & e) and non-filled symbols represent male mice (b, d & f). Each symbol represents an individual mouse and a median bar is shown. n = 5-10 and at least 2 repetitions for each group.

* $p < 0.05$; ** $p < 0.01$ and *** $p < 0.001$

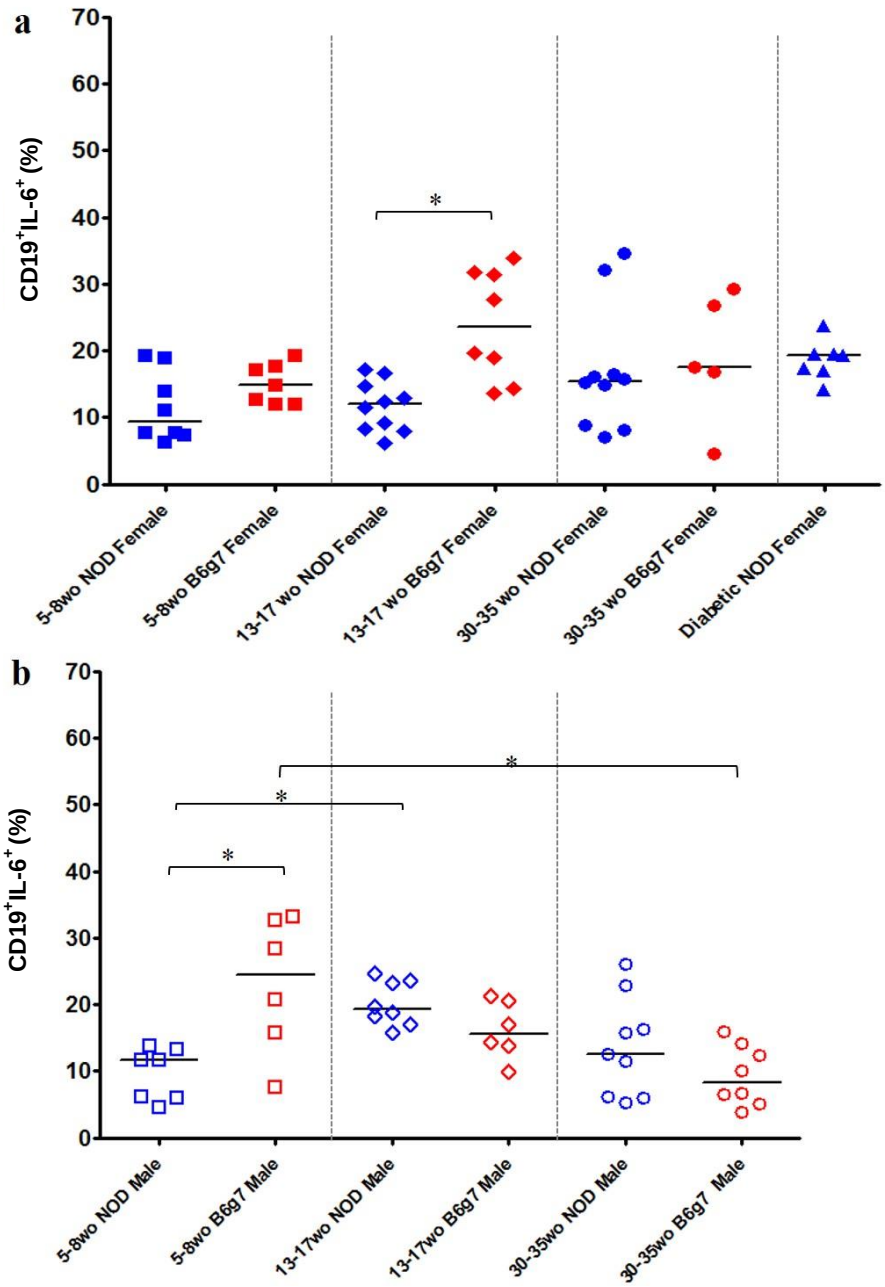

Figure 3.4Frequency of IL-6-producing B cells stimulated with CpG. Spleens from male and female NOD and B6^{g7} mice were collected, erythrocytes were lysed and removed and spleen cells were cultured for 24h with CpG; PMA, ionomycin and monensin were added for the last 3 hours and then cells were stained for extracellular markers and intracellular IL-6. Samples were examined by flow cytometry and tested with Kruskal-Wallis, followed by Dunn's post hoc test and Bonferroni correction. Filled symbols represent female mice of both strains (a) and open symbols represent male mice (b). Each symbol represents an individual mouse and a median bar is shown.

n = 5-10 and at least 2 repetitions for each group.

* $p < 0.05$; ** $p < 0.01$ and *** $p < 0.001$

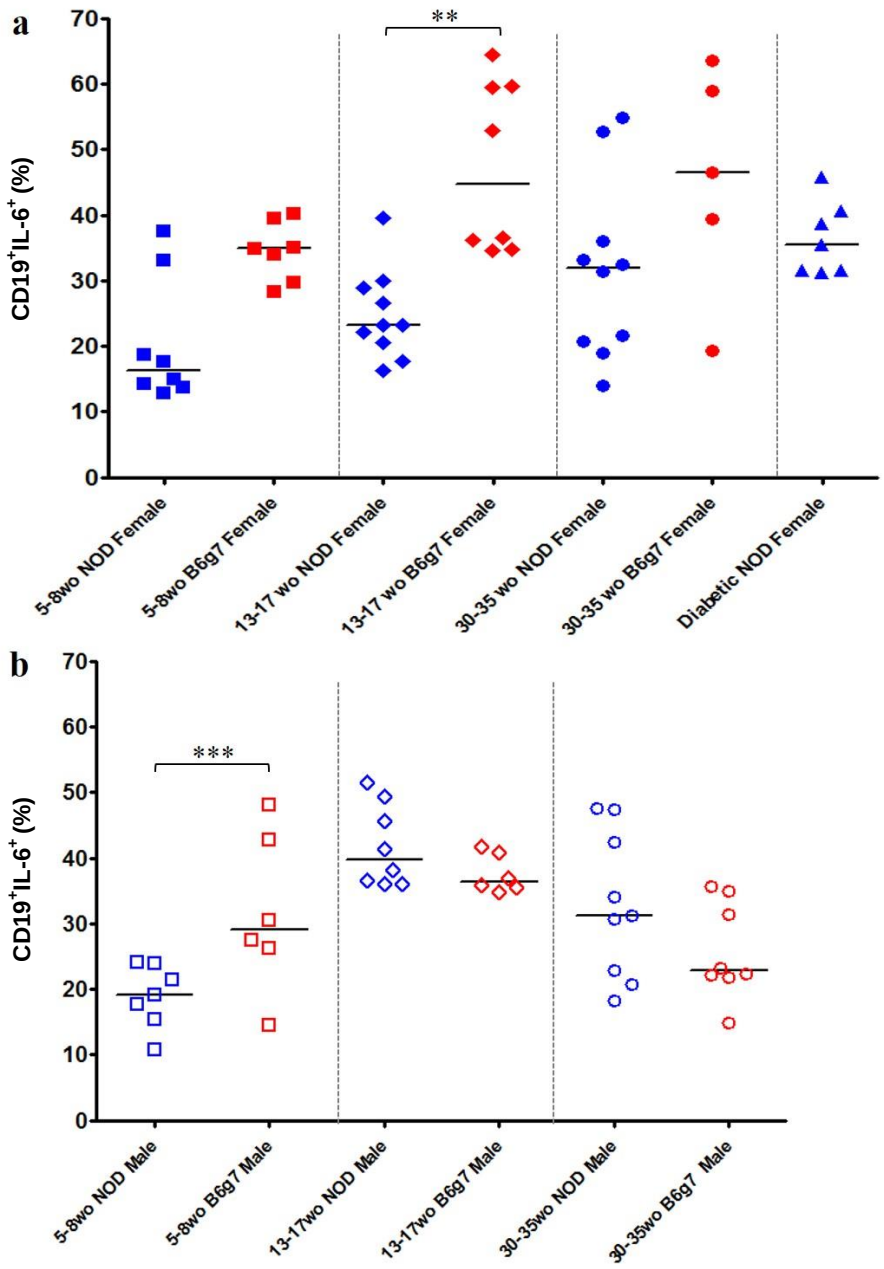

Figure 3.5 Frequency of IL-6-producing B cells stimulated with anti-CD40 and CpG. Spleens from male and female, NOD and B6^{g7} mice were collected, erythrocytes were lysed and removed and spleen cells were cultured for 24h with anti-CD40 and CpG; PMA, ionomycin and monensin were added for the last 3 hours and then cells were stained for extracellular markers and intracellular IL-6. Samples were examined by flow cytometry and tested with Kruskal-Wallis, followed by Dunn's post hoc test and Bonferroni correction. Filled symbols represent female mice of both strains (b). Each symbol represents an individual mouse and a median bar is shown.

n = 5-10 and at least 2 repetitions for each group.

* $p < 0.05$; ** $p < 0.01$ and *** $p < 0.001$

3.2.1.4 Summary

In summary, the production of IL-6 by B cells is highly determined by the nature of the stimulants added to the cell culture. B cells do not produce IL-6 when the cells are unstimulated or stimulated with LPS or anti-CD40 alone. However, when anti-CD40 is added in combination with CpG, a synergistic effect is observed. The percentages of B cells producing IL-6 in female mice increased with age and were higher in $B6^{g7}$ mice when compared to NOD mice. Results in male mice were more heterogeneous, but in general, the frequency peaked in intermediate NOD male mice and decreased with age in male $B6^{g7}$ mice.

There were no significant differences in the percentages of IL-6-producing B cells in 30-35 w.o. and diabetic NOD mice, which suggests the protection seen in these mice was not due to impairment in the production of this inflammatory cytokine.

3.2.2 TGF-β-producing B cells

3.2.2.1 Unstimulated B cells

The next cytokine studied was TGF-β. Frequency of TGF-β-producing B cells was less than 1.5% for all the groups in unstimulated cell cultures, as presented in Figures 3.6a and 3.6b. Although there were some statistically significant differences, the percentages were very small and the biological impact is questionable.

3.2.2.2. LPS-stimulated B cells

The increased percentage of $CD19^{+}TGF\text{-}\beta^{+}$ cells in female NOD mice was related to diabetes, but also with age (intermediate: 0.5%; protected: 4.2% and diabetic: 5.6%) and age-related increase was also seen in female $B6^{g7}$ mice, from young (1.8%) to 30-35 week old mice (3.9%, Figure 3.7a). Male $B6^{g7}$ mice had the same increasing percentage of TGF-β-producing B cells seen in female mice, increasing from 5% in young to 8.6% in 30-35 w.o. male mice. On the other hand, as presented in Figure 3.7b, TGF-β-producing B cells in male NOD mice reduced with age, from 9.8% in young mice to 2.6% in protected male NOD mice.

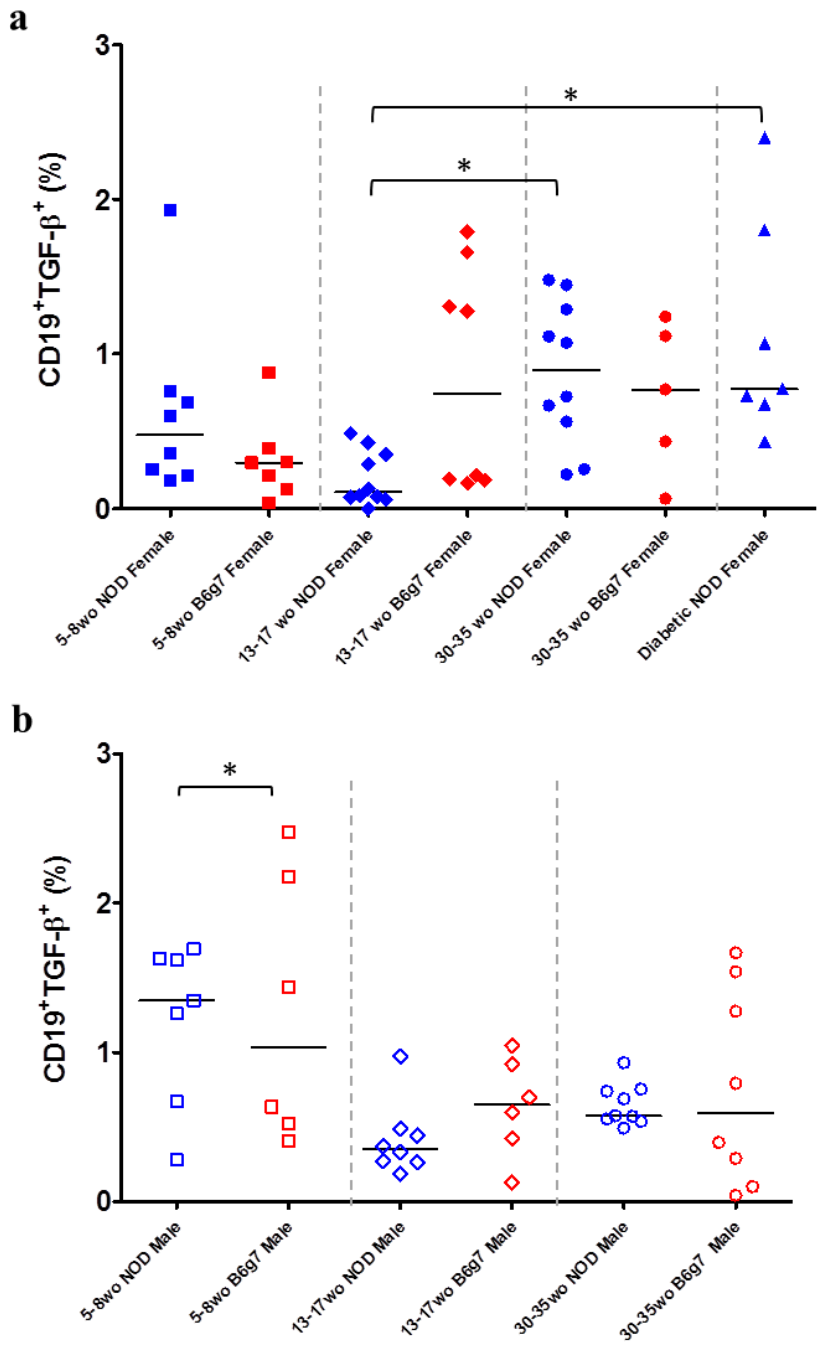

Figure 3.6 Frequency of TGF-β production in unstimulated B cells. Spleens from male and female NOD and B6^{g7} mice were collected, erythrocytes were lysed and removed and spleen cells were cultured for 24h with no stimulants; PMA, ionomycin and monensin were added for the last 3 hours and then cells were stained for extracellular markers and intracellular TGF-β. Samples were examined by flow cytometry and tested with Kruskal-Wallis, followed by Dunn's post hoc test and Bonferroni correction. Filled symbols represent female mice of both strains (a) and open symbols represent male mice (b). Each symbol represents an individual mouse and a median bar is shown.

n = 5-10 and at least 2 repetitions for each group.

* $p < 0.05$; ** $p < 0.01$ and *** $p < 0.001$

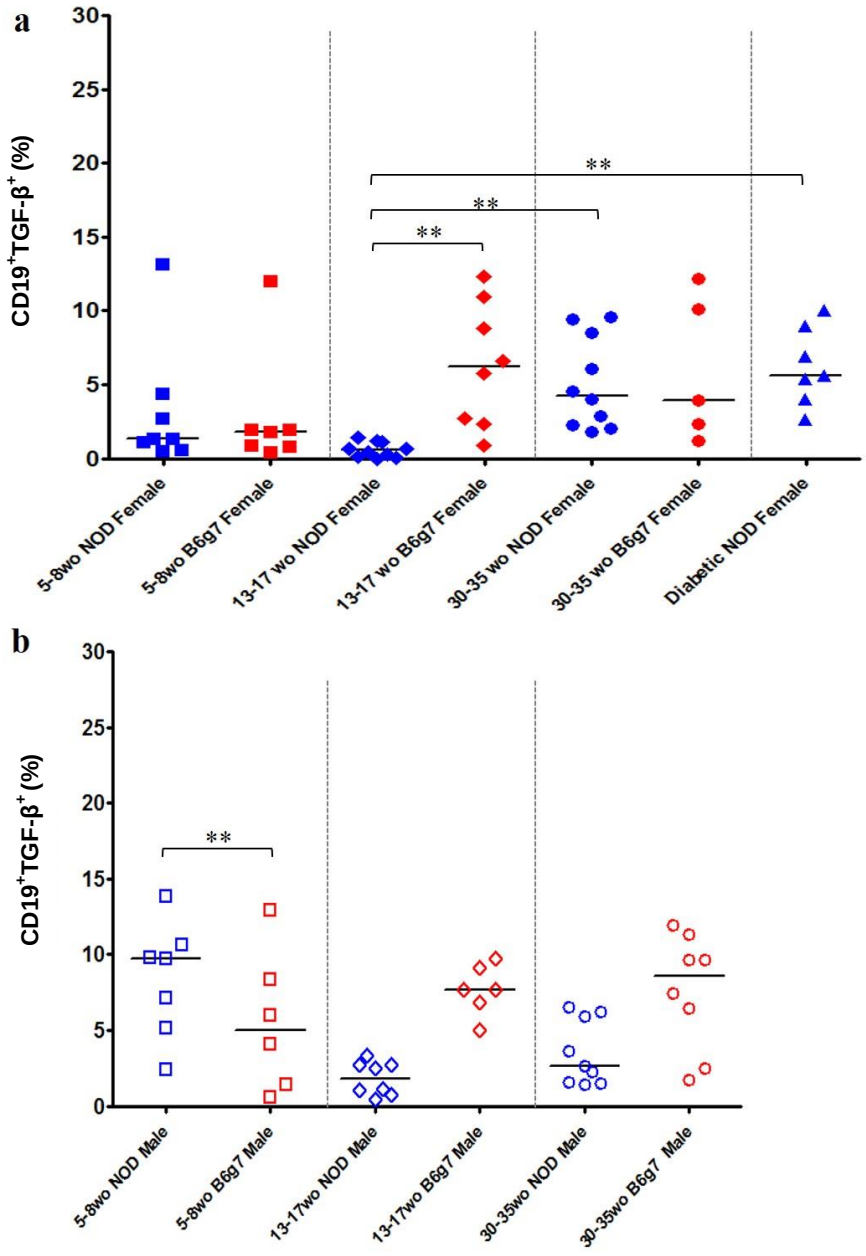

Figure 3.7 Frequency of TGF-β-producing B cells stimulated with LPS. Spleens from male and female NOD and B6^{g7} mice were collected, erythrocytes were lysed and removed and spleen cells were cultured for 24h with LPS; PMA, ionomycin and monensin were added for the last 3 hours and then cells were stained for extracellular markers and intracellular TGF-β. Samples were examined by flow cytometry and tested with Kruskal-Wallis, followed by Dunn's post hoc test and Bonferroni correction. Filled symbols represent female mice of both strains (a) and open symbols represent male mice (b). Each symbol represents an individual mouse and a median bar is shown.

n = 5-10 and at least 2 repetitions for each group.

* $p < 0.05$; ** $p < 0.01$ and *** $p < 0.001$

3.2.2.3 anti-CD40-stimulated B cells

Results for B cells cultured with anti-CD40 were consistent with those seen with LPS stimulation. In both female strains (Figure 3.8a), the frequencies of $CD19^{+}TGF\text{-}\beta^{+}$ cells increased with age and this trend was also followed by diabetic NOD mice (NOD mice: young 1.3%; intermediate 0.9%; protected 4.4% and diabetic 5.9%. $B6^{g7}$: young 1.7%; intermediate 6% and 30-35 weeks old 5.1%). Again, similar to LPS stimulation, B cells from young male NOD mice were able to produce TGF-β (7.6%) and this percentage decreased (2.5%) in old male NOD mice (Figure 3.8b). In contrast, male $B6^{g7}$ mice presented an increased frequency of TGF-β-producing B cells, increasing from 3.4% in young to 6.5% in 30-35 week old mice.

3.2.2.4 CpG-stimulated B cells

Figure 3.9a illustrates the variations in $CD19^{+}TGF\text{-}\beta^{+}$ cells from female mice, when cell cultures were stimulated with CpG. One interesting finding was that $B6^{g7}$ mice responded better to CpG than NOD mice. However, both strains showed increased percentages of TGF-β-producing B cells with age, in response to CpG. The percentages in female NOD mice varied less (young: 0.8%; protected: 2.3% and diabetic: 2.9%) than $B6^{g7}$ mice (young: 1.5%; 30-35 w.o: 6%). The strain difference was more pronounced in older male mice (Figure 3.9b). Although both male NOD and $B6^{g7}$ mice had decreased percentages of TGF-β-producing B cells with age in response to CpG, male $B6^{g7}$ mice started higher and were more variable than male NOD mice (11.6% versus 4.1%, respectively) and were still higher when mice were 30-35 weeks old ($B6^{g7}$: 7.6%; NOD: 1.1%).

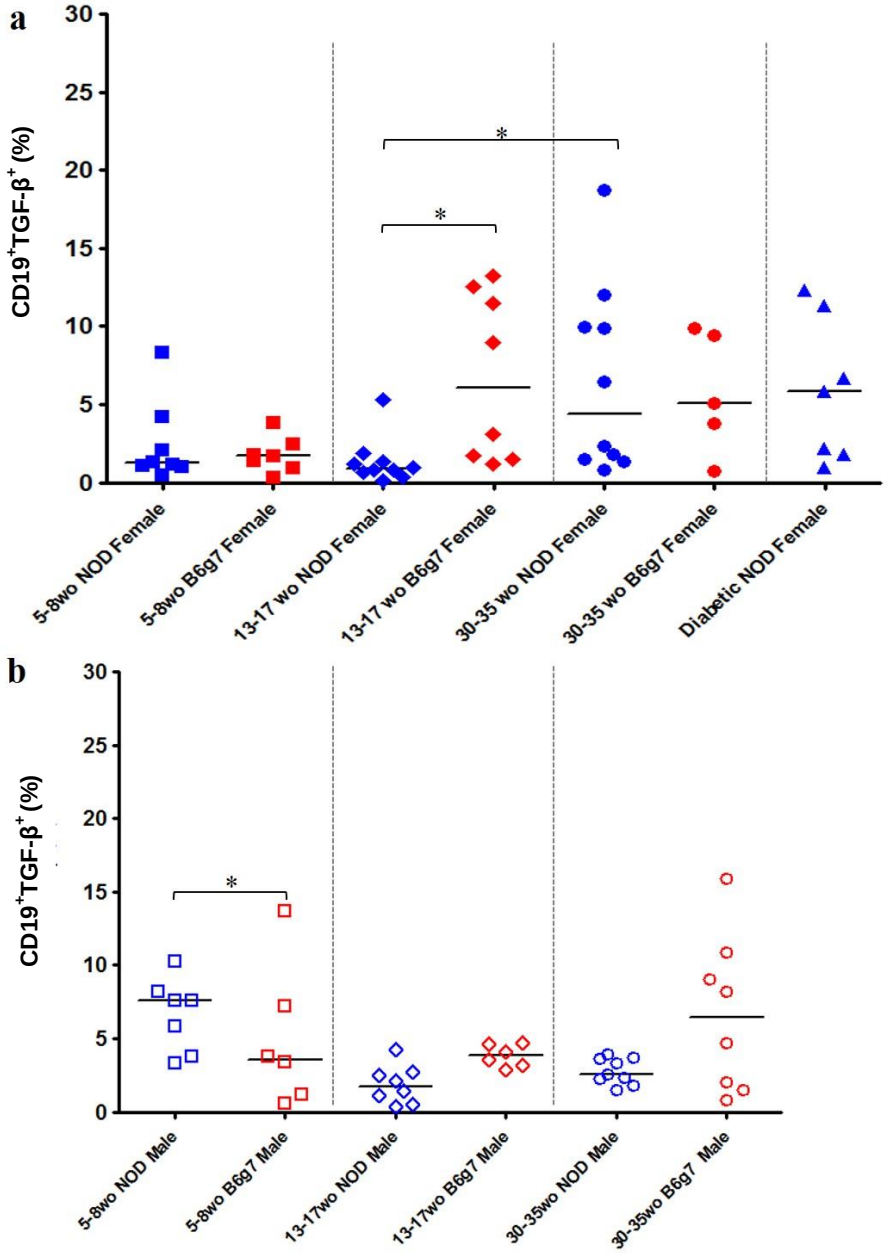

Figure 3.8 Frequency of TGF-β-producing B cells stimulated with anti-CD40. Spleens from male and female, NOD and B6^{g7} mice were collected, erythrocytes were lysed and removed and spleen cells were cultured for 24h with anti-CD40; PMA, ionomycin and monensin were added for the last 3 hours and then cells were stained for extracellular markers and intracellular TGF-β. Samples were examined by flow cytometry and tested with Kruskal-Wallis, followed by Dunn's post hoc test and Bonferroni correction. Filled symbols represent female mice of both strains (a) and open symbols represent male mice (b). Each symbol represents an individual mouse and a median bar is shown.

n = 5-10 and at least 2 repetitions for each group.

* $p < 0.05$; ** $p < 0.01$ and *** $p < 0.001$

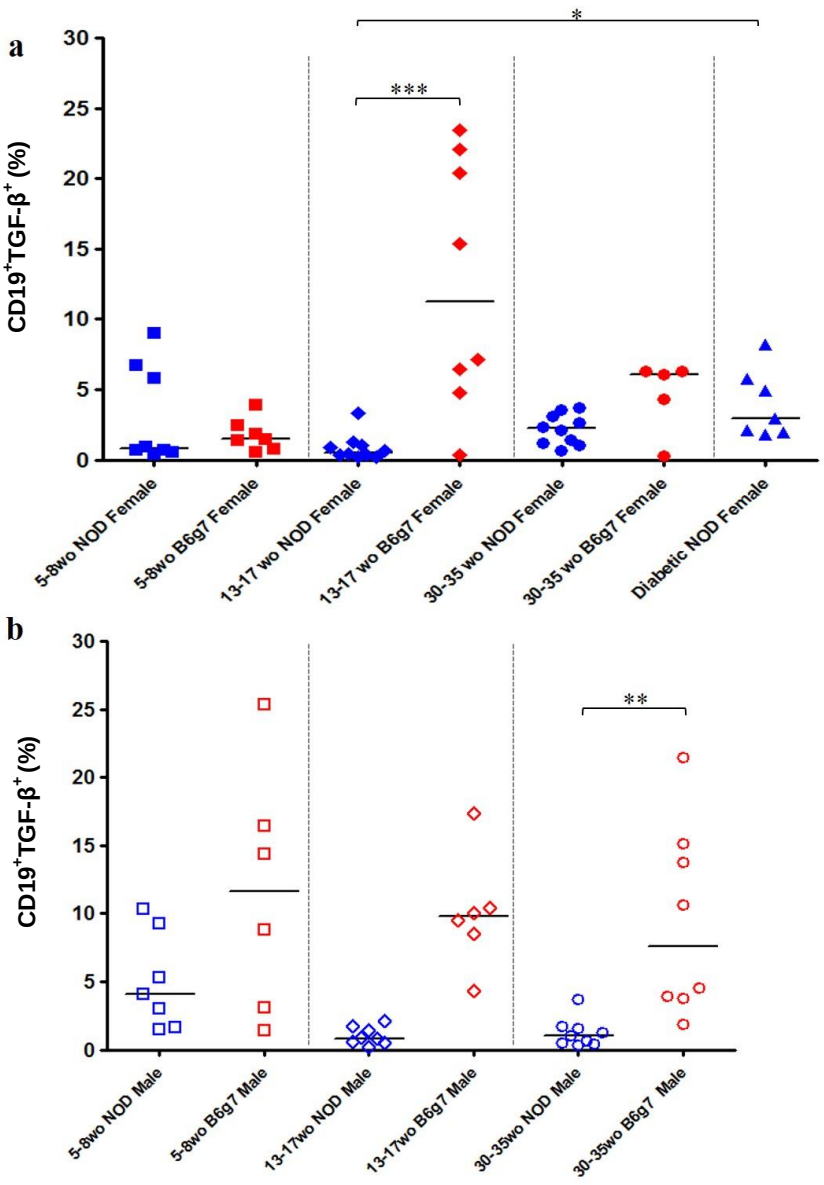

Figure 3.9 Frequency of TGF-β-producing B cells stimulated with CpG. Spleens from male and female NOD and B6^{g7} mice were collected, erythrocytes were lysed and removed and spleen cells were cultured for 24h with CpG; PMA, ionomycin and monensin were added for the last 3 hours and then cells were stained for extracellular markers and intracellular TGF-β. Samples were examined by flow cytometry and tested with Kruskal-Wallis, followed by Dunn's post hoc test and Bonferroni correction. Filled symbols represent female mice of both strains (a) and open symbols represent male mice (b). Each symbol represents an individual mouse and a median bar shown. n = 5-10 and at least 2 repetitions for each group.

* $p < 0.05$; ** $p < 0.01$ and *** $p < 0.001$

3.2.2.5 anti-CD40/CpG-stimulated B cells

Cell culture stimulation with both anti-CD40 and CpG did not further increase TGF-β production by B cells. The frequencies were, in fact, similar to CpG alone. Again, $B6^{g7}$ mice had higher percentages of $CD19^{+}TGF\text{-}\beta^{+}$ cells compared to NOD mice in both genders. In female mice, as seen in Figure 3.10a, the frequency of TGF-β production by B cells increased with age, being less in female NOD mice (young: 0.9%; protected: 1.4% and diabetic: 2.8%) compared with female $B6^{g7}$ mice (young: 0.9%; intermediate: 11.2% and 30-35w.o: 4%). In male NOD mice, a decrease in the frequency from young (3%) to protected mice (1%) was observed. Male $B6^{g7}$ mice did not have variation in the percentage of $CD19^{+}TGF\text{-}\beta^{+}$ cells over time (young: 4.3%; intermediate: 5.7% and 30-35 weeks old: 3.6%), as observed in Figure 3.10b.

3.2.2.6 Summary

In summary, TGF-β production was low in unstimulated B cells and cultures stimulated with LPS and anti-CD40 exhibited similar frequencies of $CD19^{+}TGF\text{-}\beta^{+}$ cells. There was no difference in the percentages of TGF-β-producing B cells between diabetic mice and protected female NOD mice. The difference between diabetic mice and the other healthy NOD groups is probably more associated with age than with the development of the disease. Male NOD mice presented a different dynamic and the percentages of $CD19^{+}TGF\text{-}\beta^{+}$ cells decreased with age.

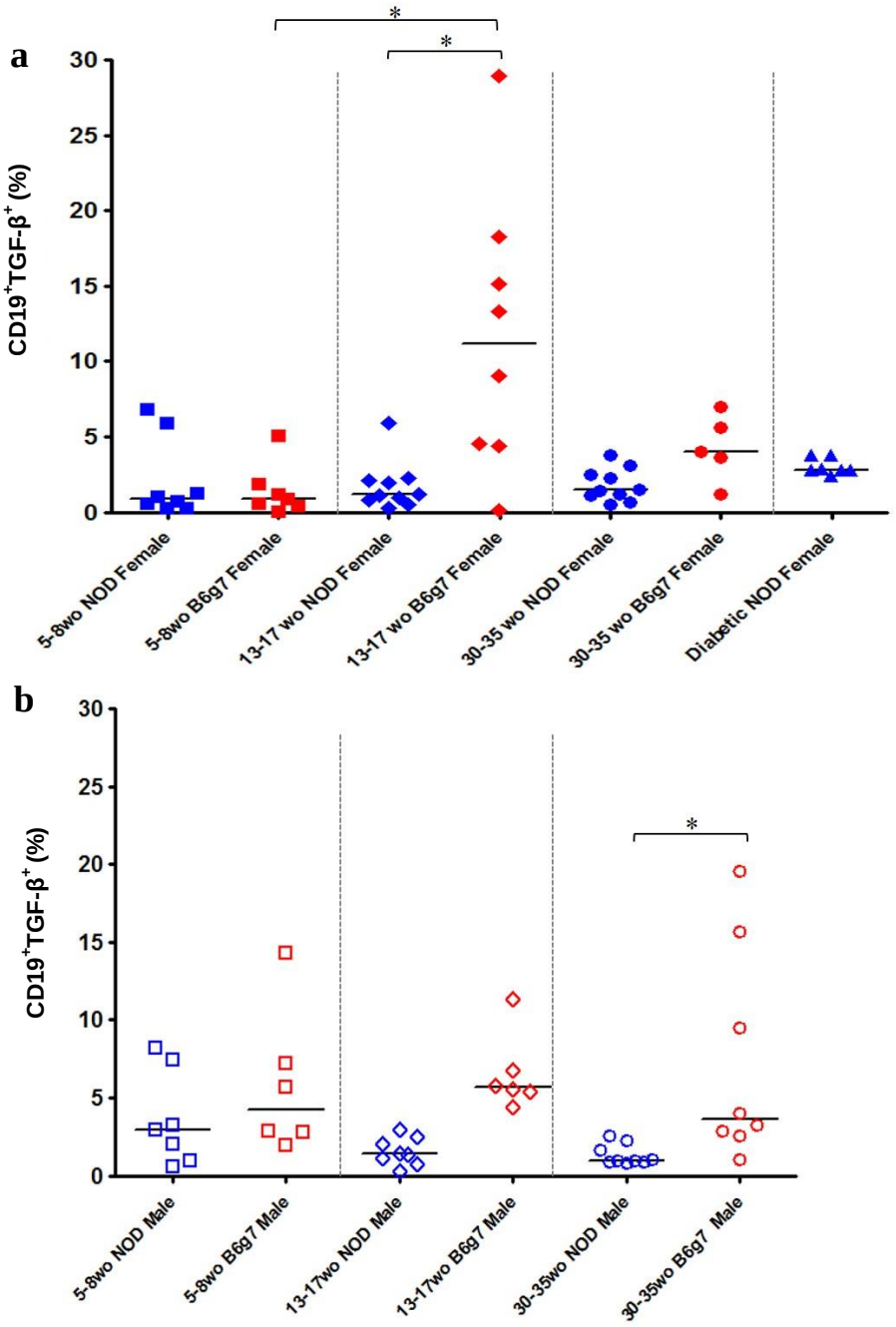

Figure 3.10 Frequency of TGF-β-producing B cells stimulated with anti-CD40 and CpG. Spleens from male and female NOD and B6^{g7} mice were collected, erythrocytes were lysed and removed and spleen cells were cultured for 24h with anti-CD40 and CpG; PMA, ionomycin and monensin were added for the last 3 hours and then cells were stained for extracellular markers and intracellular TGF-β. Samples were examined by flow cytometry and tested with Kruskal-Wallis, followed by Dunn's post hoc test and Bonferroni correction. Filled symbols represent female mice of both strains (a) and open symbols represent male mice (b). Each symbol represents an individual mouse and a median bar is shown.

n = 5-10 and at least 2 repetitions for each group.

* $p < 0.05$; ** $p < 0.01$ and *** $p < 0.001$

3.2.3 IL-10-producing B cells

3.2.3.1 Unstimulated B cells

Unstimulated B cells from the NOD mouse had more IL-10^+ B cells compared to $B6^{g7}$ B cells. There was a significant difference when female mice from both strains were compared at 30-35 weeks old ($p < 0.01$). Unstimulated B cells from diabetic NOD mice did not produce IL-10 and this was significantly different from other mice at all ages, as seen in Figure 3.11a. A significantly increased percentage of IL-10-producing B cells was found in NOD male mice and decreased percentage was seen in $B6^{g7}$ mice with age (0.7%; 4.6% and 4.5% in young, intermediate and protected NOD mice, respectively, compared to 1.9%, 0.06% and 0.9% in $B6^{g7}$ mice), in Figure 3.11b.

3.2.3.2 LPS-stimulated B cells

When the cells were stimulated with LPS, they showed a different pattern from TGF-β-producing B cells. Here, the percentage of IL-10^+ B cells from female protected NOD mice (11%) was significantly increased compared to NOD diabetic mice (5.8%; $p < 0.001$), as demonstrated in Figure 3.12a. The percentage of IL-10-producing B cells in female $B6^{g7}$ mice decreased with age (7.5% to 2.4%, from young to old, respectively). In male NOD mice (Figure 3.12b) the increase in the percentage of IL-10-producing B cells with age was even more accentuated (young: 4.9%; intermediate: 5.4% and protected: 12.4%). Male $B6^{g7}$ mice maintained the frequency of $CD19^+IL\text{-}10^+$ cells around 2-4%.

3.2.3.3 anti-CD40-stimulated B cells

As observed in Figure 3.13a, B cells from diabetic NOD mice, when stimulated with anti-CD40, had few IL-10-B cell producers (<1%). This frequency was significantly lower than the $CD19^+IL10^+$ cells at all other time-points in non-diabetic mice (young: $p < 0.01$; intermediate: $p < 0.01$ and protected mice: $p < 0.001$). A significant decrease of IL-10 producing B cells was found between young and 30-35 week old $B6^{g7}$ mice (7.7% versus 1.4%, respectively). Furthermore, a significant difference was found between protected/old female NOD mice and old $B6^{g7}$ mice. Figure 3.13b shows that B cells from male mice stimulated with anti-CD40 behaved very similarly as when they were stimulated with LPS. Once again, the frequency of $CD19^+IL\text{-}10^+$ cells significantly

increased with age in male NOD mice (young: 1.7%; intermediate: 4.6% and protected mice: 7.5%), while the frequency of $CD19^{+}IL\text{-}10^{+}$ cells in male $B6^{g7}$ mice remained low through young and intermediate groups, with a higher percentage in the 30-35 w.o. (young: 1.9%; intermediate: 0.6% and 30-35 w.o: 3.1%).

3.2.3.4 CpG-stimulated B cells

The next stimulant analysed was CpG (Figure 3.14). Interestingly, unlike LPS and anti-CD40, B cells from young female $B6^{g7}$ mice had a higher percentage of IL-10-producing B cells compared with young female NOD mice (16% versus 10.6%, respectively). When female mice were 13-17 weeks old, this frequency decreased in both strains (11.6%: 4.9%, $B6^{g7}$: NOD mice). However, at 30-35 weeks old, female NOD mice had a significantly higher percentage of IL-10 producing B cells (10.3%), when compared to female $B6^{g7}$ mice (1.4%). The percentage of $CD19^{+}IL\text{-}10^{+}$ cells in diabetic mice in response to CpG was 4.7%, similar to the intermediate group (Figure 3.14a). These differences were not seen in males, which had a similar percentage of IL-10-producing B cells between strains in young (NOD: 5.3%; $B6^{g7}$: 5.4%) and intermediate groups (NOD: 3.9%; $B6^{g7}$: 5.5%). However, in mice 30-35 weeks old, the percentage of $CD19^{+}IL\text{-}10^{+}$ was significantly higher ($p < 0.01$) in NOD mice (8.7%) than in male $B6^{g7}$ mice (2.8%). These results are shown in Figure 3.14b.

3.2.3.5 anti-CD40/CpG-stimulated B cells

Lastly, combining CpG and anti-CD40 only produces an additive effect in the production of IL-10 by B cells in female $B6^{g7}$ mice. For both genders of NOD and male $B6^{g7}$ mice, the trend was similar to when cells were stimulated with CpG alone. Figure 3.15a illustrates the significantly decreasing frequency of $CD19^{+}IL\text{-}10^{+}$ cells in female young $B6^{g7}$ mice over time (young: 21.2%; intermediate: 14.9% and 30-35 w.o. mice: 1.5%). Female NOD mice, on the other hand, had an increased frequency of IL-10-producing B cells in protected mice, unless they were diabetic (young: 6.1%; protected: 8% and diabetic: 3.2%). In male NOD mice, the percentage of $CD19IL\text{-}10^{+}$ cells increased with age (young: 2.9%; protected: 5.2%), while $CD19^{+}IL\text{-}10^{+}$ cells from male young $B6^{g7}$ increased (1.7%) compared to mice that were 13-17 weeks old (5.6%) and decreased again (1.6%) in 30-35 week old $B6^{g7}$ mice (Figure 3.15b).

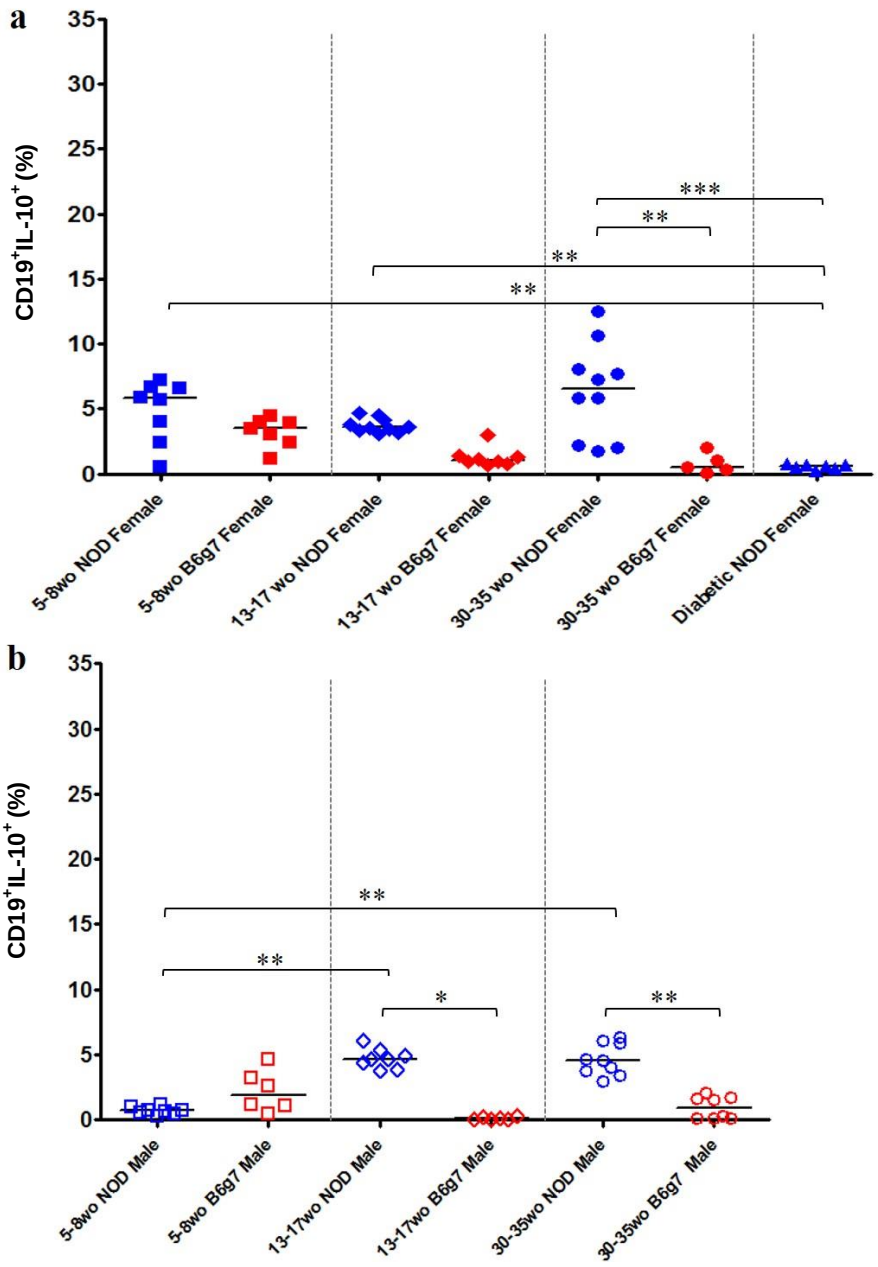

Figure 3.11 Frequency of IL-10 production in unstimulated B cells. Spleens from male and female NOD and B6^{g7} mice were collected, erythrocytes were lysed and removed and spleen cells were cultured for 24h with no stimulant; PMA, ionomycin and monensin were added for the last 3 hours and then cells were stained for extracellular markers and intracellular IL-10. Samples were examined by flow cytometry and tested with Kruskal-Wallis, followed by Dunn's post hoc test and Bonferroni correction. Filled symbols represent female mice of both strains (a) and open symbols represent male mice (b). Each symbol represents an individual mouse and a median bar is shown.

n = 5-10 and at least 2 repetitions for each group.

* $p < 0.05$; ** $p < 0.01$ and *** $p < 0.001$

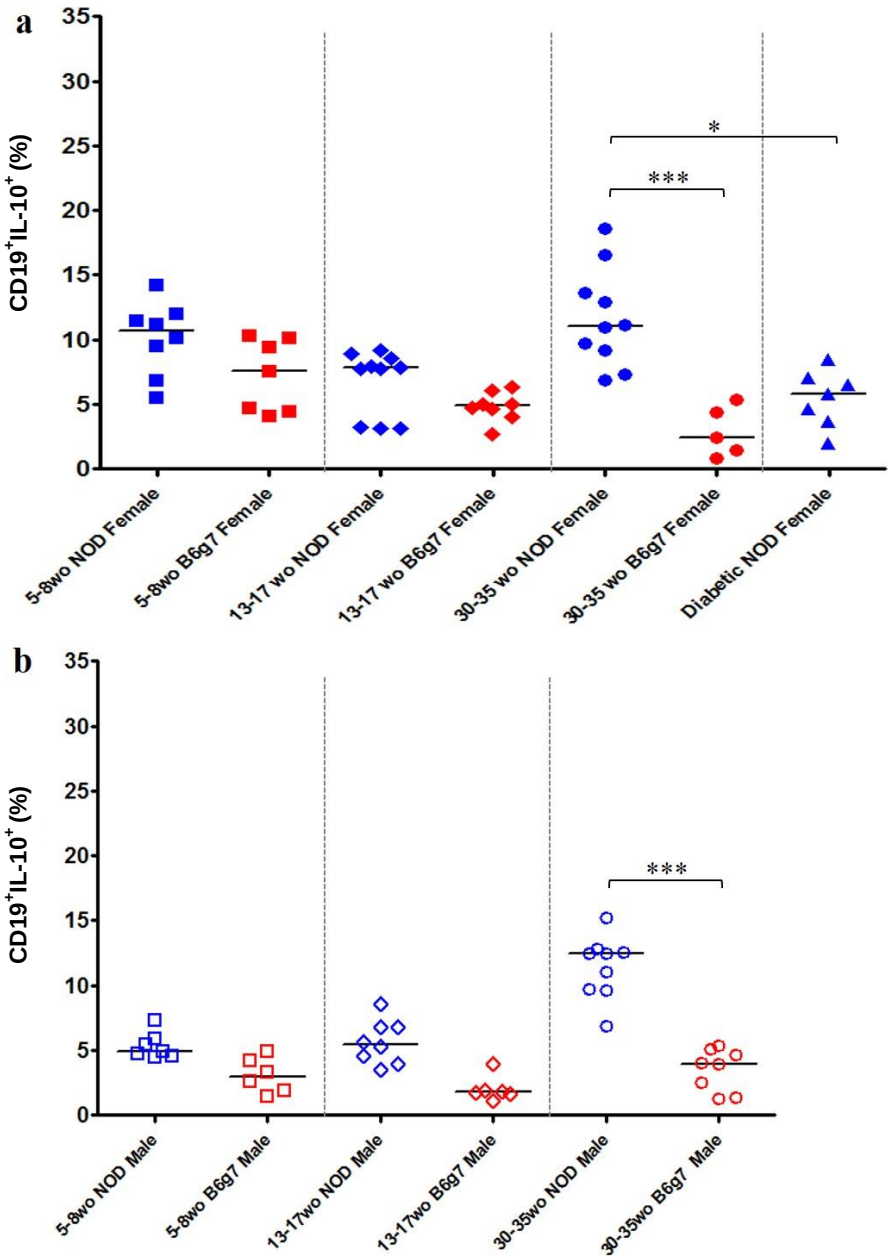

Figure 3.12 Frequency of IL-10-producing B cells stimulated with LPS. Spleens from male and female NOD and B6^{g7} mice were collected, erythrocytes were lysed and removed and spleen cells were cultured for 24h with LPS; PMA, ionomycin and monensin were added for the last 3 hours and then cells were stained for extracellular markers and intracellular IL-10. Samples were examined by flow cytometry and tested with Kruskal-Wallis, followed by Dunn's post hoc test and Bonferroni correction. Filled symbols represent female mice of both strains (a) and open symbols represent male mice (b). Each symbol represents an individual mouse and a median bar is shown.

n = 5-10 and at least 2 repetitions for each group.

* $p < 0.05$; ** $p < 0.01$ and *** $p < 0.001$

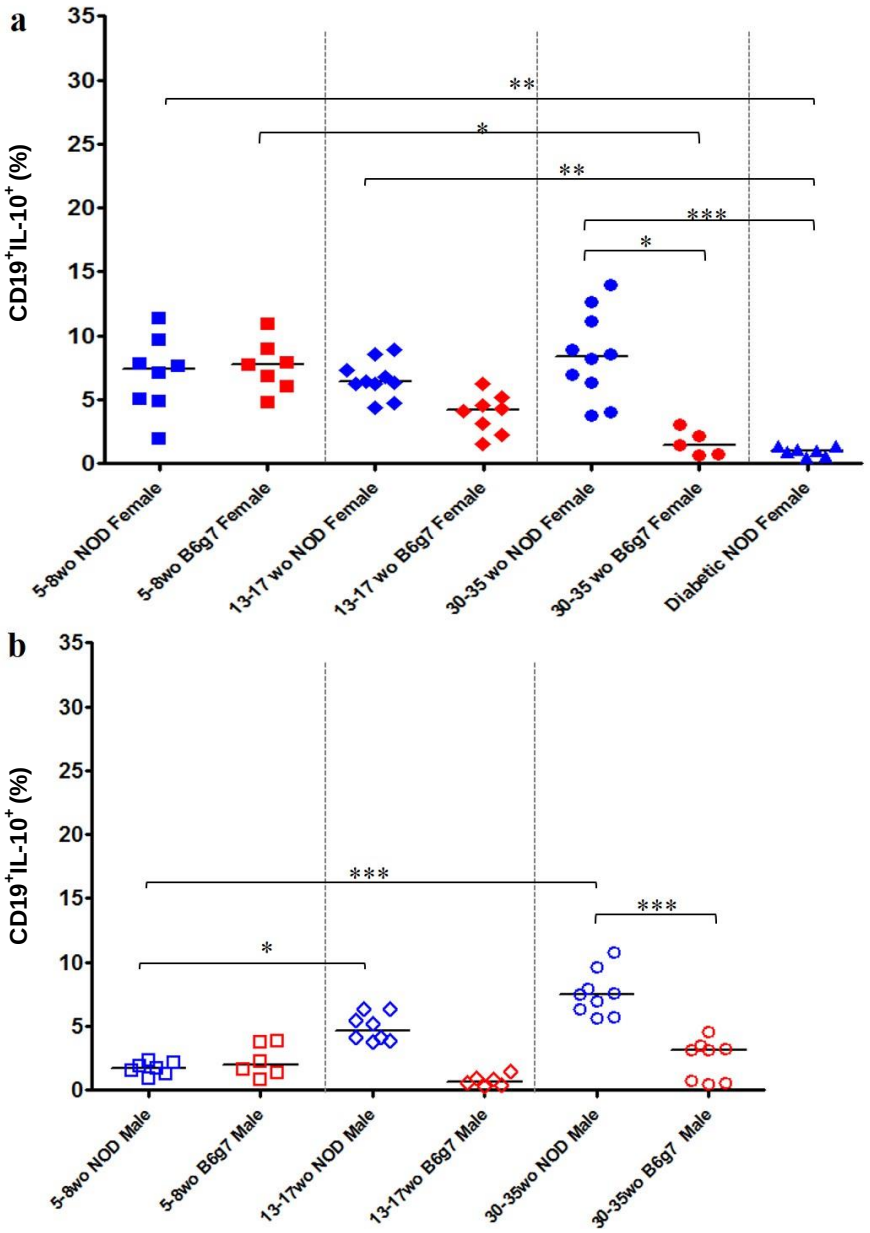

Figure 3.13 Frequency of IL-10-producing B cells stimulated with anti-CD40. Spleens from male and female NOD and B6^{g7} mice were collected, erythrocytes were lysed and removed and spleen cells were cultured for 24h with anti-CD40; PMA, ionomycin and monensin were added for the last 3 hours and then cells were stained for extracellular markers and intracellular IL-10. Samples were examined by flow cytometry and tested with Kruskal-Wallis, followed by Dunn's post hoc test and Bonferroni correction. Filled symbols represent female mice of both strains (a) and open symbols represent male mice (b). Each symbol represents an individual mouse and a median bar is shown.

n = 5-10 and at least 2 repetitions for each group.

* $p < 0.05$; ** $p < 0.01$ and *** $p < 0.001$

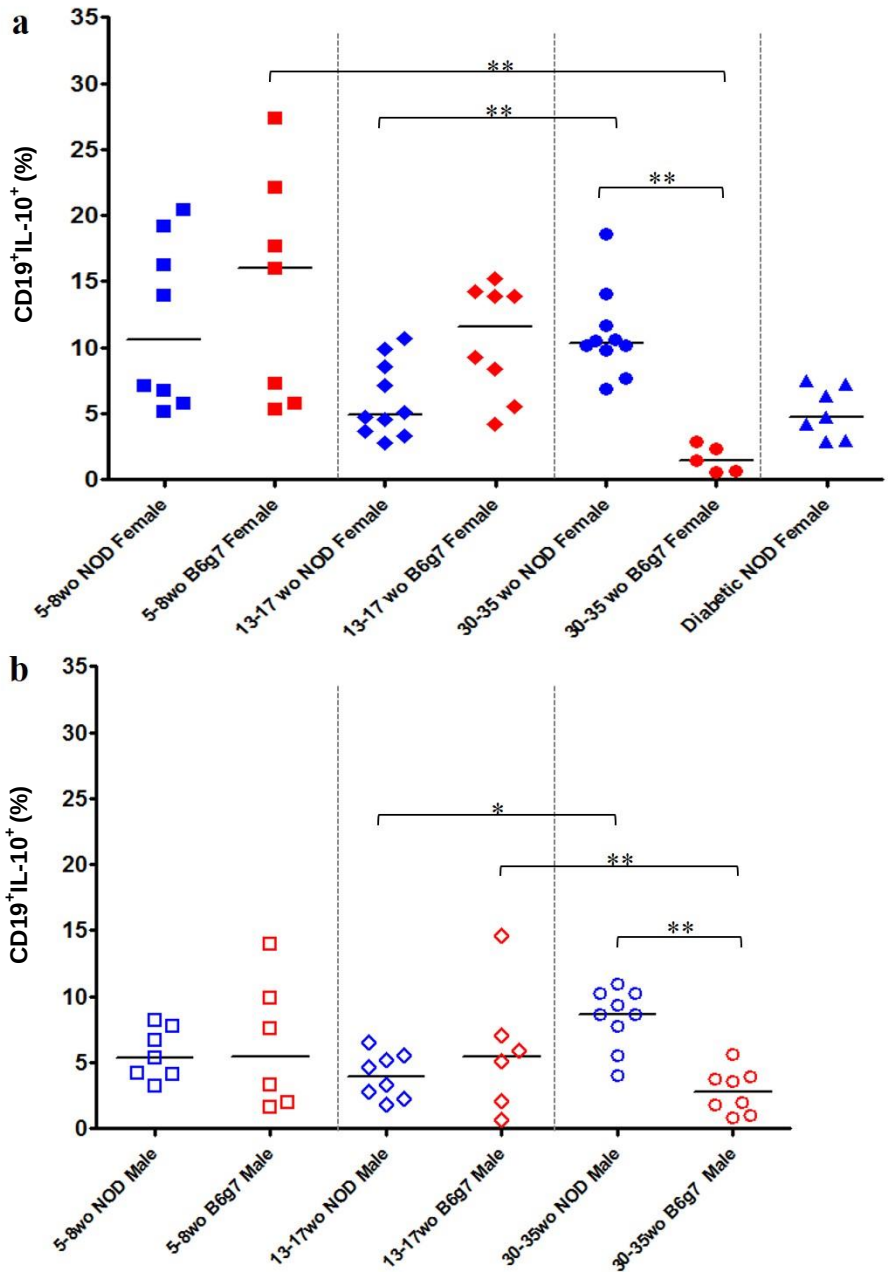

Figure 3.14 Frequency of IL-10-producing B cells stimulated with CpG. Spleens from male and female NOD and B6^{g7} mice were collected, erythrocytes were lysed and removed and spleen cells were cultured for 24h with CpG; PMA, ionomycin and monensin were added for the last 3 hours and then cells were stained for extracellular markers and intracellular IL-10. Samples were examined by flow cytometry and tested with Kruskal-Wallis, followed by Dunn's post hoc test and Bonferroni correction. Filled symbols represent female mice of both strains (a) and open symbols represent male mice (b). Each symbol represents an individual mouse and a median bar is shown.

n = 5-10 and at least 2 repetitions for each group.

* $p < 0.05$; ** $p < 0.01$ and *** $p < 0.001$

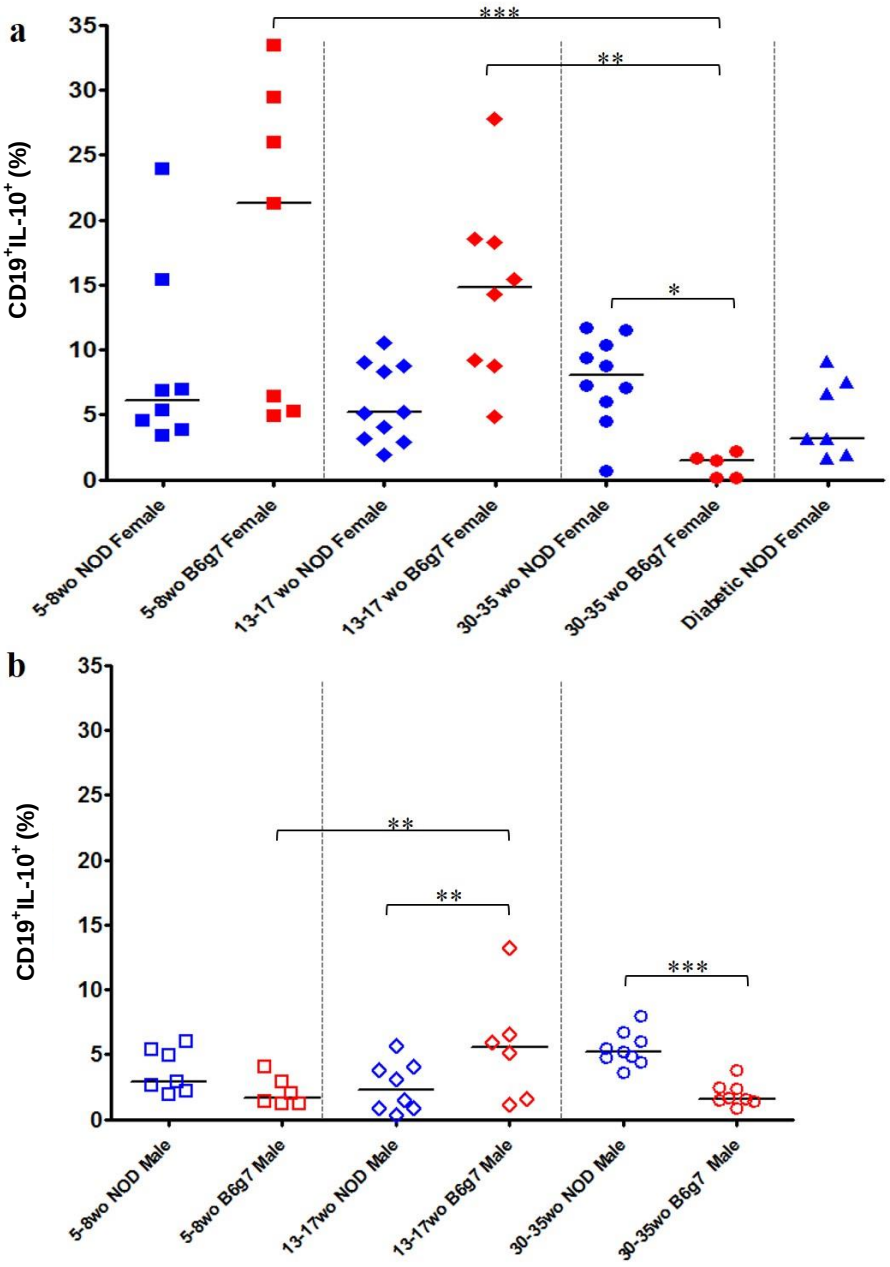

Figure 3.15 Frequency of IL-10-producing B cells stimulated with anti-CD40 and CpG. Spleens from male and female NOD and B6^{g7} mice were collected, erythrocytes were lysed and removed and spleen cells were cultured for 24h with anti-CD40 and CpG; PMA, ionomycin and monensin were added for the last 3 hours and then cells were stained for extracellular markers and intracellular IL-10. Samples were examined by flow cytometry and tested with Kruskal-Wallis, followed by Dunn's post hoc test and Bonferroni correction. Filled symbols represent female mice of both strains (a) and open symbols represent male mice (b). Each symbol represents an individual mouse and a median bar is shown.

n = 5-10 and at least 2 repetitions for each group.

* $p < 0.05$; ** $p < 0.01$ and *** $p < 0.001$

3.2.3.6 Summary

In summary, B cells responded differently to various stimulants and showed an age variation, associated with strain and whether they developed diabetes or not. While B cells from both male and female $B6^{g7}$ mice had a decreasing frequency of IL-10-producing B cells over time, the B cells from NOD mice had the opposite trend and showed higher percentages of $CD19^{+}IL\text{-}10^{+}$ cells in protected mice. The diabetic NOD mouse group comprised female NOD mice with an age-range that varied between 11.9 and 31 weeks old. Therefore, if female NOD mouse results are analysed without the protected groups, they follow the trend seen in $B6^{g7}$ mice. The results suggested that protected NOD mice had a clear increase in frequency of IL-10-producing B cells, which may contribute to the protection against diabetes.

The expression of regulatory markers on these IL-10-producing B cells will be discussed in the next section.

3.3 Expression of regulatory B cell subpopulation markers in the IL-10-producing B cells

Considering the results for the production of IL-10 by B cells and the differences observed between diabetic, 30-35 w.o. NOD and $B6^{g7}$ mice, we decided to focus on these groups to study the cell-surface markers associated with the IL-10-producing B cells.

There were two possible gating strategies to analyse the frequency of IL-10-producing Breg subpopulations: 1) Gating the putative regulatory subpopulations, using cell surface markers previously identified to be expressed in Bregs, in the whole $CD19^{+}$ B cell population and then gate the positive cells for the cytokine of interest in this population. However, as discussed previously, the subpopulations needed to be divided into 3 different panels. As B cells could express all the surface markers concomitantly, this division would represent a misleading result. Therefore, the strategy adopted was 2) Gating the IL-10-producing cells within the total B cells (results shown in section 3.2.3) and then study how each of the regulatory markers were expressed in these B cells. Examples of both gating strategies are illustrated in Figure 3.16.

Thus, the following graphs represent the percentage of the markers $CD21^{+}CD23^{+}$ (transitional cells), $CD21^{+}CD23^{-}$ (marginal zone), $CD1d^{hi}CD5^{+}$ and $CD24^{hi}CD38^{hi}$, taking the percentage of $CD19^{+}IL\text{-}10^{+}$ cells of each group as 100%.

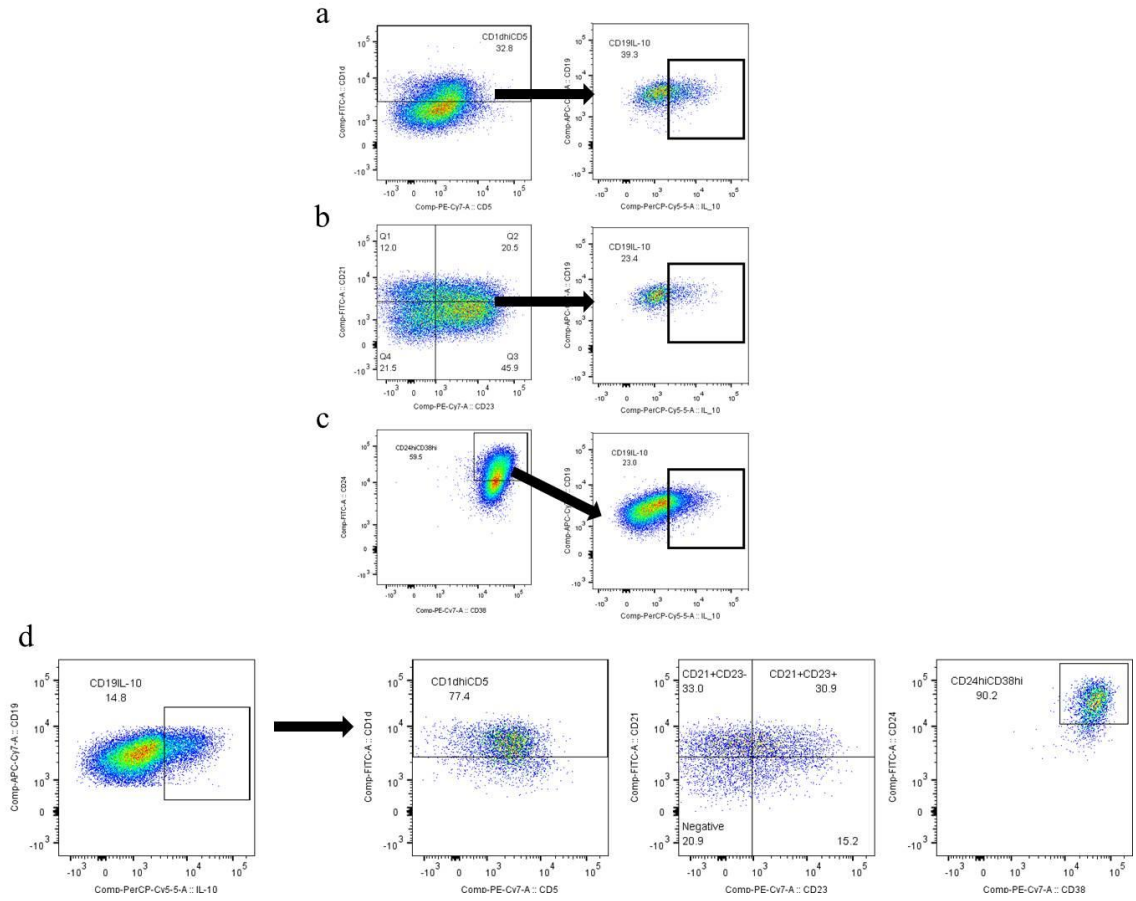

Figure 3.16 Example of the two possible flow cytometric gating strategies for the cytokine-producing regulatory B cell subpopulation analysis. Spleens from NOD and $B6^{g7}$ mice were collected, erythrocytes were lysed, cells were counted and left in culture with or without stimulants for 24h. Surface markers and intracellular cytokines were examined by flow cytometry. For every sample, 30,000 $CD19^{+}$ cells were acquired. In the first strategy, the three putative regulatory subsets ($CD1d^{hi}CD5^{+}$ in (a); CD21 and CD23 in (b) and $CD24^{hi}CD38^{hi}$ in (c)) were gated first and then, the frequency of IL-10-producing B cells was analysed. In the second strategy (d), chosen for this thesis, the IL-10-producing B cells were gated first and the expression of regulatory surface markers in these cells was analysed subsequently. In both cases, the markers are not all in the same panel, but they are not exclusive. Gates were set, based on FMOs and isotype controls – Figure A1, in the appendix.

3.3.1 Regulatory markers in unstimulated IL-10–producing B cells

When B cells were unstimulated, there were no differences in the T2 phenotype markers ($CD21^{hi}CD23^{hi}$ – Figures 3.17a and b) in $CD19^{+}IL\text{-}10^{+}$ cells between the 3 groups. There were also no statistically significant differences observed between the groups in female or male mice. For IL-10-producing B cells expressing the Marginal zone phenotype ($CD21^{hi}CD23^{-}$ – Figures 3.17c and d), the same pattern was observed.

When the expression of $CD1d^{hi}CD5^{+}$ was examined in unstimulated IL-10-producing B cells, statistically significant strain differences were observed in both female ($p < 0.05$ – Figure 3.17e) and male mice ($p < 0.001$ – Figure 3.17f). The strain difference was also observed for the expression of $CD24^{hi}CD38^{hi}$; however the $CD24^{hi}CD38^{hi}$ population was only higher in NOD male mice, when compared to B6g7 mice (Figures 3.17g and h). The frequencies of $CD1d^{hi}CD5^{+}$ and $CD24^{hi}CD38^{hi}$ increased in diabetic mice, compared with protected NOD mice, but the difference was not statistically significant.

3.3.2 Regulatory markers in IL-10–producing B cells stimulated with LPS

Compared to unstimulated cells, IL-10-producing B cells stimulated with LPS had an increase in the expression of regulatory markers.

Although there was no significant difference, it is interesting to note that, for this stimulant, the expression of T2 markers was higher in 30-35 w.o. $B6^{g7}$ mice, compared to NOD mice (mainly in male mice – Figures 3.18a and b). Nevertheless, the expression of marginal zone markers was still higher (though not significant) in NOD mice. The percentage of $CD19^{+}IL\text{-}10^{+}$ cells from diabetic mice expressing $CD21^{hi}CD23^{-}$ was even higher. This could suggest that IL-10 is being produced by different populations of B cells depending on the strain (Figures 3.18c and d).

As described previously in the literature (Yanaba et al. 2008), the majority of the B cells stimulated with LPS and producing IL-10 expressed $CD1d^{hi}CD5^{+}$, as illustrated in Figures 3.18e and f. The expression was higher in NOD mice, when compared to $B6^{g7}$ mice. This difference was statistically significant in male mice ($p < 0.05$).

When stimulated with LPS, more than 80% of the B cells producing IL-10 expressed $CD24^{hi}CD38^{hi}$ in all strains and genders and there was no significant difference between the groups (Figures 3.18g and h).

3.3.3 Regulatory markers in IL-10–producing B cells stimulated with anti-CD40

When B cells were stimulated with anti-CD40, there was an upregulation of the surface markers $CD21^{hi}CD23^{hi}$ and it was independent of the gender or strain being analysed. As a counterbalance to this upregulation, the expression of MZ phenotype in B cells producing IL-10 was very low (Figures 3.19a-d). This observation could suggest a downregulation or upregulation of markers dependent on stimulation and/or that IL-10 production varies on B cell subpopulations depending on the stimulant used.

Despite the difference in T2 and MZ markers, the expression of $CD1d^{hi}CD5^{+}$ in cells stimulated with anti-CD40 was still higher than 50% in all the groups (Figures 3.19e and f). Male NOD mice had a statistically higher percentage of IL-10-producing B cells expressing $CD1d^{hi}CD5^{+}$, in comparison to $B6^{g7}$ mice ($p < 0.05$).

As observed in Figures 3.19g and h, the expression of $CD24^{hi}CD38^{hi}$ in $CD19^{+}IL\text{-}10^{+}$ cells stimulated with anti-CD40 was strikingly higher in NOD mice, compared to $B6^{g7}$ mice; however, there were no statistically significant differences. As observed for LPS-stimulated cells, the anti-CD40 stimulated cells from diabetic mice expressed more putative regulatory markers than protected mice.

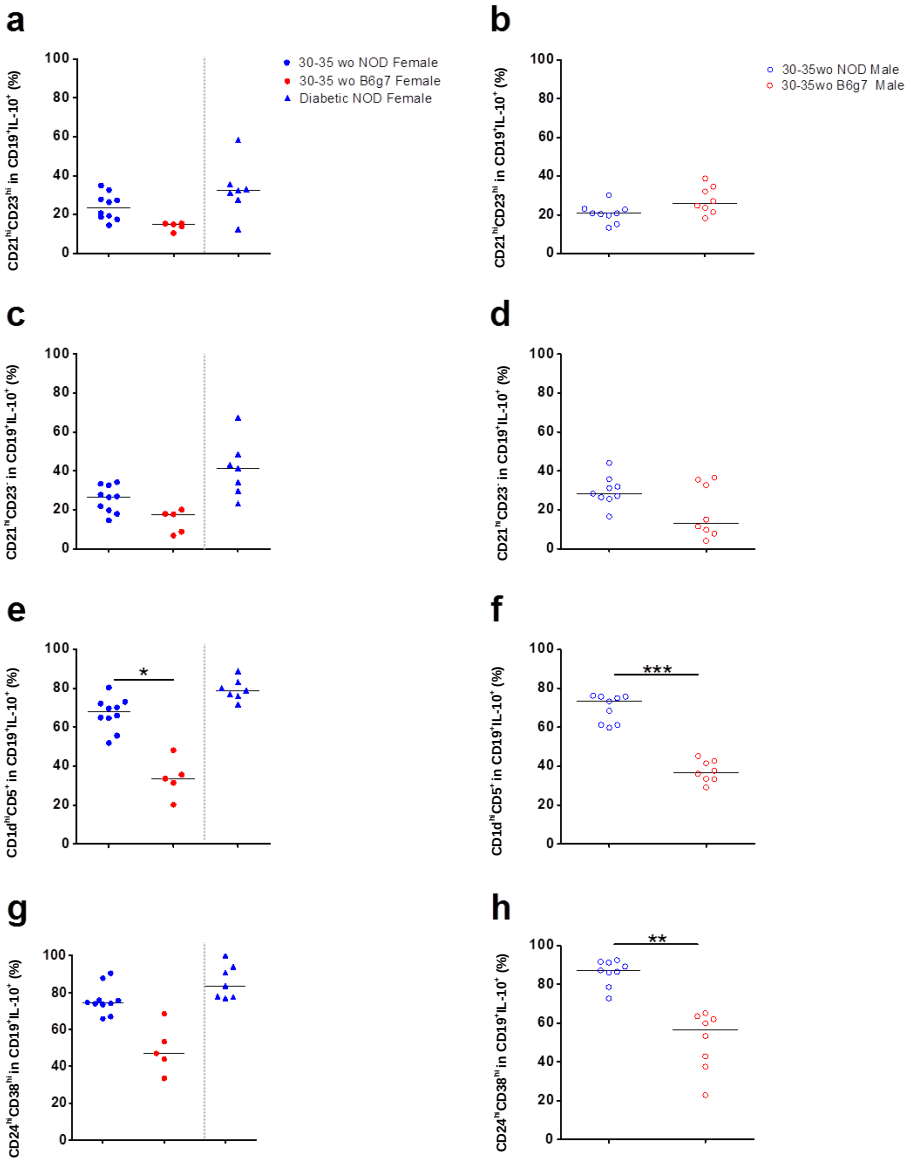

Figure 3.17 Frequency of regulatory markers expression in unstimulated IL-10-producing B cells. Spleens from 30-35 w.o. male and female NOD and B6^{g7} mice, as well as diabetic female NOD mice, were collected, erythrocytes were lysed and removed and spleen cells were cultured for 24h with no stimulant added; PMA, ionomycin and monensin were added for the last 3 hours and then cells were stained for extracellular markers and intracellular cytokines. Samples were examined by flow cytometry and tested with Kruskal-Wallis, followed by Dunn's post hoc test and Bonferroni correction. Filled symbols represent female mice of both strains and open symbols represent male mice. Frequency of CD21^{hi}CD23^{hi} expression in CD19^{+}IL-10^{+} cells is shown in (a) female mice and in (b) male mice; frequency of CD21^{hi}CD23^{-} expression in CD19^{+}IL-10^{+} cells is shown in (c) female mice and in (d) male mice; the frequency of CD1d^{hi}CD5^{+} expression in CD19^{+}IL-10^{+} cells is shown in (e) female mice and in (f) male mice and, lastly, frequency of CD24^{hi}CD38^{hi} expression in CD19^{+}IL-10^{+} cells is shown in (g) female mice and in (h) male mice. Each symbol represents an individual mouse and a median bar is shown.

n = 5-10 and at least 2 repetitions for each group. * $p < 0.05$; ** $p < 0.01$ and *** $p < 0.001$

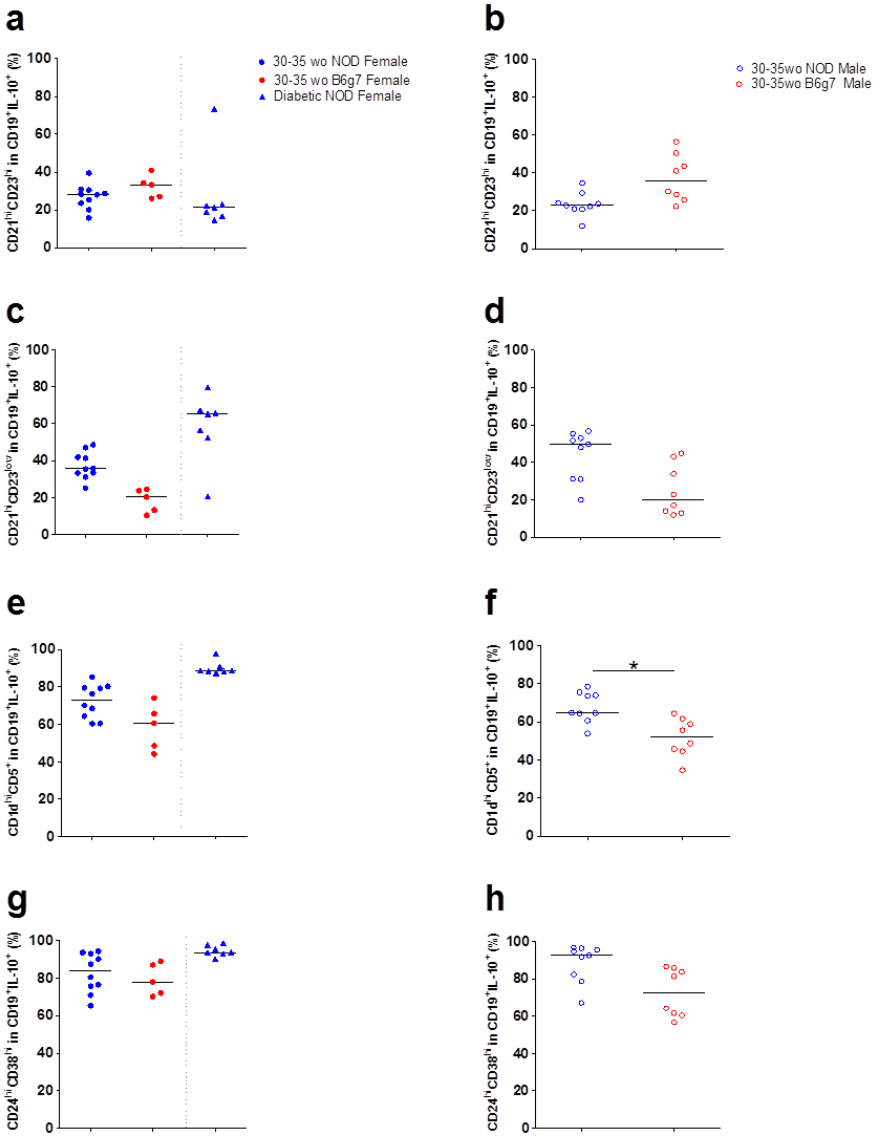

Figure 3.18 Frequency of regulatory markers expression in IL-10-producing B cells stimulated with LPS. Spleens from 30-35 w.o. male and female NOD and B6^{g7} mice, as well as diabetic female NOD mice, were collected, erythrocytes were lysed and removed and spleen cells were cultured for 24h with LPS; PMA, ionomycin and monensin were added for the last 3 hours and then cells were stained for extracellular markers and intracellular cytokines. Samples were examined by flow cytometry and tested with Kruskal-Wallis, followed by Dunn's post hoc test and Bonferroni correction. Filled symbols represent female mice of both strains and open symbols represent male mice. Frequency of CD21^{hi}CD23^{hi} expression in CD19^{+}IL-10^{+} cells is shown in (a) female mice and in (b) male mice; frequency of CD21^{hi}CD23^{-} expression in CD19^{+}IL-10^{+} cells is shown in (c) female mice and in (d) male mice; the frequency of CD1d^{hi}CD5^{+} expression in CD19^{+}IL-10^{+} cells is shown in (e) female mice and in (f) male mice and, lastly, frequency of CD24^{hi}CD38^{hi} expression in CD19^{+}IL-10^{+} cells is shown in (g) female mice and in (h) male mice. Each symbol represents an individual mouse and a median bar is shown.

n = 5-10 and at least 2 repetitions for each group. * $p < 0.05$; ** $p < 0.01$ and *** $p < 0.001$

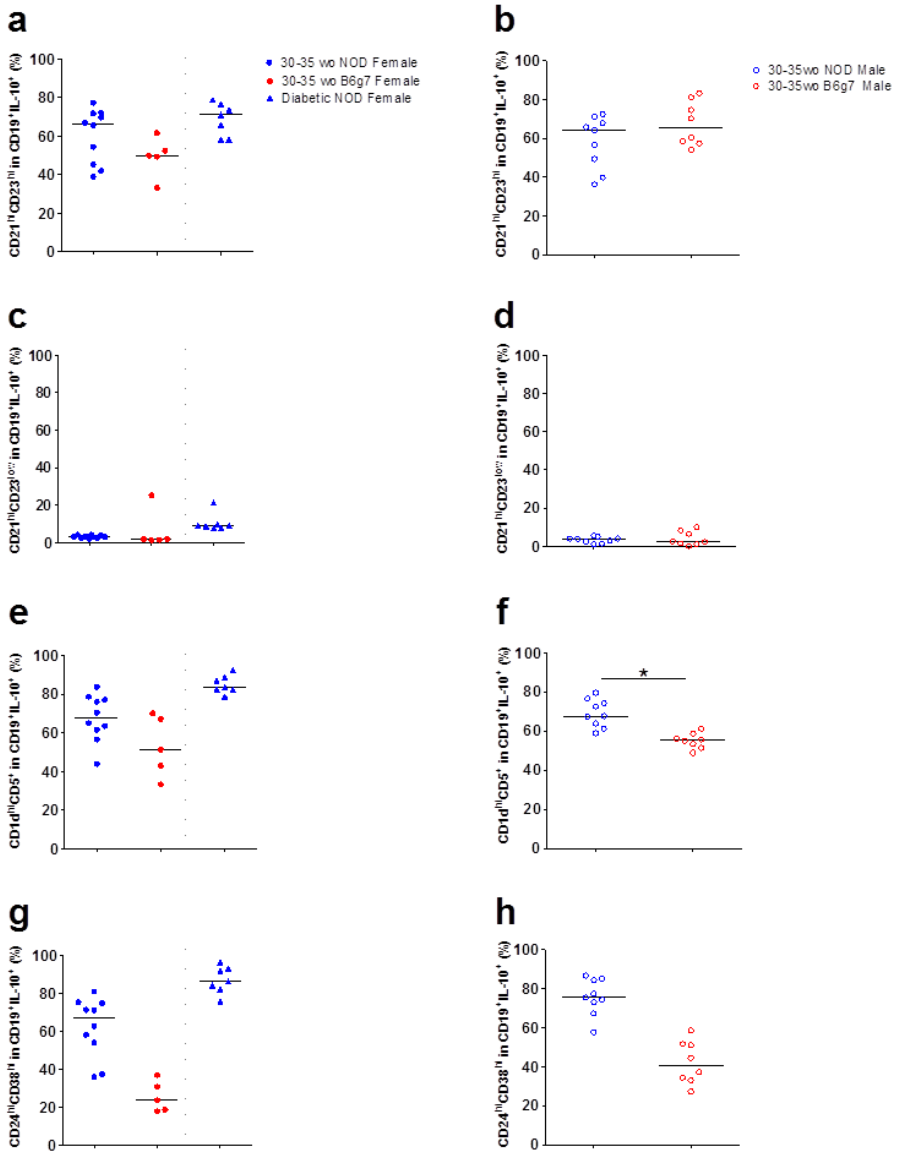

Figure 3.19 Frequency of regulatory markers expression in IL-10-producing B cells stimulated with anti-CD40. Spleens from 30-35 w.o. male and female NOD and $B6^{g7}$ mice, as well as diabetic female NOD mice, were collected, erythrocytes were lysed and removed and spleen cells were cultured for 24h with anti-CD40; PMA, ionomycin and monensin were added for the last 3 hours and then cells were stained for extracellular markers and intracellular cytokines. Samples were examined by flow cytometry and tested with Kruskal-Wallis, followed by Dunn's post hoc test and Bonferroni correction. Filled symbols represent female mice of both strains and open symbols represent male mice. Frequency of $CD21^{hi}CD23^{hi}$ expression in $CD19^{+}IL\text{-}10^{+}$ cells is shown in (a) female mice and in (b) male mice; frequency of $CD21^{hi}CD23^{-}$ expression in $CD19^{+}IL\text{-}10^{+}$ cells is shown in (c) female mice and in (d) male mice; the frequency of $CD1d^{hi}CD5^{+}$ expression in $CD19^{+}IL\text{-}10^{+}$ cells is shown in (e) female mice and in (f) male mice and, lastly, frequency of $CD24^{hi}CD38^{hi}$ expression in $CD19^{+}IL\text{-}10^{+}$ cells is shown in (g) female mice and in (h) male mice. Each symbol represents an individual mouse and a median bar is shown.

n = 5-10 and at least 2 repetitions for each group. * $p < 0.05$; ** $p < 0.01$ and *** $p < 0.001$

3.3.4 Regulatory markers in IL-10–producing B cells stimulated with CpG

As observed with LPS-stimulated B cells, when stimulated with CpG, the frequency of $CD19^{+}IL\text{-}10^{+}$ cells expressing the T2 phenotype was higher in $B6^{g7}$ mice (however the difference was not statistically significant – Figures 3.20a and b). The expression of $CD21^{hi}CD23^{-}$, $CD1d^{hi}CD5^{+}$ and $CD24^{hi}CD38^{hi}$ on IL-10-producing B cells stimulated with CpG was similar between 30-35 w.o. NOD and $B6^{g7}$ mice, from both genders (Figures 3.20c-h). Diabetic mice expressed the highest frequencies of regulatory markers (non-significant - ns).

3.3.5 Regulatory markers in IL-10–producing B cells stimulated with anti-CD40/ CpG

The combination of anti-CD40 and CpG did not show a synergistic effect for the expression of regulatory markers and the frequencies were very similar to the cells stimulated with CpG only. The expression of regulatory markers on IL-10-producing B cells was not as high as in LPS-stimulated B cells and was heterogeneous between the individual mice.

The expression of the T2 phenotype ($CD21^{hi}CD23^{hi}$ – Figures 3.21a and b) in IL-10-producing B cells was higher in $B6^{g7}$ mice (ns). The expression of MZ phenotype markers and $CD1d^{hi}CD5^{+}$, on the other hand, was similar in all groups, with non-significant higher frequencies in NOD mice (Figures 3.21c-f).

The expression of $CD24^{hi}CD38^{hi}$ on IL-10-producing B cells stimulated with anti-CD40 and CpG was significantly higher in diabetic mice, when compared to 30-35 w.o. mice ($p < 0.05$ – Figure 3.20g).

3.3.6 Summary

Although there was a statistically significant difference between protected and diabetic NOD mice in the percentage of total B cells producing IL-10, the expression of regulatory markers on these cells was generally very similar in both groups, with a non-significant upregulation in diabetic mice. NOD mice, both male and female, had overall higher frequencies of regulatory markers when compared to $B6^{g7}$ mice. Different

stimulants stimulated different phenotypes of IL-10-producing B cells (LPS stimulated MZ B cells and anti-CD40 stimulated T2 B cells).

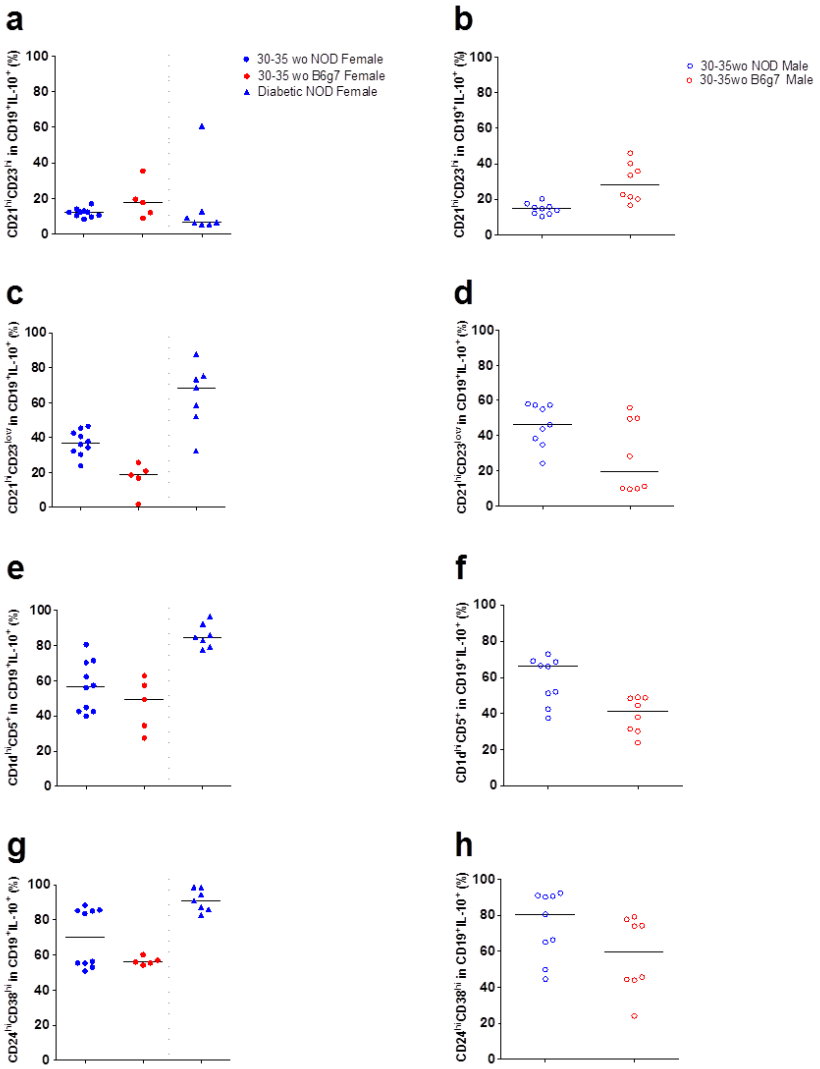

Figure 3.20 Frequency of regulatory markers expression in IL-10-producing B cells stimulated with CpG. Spleens from 30-35 w.o. male and female NOD and $B6^{g7}$ mice, as well as diabetic female NOD mice, were collected, erythrocytes were lysed and removed and spleen cells were cultured for 24h with CpG; PMA, ionomycin and monensin were added for the last 3 hours and then cells were stained for extracellular markers and intracellular cytokines. Samples were examined by flow cytometry and tested with Kruskal-Wallis, followed by Dunn's post hoc test and Bonferroni correction. Filled symbols represent female mice of both strains and open symbols represent male mice. Frequency of $CD21^{hi}CD23^{hi}$ expression in $CD19^{+}IL\text{-}10^{+}$ cells is shown in (a) female mice and in (b) male mice; frequency of $CD21^{hi}CD23^{-}$ expression in $CD19^{+}IL\text{-}10^{+}$ cells is shown in (c) female mice and in (d) male mice; the frequency of $CD1d^{hi}CD5^{+}$ expression in $CD19^{+}IL\text{-}10^{+}$ cells is shown in (e) female mice and in (f) male mice and, lastly, frequency of $CD24^{hi}CD38^{hi}$ expression in $CD19^{+}IL\text{-}10^{+}$ cells is shown in (g) female mice and in (h) male mice. Each symbol represents an individual mouse and a median bar is shown. n = 5-10 and at least 2 repetitions for each group.

* $p < 0.05$; ** $p < 0.01$ and *** $p < 0.001$

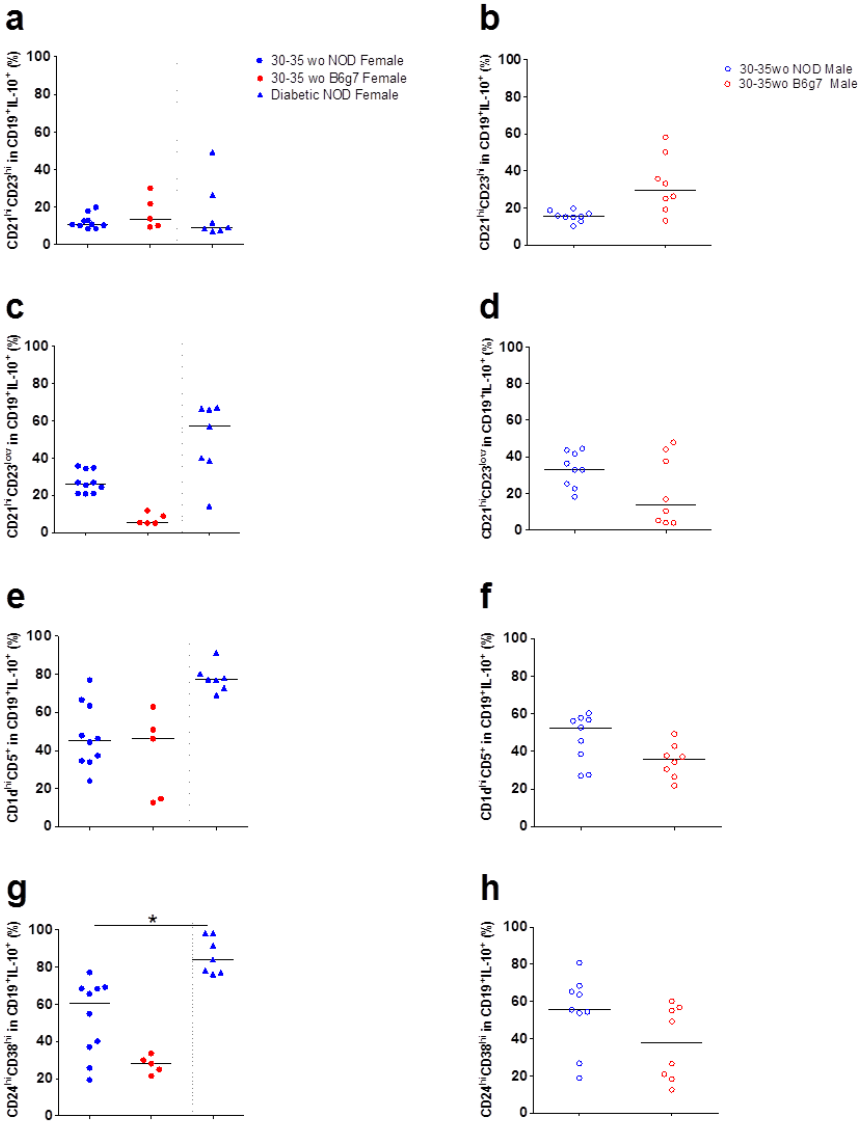

Figure 3.21 Frequency of regulatory markers expression in IL-10-producing B cells stimulated with anti-CD40 and CpG. Spleens from 30-35 w.o. male and female NOD and B6^{g7} mice, as well as diabetic female NOD mice, were collected, erythrocytes were lysed and removed and spleen cells were cultured for 24h with anti-CD40 and CpG; PMA, ionomycin and monensin were added for the last 3 hours and then cells were stained for extracellular markers and intracellular cytokines. Samples were examined by flow cytometry and tested with Kruskal-Wallis, followed by Dunn's post hoc test and Bonferroni correction. Filled symbols represent female mice of both strains and open symbols represent male mice. Frequency of CD21^{hi}CD23^{hi} expression in CD19^{+}IL-10^{+} cells is shown in (a) female mice and in (b) male mice; frequency of CD21^{hi}CD23^{-} expression in CD19^{+}IL-10^{+} cells is shown in (c) female mice and in (d) male mice; the frequency of CD1d^{hi}CD5^{+} expression in CD19^{+}IL-10^{+} cells is shown in (e) female mice and in (f) male mice and, lastly, frequency of CD24^{hi}CD38^{hi} expression in CD19^{+}IL-10^{+} cells is shown in (g) female mice and in (h) male mice. Each symbol represents an individual mouse and a median bar is shown.

n = 5-10 and at least 2 repetitions for each group.

* $p < 0.05$; ** $p < 0.01$ and *** $p < 0.001$

3.4 Discussion

For a long time it was believed that the role of B cells was restricted to pathogenic effects in type 1 diabetes. However, although not new, the concept of regulatory B cells (Bregs) has previously been studied mainly in other autoimmune diseases, such as arthritis (Mauri et al. 2003), Systemic Lupus Erythematosus – SLE (Blair et al. 2009) and Experimental Autoimmune Encephalomyelitis – EAE (Fillatreau et al. 2002), but not in great detail in type 1 diabetes. Therefore, our aim in this investigation was to characterize cytokine-producing B cells and the expression of regulatory markers in NOD mice, compared with a non-diabetes-prone congenic strain, the $B6^{g7}$ mice.

The first cytokine evaluated was IL-6, a pro-inflammatory cytokine. We observed that unstimulated, LPS- and anti-CD40-stimulated spleen B cells do not produce IL-6, which supports the idea of these stimulants (alone) shifting B cells to a regulatory profile. On the other hand, the combination of CpG and anti-CD40 increased the frequency of $CD19^{+}IL\text{-}6^{+}$ cells in comparison to CPG and anti-CD40 alone and the effect was synergistic.

A study that determined the role of IL-6 produced by B cells in EAE supports our findings. In their investigation, spleen cells stimulated with anti-CD40 combined with CpG produced more IL-6 than cells stimulated with LPS or anti-CD40 or CpG alone (Barr et al. 2012). The study also showed that the combination of LPS and anti-CD40 produced the same effect as CpG and anti-CD40, proving to be a result of dual stimulation of different types of receptors. A study in humans demonstrated that stimulating B cells with CpG upregulates the expression of CD40. They also observed the synergistic effect of combining CpG and a CD40-CD40L stimulation in B cells, with increased expression of IL-6 and IL-10, although IL-6 production occurred faster than IL-10 (Gantner et al. 2003). This could suggest that even if anti-CD40 by itself does not stimulate the cells to produce IL-6, it could bring B cells to a state of activation where the effect of CpG stimulation is optimised, as a second signal. The mechanism, however, is still unclear.

We then moved on to the regulatory cytokines, starting with TGF-β. Although TGF-β-producing B cells have not been studied as much as IL-10-producing B cells, the role of this cytokine in type 1 diabetes, in lymphoid organs and inside the islet, has been broadly discussed in the literature (Peng et al. 2004; Tai et al. 2013).

Our results show that the frequencies of $CD19^{+}TGF\text{-}\beta^{+}$ cells were more heterogeneous than observed for IL-10 and the main finding was the increased frequency of TGF-β-producing B cells associated with age.

As discussed in the introduction to this chapter, Tian and colleagues studied the relation between TGF-β production by B cells and NOD mice. According to their studies, B cells from young mice stimulated with LPS express more FasL and release TGF-β, and this induces apoptosis in diabetogenic T cells. Also in concordance with our results, they showed that unstimulated B cells do not produce TGF-β (Tian et al. 2001). Our results, however, show that diabetic mice have a similar percentage of $CD19^{+}TGF\text{-}\beta^{+}$ cells when compared to protected mice; this may bring into question the importance of TGF-β produced by B cells as contributing to natural protection against autoimmune diabetes. Nevertheless as protected mice have more B cells producing IL-10, B cells that produce TGF-β could be relevant in synergy. Another point to be made and possibly investigated in the future is whether effector cells in protected NOD mice are as resistant to regulation as in younger NOD mice (D'Alise et al. 2008). If they are not as resistant, the same percentage of TGF-β-producing B cells would be able to regulate the system more efficiently.

Lastly, we evaluated IL-10, a major factor determining regulatory B cell function. Our main findings were 1) Increased baseline frequency in IL-10-producing B cells in protected NOD mice in comparison to diabetic mice; 2) Different stimulants affect the production of IL-10 in diabetic NOD mice. Upon LPS and CpG stimulation, B cells from diabetic mice produced IL-10, but not after anti-CD40 stimulation; 3) NOD mice in general had higher frequencies of $CD19^{+}IL\text{-}10^{+}$ cells when compared to $B6^{g7}$ mice and 4) The expression of regulatory markers was non-significantly higher in diabetic mice, when compared to protected mice, although both groups had higher frequencies of these B cells than $B6^{g7}$ mice.

There are not many studies in the literature aiming to investigate >35 week old protected NOD mice and the regulatory role of B cells. Kleffel and colleagues compared these older mice to young and hyperglycaemic NOD mice. In the pancreatic islets, similar to young (4 weeks old) mice, they found that protected mice had preserved insulin production and reduced insulitis in comparison to diabetic mice. Moreover, it was observed that, compared to other groups, protected NOD mice (denominated Long-

term Normoglycaemic mice in the paper) had a higher frequency of IL-10^+ B cells infiltrating the pancreatic islets. Similar to our investigation, they also examined the production of IL-10 by spleen B cells over time and observed a higher percentage of IL-10^+ B cells in young mice, although it was non-significant, and they found no difference between diabetic and protected mice. The discrepancy between their and our results could be due to differences in the cell stimulation methods. Here, the stimulants were added for 24h, with a 3h boost of PMA, ionomycin and monensin, while in their paper, they added PMA, ionomycin and monensin for 5h, which is comparable only to our unstimulated cell cultures (Kleffel et al. 2014).

Although IL-10-producing B cells from diabetic mice were capable of responding to LPS stimulation, the frequency of $CD19^+IL\text{-}10^+$ cells was higher in older, protected female NOD mice. Diabetic mouse splenocytes presented an interesting variation in the frequency of $CD19^+IL10^+$ cells depending on the stimulant. Unstimulated and anti-CD40 stimulation did not increase the percentage of B cells producing IL-10. Mion and colleagues observed that, in C57BL/6 mice, B cells stimulated with anti-CD40 antibody took longer to produce IL-10 than cells stimulated with LPS and CpG. This was thought to be due to anti-CD40 mimicking a cellular interaction compared to stimulation by exogenous stimulants (Mion et al. 2014). That does not explain, however, why diabetic mice are less responsive when stimulated with anti-CD40 than other mice. One possible explanation for this could be the downregulation of CD40 receptors on the surface of B cells from diabetic mice. A study using chimeric mice, where the B cells were CD40-/-, resulted in the mice having non-remitting severe EAE when compared to control mice, supporting the idea of an association between autoimmune disease and the lack of CD40 receptors (Fillatreau et al. 2002). However, to confirm this hypothesis, a study focusing on expression of CD40 on B cells in NOD mice during aging and after diabetes onset would be necessary. Another study in patients with SLE demonstrated that $CD19^+CD24^{hi}CD38^{hi}$ B cells, a key human Breg population, derived from peripheral blood were refractory to CD40 stimulation and would not produce IL-10, as opposed to B cells collected from healthy donors. This difference, however, was not related to the expression of CD40 receptors, but to the STAT3 signalling pathway that is activated when CD40-CD40L bind and is impaired in Breg cells from SLE patients (Blair et al. 2010). These observations could suggest an association between the B cell

unresponsiveness to CD40 stimulation and autoimmune diabetes in NOD mice and needs further investigation.

The expression of $CD1d^{hi}CD5^{+}$ in IL-10-producing B cells of diabetic mice was not significantly higher, when compared to protected NOD mice and $B6^{g7}$ mice; these results were seen independent of the stimulant. The study by Mizoguchi and colleagues demonstrated an increase in the expression of CD1d and IgM in a model of intestinal inflammation. Increased expression was shown in the MLNs of diseased mice when compared to wild-type mice (mice that do not have the knock out gene and, therefore, are not prone to develop the intestinal inflammation) and healthy mice prone to development of the disease. However, in agreement with our findings, they did not observe statistically significant differences in the spleen (Mizoguchi et al. 2002).

The higher frequency of IL-10 producing B cells in NOD compared to $B6^{g7}$ mice, when spleen cells were stimulated with LPS, was also described by Yanaba and colleagues. They demonstrated that NOD mice and a lupus-prone strain had higher frequencies of $CD1d^{hi}CD5^{+}$ and IL-10-producing B cells, when compared to B6 mice (Yanaba et al. 2009). Our results for the expression of regulatory markers in IL-10-producing B cells also showed that more than 50% of $CD19^{+}IL\text{-}10^{+}$ cells from NOD mice expressed $CD1d^{hi}CD5^{+}$, when cells were unstimulated or stimulated with LPS, anti-CD40 alone or CpG alone. It was higher than 40% for cells stimulated with anti-CD40 and CpG together. For $B6^{g7}$ mice, the percentages varied more depending on the stimulant: LPS was best able to upregulate these markers, but the percentages were always lower than in NOD mice.

This observation could be explained by a higher frequency of $CD1d^{hi}$ B cells, the subpopulation believed to comprise the regulatory B cells, and marginal zone B cells in NOD mice when compared to C57BL/6 mice (Rolf et al. 2005). Mariño and colleagues demonstrated that the number of cells in the marginal zone increased with time (and, hence, with the development of insulitis) in female NOD mice. They also revealed the mechanism for this finding: marginal zone B cells from NOD mice have more S1P3 receptors and, therefore, are hyperresponsive to the chemokine (S1P) responsible for retention of cells in the marginal zone in the spleen (Marino et al. 2008).

Although $CD1d^{hi}$ cells are mainly concentrated in marginal zone, we also investigated the transitional B cells (T2), following previous studies in the literature (Evans et al.

2007). Blair and colleagues investigated regulatory B cells in a murine model for lupus erythematous and demonstrated that anti-CD40 amplified the production of IL-10 by purified T2-like B cells, in comparison to LPS and CpG. These two stimulants, when investigated in the whole B cell population, stimulated IL-10 production in marginal zone and T2-like B cells (not as abundant as anti-CD40) in the same proportion (Blair et al. 2009). Indeed our results showed that cytokine-producing B cells stimulated with anti-CD40 expressed the T2 phenotype in a higher proportion. However, when the stimulants had a bacterial origin (LPS and CpG), B cells from NOD mice producing the cytokines analysed had higher frequencies of $CD21^{+}CD23^{-}$, the marginal zone markers. These findings raise questions about the real location of regulatory B cells in the spleen *in vivo*, before the tissue is disrupted and stimulants are added for cell culture. A histological study identifying IL-10 producing B cells *in situ* in the spleen of NOD mice would have to be conducted to clarify this matter. Nevertheless, the stimulation to induce regulatory B cells might be necessary and negative results should be analysed very carefully.

In summary, this was the first time differences between the frequency of $CD19^{+}$IL-10^{+} spleen cells upon stimulation with LPS, anti-CD40 and CpG were demonstrated in protected and diabetic NOD mice. Functional experiments to analyse the regulatory effect of B cells from >35 week old protected NOD mice when cultured with dendritic cells and CD8 T cells from G9Cα-/-.NOD mice are described in chapter 4.

Although there were interesting findings, our studies were limited by the number of fluorochromes that could be analysed simultaneously in the flow cytometer available at the time of this study. IL-10 production is associated with a number of B cell phenotypes as delineated by cell surface markers. The analysis of all these surface markers together on these putative regulatory cells would facilitate our understanding of the regulatory B cells in NOD mice as a whole and answer some questions, which include: How many regulatory B cell phenotypes exist? How do the stimulants modify these phenotypes?

In conclusion, this chapter highlighted the differences in cytokine production, mainly regulatory cytokines, and the expression of regulatory markers related to type 1 diabetes, age of NOD mice and the stimulants used to trigger this production. The main result was that 30-35 week old protected female NOD mice had a higher frequency of

IL-10-producing B cells when compared to diabetic mice. An examination of whether the cells have *in vitro* protective effects will be examined in Chapter 4.

4. Effect of B cells on the interaction between antigen-specific CD8 T cells and dendritic cells

4.1 Introduction and Objectives

4.1.1 Introduction

After analysing the results in chapter 3 and observing the increased percentage of IL-10-producing B cells in protected NOD mice, the next step was to carry out functional experiments to test whether B cells from these mice were better at suppressing immune responses.

The regulatory function of B cells could have been assessed in many different assays, aiming to understand their effects on various types of cells. The cooperative effects of CD4 T cells and B cells are well known. However, for our first experiments, we chose to investigate the effect of B cells on the activation of insulin-specific CD8 T cells, derived from a transgenic NOD mice (G9Cα $^{-/-}$) developed by Professor Susan Wong (Wong et al. 2009). These experiments were to test not only direct effects on CD8 T cells but also effects through dendritic cells (DCs) as antigen presenting cells.

The importance of CD8 T cells in type 1 diabetes is now well-documented. An early study highlighted the observation that knockout NOD mice lacking β2-microglobulin (essential component of the MHC I molecule) were not able to activate cytotoxic T cells and did not develop disease (Serreze et al. 1994).

The study of islet antigen-specific CD8 T cells have given further clues for the role of these T cells on the onset of the disease: CD8 T cells with TCR specificity for a peptide of the β-chain of insulin (B:15-23) are found in the islets of NOD mice as early as 4 weeks after birth. IFN-γ producing CD8 T cells are essential for the inflammation observed in pancreatic islets of NOD mice and the damage caused by them might "open the door" for other lymphocytes, with specificity for other islet antigens (Wong et al. 1996; Wong et al. 1999). CD8 T cells recognising the autoantigen islet-specific glucose-6-phosphatase catalytic subunit related protein (IGRP) have also been shown to play an important role (Nagata et al. 1994; Verdaguer et al. 1997; Lieberman et al. 2003).

Although initially associated with the priming of CD4 T cells, DCs are essential for cross-presentation of antigens to CD8 T cells (Joffre et al. 2012). This is important for the presentation of tissue-associated antigens to CD8 T cells via MHC class I (Kurts et al. 1996). DCs play a role in the activation of antigen-specific CD8 T cells to cause type 1 diabetes: Professional antigen presenting cells presenting antigens to CD8 T cells via MHC I, rather than direct presentation of islet specific antigens by beta cells, has been shown to be essential for invasive infiltration of pancreatic islets (de Jersey et al. 2007).

As discussed in chapter 1, CD8 T cells have been shown to interact with B cells in type 1 diabetes. B cells contribute to disease by providing the signals for CD8 T cell survival, especially in late islet infiltration (Brodie et al. 2008). B cells can also cross-present autoantigens to CD8 T cells, via MHC class I, which was demonstrated by studying NOD mice lacking B cells (NOD.μMT) or B cells from transgenic $\beta 2m^{-/-}$ NOD mice (not expressing MHC I). In these mice, IGRP-CD8 T cells were not able to proliferate in the PLNs and diabetes was prevented (Marino et al. 2012). On the other hand, in the lymphoid organs, a regulatory effect of B cells on CD8 T cells was also described by Parekh and colleagues. When stimulated with LPS, B cells induced anergy in CD8 T cells in a membrane bound TGF-β1-dependent way (Parekh et al. 2003).

B cells and dendritic cells are also known to interact. B cells suppress dendritic cell IL-12 production in response to a number of different types of stimulation. For example, B cells activated to produce IL-10 by *Leishmania major* infection induced suppression of IL-12 production by DCs (Ronet et al. 2010). This mechanism of action has also been demonstrated by CpG-activated neonatal B cells, which were able to suppress IL-12 production by neonatal dendritic cells (Sun et al. 2005). Regulatory effects of B cells on DCs were described previously in the autoimmune model of multiple sclerosis EAE. In this model, when DCs were co-cultured with B10 cells ($CD1d^{hi}CD5^{+}$ B cells, producing IL-10) prior to interaction with antigen specific CD4 T cells, they were less efficient in inducing T cell proliferation, compared to DCs co-cultured with $CD1d^{low}CD5^{-}$ B cells or $IL\text{-}10^{-/-}$ B cells (Matsushita et al. 2010).

Thus, in the context of studying the role of regulatory B cells in a model of diabetes, we were interested in investigating B cell interactions with CD8 T cells, which could interact directly by cytokine production or cell-cell contact, but also indirectly, by modulating the dendritic cell function.

4.1.2 Objectives

Based on previous findings from chapter 3 and the studies described above, we aimed to study how B cells from older NOD and B6^{g7} mice (> 35 w.o.) and diabetic NOD mice may affect the activation of CD8 T cells (specific for an insulin peptide) by DCs. Our hypothesis was that B cells from protected NOD mice could potentially have more accentuated regulatory properties and be more efficient than B cells from diabetic NOD mice or B6^{g7} mice in suppressing the cytotoxic function of CD8 T cells.

4.2 Experimental Design

To investigate the interaction between B cells, dendritic cells and CD8 T cells, a number of mouse strains were used. A diagram of the interactions studied and the timeline for the experimental set-up is shown in Figure 4.1.

To make it possible to study interactions between B cells and dendritic cells in culture with CD8 T cells, without the addition of exogenous peptide in the cell culture, we utilized dendritic cells from transgenic mice that express proinsulin 2 (PI2) under the promoter of MHC class II I-E^{k} (French et al. 1997), here designated PI homo mice.

DCs from 6-12 week-old PI homo mice (4 mice pooled for each experiment) were processed as described in the Methods chapter (section 2.4) and were activated with LPS one day before the set-up.

B cells from the spleen of > 35 weeks old NOD (protected) and B6^{g7} mice and diabetic NOD mice (3-4 mice pooled for each group) were magnetically separated, stimulated with LPS or left unstimulated for 24h prior to the set-up. In addition to LPS being the main stimulant used to generate regulatory B cells in the literature, the choice of LPS as the stimulant for the B cells was based on the results seen in chapter 3.

We studied a number of CD8 T cell functions including activation, proliferation and degranulation as a surrogate measure of cytotoxicity, as well as cytokine production. CFSE was used to measure proliferation, CD69 was used as a marker for early activation and CD107a is found on the membrane of granzyme/perforin granules, and so measurement of CD107a gave an induction of degranulating cytotoxic CD8 T cells (Betts et al. 2003). In addition to the anti-inflammatory (IL-10) and inflammatory (IL-6, IFN-γ and TNF-α) cytokines, we also evaluated the production of MIP1-β. This

chemokine is secreted by various cells, like lymphocytes, macrophages and DCs and is responsible for the attraction of T cells to the site of inflammation (Maurer and von Stebut 2004).

On day 0, insulin-specific CD8 T cells were collected from the spleen of 6-12 week-old G9Cα$^{-/-}$ mice and labelled with CFSE on the day of the set-up (methods described in section 2.7). Cells were added to the wells of a 24-well culture plate at a ratio of 1 CD8 T cell : 2 DCs : 7 B cells, a proportion determined previously by titration. The total number of cells was: $2x10^5$ CD8 T cells : $4x10^5$ DCs : $1.4x10^6$ B cells. The 3 types of individual cells cultured alone and controls were set-up with wells containing CD8 T cells + DCs, but without B cells. One day after the set-up, half of the plates were harvested for the analysis of the expression of CD69 and CD107a by flow cytometry; from the remaining plates, supernatants were collected 2 days after the set-up (for multiplex cytokine assay). Finally, CFSE and CD69 were assessed by flow cytometry 3 days after the set-up. Experiments were performed at least 3 times for all the groups.

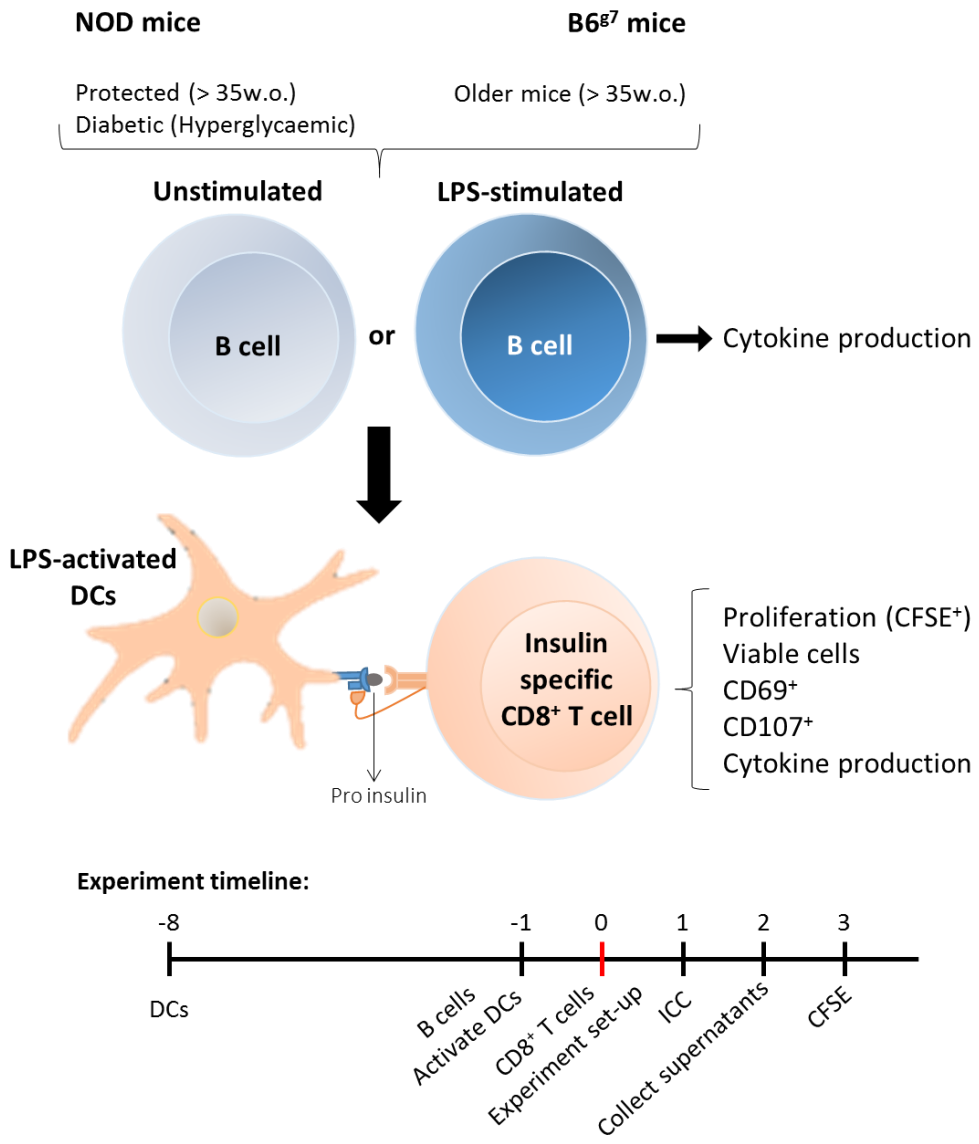

Figure 4.1 Experimental design for chapter 4 – the effect of B cells, as bystanders, on the activation of CD8 T cells. To evaluate B cell potential to regulate responses, unstimulated and LPS-stimulated B cells were cultured with CD8 T cells and PI homo DCs (endogenously expressing PI2). These B cells were from NOD and B6^{g7} mice, older than 35 weeks of age and also diabetic NOD mice (hyperglycaemic mice aged between 12-30 w.o.). In this system, B cells would not act as APCs to the CD8 T cells, as there was no exogenous antigen present. The read-outs for CD8 T cells and B cells are listed. The experimental timeline was as following: Dendritic cells were prepared from the bone marrow of PI homo mice on day -8 and were activated with LPS on day -1. Also on day -1, spleens from NOD or B6^{g7} mice were collected, processed, and the B cells were magnetically sorted and incubated for 24h with LPS or left unstimulated. On day 0, CD8 T cells from G9 mice were collected, processed, magnetically sorted, CFSE labelled and the three types of cells were incubated together. On day 1, cells were harvested for the analysis of CD107a and CD69 by flow cytometry. On day 2, supernatants were collected for cytokine multiplex assay. Finally on day 3, cells were harvested for proliferation, determination of viable cells and CD69.

4.3 The effect of B cells as bystanders in the activation of CD8 T cells by DCs

4.3.1 Proliferation, viable CD8 T cells and activation

To evaluate the effect of B cells on the activation of insulin-specific CD8 T cells, we analysed T cell proliferation, percentage of viable cells and activation (1 and 3 days after set-up).

Proliferation was determined by CFSE labelling 72h after the set-up (Day 0) and the gating strategy is explained in Figure 4.2a. Because the experiments were repeated at least 3 times and the staining for CFSE may vary, data shown in Figure 4.3a was normalized: Wells where B cells were not added (DCs and CD8 T cells only – a positive control) were taken as 100% for each experiment (represented by the dashed line in the graph). The percentages represent the increase or decrease from this control parameter, with the addition of unstimulated or LPS-stimulated B cells.

In all groups, the addition of unstimulated B cells to CD8 T cells + DCs led to T cell proliferation similar to or more than the proliferation seen in the control, implying they did not affect proliferation. However, when LPS-stimulated B cells were added to the system, the percentage of proliferation decreased from the control level in all groups. This difference was statistically significant when stimulated B cells were derived from NOD mice (protected and diabetic – $p < 0.01$ and $p < 0.05$, respectively), but was not as remarkable with $B6^{g7}$ B cells.

It is important to note that the analysis of proliferation as the percentage of dividing cells (decreasing signal for CFSE), as shown in this chapter, is incomplete and does not discriminate the nature of the dividing cells. It is not possible to determine, for example, if it is a case of few CD8 T cells dividing many times or many CD8 T cells dividing less. To complement the data shown here, an index of division should be performed and the graphs should be represented as histograms.

To evaluate whether this decreased proliferation was due to cell death, the percentage of live T cells was analysed. The gating strategy here was different (Figure 4.2b), to focus on the percentage of viable CD8 T cells, 72h after the set-up. Compared to the percentage of live T cells in the control well (black bar), the addition of unstimulated B cells or LPS-stimulated B cells from $B6^{g7}$ mice did not cause more CD8 T cell death. However, when activated B cells from NOD mice (protected and diabetic) were added

to the system, the percentage of viable T cells significantly decreased, compared to the system containing unstimulated NOD B cells, as illustrated in Figure 4.3b.

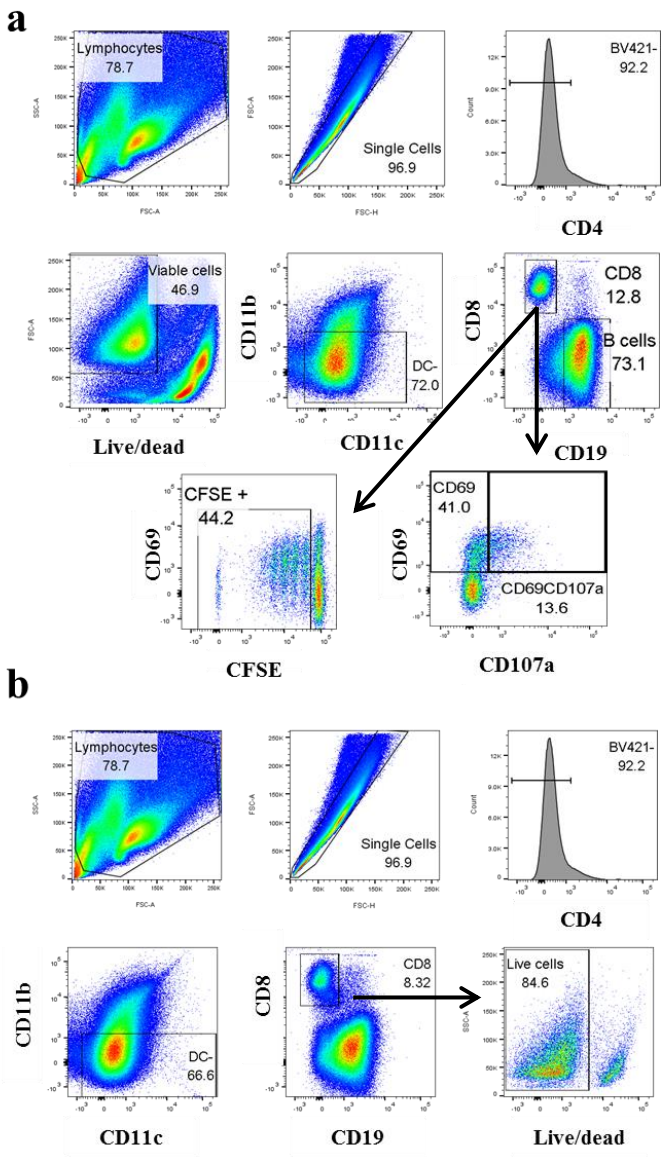

Figure 4.2 Example of the gating of flow cytometric plots used for the determination of CD8 T cell proliferation (CFSE), activation (CD69), degranulation (CD107a) and percentage of live CD8 T cells. After one week of culture, bone marrow DCs of PI homo mice were stimulated with LPS for 18h. Splenic B cells purified from NOD or $B6^{g7}$ mice were stimulated with LPS for 24h or left unstimulated. Splenic CD8 T cells (from G9 mice) were purified on the day of the set-up of the experiment and then labelled with CFSE for the evaluation of CD8 T cell proliferation. The experimental procedure was as follows: $2x10^5$ CD8 T cells, $4x10^5$ stimulated DCs and $1.4x10^6$ stimulated or unstimulated B cells were added to each well. After 24h and 72h of incubation, cells were harvested for antibody-staining and flow cytometric analysis. One example of the gating strategy for these experiments is found in (a): Lymphocytes ➔Single cells ➔Exclusion of any CD4 T cells in the culture ➔Viable cells ➔ Exclusion of DCs ($CD11b^-CD11c^-$) ➔Distinction between CD8 T cells and B cells (CD19). In the CD8 T cell pool, proliferation (CFSE dilution), activation ($CD69^+$) and degranulation ($CD107a^+$) were assessed. For the analysis of live CD8 T cells (b), the order of gating was Lymphocytes ➔Single cells ➔Exclusion of any CD4 T cells in the culture ➔ Exclusion of DCs ($CD11b^-CD11c^-$) ➔ Distinction between CD8 T cells and B cells (CD19) ➔ Viable cells.

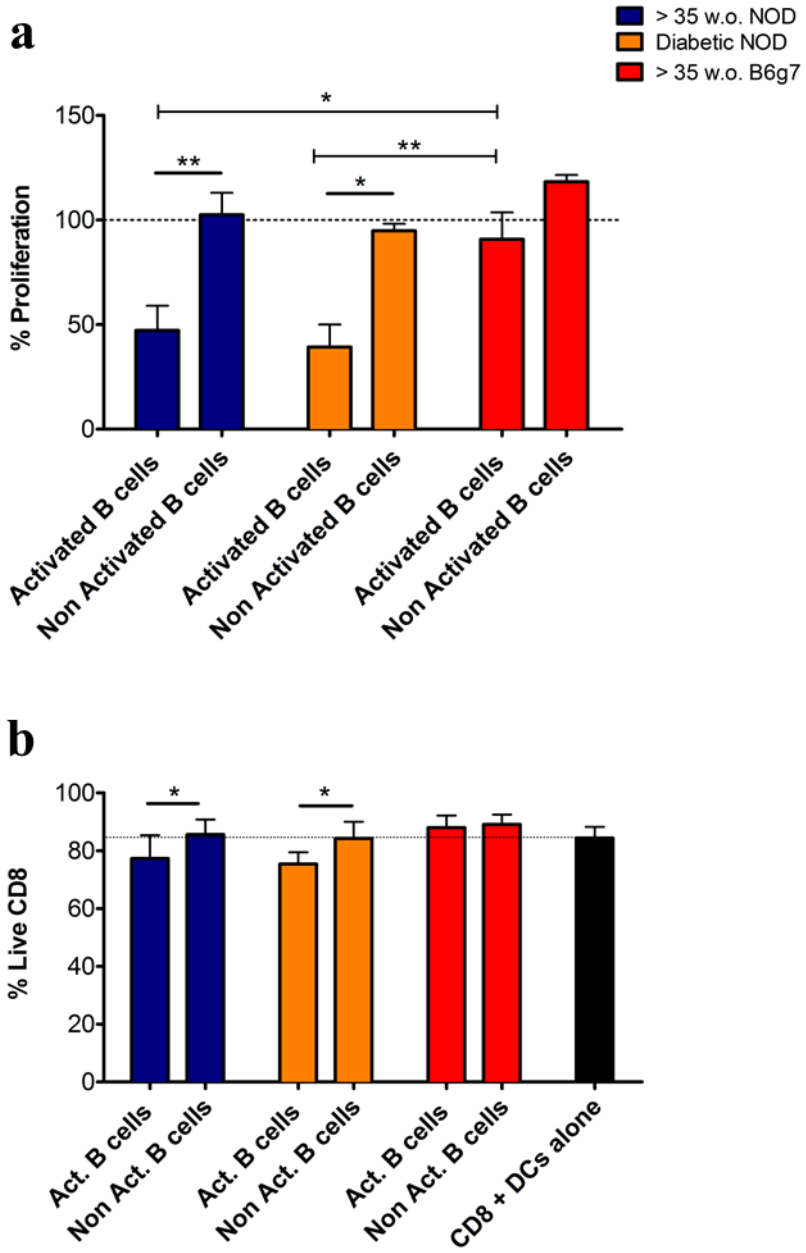

Figure 4.3 Decreased antigen-specific CD8 T cell proliferation and percentage of viable cells in the presence of LPS-stimulated NOD B cells. After culture for one week, bone marrow DCs from PI homo mice were stimulated with LPS for 18h. Splenic B cells from NOD or $B6^{g7}$ mice were stimulated with LPS for 24h or left unstimulated. Splenic CD8 T cells (from G9 mice) were purified on the day of the set-up of the experiment and labelled with CFSE for the evaluation of CD8 proliferation (a). The experimental procedure was as follows: $2x10^5$ CD8 T cells, $4x10^5$ stimulated DCs and $1.4x10^6$ stimulated or unstimulated B cells were added to each well. After 72h of incubation, cultures were harvested for flow cytometric staining – Live cells were gated as described previously and the percentages are shown in (b). The data are represented as mean and standard error and were analysed by Two-way ANOVA. n=3-4 individual experiments, each experiment using pooled spleen cells from 3-4 mice.

The percentages of CD8 T cells expressing CD69 were analysed 24h (Figure 4.4a) and 72h (Figure 4.4b) after the set-up.

Twenty-four hours after the set-up, CD8 T cells cultured with DCs alone had the highest frequencies of CD69, followed closely by CD8 T cells cultured with DCs and unstimulated B cells from NOD mice. The other groups had lower percentages of $CD8^{+}CD69^{+}$ T cells.

On the next time point, 72h after the set-up, most of the frequencies of $CD8^{+}CD69^{+}$ cells had increased when compared to the results seen at 24h. T cells cultured with DCs alone still had the highest frequencies of CD69 expression, but the percentages increased to almost the same level when B cells from $B6^{g7}$ mice were added. When LPS-stimulated B cells from NOD mice (protected and diabetic) were added to the system, the percentage of T cells expressing CD69 was the lowest and did not vary between the time points.

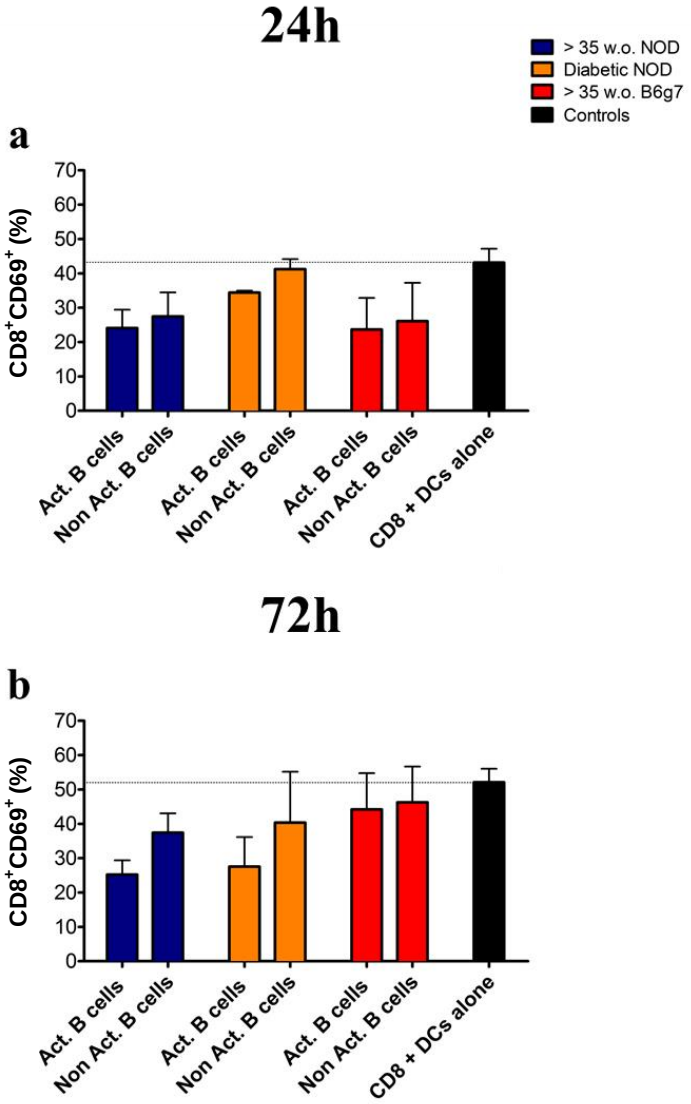

Figure 4.4 Activation of CD8 T cells cultured with B cells and DCs (percentage of $CD8^+CD69^+$ T cells). After culture for one week, bone marrow DCs from PI homo mice were stimulated with LPS for 18h. Splenic B cells from NOD or $B6^{g7}$ mice were stimulated with LPS for 24h or left unstimulated. Splenic CD8 T cells (from G9 mice) were purified on the day of the set-up of the experiment and labelled with CFSE for the evaluation of CD8 proliferation. The experimental procedure was as follows: $2x10^5$ CD8 T cells, $4x10^5$ stimulated DCs and $1.4x10^6$ stimulated or unstimulated B cells were added to each culture. After 24h (a) or 72h (b) of incubation, cultures were harvested for flow cytometric staining. The data are represented as mean and standard error and were analysed by Two-way ANOVA. n=3-4 individual experiments, each experiment using pooled spleen cells from 3-4 mice.

4.3.2 Markers of cytotoxicity (MIP1-β and CD107a)

Although proliferation and activation of T cells are essential parameters to study, the most important read-outs for CD8 T cells are those involved with inflammation and cytotoxic function. Hence, we analysed the concentration of MIP1-β, a chemokine that attracts cells to the site of inflammation, in the supernatants, together with the expression of CD107a, marker of degranulation, on CD8 T cells.

As illustrated in Figure 4.5a, all three types of cells (DCs, B and T cells) were able to secrete MIP1-β when cultured alone. Curiously, LPS-stimulated B cells from protected mice cultured alone secreted the highest concentration of this chemokine, followed by diabetic mice and then $B6^{g7}$ mice. Adding CD8 T cells and DCs together only resulted in an additive amount of MIP1-β secreted in the supernatant. The addition of unstimulated B cells to the system increased the concentration of this chemokine for all groups. This increase was seen on adding stimulated $B6^{g7}$ B cells. Although the high concentrations of MIP1-β secreted by LPS-stimulated B cells from protected mice cultured alone (indicating they were able to produce this chemokine), when cultured with CD8 T cells and DCs, the concentration was lower than for T cells + DCs alone. The same was observed for stimulated B cells from diabetic mice. In summary, the addition of LPS-stimulated B cells from NOD mice reduced the levels of MIP1-β in the supernatant, while unstimulated B cells had the opposite effect. However, as the assay was based on cytokines in the supernatants, it was not possible to determine which cell/cell groups was/were producing less MIP1-β in this system.

The next parameter analysed was the percentage of CD8 T cells expressing CD107a, a marker for degranulating cytotoxic cells (Figure 4.5b). While the percentage was around 15% for CD8 T cells cultured with DCs alone, when unstimulated B cells from diabetic mice were added to the system, this percentage increased. For all other culture conditions, the percentage of $CD8^{+}CD69^{+}CD107a^{+}$ T cells was lower; however, when LPS-stimulated B cells from diabetic mice were added the frequency was similar to the control cultures with CD8 T cells and DCs alone. Interestingly, addition of either stimulated or unstimulated B cells from protected mice and > 35 w.o. $B6^{g7}$ mice inhibited the expression of CD107a.

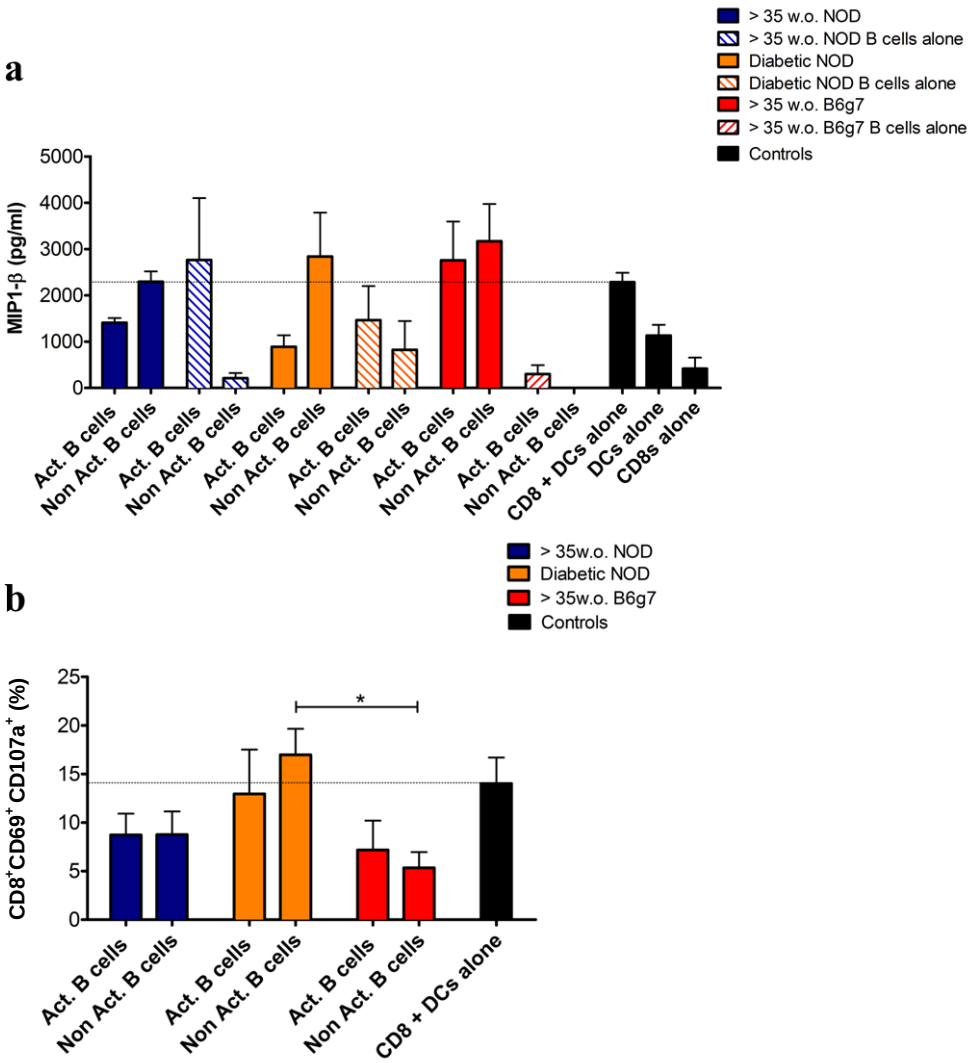

Figure 4.5 Concentration of MIP1-β in the supernatants of B cells cultured with CD8 T cells and DCs and percentage of T cell degranulation (percentage of $CD8^+CD69^+CD107a^+$). After culture for one week, bone marrow DCs from PI homo mice were stimulated with LPS for 18h. Splenic B cells were collected from NOD or $B6^{g7}$ mice and were left unstimulated or stimulated with LPS for 24h. Splenic CD8 T cells (from G9 mice) were purified on the day of the set-up of the experiment and labelled with CFSE for the evaluation of CD8 proliferation. The experimental procedure was as follows: $2x10^5$ CD8 T cells, $4x10^5$ stimulated DCs and $1.4x10^6$ stimulated or unstimulated B cells were added to each well. After 24h of incubation, wells were harvested for flow cytometric staining and after 48 hours the supernatants were collected for chemokine analysis. (a) MIP1-β was measured in the supernatant after 48 hours. The dashed line indicates the levels of MIP1-β produced by CD8 T cells + DCs cultured together. (b) For CD107a staining, the antibody was added to the wells 3h before harvesting. The dashed line indicates the percentage of cells expressing CD107a when CD8 T cells were cultured together with DC in the absence of B cells. The data are represented as mean and standard error and were analysed by Two-way ANOVA. n=3-4 individual experiments, each experiment using pooled spleen cells from 3-4 mice.

* $p < 0.05$

4.3.3 Secretion of inflammatory cytokines

The analysis of the results so far showed greater suppression of CD8 T cell activity by B cells stimulated with LPS when compared to unstimulated B cells. The results also showed that these findings were more accentuated when B cells were from NOD mice, especially protected NOD mice.

To better understand the effect of LPS stimulation on B cells, we also analysed the secretion of cytokines, starting with pro-inflammatory cytokines.

IFN-γ was undetectable from all of the cell types when cultured by themselves (B cells alone not shown). As observed in Figure 4.6a, when CD8 T cells were cultured with DCs, IFN-γ was secreted. The addition of unstimulated B cells from all groups resulted in no difference compared to positive control. LPS-stimulated B cells from protected mice and > 35 w.o. $B6^{g7}$ mice did not contribute or inhibit the concentration shown in the control well (similar values for the 3 groups). The addition of stimulated B cells from diabetic mice to the system inhibited the secretion of IFN-γ.

For TNF-α (Figure 4.6b), CD8 T cells and DCs, but not B cells produced the cytokine when cultured by themselves, (B cells not shown). TNF-α was considerably increased when DCs were cultured with CD8 T cells and the addition of unstimulated B cells did not affect this secretion. The addition of LPS-stimulated B cells of all three groups decreased the levels of TNF-α in the cultures, especially when B cells were from diabetic mice, which was statistically different from unstimulated B cells.

The IL-6 found in the supernatants (Figure 4.6c), appeared to be mostly secreted by DCs, as the levels in the cultures of DCs alone was similar to the levels when CD8 T cells and DCs were cultured together. The addition of B cells (stimulated or unstimulated) from diabetic mice did not alter these levels, while the addition of B cells from protected or > 35 w.o. $B6^{g7}$ mice decreased the concentration of IL-6, especially $B6^{g7}$ B cells.

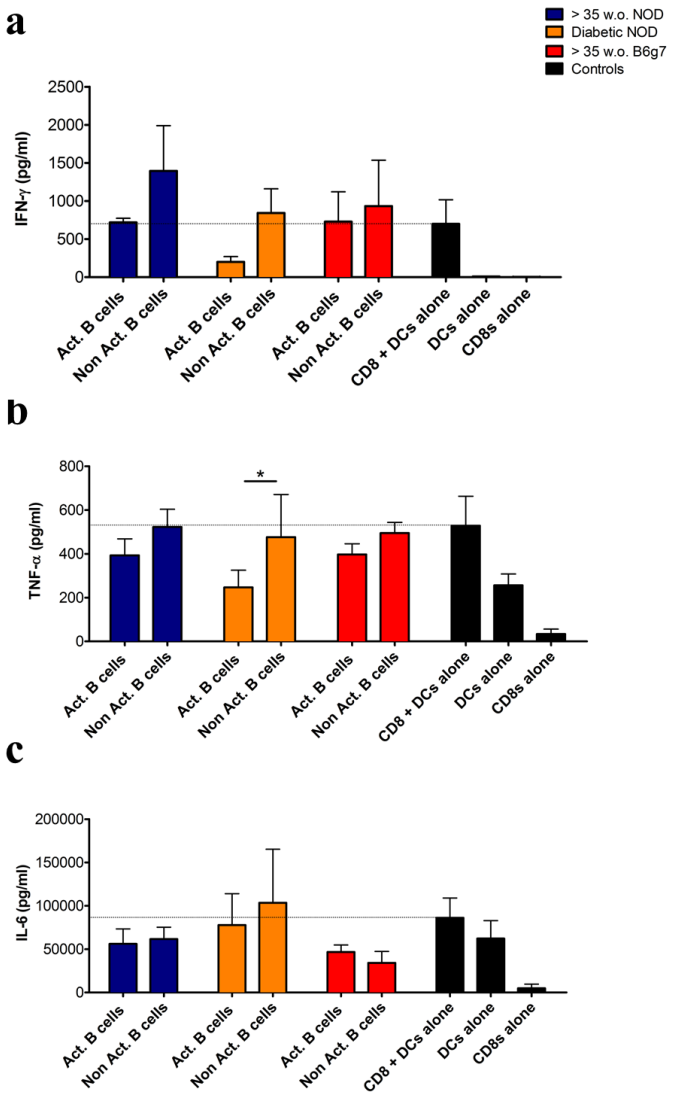

Figure 4.6 Concentration of IFN-γ, TNF-α and IL-6 in the supernatants of B cells cultured with CD8 T cells and DCs. After culture for one week, bone marrow DCs from PI homo mice were stimulated with LPS for 18h. Splenic B cells from NOD or $B6^{g7}$ mice were stimulated with LPS for 24h or left unstimulated. Splenic CD8 T cells (from G9 mice) were purified on the day of the set-up of the experiment and labelled with CFSE for the evaluation of CD8 proliferation. The experimental procedure was as follows: $2x10^5$ CD8 T cells, $4x10^5$ stimulated DCs and $1.4x10^6$ stimulated or unstimulated B cells were added to each well. After 48h, supernatants were collected and IFN-γ (a), TNF-α (b) and IL-6(c) were measured. The dashed line indicates the levels of the cytokines produced by CD8 T + DCs cells alone (no B cells added). The data are represented as mean and standard error and were analysed by Two-way ANOVA. n=3-4 individual experiments, each experiment using pooled spleen cells from 3-4 mice.

* $p < 0.05$

[One single outlying value was excluded from the IFN-γ results from the "> 35 w.o. NOD/Act B cells" group as the level far exceeded values obtained from these types of cultures (4650 pg/ml), compared to all other repetitions].

4.3.4 Secretion of IL-12p70

IL-12p70 is a cytokine produced mainly by DCs to induce Th1 responses. As illustrated in Figure 4.7, DCs cultured with CD8 T cells had higher levels than DCs cultured alone. The addition of B cells only altered IL-12p70 levels when B cells (stimulated and unstimulated) were from diabetic mice, inducing more secretion of IL-12p70. B cells from protected mice did not alter the levels and cultures with B cells from $B6^{g7}$ mice had lower concentrations of this cytokine.

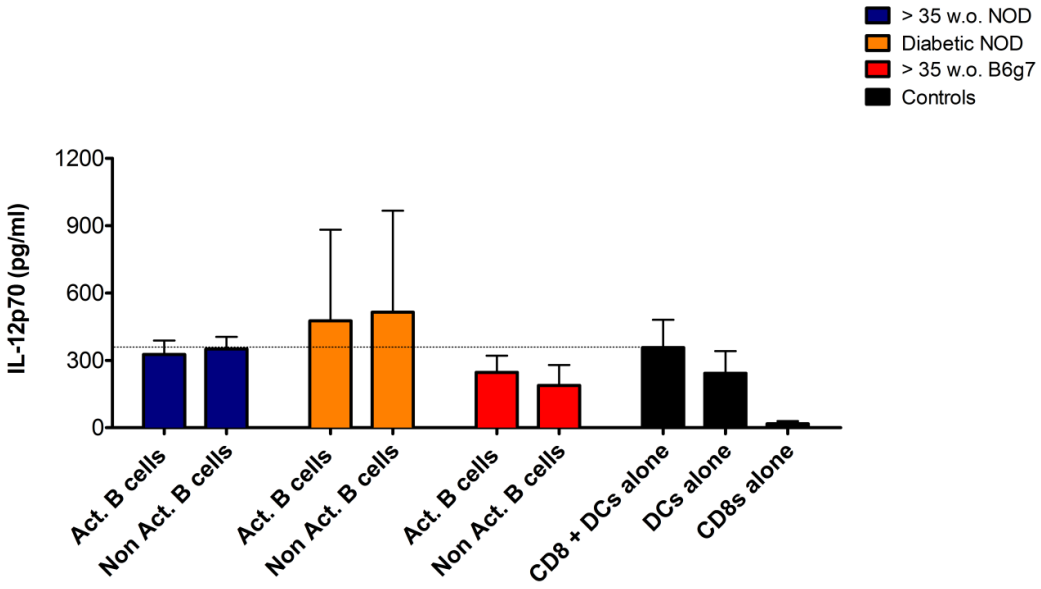

Figure 4.7 Concentration of IL-12p70 in the supernatants of B cells cultured with CD8 T cells and DCs. After culture for one week, bone marrow DCs from PI homo mice were stimulated with LPS for 18h. Splenic B cells from NOD or $B6^{g7}$ mice were stimulated with LPS for 24h or left unstimulated. Splenic CD8 T cells (from G9 mice) were purified on the day of the set-up of the experiment and labelled with CFSE for the evaluation of CD8 proliferation. The experimental procedure was as follows: $2x10^5$ CD8 T cells, $4x10^5$ stimulated DCs and $1.4x10^6$ stimulated or unstimulated B cells were added to each well. Forty-eight hours after the set-up, supernatants were collected and IL-12p70 was measured. The dashed line indicates the levels of the cytokines produced by CD8 T cells + DCs alone (no B cells added). The data are represented as mean and standard error and were analysed by Two-way ANOVA. n=3-4 individual experiments, each experiment using pooled spleen cells from 3-4 mice.

4.3.5 Secretion of regulatory cytokines

Ideally, IL-10 and TGF-β would be analysed by intracellular cytokine staining and analysed by flow cytometry as well as in the supernatants, to make this data comparable to the data in chapter 3. However, here, the percentages of B cells producing regulatory cytokines, as measured by intracellular cytoplasmic staining, were very low for all groups in this set of experiments. TGF-β was also undetectable by ELISA. Thus, the results shown here are only for the secretion of IL-10 in the supernatants.

The levels of IL-10 from the cultures of CD8 T cells alone, DCs alone or T cells and DCs together were also very low, indicating that it is likely that the IL-10 detected after the addition of B cells was secreted by the B cells.

As expected, based on the results of chapter 3, the levels of IL-10 were higher when B cells alone were stimulated with LPS, compared to unstimulated B cells (Figure 4.8). The difference between the groups was also in agreement with the data from the previous chapter. LPS-stimulated B cells from protected NOD mice produced more IL-10 than B cells from diabetic and $B6^{g7}$ mice.

When all cell types were cultured together, the secretion of IL-10 was boosted. Compared to CD8 T cells + DCs, the addition of unstimulated B cells increased the levels of IL-10; however, the increase was less in comparison to the addition of activated B cells. LPS-stimulated B cells, especially when B cells were derived from NOD mice, secreted high levels of IL-10 when in culture with T cells and DCs. The IL-10 level reached its highest (and was significantly different from control) when B cells were from protected mice.

4.3.6 Summary

The most important finding determined by the analysis of these results was the suppressive effect of activated B cells on antigen-specific CD8 T cells when in the presence of an antigen presenting cell (DC). Compared to cultures where B cells were not added or to cultures with unstimulated B cells, LPS-stimulated B cells reduced proliferation, activation (percentage of $CD69^+$ cells), degranulation (frequency of $CD69CD107a^+$ cells) and secretion of MIP1-β, IFN-γ, TNF-α and IL-6. On the other hand, activated B cells also increased CD8 T cell death and the secretion of IL-10. This

effect was more accentuated in B cells from NOD mice, especially protected NOD mice, when compared to B cells from $B6^{g7}$ mice.

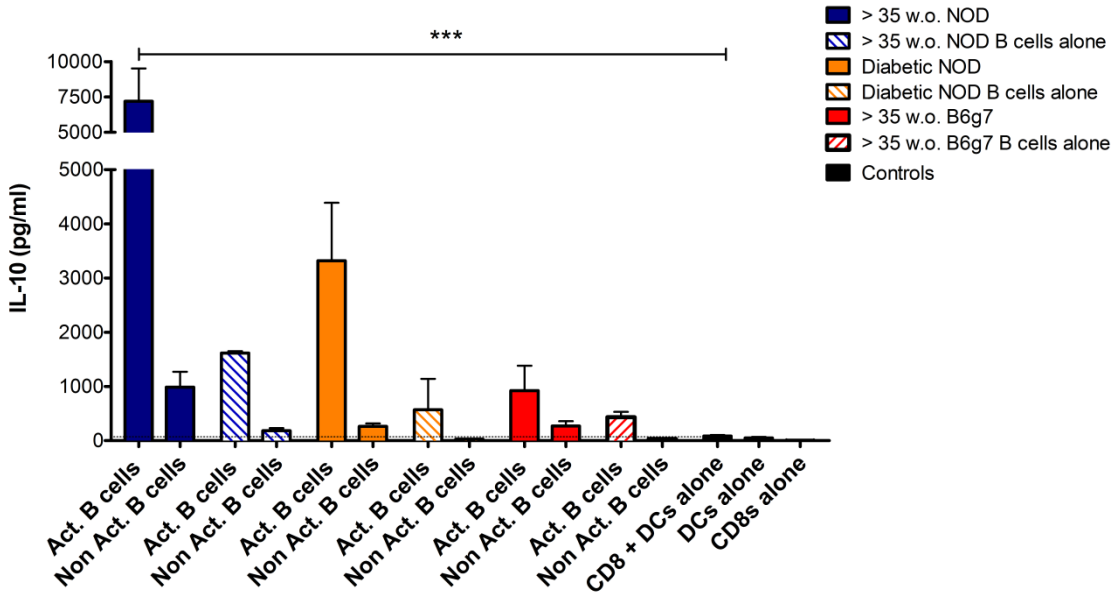

Figure 4.8 Concentration of IL-10 in the supernatants of B cells cultured with CD8 T cells and DCs. After culture for one week, bone marrow DCs from PI homo mice were stimulated with LPS for 18h. Splenic B cells from NOD or $B6^{g7}$ mice were stimulated with LPS for 24h or left unstimulated. Splenic CD8 T cells (from G9 mice) were purified on the day of the set-up of the experiment and labelled with CFSE for the evaluation of CD8 proliferation. The experimental procedure was as follows: $2x10^5$ CD8 T cells, $4x10^5$ stimulated DCs and $1.4x10^6$ stimulated or unstimulated B cells were added to each well. Forty-eight hours after the set-up, supernatants were collected and IL-10 was measured. The data are represented as mean and standard error and were analysed by Two-way ANOVA. n=3-4 individual experiments, each experiment using pooled spleen cells from 3-4 mice.

* $p < 0.05$

[One single outlying value was excluded from the "Diabetic NOD/Act B cells" group as the level far exceeded values obtained from these types of cultures (23700 pg/ml), compared to all other repetitions].

4.4 Discussion

After demonstrating that protected NOD mice had more baseline IL-10 producing B cells than diabetic mice and age-matched $B6^{g7}$ mice which increased more on stimulation, it was of importance to test whether these B cells would also be able to suppress inflammatory responses in a more efficient manner.

To analyse the suppressive effect of B cells, we used a system where dendritic cells present proinsulin to insulin-specific CD8 T cells without the addition of exogenous peptide in the culture. In this system, the B cells added in culture would only modulate the response by interacting with one or both of the cells, in a non-antigen-specific manner. B cells from all three groups (protected and diabetic NOD mice and > 35 w.o. $B6^{g7}$ mice) were left unstimulated or cultured with LPS for 24h prior to the set-up of cultures with CD8 T cells and the dendritic cells.

We investigated the role of B cells in influencing proliferation, the cytotoxic activity of CD8 T cells and chemokine and cytokine production. As discussed previously, in type 1 diabetes the interaction between B and CD8 T cells has been shown to induce pathogenic activity (Brodie et al. 2008). Indeed, here we showed that unstimulated B cells increased markers of degranulation and the levels of inflammatory cytokines.

Interestingly, when LPS-stimulated B cells were added to the wells with DCs and CD8 T cells, the effect was the opposite. Activated B cells inhibited the activation of CD8 T cells and suppressed inflammatory cytokine production, surprisingly mostly by the stimulated B cells from the diabetic mice. Conversely, the levels of IL-10 increased to their highest with the stimulated B cells. Once again, the outcomes were more noticeable with B cells from NOD mice, compared with B cells from $B6^{g7}$ mice.

Although B cells from protected mice added to the system caused less degranulation of CD8 T cells, the reduced percentage of live T cells was observed when these cells were cultured with B cells from both protected and diabetic mice. The ability of LPS-stimulated B cells from NOD mice to cause apoptosis of diabetogenic T cells has been described in the literature and was TGF-β-dependent (Tian et al. 2001). As shown in chapter 3, B cells from protected and diabetic NOD mice had similar percentages of B cells producing this cytokine; therefore, our new observations agree with previous findings. One limitation of this investigation was not having data for TGF-β being

released by B cells, as there are also studies in the literature associating B cell regulation of CD8 T cells to this cytokine (Parekh et al. 2003).

Oncogenic viruses designated Py can induce two different fates, depending on the strain of mice into which they are inoculated. In some mice, showing a predominant production of IL-12 in the spleen, the cytotoxic response was optimal and tumours were controlled; however, in another strain, IL-10 was the dominant cytokine and CD8 T cells did not exert optimal cytotoxicity. They observed that the main cells producing this IL-10 were B cells and the main difference between both strains was the expression of TLR-4 (Velupillai et al. 2006). Although TLR-4 is associated with development of diabetes (inducing the secretion of inflammatory cytokines when activated in monocytes), TLR-4$^{-/-}$ transgenic NOD mice have accelerated diabetes (Gulden et al. 2013). Therefore, the difference between the expression of TLR-4 on B cells of protected and diabetic NOD mice (which has already been raised as a question arising from the results presented in chapter 3) might be the key to understanding these results.

One interesting finding here was that B cells from diabetic NOD mice helped DCs to increase their production of IL-12p70, while in protected NOD mice the levels were similar to DCs cultured with CD8 T cells alone. These observations were similar for stimulated and unstimulated B cells. It is already known that DCs tend to shift from the Th1 path and have reduced secretion of IL-12 when cultured in the presence of IL-10 (De Smedt et al. 1997). In our system, however, the reduction of DC activity might have not been completely dependent on IL-10, as the effect was also seen with unstimulated B cells from protected mice (less IL-10 in the supernatant than cultures with activated B cells from diabetic NOD mice). Experiments utilising the addition of anti-IL-10 to the system might give us an insight of how much of this effect was IL-10-dependent.

The addition of LPS-stimulated B cells from protected mice did not change or in fact increased the secretion of IFN-γ, TNF-α and IL-6 (in comparison to control CD8 T cells + DCs and to stimulated B cells from the other groups). These results indicate that the pool of B cells was heterogenous, containing not only regulatory B cells. They also suggest that protected mice are as able to generate inflammatory responses as are diabetic mice, but they may also have more capacity to regulate this response.

Furthermore, IL-10 production from B cells cultured alone was less than when B cells were cultured with CD8 T cells and DCs which suggests that regulatory B cells need

some inflammatory signals to produce increased concentrations of IL-10. This observation confirms findings of others as discussed before in the literature (Rosser et al. 2014).

As explained in the section 4.3.5, ideally both intracellular cytoplasmic cytokine (ICC) staining as well as concentration of cytokines in the supernatant would be analysed. Each provides different information that would help us better understand the interaction between the cells: ICC gives valuable information about which cell is producing the cytokine, while with MSD data, this is not possible. On the other hand, cytoplasmic cytokine is not necessarily cytokine that will be secreted; and that is where MSD is also important.

These findings propose a regulatory function of LPS-stimulated B cells when cultured with CD8 T cells and DCs, but there are many questions raised from these results. The direction these experiments could take for further investigations will be discussed in more detail in chapter 6.

5. Effect of depletion and repopulation in regulatory B cell subsets in Type 1 Diabetes

5.1 Introduction and Objectives

CD20 is a molecule expressed by B cells from early stages (late pre-B cells) until plasma cells and is well conserved in mice and humans (73% homologous). It is involved in the regulation of calcium influx, being important for the initiation of the transition from the G_0 phase to G_1 in the cell cycle (Golay et al. 1985; Tedder and Engel 1994). CD20 is considered to be a good target for depletion strategies as it is expressed in the majority of B cells and is not internalized or solubilized (Reff et al. 1994).

5.1.1 Anti-CD20-mediated B cell depletion in humans

Monoclonal antibodies targeting CD20 were first used as a treatment for non-Hodgkin's lymphomas. A chimeric anti-CD20 (murine variable regions and human Fc) called C2B8 (now known as Rituximab) was designed by Reff and colleagues and proved to be more effective than murine anti-CD20 in killing neoplastic B cells, with just mild adverse effects. As CD20 is not expressed by fully differentiated plasma cells (hence they are not depleted), antibody serum levels were not altered and susceptibility to infections was not increased (Reff et al. 1994; Maloney et al. 1997).

The main mechanism of action of the CD20 antibody is antibody-dependent cellular cytotoxicity, transforming B cells to be targets for macrophages. Binding to CD20 antibodies can also induce apoptosis and complement-mediated lysis (Gopal and Press 1999). It is important to note, however, that in NOD mice this last mechanism might not be as relevant, as they are not able to produce the C5 factor of complement (Baxter and Cooke 1993).

Having been approved for treatment of patients with lymphomas, the use of anti-CD20 mAbs in clinical trials was expanded to autoimmune diseases. Clinical trials in patients with systemic lupus erythematous (Leandro et al. 2002), and even diseases that are more T-cell related, such as rheumatoid arthritis (Edwards and Cambridge 2001) and multiple sclerosis (Cross et al. 2006) resulted in reduced symptoms, lasting longer than the

treatment. As seen in lymphomas, they had good efficacy and no severe adverse events were reported.

In Type 1 Diabetes, as discussed in chapter 1, patients who received rituximab needed less daily insulin and had better preserved beta-cell function. Compared to placebo, the treatment delayed C-peptide fall by 8.2 months. The effects, however, were temporary (Pescovitz et al. 2009; Pescovitz et al. 2014).

5.1.2 Anti-CD20-mediated B cell depletion in mice

Monoclonal anti-CD20 antibodies are already used therapeutically in humans. A full understanding of the mechanisms and the degree of B depletion in lymphoid organs in different diseases has been obtained by a number of complementary studies in animal models.

To mimic the treatment in humans as closely as possible, Gong and colleagues created C57BL/6 mice carrying genes encoding human CD20. As seen in humans, peripheral B cells were completely depleted after treatment. In lymphoid organs, the efficiency of B cell depletion was dependent on the cell flux: B cells in lymph nodes, with high circulation of cells, were depleted more quickly than peritoneal B cells (B cells recirculate more slowly). Depletion of macrophages impaired anti-CD20 action, indicating that they are the major cell type involved in killing the B cells (Gong et al. 2005).

Mark Shlomchik's group, almost at the same time, crossed a SLE-prone mouse strain (MRL/*lpr*) with transgenic mice expressing human CD20 (hCD20), initiating the investigation of B cell depletion in autoimmune diseases (Ahuja et al. 2007). They observed that, independent of the anti-CD20 used (they tested rituximab, 2H7, 8B9 and anti-mCD20 antibodies), the depletion of B cells was always better in BALB/c transgenic mice than in the autoimmune models. For all antibodies tested, lymph node B cells were more susceptible to depletion than splenic and peritoneal cavity B cells. Murine anti-human CD20 clone 2H7 binds to the same peptide targeted by rituximab (Du et al. 2008) and was chosen for subsequent experiments.

After dose adjustments for better results, the effect of B cell depletion in SLE was investigated. The treatment decreased the percentage of memory T cells, the infiltration

in the kidneys and the serum levels of IgG1 and IgG2a (but not IgM and IgG2b). Although CD20 molecules are known to not be expressed in plasma cells, around 20% of $CD138^+$ plasmablasts expressed the molecule in these experiments, which probably contributed to decreased antibody levels in the blood (Ahuja et al. 2007). The rationale for the use of B cell depletion as a treatment in SLE is clear, as autoantibodies have a major role in SLE.

As discussed previously, T cells are the main type of lymphocytes linked to type 1 diabetes. Despite the measurement of autoantibodies to insulin and other islet proteins as markers for the development of the disease, they have not been shown to be major contributors in the pathogenesis of T1D. However, B cells can exert a role as APC and modulate T cell responses by producing cytokines, and clinical trials of anti-B cell therapy have shown some promising results, although the effects were transient.

Therefore, to investigate the mechanisms behind the efficacy of B cell depletion in type 1 diabetes, NOD mice were crossed with transgenic mice expressing human CD20 to generate hCD20/NOD mice (Hu et al. 2007).

The hCD20/NOD mice were evaluated and compared to NOD mice and there were no significant differences between the strains for number and function of cells, expression of surface markers and incidence of diabetes (Hu et al. 2007). These mice then received 4 intravenous (i.v.) injections of 2H7 or control IgG in 9 days (one every 3 days). Depletion could be detected in peripheral blood as early as 1 hour after the first injection, repopulation started 3 weeks after last injection and B cell populations were fully recovered after 12 weeks. The cycle of injections was given at different ages (pre-insulitis, pre-diabetes and after the diagnosis of diabetes), to study the role of B cells in different phases of type 1 diabetes development.

Mice injected at pre-insulitis and pre-diabetes stages (4 weeks of age or 9 weeks of age, respectively) had delayed disease and a reduced overall percentage incidence. In the pancreas, the infiltration was significantly smaller in mice treated with 2H7 for the first two months, when compared to controls. By the end of the observations, however, there was no difference in the score of insulitis in treated and control mice. Nevertheless, this analysis was done by histology and the quality of the infiltration was not investigated at that time (Hu et al. 2007).

Diabetic mice (receiving daily insulin to remain as healthy as possible for the experiments) also received one cycle of injections. Five of fourteen hCD20/NOD mice receiving 2H7 returned to euglycaemia after the treatment and the daily insulin injections were withdrawn. In contrast, no mice in the control group had blood glucose levels that reverted to normal (Hu et al. 2007).

These experiments showed not only that B cells are important at the onset and development of type 1 diabetes, but they also confirmed the effect of B cell depletion as a treatment. However the effects lasted longer than the period when the cells were absent and it was postulated that the mechanisms involved were other than simple deletion of pathogenic B cells.

The adoptive co-transfer of whole splenocyte populations or B cells alone or CD4 T cells alone from 2H7-treated mice to NOD/SCID mice (also receiving spleen cells from diabetic mice to trigger the disease), conferred protection against diabetes, when compared to mice receiving the same populations of cells from IgG-control treated hCD20/NOD mice. Together with the increased percentage of transitional B cells, $CD4^+CD25^+Foxp3^+$ T cells and CTLA-4^+ cells, these results showed that after B cell depletion, the repopulated B cell compartment was more regulatory and modulated the T cell compartment as well (Hu et al. 2007).

The increased interest in regulatory B cells in the past years led to questions about how B cell depletion affects these populations. Obtaining the answer to some of these questions is the subject of this chapter.

5.1.3 Objectives

The aims of the experiments shown in this chapter were:

1) To study the effect of B cell depletion and repopulation on the subpopulations of B cells in hCD20 NOD mice, particularly regulatory B cell subsets;

2) To evaluate cytokine production after B cell depletion in young hCD20 NOD mice;

Our hypothesis was that regulatory B cells could be important in the protection against type 1 diabetes seen in mice treated with anti-CD20.

5.2 Experimental design

5.2.1 B cell depletion protocol

The experiments shown here were designed based on the work done by Hu and colleagues (Hu et al. 2007) and the results from previous chapters.

Female NOD mice have a higher incidence of diabetes and are usually chosen for the study of type 1 diabetes. For that reason, B cell depletion was not performed in male hCD20/NOD mice for these studies.

The cycle of injections was modified in two aspects from the methods described by Hu and colleagues: 1) Pilot experiments showed that 4 intravenous (i.v.) injections compared with 1 i.v. and 3 intraperitoneal (i.p.) injections induced a similar degree of depletion, so we decided to have a cycle with 1 intravenous and 3 administrations via the intraperitoneal route, to reduce stress for the mice. 2) The second, third and fourth injections were reduced from 0.25mg/mouse to 0.2mg/mouse. Once again, the amplitude of the depletion was not affected.

To study the effect of B cell depletion, mice were injected when they were pre-diabetic (6-8 weeks old – young group). Depletion of diabetic mice, although done previously by other groups, proved to be difficult. It was rare to have two hCD20/NOD mice with hyperglycaemia at the same time (one control, one depleted) and different concentrations of insulin (administered daily to keep diabetic mice healthy) were needed, to avoid hypoglycaemia and death. Therefore, diabetic mice were not included in our studies reported here.

Female hCD20/NOD mice received one cycle of injections (anti-hCD20 antibody, clone 2H7 or an IgG control, clone MPC-11) and the time points chosen had the last injection as the start point. Cells from spleen, pancreatic and mesenteric lymph nodes, Peyer's patches and bone marrow were studied at 24h, 1 week, 8 weeks, 12 weeks after last injection (Figure 5.1) and spleen cells were also collected 30 weeks after the last injection, for functional studies. Data from all organs were also collected at the 4th week, but it is not shown here because of similarity to results seen 1 week after the last injection.

By 12 weeks, B cells had returned and mice were repopulated in the bone marrow and the lymphoid organs. Pancreata from these mice were collected for the study of the effect of B cell depletion on the quality of lymphocyte infiltration by Joanne Boldison, collaborating in this project.

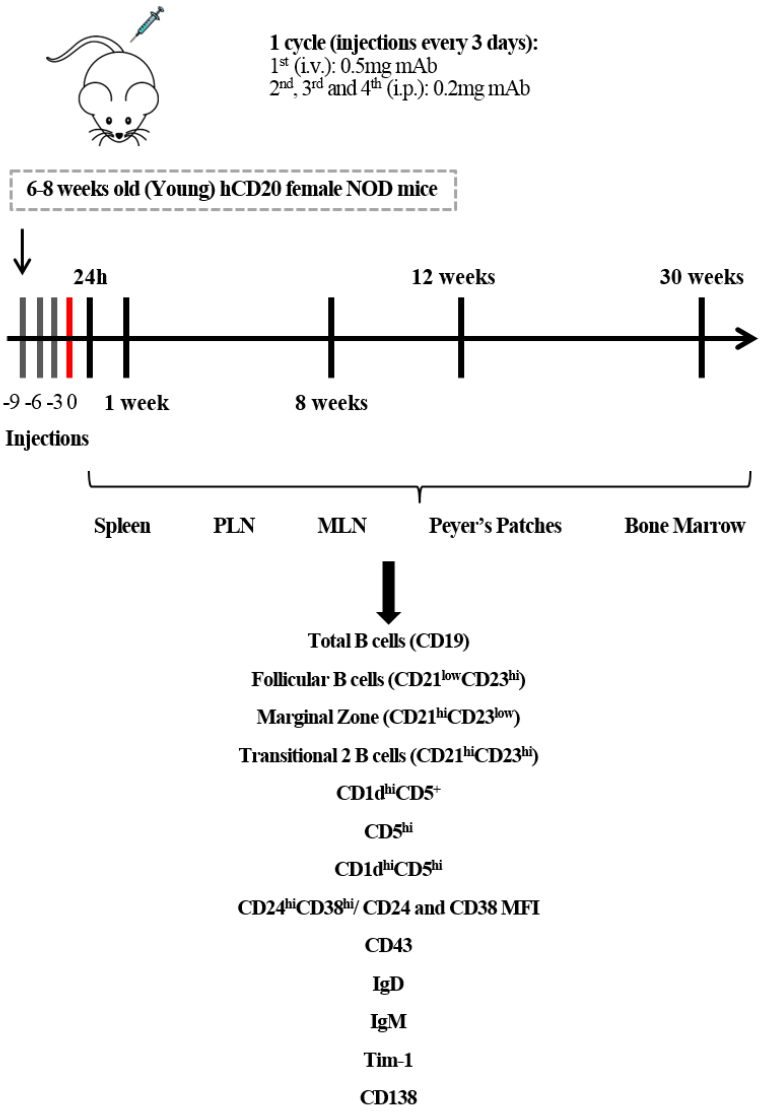

Figure 5.1 Experimental design for the studies of B cell depletion and repopulation in NOD mice expressing human CD20. Female hCD20/NOD mice received one cycle of injections with 2H7 antibodies or control IgG. One cycle comprised 4 injections and the time points for experiments were determined after the last injection. The organs chosen for the investigations were: spleen, pancreatic and mesenteric lymph nodes, Peyer's patches and bone marrow. The subpopulations chosen for investigation are also listed.

5.2.2 B cell markers analysed by flow cytometry

Figure 5.2 shows an example of the gating strategy used for spleen B cells for the flow cytometric plots used to investigate subpopulations in this chapter. The same gates were used for the other lymphoid organs, with the exception of $CD19^{+}CD24^{hi}CD38^{hi}$ (Figure 5.2c). Although more than 90% of all B cells express CD24 and CD38 in the lymph nodes, Peyer's patches and bone marrow, this population of B cells is not as prominent as seen in the spleen. Therefore, the markers CD24 and CD38 were analysed separated, by their median of fluorescent intensity (MFI). The MFI demonstrates the level of expression of the markers on the cells, so a greater MFI indicates more expression of these markers on the surface of the cells. These gating strategies were also used for all further analysis.

In addition to the surface markers studied previously in chapter 3 (T2, MZ, $CD1d^{hi}CD5^{+}$ and $CD24^{hi}CD38^{hi}$), the analysis of more markers was possible for these experiments: IgM, IgD, CD43, CD138 and Tim-1 were studied. IgM and IgD are isotypes of the membrane-bound antibody (BCR) expressed on the surface of B cells, CD43 is a marker present in pro-B cells in the bone marrow and also in B-1 B cells in the periphery (Wells et al. 1994). CD138 is a marker for plasma cells and Tim-1 is believed to be involved with IL-10 production (Ding et al. 2011).

At each time point, lymphocytes were stained for surface markers. At the 8^{th}, 12^{th} and 30^{th} week after the last injection, in addition to extracellular molecules, the cytokine production in the spleen by intracellular staining was also analysed by flow cytometry.

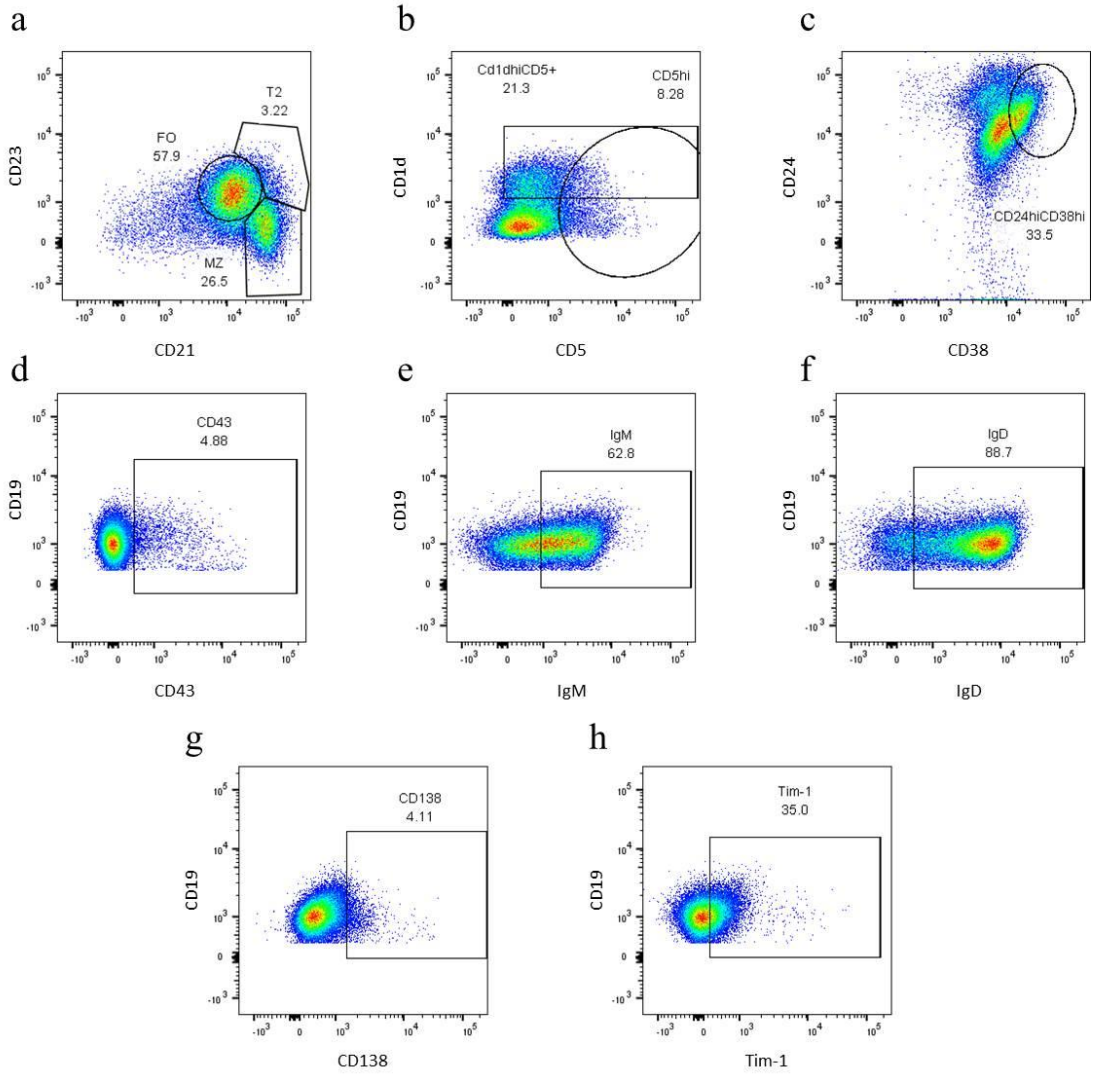

Figure 5.2 Example of flow cytometric plots used for the B cell depletion analysis in the spleen. These experiments were performed *ex vivo* with cells from lymphoid organs of female hCD20/NOD mice and stained with monoclonal antibodies. For every sample, 30,000 CD19 cells were acquired. The division of B cells into Follicular B cells (FO), Marginal zone (MZ) and Transitional B cells (T2) is shown in (a); $CD1d^{hi}CD5^{+}$ and $CD5^{hi}$ are shown in (b). The intersection of these two populations was calculated as a Boolean gate and called $CD1d^{hi}CD5^{hi}$ in this chapter (not shown). Figure (c) represents the $CD24^{hi}CD38^{hi}$ gate in the spleen. The expression of CD43, a marker for B-1 cells, is shown in (d). Figures (e) and (f) illustrate the two immunoglobulin isotypes expressed on the B cell surface and exerting the B cell receptor functions: IgM and IgD, respectively. Lastly, figure (g) shows the expression of CD138, marker for plasma cells and (h) shows the expression of Tim-1, a receptor believed to be involved in the production of IL-10. Gates were set based on FMOs and isotype controls – Figure A2, in the appendix.

5.3 Expression of hCD20 in different populations and organs

To confirm that the phenotype of our hCD20/NOD mice was similar to those described in the literature, we analysed the percentage of B cells expressing human CD20 in the organs to be studied and the markers of interest (described previously and shown in Figure 5.2). Figure 5.3a shows the percentage of $hCD20^{+}$ cells in total B cells (CD19, the first column) and all subpopulations studied in the spleen. Although the percentage of B cells expressing hCD20 was close to 100%, the highest frequencies were seen in Transitional B cells ($CD21^{hi}CD23^{hi}$) and $CD24^{hi}CD38^{hi}$ cells, while $CD19^{+}CD43^{+}$ cells had the lowest percentage of cells expressing hCD20.

In the pancreatic lymph nodes (PLN), Figure 5.3b, $CD19^{+}CD43^{+}$ cells and $CD5^{hi}$ cells were seen at a lower frequency, in contrast to the higher percentage found in the spleen. As MZ and T2 subsets were only seen in the spleen in mice, the percentages of hCD20 expressed in the marginal zone cells (including CD1d) and transitional B cell phenotypes were not investigated in lymph nodes and bone marrow.

The same pattern observed in PLNs was also seen in mesenteric lymph nodes (MLN - Figure 5.4a). Compared to the LNs and spleen, Peyer's patches (PP - Figure 5.4b) had lower percentages of hCD20 expressed in their B cells (an average of around 89%, while the other organs were 94-96%).

In the bone marrow, Figure 5.4c, the cells were more heterogeneous. This was expected, as the bone marrow contains B cells at different stages of development, some of them expressing CD20 and others not. As expected, the percentages were comparable to the spleen in the B cells expressing CD21, CD23 and IgD, as they are the cells that have been recirculating. $CD43^{+}$ B cells again had the lowest frequencies of hCD20, followed by $CD19^{+}CD5^{hi}$ cells. In this case, the percentage of cells expressing hCD20 was lower than 50%.

It is interesting to note that, in contrast to the literature, $CD138^{+}$ B cells in our hCD20/NOD mice had high expression of hCD20 (> 90% in the spleen, LNs and Peyer's patches). Nevertheless, these $CD138^{+}$ cells were gated in $CD19^{+}$ B cells, so they are considered short-lived plasmablasts and not fully mature plasma cells (Nutt et al. 2015). In the bone marrow, the percentage of $CD19^{+}CD138^{+}$ cells expressing hCD20 was around 40%. Thus, these plasmablasts are likely to become plasma cells.

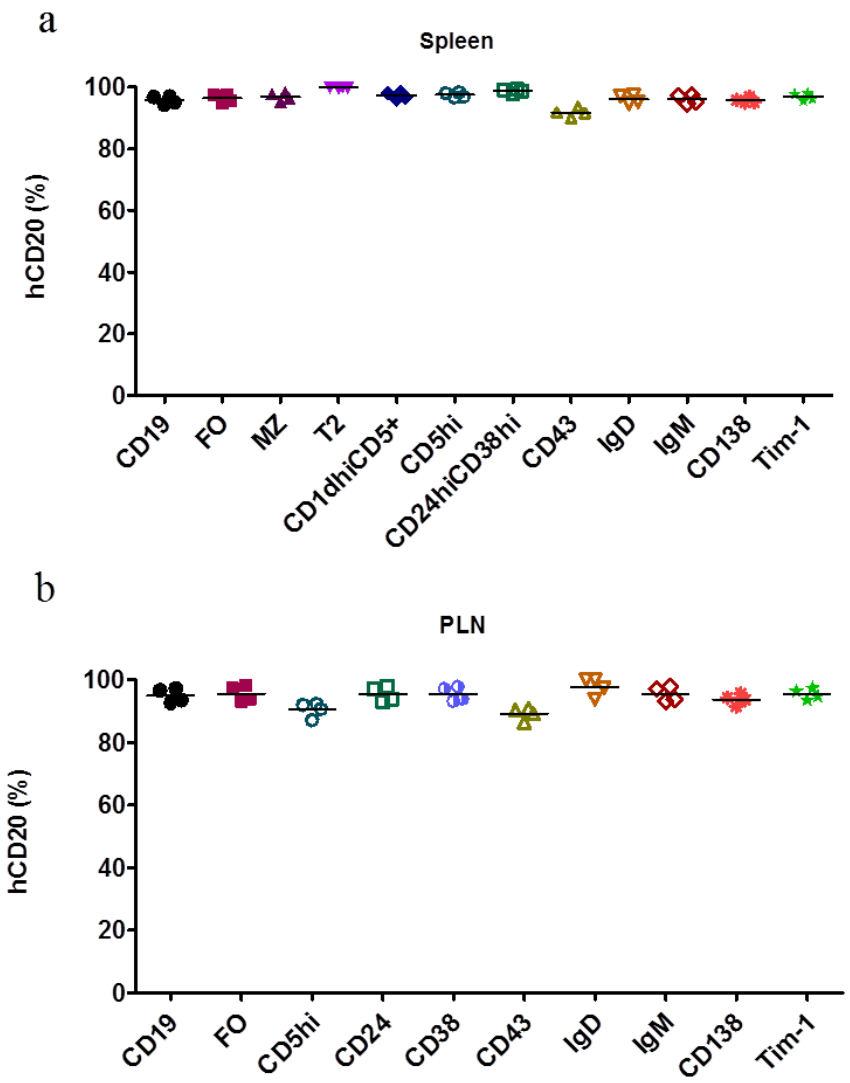

Figure 5.3 Frequency of human CD20 in B cells and their subpopulations. Spleen cells (a) and cells from pancreatic lymph nodes (b) were stained for CD19, hCD20 and other B cell markers, for *ex vivo* analysis by flow cytometry. Each symbol represents one mouse. CD19, the first column, represents the whole B cell population and all the following markers were analysed on cells gated using these individual markers. "FO" represents the column for follicular B cells ($CD21^{low}CD23^{hi}$); "MZ" represents marginal zone B cells ($CD21^{hi}CD23^{low}$) and T2 represents transitional 2 B cells ($CD21^{hi}CD23^{hi}$). The assay was performed in four hCD20 female mice aged 11 weeks old.

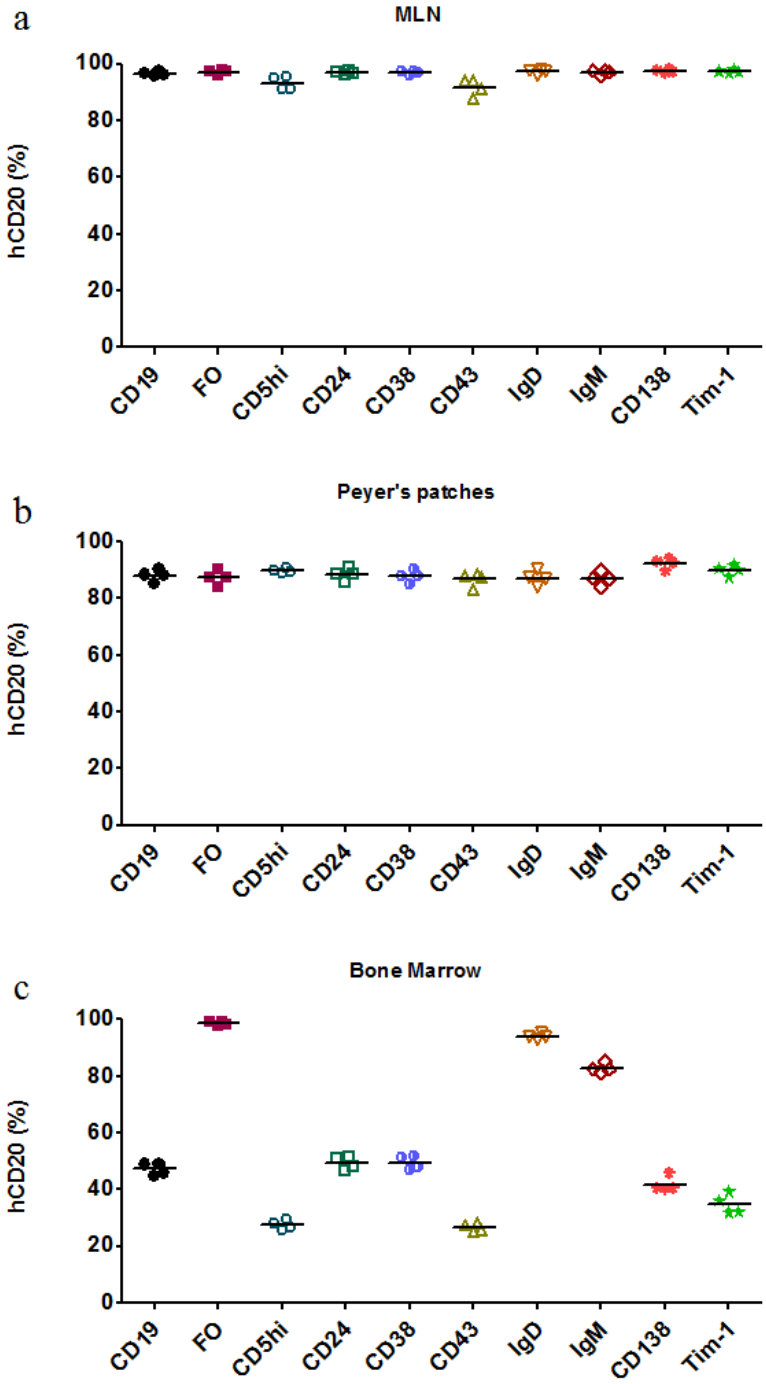

Figure 5.4 Frequency of human CD20 in B cells and their subpopulations. Cells from mesenteric lymph nodes (a), Peyer's patches (b) and bone marrow (c) were stained for CD19, hCD20 and other B cell markers, for *ex vivo* analysis by flow cytometry. Each symbol represents one mouse. CD19, the first column, represents the whole B cell population and all the following markers were analysed on cells gated using these individual markers. "FO" represents the column for follicular B cells ($CD21^{low}CD23^{hi}$). The assay was performed in four hCD20 female mice aged 11 weeks old.

As the majority of the B cell subpopulations had a high hCD20 expression and a similar percentage of cells expressing hCD20, we also investigated the MFI of hCD20 on each B cell subset.

In the spleen (Figure 5.5a), the highest MFI of hCD20 on the cells was seen in T2 B cells. Unexpectedly, the MFI in $CD138^+$ cells was also high, compared to the other subpopulations. In the PLNs (Figure 5.5b), on the other hand, there was less variation in the MFIs (between 1300 and 2300) on the B cells.

In the MLNs (Figure 5.6a), the variation was larger than in the PLNs and the highest MFIs were again seen in $CD138^+$ B cells. B cells from Peyer's patches (Figure 5.6b) not only had lower frequencies of hCD20, but also lower MFIs, when compared to the LNs and spleen.

In the bone marrow (Figure 5.6c), as seen for the percentages, the results were very heterogeneous. The MFI in cells expressing FO markers was very similar to those observed in the spleen. In this organ, the MFI in $CD138^+$ was low, combined with a low frequency of cells expressing the marker.

In summary, the investigation of the expression of hCD20 in the whole population and subpopulations of B cells showed that in the spleen, LNs and Peyer's patches, the expression was high in all subsets (with a lower frequency observed only in $CD43^+$ B cells). Therefore, any heterogeneity in depletion effects observed was unlikely to be related to the level of expression of hCD20 on the cells.

The MFI results showed that B cells in the spleen express more hCD20 than in the LNs and Peyer's patches. The results in cells from the bone marrow were more diverse than the other organs. However this is not surprising, as the B cell population in the bone marrow comprises B cells in developmental stages prior to CD20 expression and plasmablasts/plasma cells.

Given the levels of depletion were different in the lymphoid organs studied, the effects of this depletion and repopulation were studied separately in the spleen, lymph nodes and bone marrow and these are described in turn in the following sections.

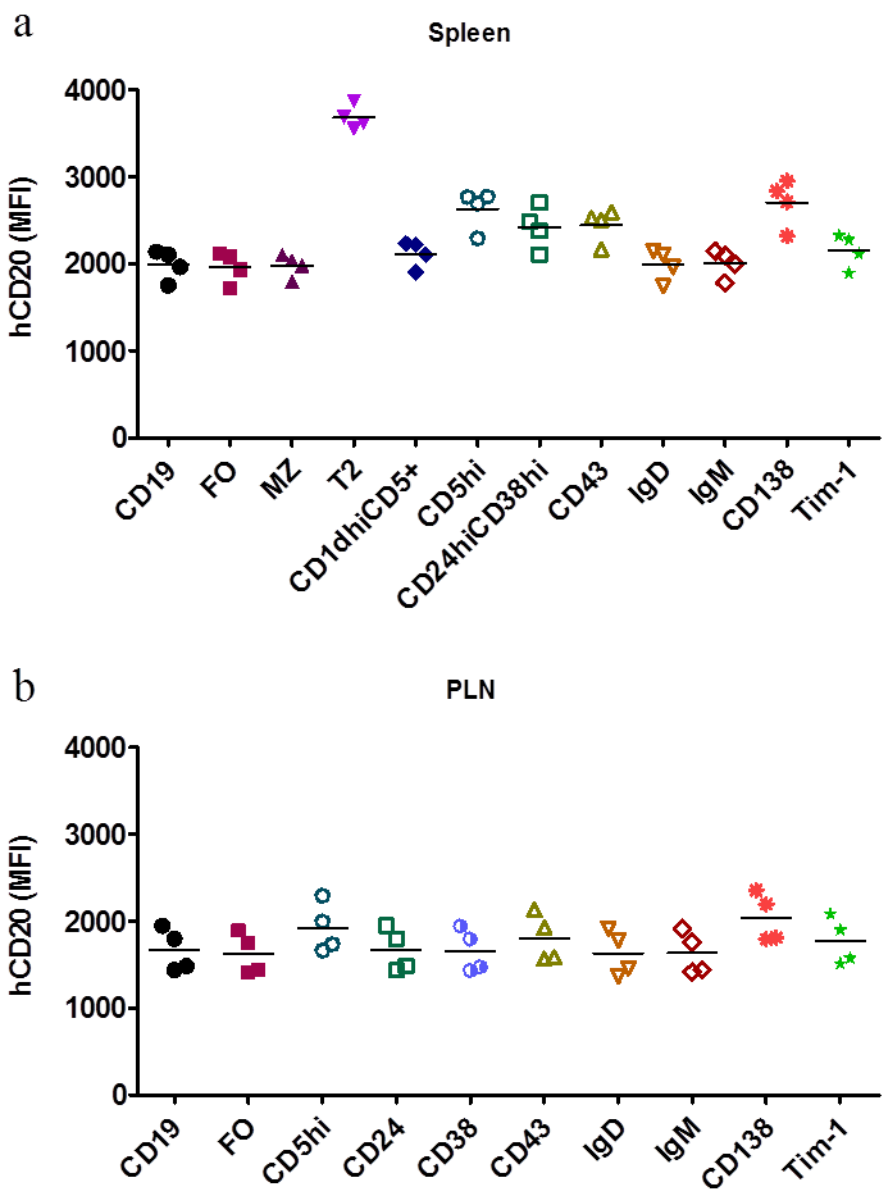

Figure 5.5 MFI of human CD20 in B cells and their subpopulations. Spleen cells (a) and cells from pancreatic lymph nodes (b) were stained for CD19, hCD20 and other B cell markers, for *ex vivo* analysis by flow cytometry. Each symbol represents one mouse. CD19, the first column, represents the whole B cell population and all the following markers were analysed on cells gated using these individual markers. "FO" represents the column for follicular B cells ($CD21^{low}CD23^{hi}$); "MZ" represents marginal zone B cells ($CD21^{hi}CD23^{low}$) and T2 represents transitional 2 B cells ($CD21^{hi}CD23^{hi}$). The assay was performed in four hCD20 female mice aged 11 weeks old.

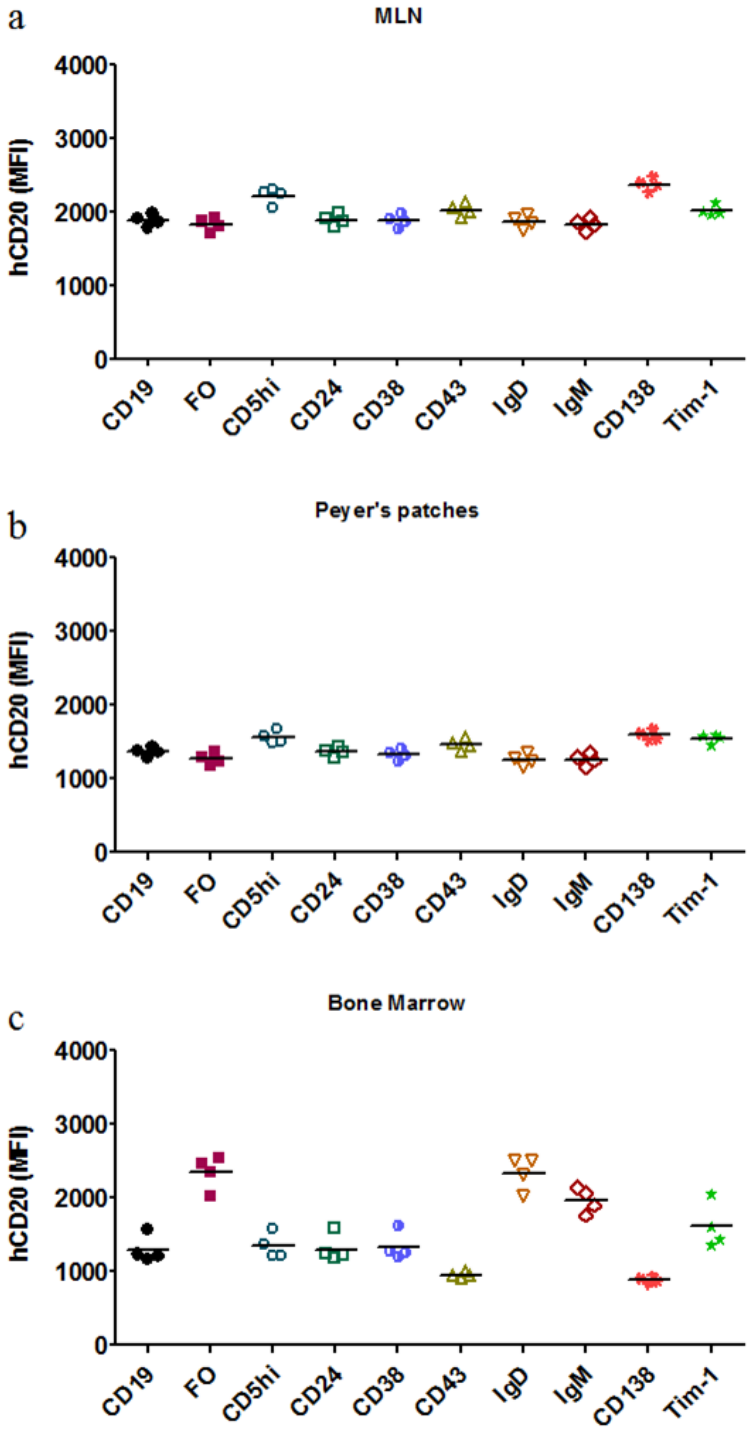

Figure 5.6 MFI of human CD20 in B cells and their subpopulations. Cells from mesenteric lymph nodes (a), Peyer's patches (b) and bone marrow (c) were stained for CD19, hCD20 and other B cell markers, for ex vivo analysis by flow cytometry. Each symbol represents one mouse. CD19, the first column, represents the whole B cell population and all the following markers were analysed on cells gated using these individual markers. "FO" represents the column for follicular B cells ($CD21^{low}CD23^{hi}$). The assay was performed in four hCD20 female mice aged 11 weeks old.

5.4 Effect of B cell depletion and repopulation in the Spleen

After analysing the expression of human CD20 in hCD20/NOD mice, the effects of B cell depletion and repopulation in the lymphoid organs were studied. The results are presented divided by markers.

It is important to clarify some aspects of the data described here: For these experiments, similar to the protocol for previous experiments, we aimed to analyse 30,000 $CD19^+$ cells for each sample. This was not achievable for hCD20-depleted mice and so, in these cases; the samples were run completely (until the FACS tube was dry). The percentage for all subpopulations, in all groups and samples, was calculated using $CD19^+$ B cells of the sample as 100%. Thus, the percentages in the depleted groups represented percentages in a smaller total number of cells.

When frequencies were equal in control and depleted mice, it indicated that, although the number of cells was smaller in 2H7 group, the subpopulation was proportionally depleted. Lower percentages indicated susceptibility to depletion. However, higher percentages in treated mice did not indicate higher numbers than controls, but rather a higher proportion of the subset in a depleted environment. In other words, while all other subpopulations were depleted, the ones showing higher frequencies were less depleted and became the dominant subpopulations. The diagram in Figure 5.7 summarizes these observations.

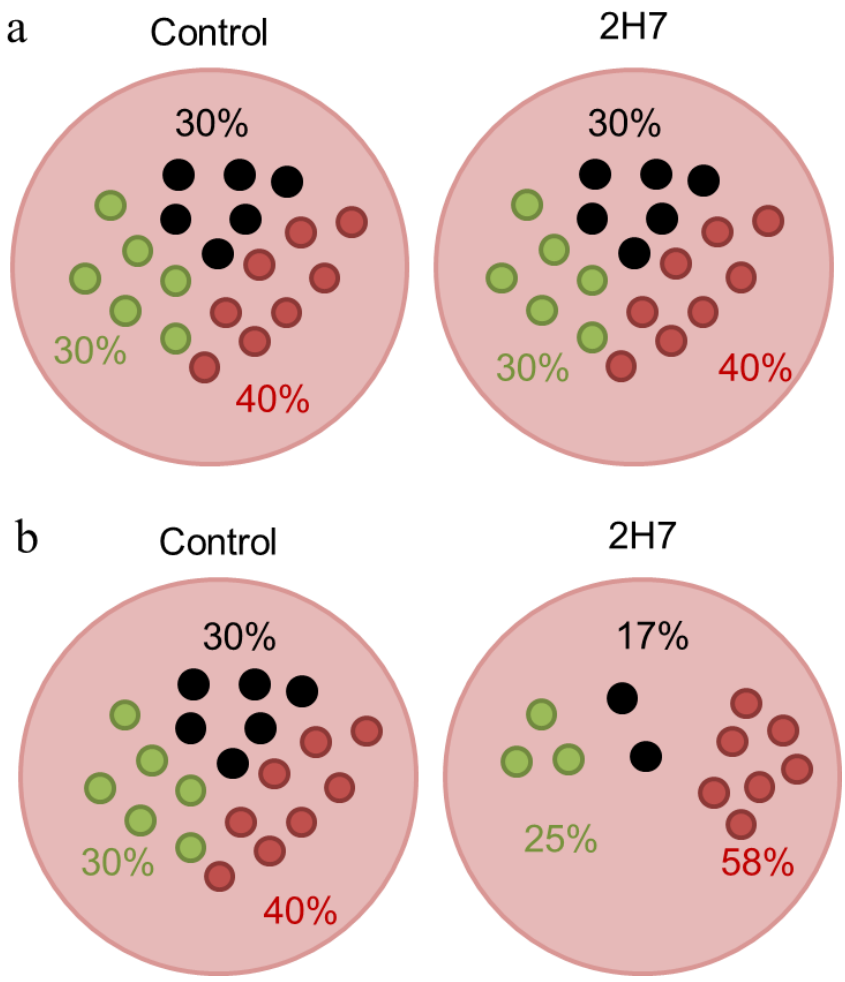

Figure 5.7 Visual representation of possible proportional variations in subpopulations after B cell depletion. It was not possible to evaluate B cell subpopulations in lymphoid organs (represented here by black, green and red circles) from mice that were to receive treatment. However we considered that, at time point -9, all hCD20/NOD mice were the same (a). After receiving anti-hCD20 (2H7), treated mice were B cell-depleted. In these mice, the B cell subpopulation frequencies varied in 3 different ways (b): Some populations were depleted proportionally (represented here by the green circles). Although their numbers were lower in depleted compared to control mice, the percentage was similar. Some subsets were more susceptible to depletion (black circles) and the percentages were much lower than the percentages seen in Controls (as well as their numbers). On the other hand, other populations were resistant to depletion. In these cases (represented by the red circles), although the number of cells was lower than in control mice, the proportion was higher because they were in a depleted environment where other cells were removed.

5.4.1 Extracellular markers: Total B cells (CD19)

When 6-8 w.o. hCD20/NOD mice were injected with one cycle of either 2H7 or the control IgG, the differences in the percentages were evident 24h after the last injection.

The total number of B cells (Figure 5.8) significantly decreased from 1.9 x 10^7 cells in the spleen of control mice to 1.2 x 10^6 cells in depleted mice 24h after the last injection, indicating 94% depletion. This level of depletion was also seen 1 week after the last injection, and were still low at 4 weeks (not shown), and just 8 weeks later, the first signs of repopulation were observed: the numbers in depleted mice had increased such that there was 60% depletion ($2x10^7$ cells in control mice versus $8x10^6$ cells in depleted mice). By the 12^{th} week after the last injection, both groups had numbers of B cells around $2.8x10^7$ cells and the values were not statistically different.

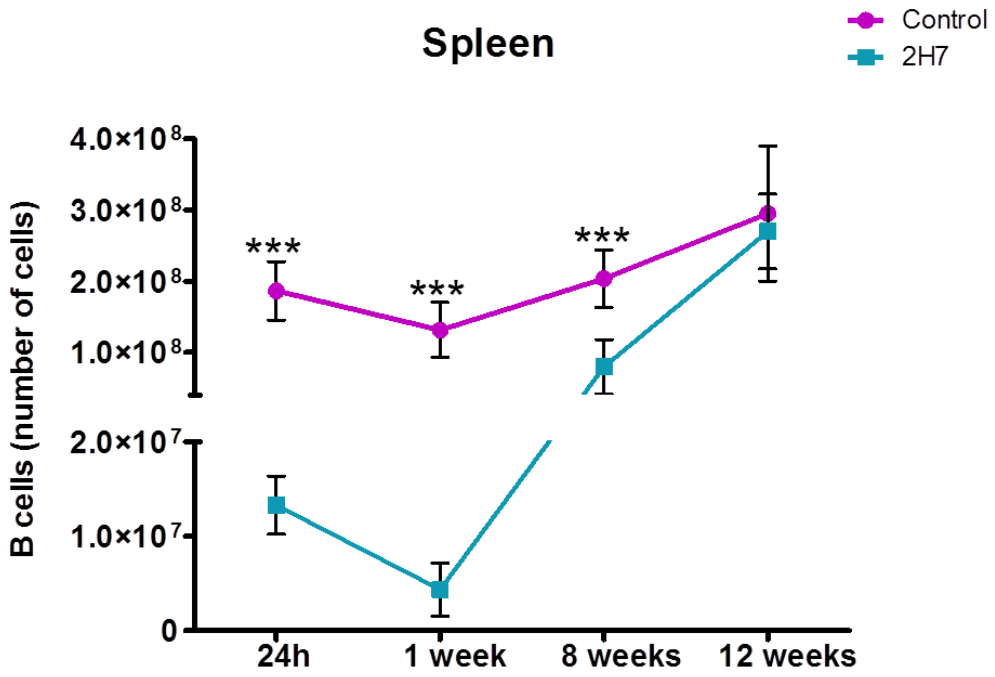

Figure 5.8 Effect of B cell depletion and repopulation in the total number of spleen B cells of young mice. 6-8 week-old female transgenic NOD mice expressing human CD20 received a cycle of 4 injections of either control IgG (in pink) or anti-human CD20 (clone 2H7 – in turquoise). Spleens from hCD20/NOD mice were collected at the time points, erythrocytes were lysed and lymphocytes were stained for extracellular markers *ex vivo*. Total lymphocytes were counted with Trypan Blue and the total numbers were multiplied by the percentage of $CD19^+$ cells determined by flow cytometry for each sample. Each time point illustrates mean of 6-8 mice and standard error. Data were analysed by t-test.

* $p < 0.05$; ** $p < 0.01$; *** $p < 0.001$

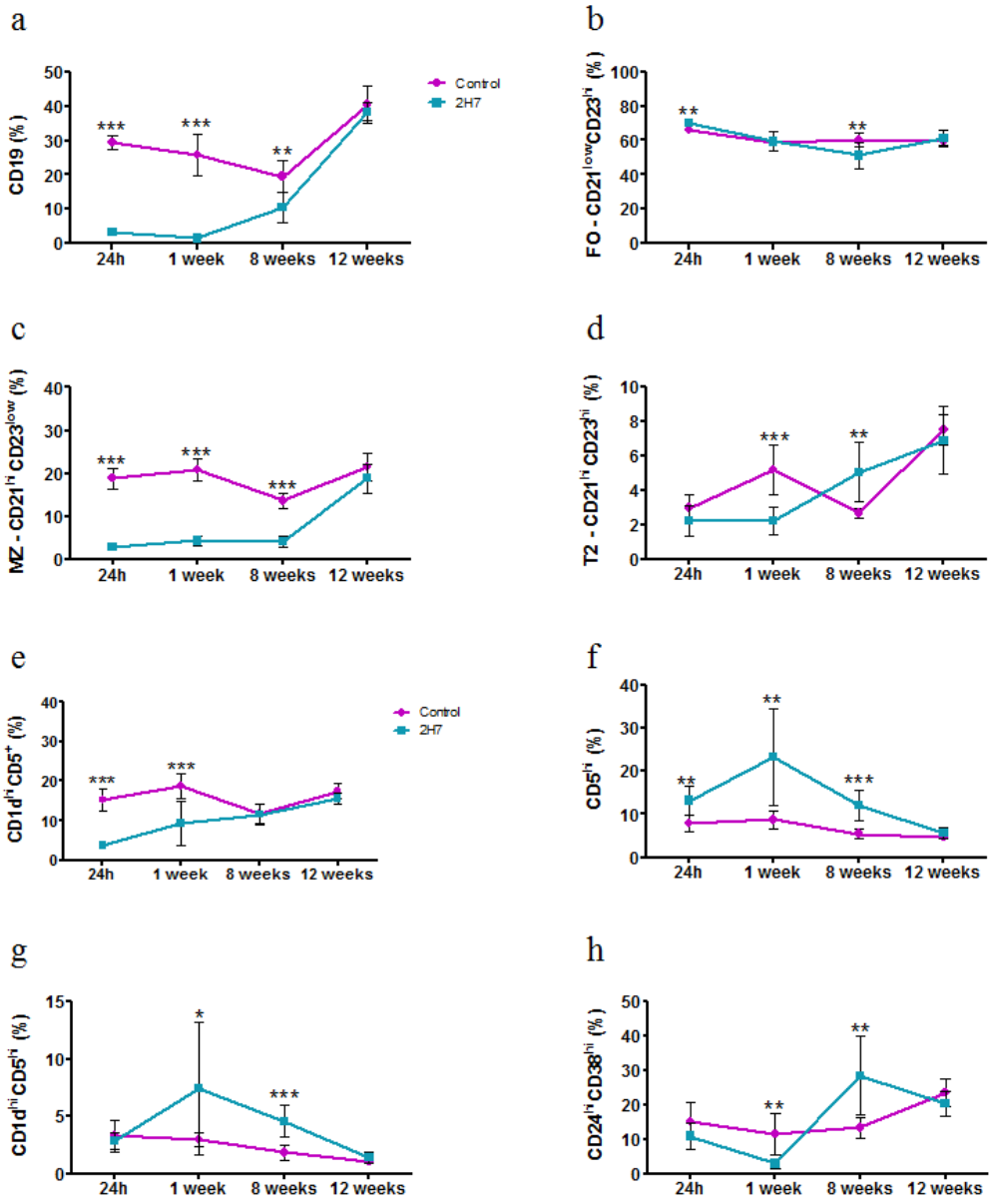

Figure 5.9 Effect of B cell depletion and repopulation in spleen B cells of young mice. 6-8 week-old female transgenic NOD mice expressing human CD20 received a cycle of 4 injections of either control IgG (represented in pink) or anti-human CD20 (clone 2H7 – represented in turquoise). Spleens from hCD20/NOD mice were collected at the determined time points, erythrocytes were lysed and lymphocytes were stained for extracellular markers *ex vivo*. The subsets analysed were: $CD19^{+}$ (a); $CD21^{low}CD23^{hi}$ (b); $CD21^{hi}CD23^{low}$ (c); $CD21^{hi}CD23^{hi}$ (d); $CD1d^{hi}CD5^{+}$ (e); $CD5^{hi}$ (f); $CD1d^{hi}CD5^{hi}$ (g) and $CD24^{hi}CD38^{hi}$ (h). The percentage of $CD19^{+}$ cells (a) is the percentage of whole splenocytes, whereas the percentages for the subsets (b-h) are percentages of the $CD19^{+}$ B cells. Each time point illustrates a mean of 6-8 mice and standard error. The percentages of cells at each time point were compared between the depleted and control group and the data were analysed by t-test.

* $p < 0.05$; ** $p < 0.01$; *** $p < 0.001$

The percentage of total B cells ($CD19^+$; Figure 5.9a) in the spleen decreased significantly from 29% in control mice to 3% in 2H7-depleted mice. This represented a depletion of 90% of B cells in the spleen after 4 injections. One week after the last injection, the depletion process was still occurring in young mice. At this time, the percentage of B cells was reduced by 94%. By eight weeks, the cells were starting to return and 12 weeks after the last injection, the cells were fully returned and there was no significant difference between the groups.

5.4.2 Extracellular markers: CD21 and CD23

This depletion observed in the number and percentage of total B cells also caused different effects in the subpopulations. All the percentages shown here for subsets are considering $CD19^+$ B cells (the first graph (a) in the first figure for all organs) as 100%. Thus, although the percentages might be higher or lower in the depleted group, the number of cells is very likely to be always lower in the 2H7 group, during depletion.

Twenty-four hours after the last injection, the proportion of follicular zone B cells ($CD21^{low}CD23^{hi}$ – Figure 5.9b) significantly increased in depleted mice, compared to control mice. The difference between the two groups was lost 1 week after the last injection. Eight weeks after the last injection, the percentage of FO B cells decreased and was significantly lower than in control mice. By the 12^{th} week, it was back to similar levels (non-significant, when compared to the control group). Compared to MZ and T2 B cells, it seemed like FO B cells were less susceptible to depletion.

Marginal zone B cells ($CD21^{hi}CD23^{low}$ – Figure 5.9c) were significantly depleted 24h after the last injection. The depletion was very striking and even 8 weeks after the last injection, the levels in depleted mice were lower than 5% (in contrast to the 15-20% in control mice). The proportion, however, was back to normal after 12 weeks.

The percentages of T2 B cells ($CD21^{hi}CD23^{low}$ – Figure 5.9d), 24h after the last injection, were variable in 2H7 mice, but there was no significant difference observed when compared to the control mice. One week later, the percentage of T2 B cells continued to be lower in depleted mice. However, 8 weeks after the last injection, there was a significant increase in transitional B cells in depleted mice, compared to control mice. This could be explained as the new B cells arriving from the bone marrow to

repopulate the spleen express this phenotype. By 12 weeks, both control and depleted mice had similar percentages of transitional B cells.

5.4.3 Extracellular markers: CD1d and CD5

As a confirmation of the depletion of the marginal zone, the percentage of $CD1d^{hi}CD5^{+}$ cells also decreased significantly (Figure 5.9e), 24h and 1 week after the last injection. As discussed in chapter 3, $CD1d^{hi}$ cells are located in the marginal zone, which was depleted in mice receiving anti-hCD20 antibody. Eight weeks after the last injection, the percentage of cells expressing $CD1d^{hi}CD5^{+}$ was similar in control and depleted mice. This result did not correlate to the pattern seen in the marginal zone, but it was likely to be an outcome of new T2 cells in the spleen. The frequencies were similar in both groups when cells were completely repopulated.

On the other hand, the proportion of $CD5^{hi}$ cells (Figure 5.9f) significantly increased in depleted mice 24h after the last injection. CD5 is a marker for B-1a cells and these cells are more resistant to depletion (Hamaguchi et al. 2005). The resistance of $CD5^{hi}$ cells was even more accentuated 1 week after the depletion, when compared to control mice. Eight weeks after the last injection, with the return of other subpopulations, the difference between the frequencies of $CD5^{hi}$ B cells in depleted and control mice was similar to the first measurement. By 12 weeks, there was no statistically significant difference between the groups.

The proportions of $CD1d^{hi}CD5^{hi}$ (the intersection between the gates for $CD1d^{hi}CD5^{+}$ and $CD5^{hi}$) was not altered by the depletion at the early stage (Figure 5.9g). One week after the last injection, the percentages of $CD1d^{hi}CD5^{hi}$ B cells followed the pattern seen in $CD5^{hi}$ B cells, being significantly higher in depleted mice. The higher proportion was maintained in the 2H7 group 8 weeks later and returned to levels similar to control mice by the 12^{th} week.

5.4.4 Extracellular markers: CD24 and CD38

The percentages of B cells expressing $CD24^{hi}CD38^{hi}$ (Figure 5.9h) were similar in depleted and control mice 24h after the last injection. As these markers are mainly expressed in Transitional 2 B cells, this finding was not a surprise, as it followed the

pattern of results seen in Figure 5.9d. One week after the last injection, the frequency of $CD24^{hi}CD38^{hi}$ B cells decreased in depleted mice, being significantly lower than control mice. Eight weeks later, however, the proportion of B cells expressing $CD24^{hi}CD38^{hi}$ increased significantly. This observation followed again the pattern seen in T2 B cells. By the 12^{th} week after the last injection, the percentages were similar in both groups.

In addition to the regulatory subsets, we also investigated the effect of the depletion on cells expressing other B cell markers.

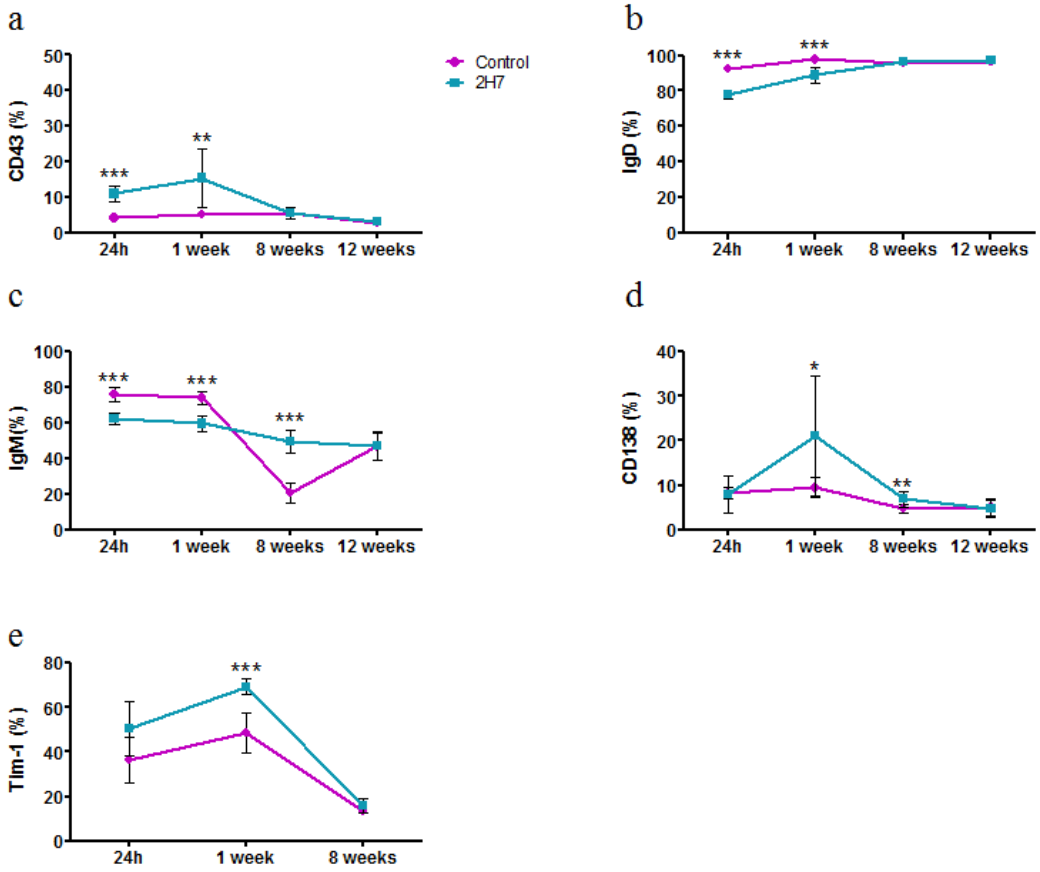

Figure 5.10 Effect of B cell depletion and repopulation in spleen B cells of young mice. 6-8 week-old female transgenic NOD mice expressing human CD20 received a cycle of 4 injections of either control IgG (represented in pink) or anti-human CD20 (clone 2H7 – represented in turquoise). Spleens from hCD20/NOD mice were collected at the determined time points, erythrocytes were lysed and lymphocytes were stained for extracellular markers *ex vivo*. The subsets analysed were: CD43 (a); IgD (b); IgM (c); CD138 (d) and Tim-1 (e). Each time point illustrates mean of 6-8 mice and standard error. The percentages of cells at each time point were compared between the depleted and control group and the data were analysed by t-test.

* $p < 0.05$; ** $p < 0.01$; *** $p < 0.001$

5.4.5 Extracellular marker: CD43

The first new marker added to the panel (compared with those studied in experiments reported in chapter 3) was CD43. B cells expressing this marker (Figure 5.10a) were resistant to depletion and even 24h after the last injection, the percentage was significantly higher in the 2H7 group. As explained previously, this did not mean the number of cells was increased, but rather that the proportion of these B cells expressing CD43 was higher due to the depletion of other subpopulations. The higher proportion was seen one week after the last injection; however, eight and twelve weeks later, the proportions were back to normal and there was no difference between control and depleted mice.

5.4.6 Immunoglobulin expression: IgD and IgM

Almost 100% of B cells in control mice expressed IgD (Figure 5.10b). In depleted mice, the percentages significantly decreased 24h and 1 week after the last injection. The percentages, however, returned to levels comparable to the control group 8 weeks after the last injection.

Following the results seen in B cells expressing IgD, the percentage of $CD19^{+}IgM^{+}$ was significantly lower in depleted mice at the first two time points (Figure 5.10c). Eight weeks after the last injection, although there was no alteration in the mean for depleted mice, the percentage in control mice decreased, which, by comparison, made the frequencies in the 2H7 significantly higher. However, it is not clear whether the apparent decrease in the IgM at 8 weeks in the control group is a true difference, as this is not in keeping with the trend and not easily explainable. By 12 weeks after the last injection, both groups had similar percentages and the results were not significantly different.

5.4.7 Extracellular marker: CD138

Although most of the $CD138^{+}$ B cells expressed hCD20 in our colony, no significant difference was observed in the percentage of cells in depleted mice, compared to control mice 24h after the last injection (Figure 5.10d). After one week, with the depletion of other subpopulations and the resistance of B cells expressing CD138, the percentage was significantly higher in depleted mice. By eight weeks, the difference between the

groups was smaller, but depleted mice still had significantly higher percentages. The frequencies were back to similar levels in both groups 12th week after the last injection.

5.4.8 Extracellular marker: Tim-1

B cells expressing Tim-1 were also resistant to depletion; a finding observed even 24h after the last injection, as the frequencies in the 2H7 group were significantly higher, compared to the control group. This pattern was also seen one week after the last injection. However, eight weeks after the last injection, the difference in the proportions between the groups was not observed.

5.4.9 Summary of effects of anti-hCD20 B cell depletion on cellular subsets *ex vivo*

The use of anti-hCD20 to deplete B cells affected splenic B cell subpopulations differently. Some subsets were susceptible to depletion, as occurred with the B cells in the marginal zone, which were severely depleted (confirmed by the depletion also observed in CD1d^{hi}CD5^{+} cells) when compared to control mice. On the other hand, B cells expressing CD5^{hi}, CD43^{+}, CD138^{+} or Tim-1 were resistant to depletion, a result demonstrated by the higher frequencies of these cells in depleted mice especially at the first two time points, when repopulation had not commenced.

The total of B cells and the majority of subpopulations were completely repopulated by the 12th week, but some of them had similar frequencies to control mice even 8 weeks after the last injection. These finding suggests that the return of B cell subsets to the spleen does not occur with the same kinetics.

5.4.10 Cytokine production and *in vitro* effects on subsets following anti-hCD20 B cell depletion in spleen B cells

5.4.10.1 Eight weeks after the last injection

As the percentage of B cells was returning to control levels in the depleted mice, spleen cells were cultured for 24h, either unstimulated, or stimulated with LPS or anti-CD40. 3h before harvesting, they received monensin, PMA and ionomycin, following the protocol described in previous chapters. LPS and anti-CD40 were chosen to represent two different pathways by which to stimulate B cells: via TLR (LPS) and mimicking T cell/costimulatory interaction (anti-CD40). In addition to the analysis of cytokine production, the effect of depletion and repopulation on other B cell markers that indicated changes in B cell subsets was also evaluated.

Figures 5.11a, 5.11b and 5.11c illustrate the percentage of $CD19^+$ cells after *in vitro* culture. When compared to the frequency of B cells *ex vivo* (Figure 5.9a), the percentage of B cells doubled similarly in both groups. Therefore, the 50% significant difference between control and 2H7 groups was preserved and it was stimulant independent.

A number of additional surface markers were examined, and the first of these was CD40. CD40 in B cells (and other APCs) is activated by interaction with CD40L in T cells, which leads to cytokine production (Mauri et al. 2003). Although the percentages of unstimulated $CD19^+CD40^+$ cells were low and similar in control and depleted mice (Figure 5.11d), stimulation with LPS increased the frequency of B cells expressing CD40 (Figure 5.11e). The percentage was not significantly different in either group. When B cells were stimulated with anti-CD40 (Figure 5.11f), the percentage of $CD19^+CD40^+$ cells was similar to those in unstimulated cells in control cultures. In depleted mice, the percentage was significantly lower when compared to the control group. It was also lower when compared to the percentage of unstimulated B cells in depleted mice.

The expression of hCD20 after cell culture was also examined. When B cells were cultured without stimulant (Figure 5.11g), or with LPS (Figure 5.11h) or anti-CD40 (Figure 5.11i), spleen cells from control mice had a significantly higher frequency of B cells expressing hCD20 than mice treated with 2H7. Because hCD20 was not assessed

in cells when studied directly *ex-vivo*, it is not known if this reduction was pre-existent before culture.

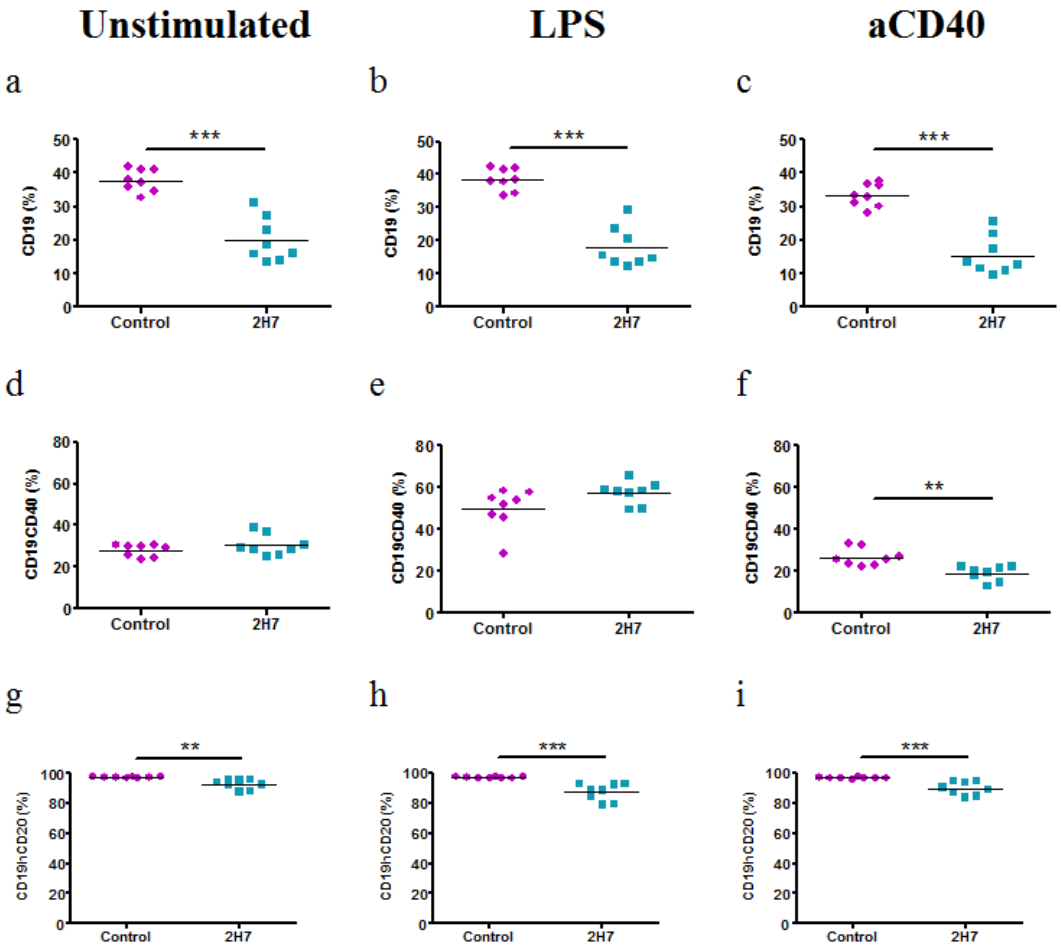

Figure 5.11 Effect of B cell depletion and repopulation *in vitro* in B cells of young mice. 6-8 week-old female transgenic NOD mice expressing human CD20 received a cycle of 4 injections of either control IgG (represented in pink) or anti-human CD20 (clone 2H7 – represented in turquoise). Eight weeks after the last injection, spleens were collected, erythrocytes were lysed and removed and spleen cells were cultured for 24h with LPS, anti-CD40 or left unstimulated; PMA, ionomycin and monensin were added for the last 3 hours and then cells were stained for extracellular markers and intracellular cytokines. The subsets analysed were: CD19 (a-c); CD40 (d-f) and human CD20 (g-i). Each graph illustrates individual mice and the mean. Data were analysed by t-test. n = 6-8.

* $p < 0.05$; ** $p < 0.01$; *** $p < 0.001$

In these experiments CD80 (B7-1) and CD86 (B7-2), were also analysed. These markers are costimulatory molecules that bind to CD28 or CTLA-4 in T cells. They are expressed in APCs (Lim et al. 2012).

The percentage of B cells expressing CD80 was low in unstimulated cells in general, being significantly lower in depleted mice (Figure 5.21a). When stimulated with LPS (Figure 5.12b) or anti-CD40 (Figure 5.12c), the percentages increased in both groups. However, the increase was smaller in depleted mice. In LPS-stimulated B cells, percentages were not significantly different between the groups, but in B cells from depleted mice stimulated with anti-CD40, the percentage of $CD19^{+}CD80^{+}$ cells was significantly lower than in the control group.

The significantly lower expression in depleted mice was also observed for CD86. For this costimulatory molecule, statistically significant differences between control and 2H7-treated mice were observed in unstimulated (Figure 5.12d), LPS- (Figure 5.12e) and anti-CD40-stimulated B cells (Figure 5.12f).

The expression of CD138 was analysed *ex vivo* and again *in vitro*; however, the percentages were very low after cells were cultured for 24h (Figures 5.12g-i). The percentage in depleted mice was marginally higher when cells were cultured with LPS, but there was no significant difference in $CD138^{+}$ cells between groups for any of the stimulants studied.

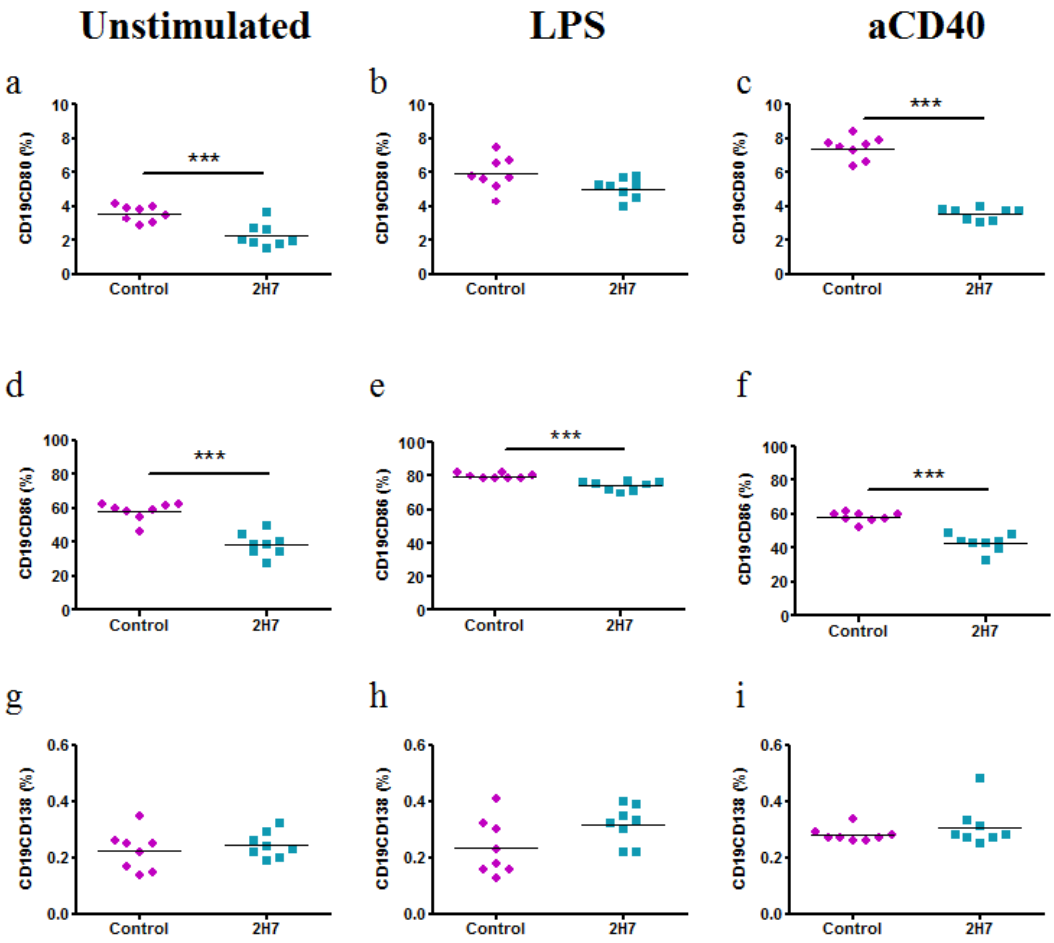

Figure 5.12 Effect of B cell depletion and repopulation *in vitro* in B cells of young mice. 6-8 week-old female transgenic NOD mice expressing human CD20 received a cycle of 4 injections of either control IgG (represented in pink) or anti-human CD20 (clone 2H7 – represented in turquoise). Eight weeks after the last injection, spleens were collected, erythrocytes were lysed and removed and spleen cells were cultured for 24h with LPS, anti-CD40 or left unstimulated; PMA, ionomycin and monensin were added for the last 3 hours and then cells were stained for extracellular markers and intracellular cytokines. The subsets analysed were: CD80 (a-c); CD86 (d-f) and human CD138 (g-i). Each graph illustrates individual mice and the mean. Data were analysed by t-test. n = 6-8.

* $p < 0.05$; ** $p < 0.01$; *** $p < 0.001$

The cytokine production by B cells was analysed under the same conditions described for the *in vitro* markers.

Eight weeks after the last injection, the percentage of B cells producing IL-10 was significant lower in B cells from depleted mice. This difference was observed in unstimulated (Figure 5.13a), LPS- (Figure 5.13b) and anti-CD40-stimulated cells (Figure 5.13c). We observed that the control mice had increased percentage of $CD19^{+}IL\text{-}10^{+}$ cells on stimulation with LPS and even more with anti-CD40 stimulation, the depleted mice responded to LPS stimulation but were less responsive to anti-CD40 stimulation. Considering that the the marginal zone of NOD mice is the main source of B10 cells (as seen in Chapter 3) and that this region was the most affected by depletion, it would explain the lower frequencies of IL-10-producing B cells in depleted mice.

On the other hand, the production of TGF-β by B cells of mice treated with 2H7 was higher than the production by the B cells of mice treated with control IgG. Although all percentages were small, depleted mice had significantly higher percentages of B cells producing TGF-β when compared to control mice, both the unstimulated (Figure 5.13d) and LPS-stimulated cells (Figure 5.13e). Anti-CD40 treatment (Figure 5.13f) also induced a higher percentage of TGF-β in the 2H7 group, but this was not statistically different from the control cells.

The stimulation of B cells producing IL-6, under these culture conditions, were also significantly increased in depleted mice, in comparison to control mice. However, it should be noted that the percentages were small, but significantly smaller in mice that received control IgG, when cells were unstimulated (Figure 5.13g) or stimulated with anti-CD40 (Figure 5.13i). In LPS-stimulated cells (Figure 5.13h), there was no significant difference.

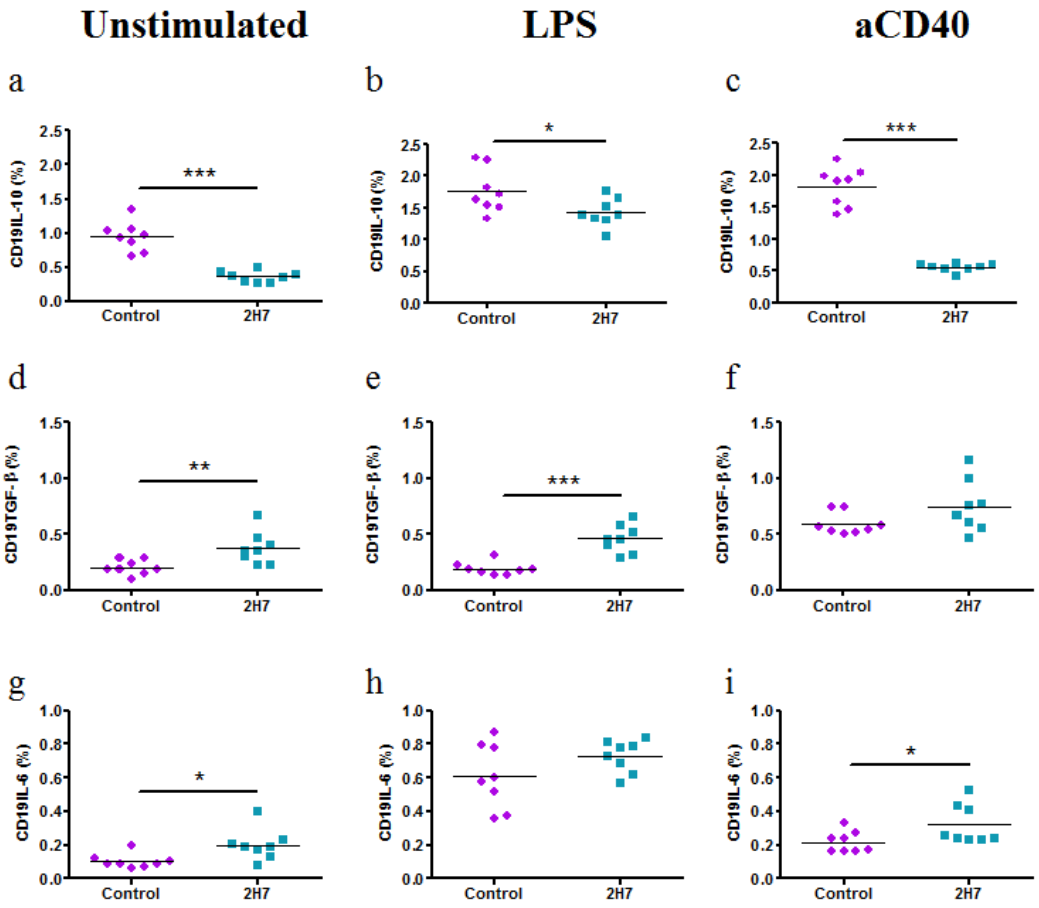

Figure 5.13 Effect of B cell depletion and repopulation *in vitro* in cytokine production by B cells of young mice. 6-8 week-old female transgenic NOD mice expressing human CD20 received a cycle of 4 injections of either control IgG (represented in pink) or anti-human CD20 (clone 2H7 – represented in turquoise). Eight weeks after the last injection, spleens were collected, erythrocytes were lysed and removed and spleen cells were cultured for 24h with LPS, anti-CD40 or left unstimulated; PMA, ionomycin and monensin were added for the last 3 hours and then cells were stained for extracellular markers and intracellular cytokines. The cytokines analysed were: IL-10 (a-c); TGF-β (d-f) and IL-6 (g-i). Each graph illustrates individual mice and the mean. Data were analysed by t-test. n = 6-8.

* $p < 0.05$; ** $p < 0.01$; *** $p < 0.001$

5.4.10.2 Twelve weeks after the last injection

Twelve weeks after the last anti-hCD20 injection in young mice, surface markers and cytokine production were evaluated *in vitro* again.

Although the percentage of $CD19^+$ cells *ex vivo* was reconstituted in depleted mice, when cultured for 24h, with no stimulant (Figure 5.14a), LPS (Figure 5.14b) or anti-CD40 (Figure 5.14c), treated mice had significantly lower frequencies of B cells in the cultures.

For B cells expressing CD40, the same pattern seen 8 weeks after the last injection was also observed four weeks later: CD40 was upregulated when cells were stimulated with LPS and anti-CD40 did not change the percentages of cells expressing CD40 at either time point when compared to unstimulated cells. Moreover, there was no significant difference in the percentages for any stimulation (Figures 5.14d-f).

There was similar expression of hCD20 in the *in vitro* cultured cells, as had been observed in *ex vivo* B cells. All cells, in both groups and for all stimulants, expressed high percentages (close to 100%) of hCD20 and there was no significant difference between control and depleted (now repopulated) mice (Figures 5.14g-i).

Although most of the markers had returned to normal levels, and were expressed equally in both groups, when B cells were repopulated in 2H7-treated mice, the expression of CD80 and CD86 were still reduced.

Unstimulated cells in depleted mice had significantly lower percentages of $CD19^+CD80^+$ cells (Figure 5.15a). When cells were stimulated with LPS (Figure 5.15b) and anti-CD40 (Figure 5.15c), the percentages were still lower in depleted mice, although not statistically significant. The percentages of $CD19^+CD86^+$ cells were also lower in unstimulated cells from the 2H7-treated group, although this was not significant (Figure 5.15d). When stimulated with LPS (Figures 5.15e) and anti-CD40 (Figures 5.15f), the percentages of B cells expressing CD86 were significantly lower in depleted mice, compared to control.

After repopulation, the percentage of $CD138^+$ B cells was similar in control and depleted mice (no significant difference between the groups). However, for all stimulants (Figures 5.15g-i), the overall percentages were lower in the 2H7-depleted group.

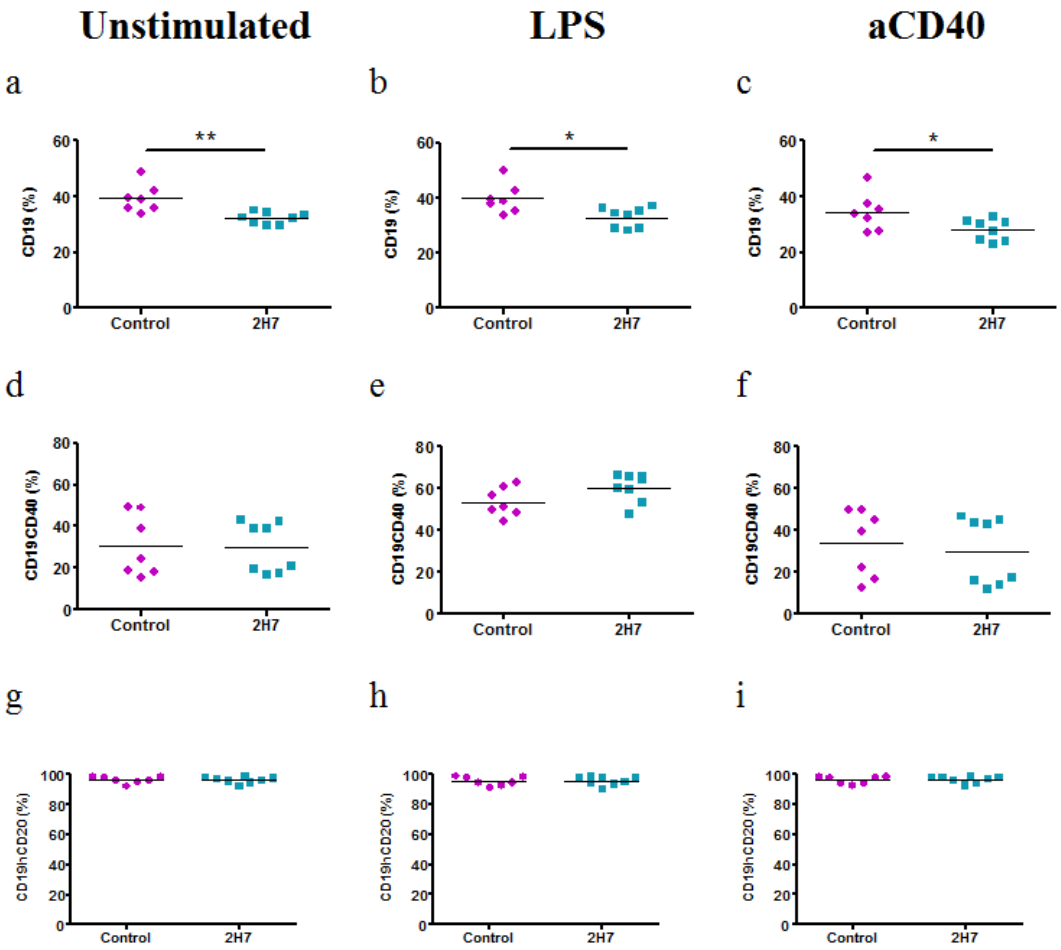

Figure 5.14 Effect of B cell depletion and repopulation *in vitro* in B cells of young mice. 6-8 week-old female transgenic NOD mice expressing human CD20 received a cycle of 4 injections of either control IgG (represented in pink) or anti-human CD20 (clone 2H7 – represented in turquoise). Twelve weeks after the last injection, spleens were collected, erythrocytes were lysed and removed and spleen cells were cultured for 24h with LPS, anti-CD40 or left unstimulated; PMA, ionomycin and monensin were added for the last 3 hours and then cells were stained for extracellular markers and intracellular cytokines. The subsets analysed were: CD19 (a-c); CD40 (d-f) and human CD20 (g-i). Each graph illustrates individual mice and the mean. Data were analysed by t-test. n = 6-8.

* $p < 0.05$; ** $p < 0.01$; *** $p < 0.001$

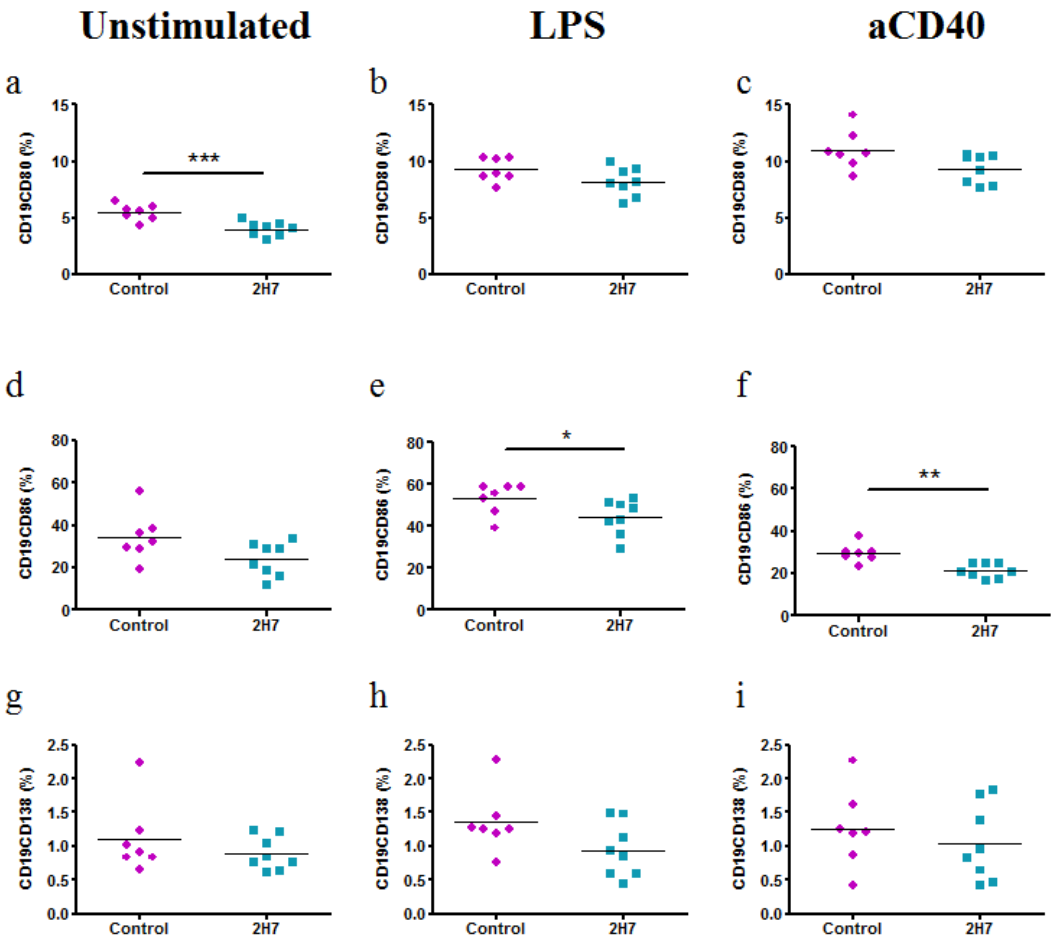

Figure 5.15 Effect of B cell depletion and repopulation *in vitro* in B cells of young mice. 6-8 week-old female transgenic NOD mice expressing human CD20 received a cycle of 4 injections of either control IgG (represented in pink) or anti-human CD20 (clone 2H7 – represented in turquoise). Twelve weeks after the last injection, spleens were collected, erythrocytes were lysed and removed and spleen cells were cultured for 24h with LPS, anti-CD40 or left unstimulated; PMA, ionomycin and monensin were added for the last 3 hours and then cells were stained for extracellular markers and intracellular cytokines. The subsets analysed were: CD80 (a-c); CD86 (d-f) and human CD138 (g-i). Each graph illustrates individual mice and the mean. Data were analysed by t-test. n = 6-8.

* $p < 0.05$; ** $p < 0.01$; *** $p < 0.001$

For $CD19^{+}IL\text{-}10^{+}$ cells, after the population was reconstituted, unstimulated (Figure 5.16a) and LPS-stimulated (Figure 5.16b) cells from depleted mice were able to reach similar levels of cytokine production seen in control mice. Cells stimulated with anti-CD40 (Figure 5.16c), however, had lower percentages of B cells producing IL-10 in depleted mice, compared to control mice. As observed in Figures 5.16d-f, this was not related to lower frequency of CD40 expression in these mice.

Although the production of TGF-β and IL-6 by B cells was higher in depleted mice at the previous time-point, 12 weeks after the last injection they were similar and not significantly different in the control and 2H7 groups (Figures 5.16d-i).

5.4.11 Summary for *in vitro* surface markers and intracellular cytokines in B cells from the spleen

The most important findings for surface markers in B cells cultured for 24h related to the frequencies of CD80 and CD86, important markers in APCs. Even 12 weeks after the last injection, when the majority of the markers returned to percentages similar to the control group, the frequencies of CD80 and CD86 were significantly lower in depleted mice.

The frequency of cytokines varied during the two time points studied and the 2H7 group had significantly lower percentages of B cells producing IL-10, and higher percentages of $CD19^{+}TGF\text{-}\beta^{+}$ cells 8 weeks after the last injection. The percentages of IL-6 producing B cells were very small. However, twelve weeks after the last injection, the frequencies were mostly similar in both groups.

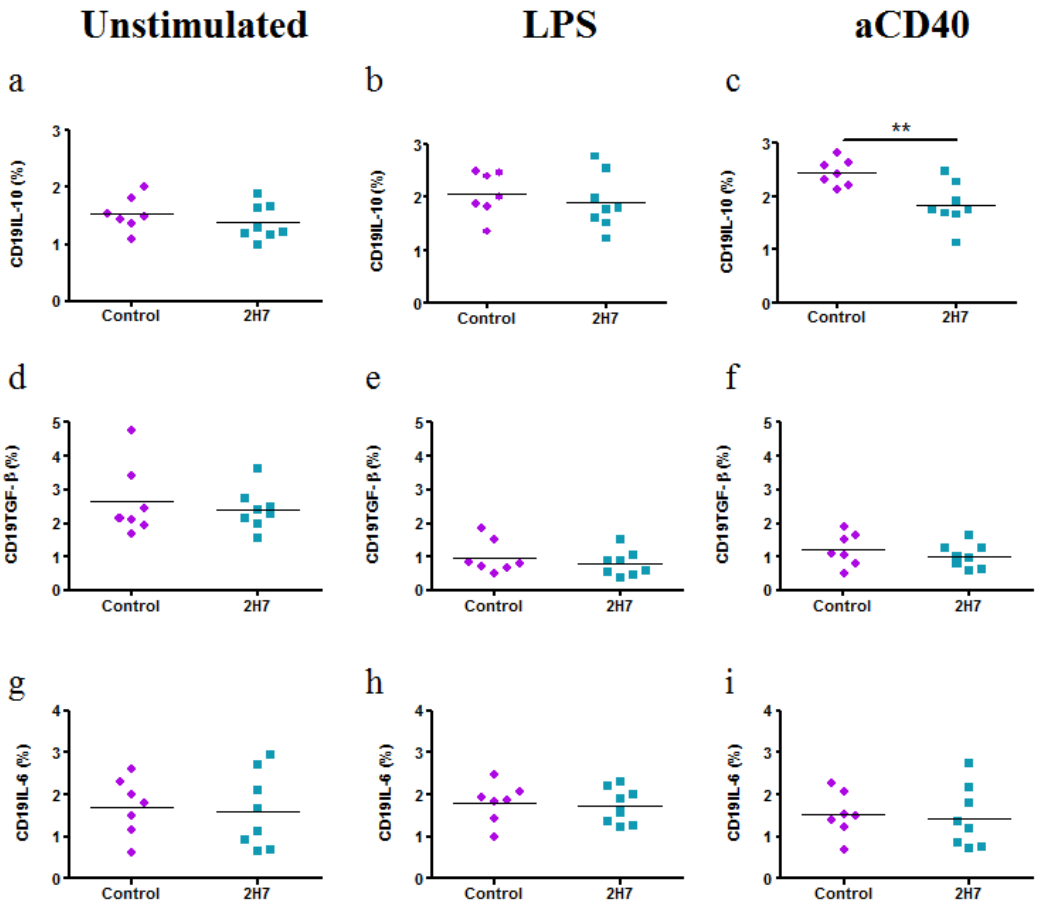

Figure 5.16 Effect of B cell depletion and repopulation *in vitro* in cytokine production by B cells of young mice. 6-8 week-old female transgenic NOD mice expressing human CD20 received a cycle of 4 injections of either control IgG (represented in pink) or anti-human CD20 (clone 2H7 – represented in turquoise). Twelve weeks after the last injection, spleens were collected, erythrocytes were lysed and removed and spleen cells were cultured for 24h with LPS, anti-CD40 or left unstimulated; PMA, ionomycin and monensin were added for the last 3 hours and then cells were stained for extracellular markers and intracellular cytokines. The cytokines analysed were: IL-10 (a-c); TGF-β (d-f) and IL-6 (g-i). Each graph illustrates individual mice and the mean. Data were analysed by t-test. n = 6-8.

* $p < 0.05$; ** $p < 0.01$; *** $p < 0.001$

5.5 Effect of B cell depletion and repopulation in the Lymph Nodes

As observed in Figures 17 and 18, the variations caused by B cell-depletion affected PLNs, MLNs and Peyer's patches (PPs) in a similar manner. Therefore, the results for these three lymph nodes are shown together.

5.5.1 Extracellular markers: Total B cells (CD19)

As observed for the spleen, the effect of anti-hCD20 treatment in lymph nodes was observed even 24h after the last injection. The percentage of B cells in the pancreatic lymph nodes of depleted mice was around 1.6%, reduced from 12% in control mice (Figure 5.17 a1); this represented a depletion of 87% of total B cells. The depletion seen in the MLNs was even greater than in the spleen and PLNs. While the percentage of total B cells was 13.9% in control mice, depleted mice had only 0.7% B cells – a depletion of 95% (Figure 5.17 a2). The depletion in the Peyer's patches was not as efficient as in other lymph nodes. The difference between the percentage of $CD19^{+}$ cells in the control group (35.3%) and 2H7 group (8.7%) was only 75%, 24h after the last injection (Figure 5.17 a3).

These statistically significant reductions were maintained during the first 3 time points and returned to control levels by the 12^{th} week in the three organs studied.

5.5.2 Extracellular markers: CD21 and CD23

As explained at the beginning of the chapter, B cells expressing marginal zone and T2 phenotypes are rare in the lymph nodes, even in control mice, so these populations were not described (including the expression of CD1d). $CD21^{low}CD23^{hi}$ (FO) B cells were significantly depleted in the lymph nodes of the 2H7 group. Following the pattern seen for the total number of B cells (Figure 5.17a), this depletion was observed for the first 3 time points and the percentages returned to levels similar to the control group 12 weeks after the last injection (Figure 5.17 b1-3).

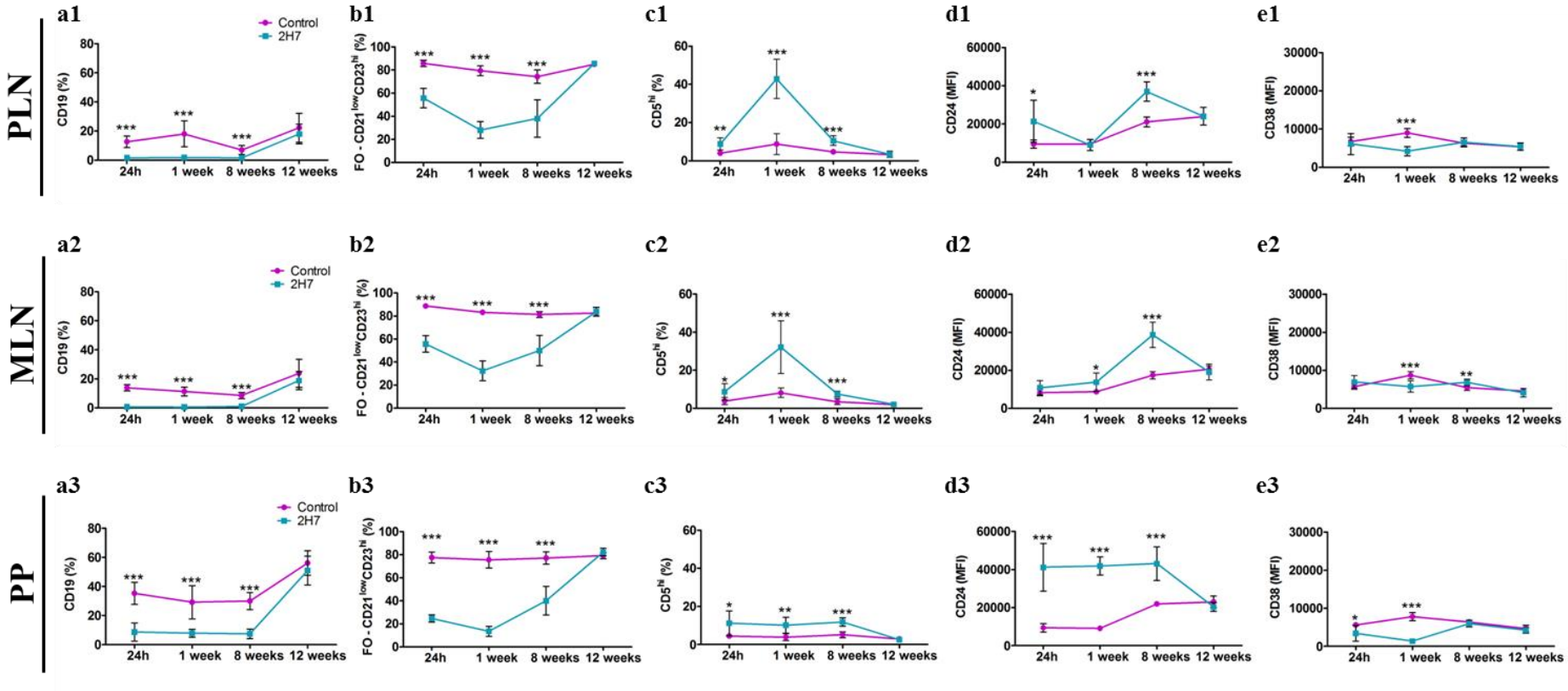

Figure 5.17 Effect of B cell depletion and repopulation in lymph node B cells of young mice. 6-8 week-old female transgenic NOD mice expressing human CD20 received a cycle of 4 injections of either control IgG (represented in pink) or anti-human CD20 (clone 2H7 – represented in turquoise). PLNs, MLNs and Peyer's patches from hCD20/NOD mice were collected at the determined time points, erythrocytes were lysed and lymphocytes were stained for extracellular markers *ex vivo*. The subsets analysed were: CD19 (a 1-3); $CD21^{low}CD23^{hi}$ (b 1-3); $CD5^{hi}$ (c 1-3); CD24 (MFI) (d 1-3) and CD38 (MFI) (e 1-3). Each time point illustrates mean of 6-8 mice and standard error. The percentages of cells at each time point were compared between the depleted and control group and the data were analysed by t-test.

* $p < 0.05$; ** $p < 0.01$; *** $p < 0.001$

5.5.3 Extracellular markers: CD5

The striking decrease of some populations made the proportion of resistant cells significantly higher. One example is seen in Figure 5.17 a1-2: The percentage of the remaining B cells expressing $CD5^{hi}$ in the PLNs and MLNs reached its peak, one week after the last injection at more than 30%. However, the number decreased as the new B cells started to repopulate the pancreatic lymph nodes and was similar to control mice by the 12^{th} week.

Compared to MLNs and PLNs, the resistance of $CD5^{hi}$ B cells to depletion in Peyer's patches was not as evident. The frequencies after depletion were no higher than 15% and varied within the groups (large error bar). By 12 weeks, the percentages were back to similar levels in depleted and control mice (Figure 5.17 c3).

5.5.4 Extracellular markers: CD24 and CD38

As the B cells in the PLNs do not express T2 and MZ phenotype, they do not express $CD24^{hi}CD38^{hi}$ B cells in the same way as the spleen. However, the expression of CD24 and CD38 was close to 100% in all groups, so the MFIs of these markers were analysed separately.

B cells that remained in the PLNs and MLNs after the treatment expressed more CD24 than B cells from control mice, as observed in figure 5.17 d1-2. The expression peaked at the 8^{th} week after the last injection. When the B cell population was repopulated, the expression of CD24 showed no difference compared to control mice. The differences in the expression of CD24 on B cells from depleted and control mice were more evident in the Peyer's patches. The remaining B cells in the 2H7 group expressed significantly more CD24 than B cells from the control group (Figure 5.17 d3).

The expression of CD38 on the B cells in the PLNs and PPs did not vary during depletion, except for the first week after the last injection, when the expression was significantly lower in B cells from depleted mice (Figure 5.17 e1 and e3). In the MLNs, the results for the expression of CD38 were very heterogeneous during the depletion period, varying in control and depleted mice (Figure 5.17 e2).

5.5.5 Extracellular marker: CD43

B cells expressing CD43 were resistant to depletion in all three LNs. From 24h until the 8th week after the last injection, the percentages of CD19^{+}CD43^{+} cells were significantly higher in the depleted group, compared to control mice. As the lymphoid organs were being repopulated, the percentages decreased to control mice levels by the 12th week (Figure 5.18 a1-3).

5.5.6 Extracellular marker: IgD and IgM

With the depletion of FO B cells, B cells expressing IgD and IgM were also reduced in the LNs. The percentage of IgD^{+} B cells in the 2H7 group was significantly decreased for the first 3 time points and increased to control levels with repopulation (Figure 5.18 b1-3).

The expression of IgM also decreased in depleted mice. However, the percentage in control mice seemed to decrease for the last two time points. It is difficult to point to the reason, but it could be an age effect. By 12 weeks, both depleted and control mice had the same frequency of B cells expressing IgM in all three LNs (Figure 5.18 c1-3).

5.5.7 Extracellular marker: CD138

As discussed previously, in our colony almost 100% of the CD19^{+}CD138^{+} B cells expressed hCD20. However these cells were still resistant to depletion; a result demonstrated by the significantly higher percentages of B cells expressing CD138, in the PLNs and MLNs, one week after the last injection and 8 weeks after the last injection in the PPs of mice treated with anti-CD20 (Figure 5.18 d1-3). The percentages returned to the low levels exhibited by control mice on the 12th week after the last injection.

5.5.8 Extracellular marker: Tim-1

Because of a change in the antibody panel, the expression of Tim-1 was not analysed at the last time point. Tim-1 was substituted in the panel by hCD20, to investigate the expression of this marker ex vivo, as a comparison to in vitro data. However, B cells expressing Tim-1 had significantly higher percentages in the 2H7 group during the depletion period, indicating that this population was resistant to the effect of anti-hCD20 (Figure 5.18 e1-3).

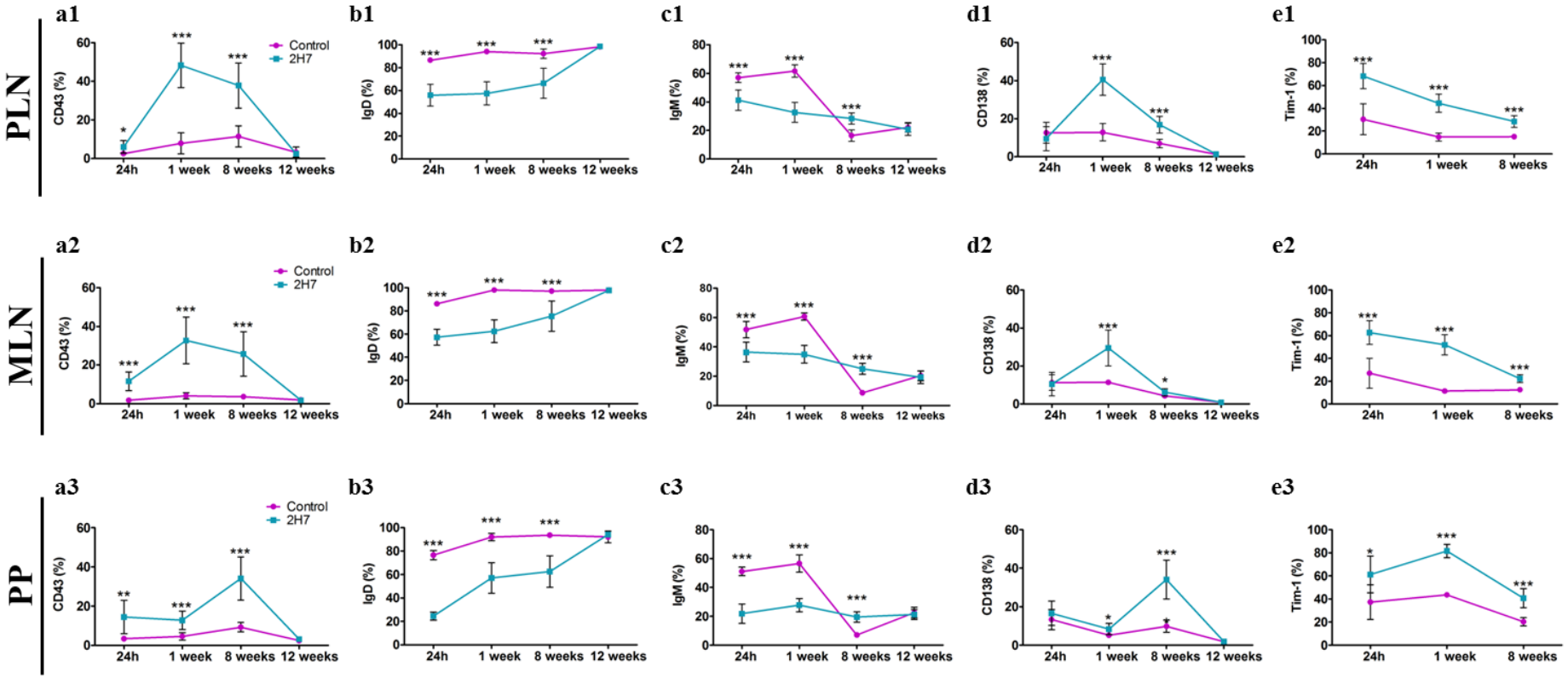

Figure 5.18 Effect of B cell depletion and repopulation in lymph node B cells of young mice. 6-8 week-old female transgenic NOD mice expressing human CD20 received a cycle of 4 injections of either control IgG (represented in pink) or anti-human CD20 (clone 2H7 – represented in turquoise). PLNs, MLNs and Peyer's patches from hCD20/NOD mice were collected at the determined time points, erythrocytes were lysed and lymphocytes were stained for extracellular markers *ex vivo*. The subsets analysed were: CD43 (a 1-3); IgD (b 1-3); IgM (c 1-3); CD138 (d 1-3) and Tim-1 (e 1-3). Each time point illustrates mean of 6-8 mice and standard error. The percentages of cells at each time point were compared between the depleted and control group and the data were analysed by t-test.

* $p < 0.05$; ** $p < 0.01$; *** $p < 0.001$

5.5.9 Summary

The results for the depletion of B cells in the LNs followed the same patterns seen in the spleen, although the depletion of total B cells in the Peyer's patches was not as efficient as in the lymph nodes. In the absence of marginal zone and T2 B cells, the cells depleted were the FO B cells. Depletion was also demonstrated by the reduction of B cells expressing IgD and IgM. $CD5^{hi}$, CD43, CD138 and Tim-1 B cells were resistant to depletion. The expression of CD24 was higher in depleted mice, while the expression of CD38 remained the same for both groups.

5.6 Effect of B cell depletion and repopulation in the Bone marrow

5.6.1 Extracellular markers: Total B cells (CD19)

The results for B cell depletion in the bone marrow were different from the other organs. Bone marrow is the site of B cell origin; however, the percentage of $CD19^{+}$ B cells was, in general, lower than in the other organs. While the percentage in control mice was 5.2%, depleted mice had 3.5% of total B cells (Figure 5.19a). This difference was not statistically significant and represented a depletion of only 32% of the B cells in the bone marrow of treated mice. One week after the last injection, the difference between the groups increased to 60%. However, as the organ that generates the new B cells that will repopulate the secondary lymphoid organs, the percentage of $CD19^{+}$ cells in the bone marrow returned to control levels earlier than the other organs studied.

5.6.2 Extracellular markers: CD21 and CD23

Unlike other lymphoid organs, the percentage of FO B cells in the bone marrow was lower than 50% of all B cells. These recirculating $CD21^{low}CD23^{hi}$ B cells were almost completely extinct from the bone marrow of depleted mice for the first 8 weeks and returned to the frequencies seen in the control group by the 12^{th} week after the last injection (Figure 5.19b).

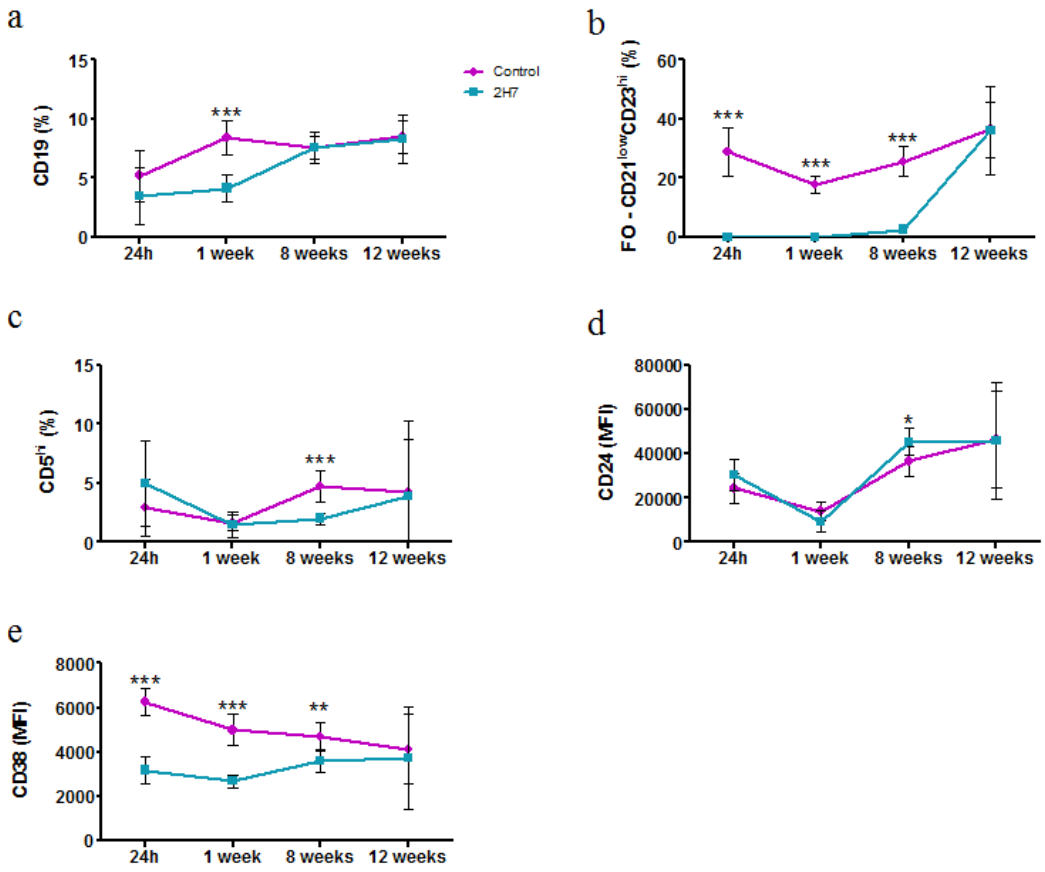

Figure 5.19 Effect of B cell depletion and repopulation in bone marrow B cells of young mice. 6-8 week-old female transgenic NOD mice expressing hCD20 received a cycle of 4 injections of either control IgG (represented in pink) or anti-hCD20 (clone 2H7 – represented in turquoise). Bone marrows from hCD20/NOD mice were collected at the determined time points, erythrocytes were lysed and lymphocytes were stained for extracellular markers *ex vivo*. The subsets analysed were: CD19 (a); $CD21^{low}CD23^{hi}$ (b); $CD5^{hi}$ (c); CD24 (MFI) (d) and CD38 (MFI) (e). Each time point illustrates the mean of 6-8 mice and standard error. Data were analysed by t-test.

* $p < 0.05$; ** $p < 0.01$; *** $p < 0.001$

5.6.3 Extracellular markers: CD5

Interestingly, the depletion in the bone marrow did not alter the percentage of $CD5^{hi}$ B cells (Figure 5.19c), which did not become a dominant population, as seen elsewhere. The numbers in both groups varied throughout the whole experiment.

5.6.4 Extracellular markers: CD24 and CD38

The expression of CD24 on B cells from control mice and on the remaining B cells from depleted mice was similar throughout the whole experiment and no significant difference was detected (Figure 5.19d). On the other hand, the expression of CD38 on B cells from mice treated with anti-hCD20 was significantly lower than control B cells for the first 3 time points (Figure 5.19e)

5.6.5 Extracellular marker: CD43

The only marker being expressed in a significantly higher proportion of B cells in depleted mice was the $CD43^{+}$ (Figure 5.20a). This high expression, however, returned to control levels faster than in the other lymphoid organs and frequencies were similar in both groups by the 8^{th} week.

5.6.6 Extracellular markers: IgD and IgM

The percentages of B cells expressing IgD (Figure 5.20b) and IgM (Figure 5.20c) in depleted mice followed the pattern seen for FO B cells in the bone marrow for the first week after depletion: The proportions were significantly lower in depleted mice. By the 8^{th} week after the last injection, however, the frequencies started to increase and it was likely that this was because of the newly generated transitional B cells.

5.6.7 Extracellular marker: CD138

As expected, the highest percentages of B cells expressing CD138 were seen in the bone marrow (varying around 20% in control mice). The depletion did not affect the percentage of $CD19^{+}CD138^{+}$ cells, which varied the same way as the control group (Figure 5.20d).

5.6.8 Extracellular marker: Tim-1

As illustrated in Figure 5.20e, the percentage of B cells expressing Tim-1 in the bone marrow was not affected by B cell depletion in treated mice. The percentages in both groups decreased at the 1st week and increased together by the 8th week after the last injection.

5.6.9 Summary

Bone marrow total B cells were the most resistant B cells to depletion, comparing all the lymphoid organs studied. Eight weeks after the last injection, total B cells in the bone marrow of depleted mice reached the same percentages seen in control mice.

The main populations affected were the B cells expressing follicular zone phenotype, and cells expressing IgD and IgM. Resistance to depletion was observed in CD43^{+} B cells, while the depletion had a less clear effect on B cells expressing CD5^{hi}, CD138^{+} and Tim-1^{+}.

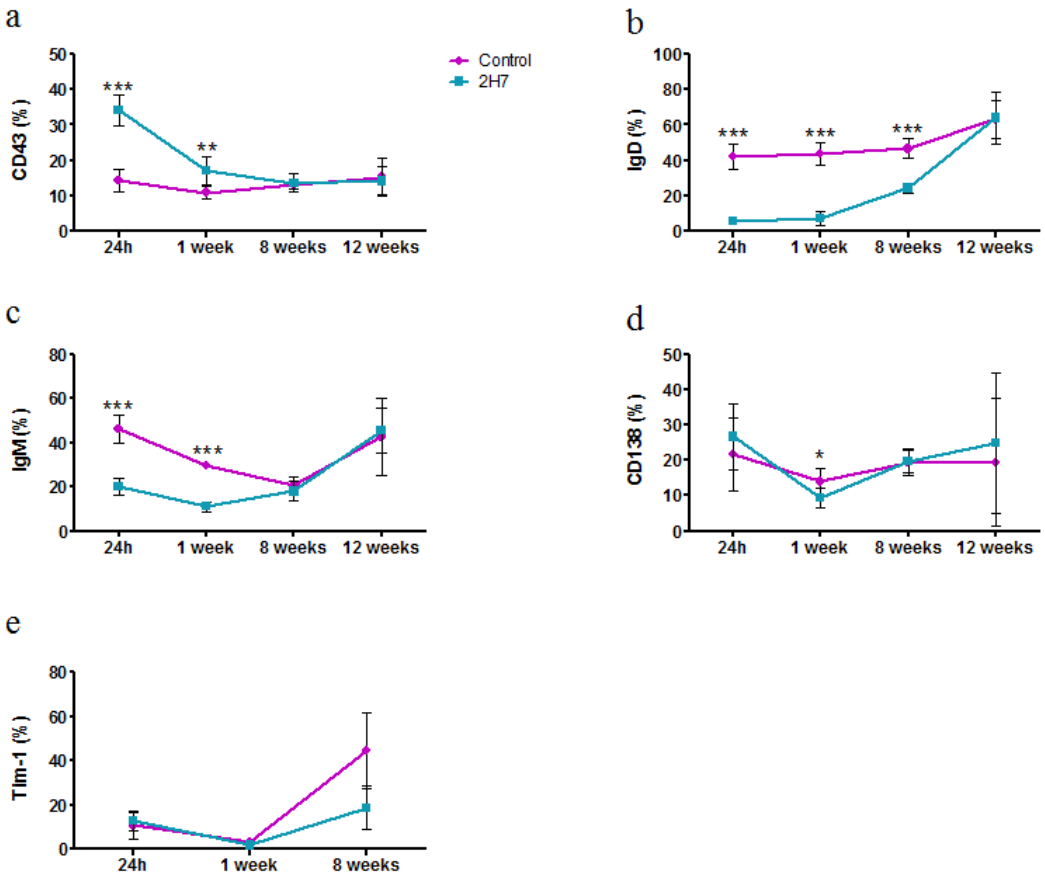

Figure 5.20 Effect of B cell depletion and repopulation in bone marrow B cells of young mice. 6-8 week-old female transgenic NOD mice expressing hCD20 received a cycle of 4 injections of either control IgG (represented in pink) or anti-hCD20 (clone 2H7 – represented in turquoise). Bone marrows from hCD20/NOD mice were collected at the determined time points, erythrocytes were lysed and lymphocytes were stained for extracellular markers *ex vivo*. The subsets analysed were: CD43 (a); IgD (b); IgM (c); CD138 (d) and Tim-1 (e). Each time point illustrates the mean of 6-8 mice and standard error. Data were analysed by t-test.

* $p < 0.05$; ** $p < 0.01$; *** $p < 0.001$

5.7 The effects of B cell depletion and repopulation in older hCD20 NOD mice

To determine the further effects of B cell depletion, hCD20 NOD mice depleted during the pre-insulitis period (6-8w.o.) were observed for > 30 weeks after the last injection. Ideally the control group would be hCD20 NOD mice injected with MPC-11 (control IgG). However, in this case, control group comprised hCD20 NOD mice that were not treated with either MPC-11 or 2H7.

5.7.1 Incidence of type 1 diabetes

The first observation about these older hCD20 mice was the incidence of type 1 diabetes (Figure 5.21). Concordant with the findings in the literature, we observed that treatment with 2H7 delayed the onset of type 1 diabetes (the first hyperglycaemic 2H7-treated mouse was detected 10 weeks after the first control mouse); the 2H7-treated group also had an overall reduced incidence of diabetes (58% in the control group versus 44% in the depleted group). The differences were not statistically significant, which was likely to be due to the number of mice. A new experiment has been set up, with mice injected with MPC-11 and 2H7, and is currently ongoing (end in May/2017).

5.7.2 Effects of the interaction between CD8 T cells, DCs and B cells from hCD20 mice

5.7.2.1 Experimental design

One of the possibilities as to why B cell depletion decreased the incidence of type 1 diabetes was that the new B cells that repopulate the lymphoid organs have a more regulatory profile than prior to depletion. To test this theory, we used the system described in chapter 4 (section 4.2) to analyse the potential of B cells from hCD20 mice previously depleted and repopulated to interfere with the activation of CD8 T cells by DCs.

Briefly, dendritic cells were purified from PI homo mice and used to present proinsulin to T cells. These DCs were stimulated with LPS for 18h and were then added in culture for 3 days with CD8 T cells from G9 mice. LPS-stimulated or unstimulated B cells were also added to the system.

LPS-stimulated and unstimulated B cells derived from 3 groups of mice: 1) > 35w.o. euglycaemic hCD20 mice that did not receive any injection (n=3; Control) and 2) > 35w.o. euglycaemic hCD20 mice that received 1 cycle of anti-hCD20 when they were 6-8 w.o (n=3; 2H7). A third group was added due to the detection of one hyperglycemic hCD20 mouse from the 2H7 group on the day of the experiment. Hence, the third group comprised one > 35w.o. hyperglycaemic hCD20 mouse that had received 1 cycle of anti-hCD20 (n=1; 2H7 diabetic).

As a consequence of such small numbers, it was not possible to apply statistics to the graphs and data shown here are preliminary and partial. As explained previously, these experiments are being repeated and the aim is to increase the number of mice and include the group "Control diabetic" for future analysis.

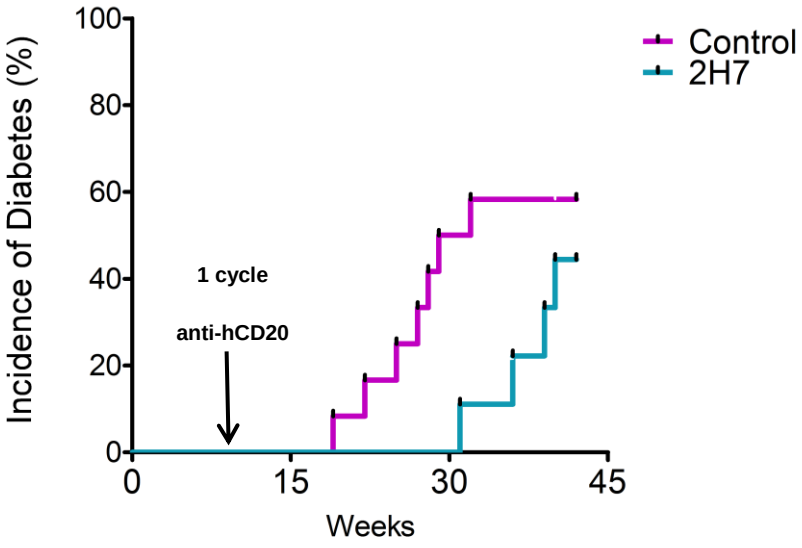

Figure 5.21 Incidence of type 1 diabetes in hCD20 NOD mice. Six to eight week-old hCD20 mice were injected with 1 cycle of 2H7 (n=9, represented in turquoise) or had no injections (n=12, represented in pink). Mice were observed for 35 weeks after the last injection for the evaluation of the incidence of type 1 diabetes. Diabetes was confirmed after two consecutive weeks of positive glycosuria and blood glucose over 13.9 mmol/L. Data were analysed by log rank test. The arrow indicates when the cycle of anti-hCD20 was injected in the 2H7-treated group.

5.7.2.2 $CD8^+$ T cell proliferation and activation

An example of the gating strategy for the graphs is shown in the previous chapter (Figure 4.2). The difference here was the activation marker was changed to CD44, as

the time point for analysis of activation was later than the optimal for examination of CD69.

As explained in Chapter 4, as a consequence of the variability of the efficiency of the CFSE labelling from one experiment to the other, all data from experimental groups were normalized to the control (CD8 T cells + DCs alone) and the percentages in Figure 5.22a represent the increase or decrease from this control parameter, with the addition of unstimulated or LPS-stimulated B cells.

Although the addition of unstimulated B cells to the system did not induce alteration in CD8 T cell proliferation, CD8 T cells from cultures that included LPS-stimulated B cells showed a decreased percentage of proliferation in all 3 groups.

The activation of the CD8 T cells was also evaluated (Figure 5.22b), as the percentage of cells expressing CD44. There was an increase in the frequency of activated cells following addition of unstimulated B cells, compared to wells with CD8 T cells and DCs alone, but the difference was not striking. The presence of stimulated B cells in the cell culture led to the decrease of the percentage of activated CD8 T cells. This decrease, however, was observed in all 3 groups of B cells, whether they were derived from control treated, 2H7 non-diabetic or the 2H7 diabetic mouse.

5.7.2.3 Viable CD8 T cells

In a new approach to the gating strategy (Figure 5.23a), the percentage of viable CD8 T cells was used to determine whether the cells were being killed in the presence of stimulated B cells, as a reason for the decreased proliferation. For all 3 groups the percentage of viable CD8 T cells was lower in the presence of LPS-stimulated B cells compared to unstimulated B cells and CD8 T cells cultured with DCs and no B cells (Figure 5.23b); however the difference was not as remarkable as seen for the proliferation, which could suggest the death of CD8 T cells was not the only reason for the differences seen in Figures 5.22. Nevertheless, it would be interesting to determine how many of these cells had induced apoptosis.

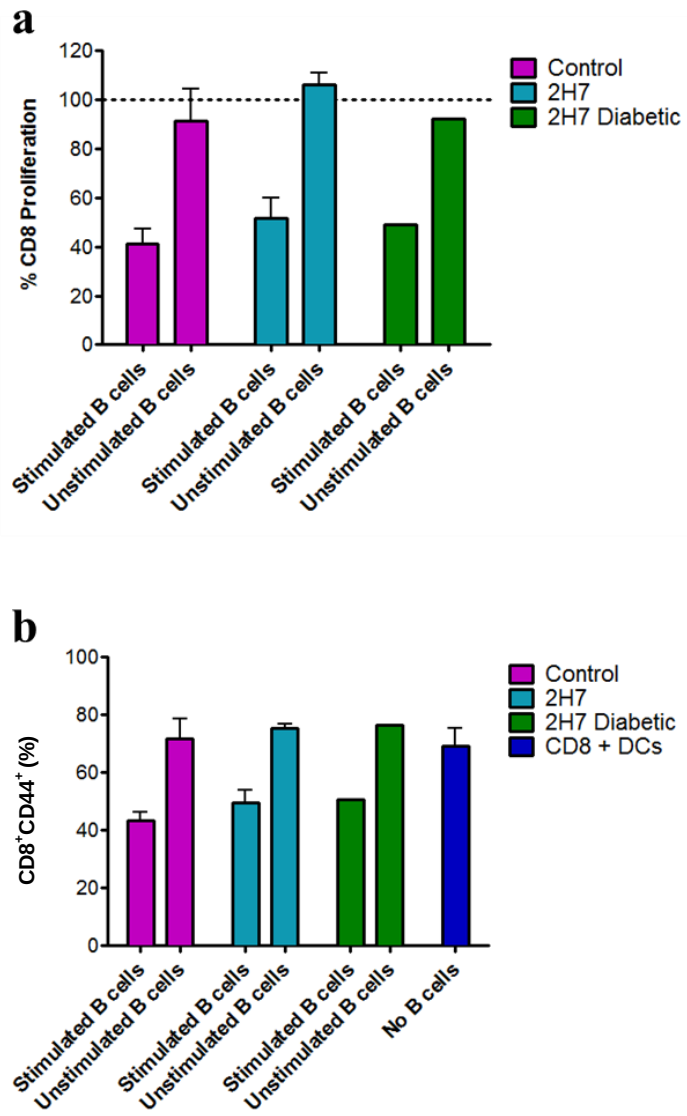

Figure 5.22 Effect of stimulated and unstimulated B cells on the activation of CD8 T cells by DCs. After culture for one week, bone marrow DCs from PI homo mice were stimulated with LPS for 18h. Splenic B cells from hCD20 mice were stimulated with LPS for 24h or left unstimulated. Spleen CD8 T cells (from G9 mice) were purified on the day of the set-up of the experiment and labelled with CFSE for the evaluation of CD8 proliferation. The experimental procedure was as follows: $2x10^5$ CD8 T cells, $4x10^5$ DCs and $1.4x10^6$ stimulated or unstimulated B cells were added to each culture. After 72h of incubation, cultures were harvested for flow cytometric staining. Forty eight hours after the set-up, supernatants were collected. The percentage of CD8 T cells proliferating and activated CD8 T cells are shown in (a) and (b), respectively. The data shown are represented as mean and standard error. n=3 for control and 2H7 groups and n=1 for 2H7 diabetic, done over 2 experiments.

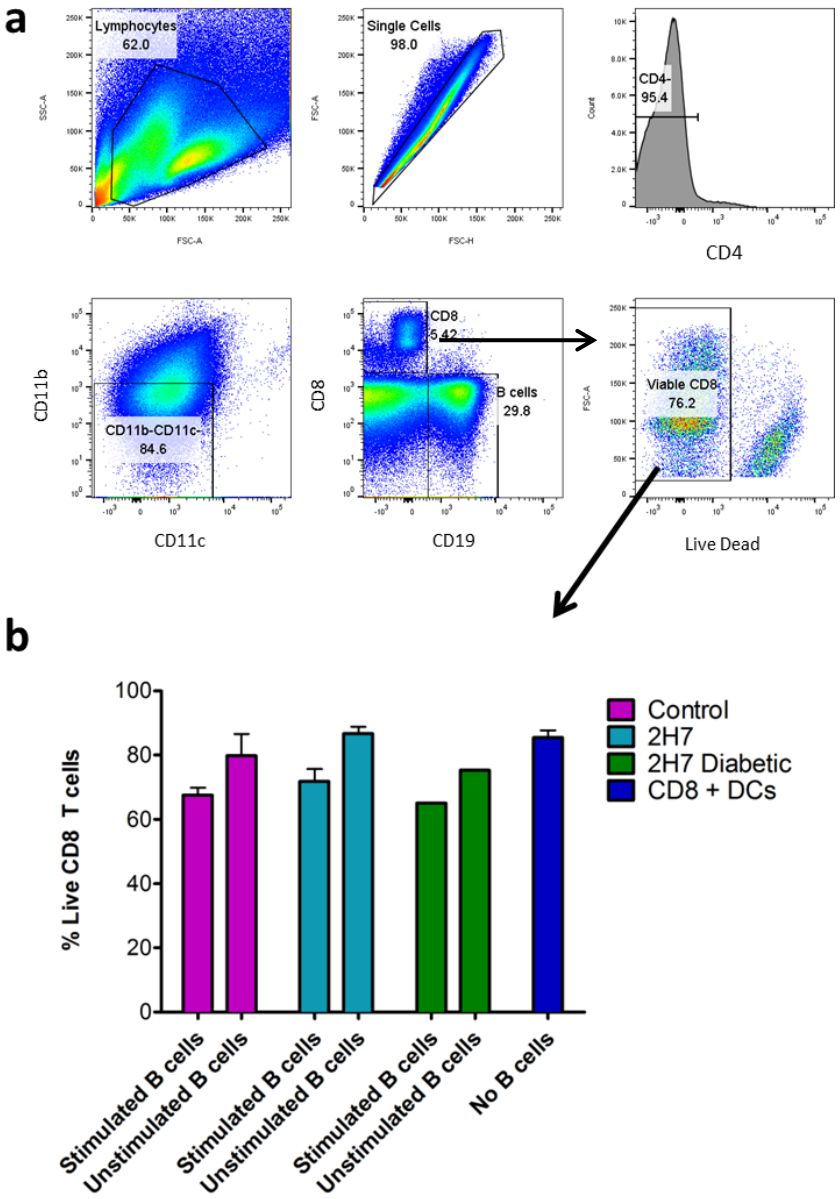

Figure 5.23 Effect of stimulated and unstimulated B cells on the death of CD8 T cells. After culture for one week, bone marrow DCs from PI homo mice were stimulated with LPS for 18h. Splenic B cells from hCD20 mice were stimulated with LPS for 24h or left unstimulated. Splenic CD8 T cells (from G9 mice) were purified on the day of the experiment set-up and labelled with CFSE for the evaluation of viable CD8 T cells. The experimental procedure was as follows: $2x10^5$ CD8 T cells, $4x10^5$ DCs and $1.4x10^6$ stimulated or unstimulated B cells were added to each culture. After 72h of incubation, cultures were harvested for flow cytometric staining. Forty-eight hours after the set-up, supernatants were also collected. One example of the gating strategy for the evaluation of viable cells is found in (a): Lymphocytes ➔ Single cells ➔ Exclusion of any CD4 T cells in the culture ➔ Exclusion of DCs ($CD11b^-CD11c^-$) ➔ Distinction between CD8 T cells and B cells (CD19) ➔ Viable CD8 T cells. The data in (b) are represented as mean and standard error. n=3 for control and 2H7 groups and n=1 for 2H7 diabetic, done over 2 experiments.

5.7.2.4 Cytokines in the supernatants

To investigate the mechanisms by which stimulated B cells were reducing the proliferation and activation of CD8 T cells, in contrast to unstimulated B cells, we investigated the concentration of cytokines in the supernatants. In agreement with the previous findings, we observed that cell cultures where LPS-stimulated B cells were added had lower levels of pro-inflammatory cytokines and more IL-10 (Figures 5.24a-d).

It is interesting to observe the differences between the groups. When B cells from the diabetic mouse were added to the cell culture, the concentration of IFN-γ was much higher, even with LPS-stimulated B cells (Figure 5.24a).

IL-10 was produced mainly by B cells, as the concentration of IL-10 produced by CD8 T cells + DCs alone was very low (Figure 5.24b) and, as expected, the stimulation with LPS boosted the production. Higher concentrations of IL-10 were seen with stimulated B cells derived from control hCD20 mice. Most of all the IL-6 in the culture was produced by DCs (Figure 5.24c). However, the addition of unstimulated B cells increased the concentrations, except when the unstimulated B cells were from the euglycaemic 2H7-treated group. For the diabetic mouse (from the 2H7-treated group), even the addition of stimulated B cells caused the increase of IL-6. The results for TNF-α (Figure 5.24d) were similar to IL-6.

5.7.3 Interaction between CD8 T cells and B cells from hCD20 mice as APC with G9 peptide as antigen

As a decrease in the costimulatory molecules (CD80 and CD86) was observed in B cell-depleted mice 8 and 12 weeks after the last injection (Figures 5.12 and 5.15), we decided to use the system to evaluate the function of B cells as APCs.

For these experiments DCs were not used; LPS-stimulated B cells were cultured with CD8 T cells. The G9 peptide (insulin B chain, amino acids 15-23) was added in two concentrations (1μg/ml and 0.5 μg/ml), as the antigen to be presented. Cell cultures were incubated for 72h and the parameters analysed, as well as the gating strategies, were the same as described above for B cells as bystander cells.

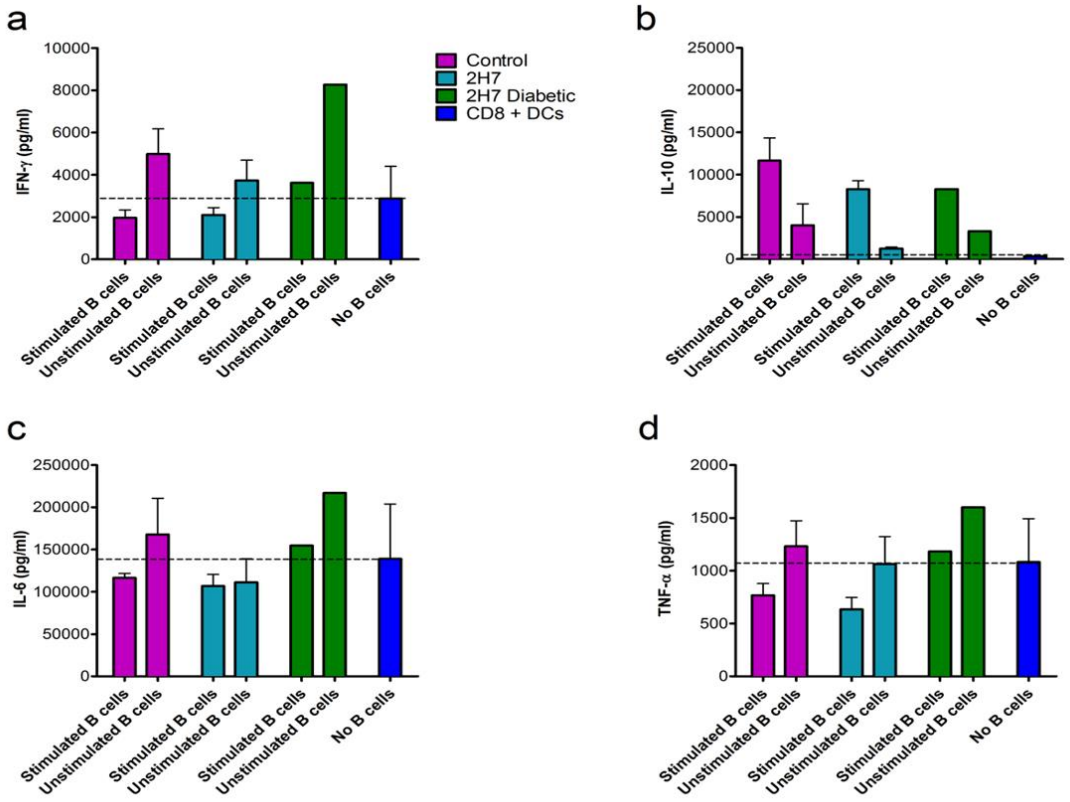

Figure 5.24 Effect of stimulated and unstimulated B cells on the secretion of cytokines. After culture for one week, bone marrow DCs from PI homo mice were stimulated with LPS for 18h. Splenic B cells from hCD20 mice were stimulated with LPS for 24h or left unstimulated. Splenic CD8 T cells (from G9 mice) were purified on the day of the experimental set-up and labelled with CFSE for the evaluation of $CD8^+$ T viable cells. The experimental procedure was as follows: $2x10^5$ CD8 T cells, $4x10^5$ DCs and $1.4x10^6$ stimulated or unstimulated B cells were added to each well. Forty-eight hours after the set-up, supernatants were also collected and cytokines were measured. The concentration of IFN-γ is shown in (a), IL-10 in (b), IL-6 (c) and TNF-α (d). Dashed lines indicate the levels of the cytokines produced by CD8 T cells + DCs. The data are represented as mean and standard error. n=3 for control and 2H7 groups and n=1 for 2H7 diabetic, done over 2 experiments.

5.7.3.1 CD8 T cell proliferation, activation and frequency of viable cells

For these experiments, both concentrations used (1µg/ml and 0.5µg/ml) led to almost 100% proliferation of CD8 T cells (Figure 5.25a). Less proliferation was observed when the unstimulated B cells derived from the diabetic mouse were in the cultures using 0.5µg/ml of peptide. On the other hand, the activation of CD8 T cells ($CD44^+$ cells) was higher in the presence of stimulated and unstimulated B cells from this same diabetic mouse (Figure 5.25b), than in the other 2 groups. However, the biological effect of such small differences is debatable.

The percentage of viable CD8 T cells did not vary among the groups and was around 80% for all of groups (Figure 5.25c).

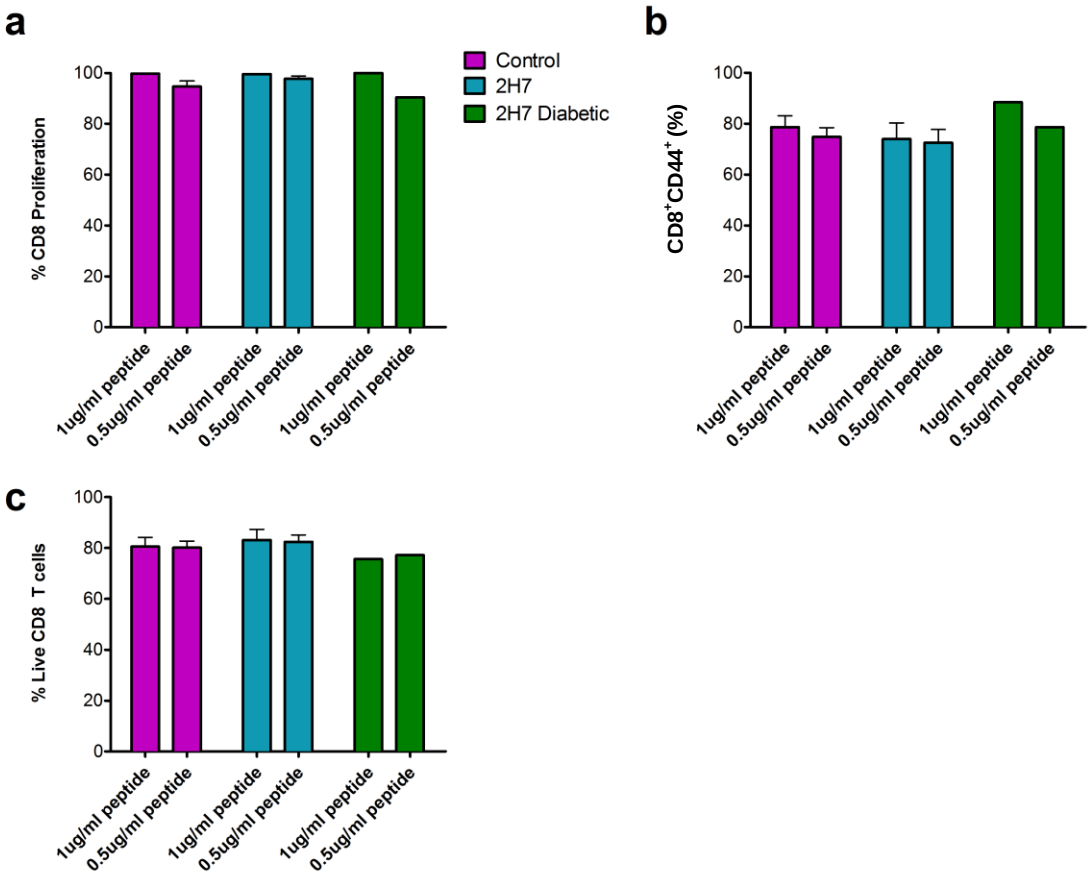

Figure 5.25 Effect of stimulated and unstimulated B cells, acting as APCs, in the proliferation and activation of CD8 T cells. Splenic B cells from hCD20 mice were stimulated with LPS for 24h or left unstimulated. Splenic CD8 T cells (from G9 mice) were purified on the day of the set-up of the experiment and labelled with CFSE for the evaluation of CD8 proliferation. The experimental procedure was as follows: $2x10^5$ CD8 T cells, $1.4x10^6$ LPS-stimulated or unstimulated B cells and G9 peptide were added together in each culture. After 72h of incubation, cultures were harvested for flow cytometric staining. Forty eight hours after the set-up, supernatants were also collected. We analysed the proliferation ($CFSE^+$ cells - a), activation ($CD44^+$ cells - b) and frequency of viable cells (c) in CD8 T cells. The data are represented as mean and standard error. n=3 for control and 2H7 groups and n=1 for 2H7 diabetic, done over 2 experiments.

5.7.3.2 Expression of co-stimulatory molecules in B cells from hCD20 mice

Contrasting with the results shown previously (where the expression of CD80 and CD86 on the B cells was lower in mice treated with 2H7), when added in culture with peptide and CD8 T cells, the percentage of B cells (from > 35 w.o. mice) expressing both costimulatory molecules was similar for all 3 groups. The expression of CD80 (Figure 5.26a) was somewhat smaller when the concentration of the peptide was lower. The percentage of B cells expressing CD86 (Figure 5.26b) was higher than the percentage of $CD19^{+}CD80^{+}$ cells in all groups.

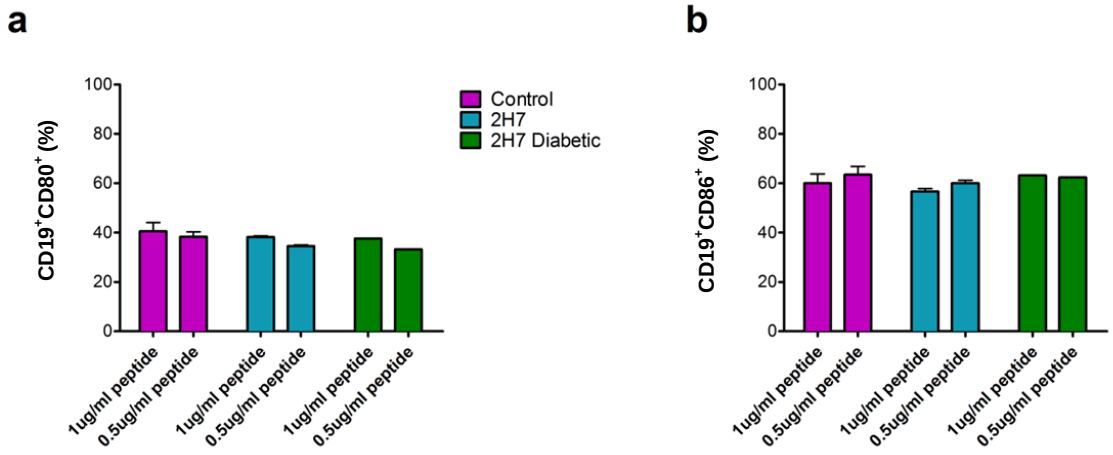

Figure 5.26 Expression of costimulatory molecules in stimulated and unstimulated B cells, acting as APCs to CD8 T cells. Splenic B cells from hCD20 mice were stimulated with LPS for 24h or left unstimulated. Splenic CD8 T cells (from G9 mice) were purified on the day of the set-up of the experiment and labelled with CFSE for the evaluation of CD8 proliferation. The experimental procedure was as follows: $2x10^{5}$ CD8 T cells, $1.4x10^{6}$ LPS-stimulated or unstimulated B cells and G9 peptide were added together in each culture. After 72h of incubation, cultures were harvested for flow cytometric staining. Forty eight hours after the set-up, supernatants were also collected. We analysed the expression of CD80 (a) and CD86 (b) on B cells. The data are represented as mean and standard error. n=3 for control and 2H7 groups and n=1 for 2H7 diabetic, done over 2 experiments.

5.7.3.3 Cytokine production in B cells working as APCs from hCD20 mice

Although the percentages of proliferation, activation and viable CD8 T cells were very similar for the 2 concentrations of the peptide, the concentration of cytokines secreted into the supernatants varied between wells that received 1μg/ml or 0.5μg/ml of G9 peptide.

The concentration of IFN-γ (Figure 5.27a) was higher in wells with 1μg/ml and the greatest difference between the two concentrations was observed in the cultures containing B cells from the diabetic mouse.

Control hCD20 mice, not injected with anti-hCD20, had lower concentrations of IFN-γ and higher IL-10 (Figure 5.27b), compared to the 2H7-treated mice.

IL-6 was not secreted in great quantities when DCs were not present; the concentrations were similar between the two euglycaemic groups and lower in the culture containing B cells from the diabetic mouse (Figure 5.27c).

TNF-α (Figure 5.27d) followed the same pattern seen for the concentrations of IFN-γ.

5.7.4 Summary

The protective effect of B cell depletion against type 1 diabetes in NOD mice described in the literature was reproduced here when 6-8 week old mice were injected with anti-hCD20, showing reduced incidence and delayed onset of the disease.

To investigate whether this protection could be related to altered regulatory B cell function, we analysed B cells from > 35 w.o. (protected) hCD20 mice, treated with 2H7 or control untreated hCD20 mice. These B cells were tested using the system described in chapter 4 (section 4.2), where antigen-specific DCs presented antigen to antigen-specific CD8 T cells, while B cells were functioning as bystanders, interacting with the cells, but not acting as APCs.

Although there were differences in the proliferation and activation of CD8 T cells and the secretion of cytokines when LPS-stimulated and unstimulated B cells were compared, the differences were seen in all groups, including the one mouse that had become diabetic from the 2H7-treated group. There were no striking differences between the groups when B cells were the antigen-presenting cells either, and where there was a small difference, lower IFN-γ and higher IL-10 in the control group. These

results suggest that if there is a role for regulatory B cells in the protection seen in B cell depleted mice, it might not be due to the effect of B cells on CD8 T cells and DCs.

The results, however, require further confirmation as a greater number of mice, over more than one experiment, are needed for more definite conclusions.

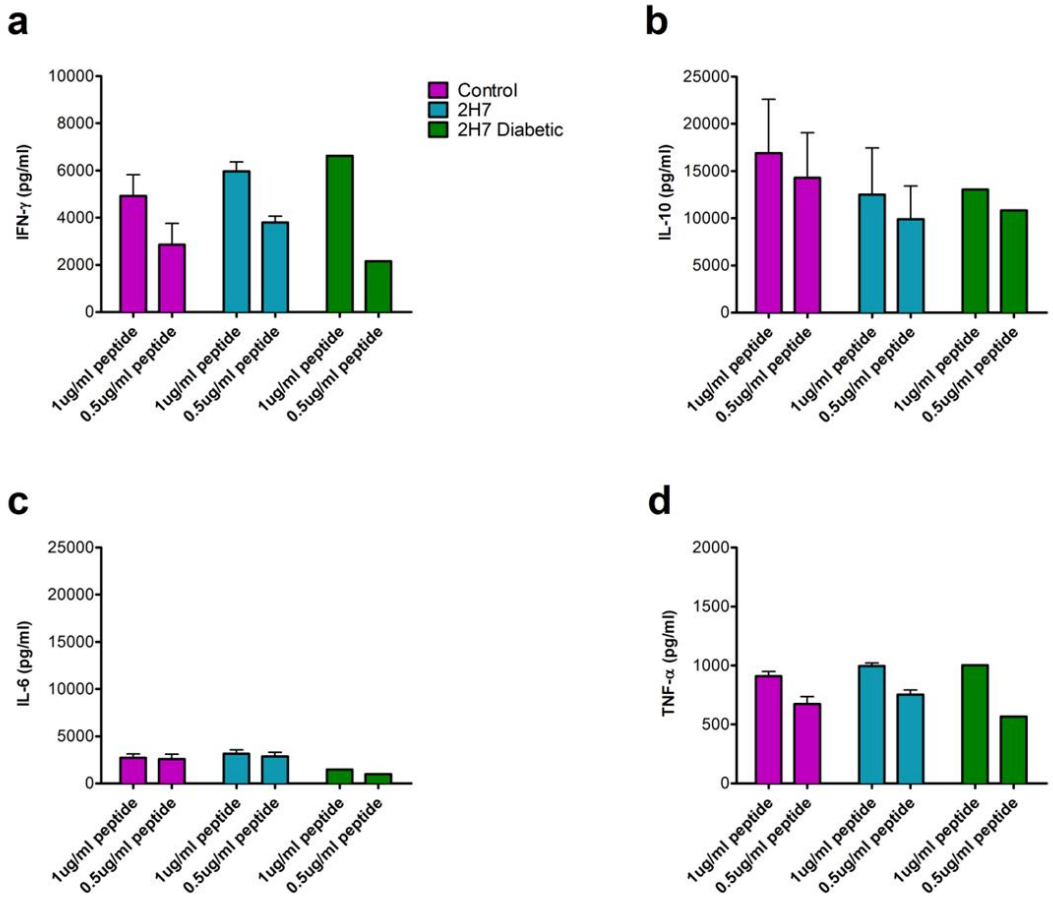

Figure 5.27 Effect of stimulated and unstimulated B cells, as APCs, on the secretion of cytokines. Splenic B cells from the spleen of hCD20 mice were stimulated with LPS for 24h or left unstimulated. Splenic CD8 T cells (from G9 mice) were purified on the day of the set-up of the experiment and labelled with CFSE for the evaluation of CD8 proliferation. The experimental procedure was as follows: $2x10^5$ CD8 T cells, $1.4x10^6$ LPS-stimulated or unstimulated B cells and G9 peptide were added together in each culture. After 72h of incubation, cultures were harvested for flow cytometric staining. Forty-eight hours after the set-up, supernatants were also collected and cytokines were measured with the multiplex assay kit (MSD). The concentration of IFN-γ is shown in (a), IL-10 in (b), IL-6 (c) and TNF-α (d). The data are represented as mean and standard error. n=3 for control and 2H7 groups and n=1 for 2H7 diabetic, done over 2 experiments.

5.8 Discussion

Anti-CD20 monoclonal antibodies were first used to deplete B cells as a treatment for lymphomas, and because of their efficacy, the use was extended for autoimmune diseases.

Rituximab (chimeric anti-CD20) has already been tested in clinical trials for SLE, arthritis and type 1 diabetes and caused few adverse events, but the effect has often been partial (Pescovitz et al. 2014; Cohen and Keystone 2015; Mok 2015). Therefore, it is important to study the mechanisms of action of this treatment on the immune system as a whole, in an effort to find ways to improve its efficacy.

To study the effects of an antibody similar to rituximab in the type 1 diabetes experimental model, a transgenic NOD mouse strain expressing human CD20 (here designated hCD20 NOD mice) was generated (Hu et al. 2007).

The aims of this study were to: 1) Evaluate the effects of B cell depletion and repopulation in B cell subsets, especially regulatory subsets; 2) Examine the production of cytokines by B cells after the depletion and 3) Determine whether the protection against type 1 diabetes seen in depleted mice was due to the effect of B cells on CD8 T cells or DCs.

Six to eight week-old hCD20 NOD mice received one cycle (4 injections in 9 days) of either anti-hCD20 (2H7) or control IgG (MPC-11) and the depletion was followed for 12 weeks after the last injection. B cells were evaluated in the spleen, lymph nodes and bone marrow and the most interesting findings are discussed below.

Different organs showed different degrees of depletion and the order was: MLN B cells were almost 100% depleted, followed by spleen and PLNs (90%), then Peyer's patches (75%) and bone marrow was where B cell depletion was least efficient (peaking at 60% one week after the last injection). The efficacy of the depletion depended more on the blood circulation in the organs than the expression of hCD20 on B cells (as more than 95% of all B cells outside the bone marrow express this marker); "hidden" organs provide protection against depletion, one example being the peritoneal cavity, where B-1 and B-2 cells are generally more resistant to depletion (Gong et al. 2005; Hamaguchi et al. 2005), and these B cells were not studied in this thesis.

The bone marrow, however, should not be analysed the same way as other lymphoid organs. They are the location for the generation of new B cells after depletion, and comprise cells at different stages of development, and therefore their population is mixed in the expression of hCD20. The disturbance of homeostasis of the number of B cells in the periphery is manifest by a decrease of recirculating FO B cells in the BM and this leads to a faster proliferation of pro/pre B cells, which will repopulate the remaining lymphoid organs (Shahaf et al. 2016).

Table 5.1 summarizes the subpopulations of B cells analysed in the lymphoid organs and how B cell depletion affected each of them.

In the spleen, the proportion of B cells with Follicular zone phenotype was generally similar in control and depleted groups throughout the experiments. Marginal zone and T2 B cells were more susceptible to depletion. This observation was made not only based on the reduction of the major phenotypes ($CD21^{hi}CD23^{low}$ and $CD21^{hi}CD23^{hi}$, respectively), but also on the depletion of $CD1d^{hi}$ and $CD24^{hi}CD38^{hi}$ B cells. Not surprisingly, Transitional B cells returned to normal proportions by the 8^{th} week after injection. As the immature phenotype of B cells entering the spleen from the bone marrow, they were likely to be an earlier subset repopulating the spleen. In the lymph nodes, depletion lasted longer than in the spleen. B cells with MZ or T2 phenotype are rare in the LNs, so the depletion was observed largely in the FO B cells. As observed in the analysis of hCD20 expression in $CD19^{+}$ B cells, these differences were not due to lower expression of the target molecule in specific subpopulations.

The reported susceptibility of B cells in the spleen to depletion is contradictory in the literature. Some publications describe MZ B cells as susceptible, agreeing with our data (DiLillo et al. 2008), while other show the opposite (Gong et al. 2005). The discrepancy could be due to different mouse strains (as discussed in previous chapters, the marginal zone in the spleen of NOD mice is thicker than in other strains) or age at which anti-CD20 is administered.

In all organs, B cells expressing $CD5^{hi}$ and CD43 were resistant to depletion. This meant that, in an environment where other populations were being reduced, the depletion of these subsets was occurring in a less clear manner, leading to a higher proportion/percentage. Both $CD5^{hi}$ and CD43 are markers related to B-1 B cells that were described previously in the literature as a subpopulation resistant to B cell

depletion (Hamaguchi et al. 2005). As discussed earlier, this resistance was not due to the lack of hCD20 expressed on these B cells. B-1 B cells are self-renewing, thus intrinsic mechanisms to resist depletion would be indispensable to avoid total extinction. Whilst Hamaguchi and colleagues postulated that B-1 B cells in the peritoneal cavity were not depleted because this environment lacked effector cells to remove anti-CD20 coated cells, this clearly does not apply in the spleen and lymph nodes. Further studies on intrinsic protection of these cells may be of importance (Hamaguchi et al. 2005).

One interesting finding in our study was the expression of hCD20 by almost all $CD19^{+}CD138^{+}$ cells in the secondary lymphoid organs and a lower percentage of $CD19^{+}CD138^{+}hCD20^{+}$ cells in the bone marrow. Regardless of their expression of hCD20, these cells were resistant to depletion, resulting in higher frequencies of B cells expressing $CD138^{+}$ in depleted mice during depletion. Reports in the literature showed that anti-CD20 did not affect the basal production of immunoglobulins and that the stable numbers of long-lived plasma cells during depletion were not derived from resistant mature B cells or memory cells, once they were susceptible to depletion (Ahuja et al. 2008; DiLillo et al. 2008). This data and the data from B-1 B cells could suggest that the populations that are resistant to depletion are self-renewable (and therefore are more resistant to apoptosis) and are involved with producing antibodies (including natural antibodies, in the case of B-1 B cells).

Table 5.1 Summary of the effect of B cell depletion on the subpopulations studied, in different lymphoid organs

	Spleen	PLN	MLN	PP	BM
CD19	depleted	Depleted	depleted	depleted	depleted**
Follicular zone	No clear difference	Depleted	depleted	depleted	depleted
Marginal zone	depleted	--	--	--	--
Transitional cells	depleted*	--	--	--	--
$CD1d^{hi}CD5^{+}$	depleted	--	--	--	--
$CD5^{hi}$	resistant	resistant	resistant	resistant	No clear difference
$CD1d^{hi}CD5^{hi}$	resistant	--	--	--	--
$CD24^{hi}CD38^{hi}$	depleted *	--	--	--	--
CD24 (MFI)	--	higher in 2H7 group	higher in 2H7 group	higher in 2H7 group	No clear difference
CD38 (MFI)	--	No clear difference	No clear difference	lower in the 2H7 group	lower in the 2H7 group
CD43	resistant	resistant	resistant	resistant	resistant
IgD	depleted *	depleted	depleted	depleted	depleted
IgM	depleted	depleted	depleted	depleted	depleted
CD138	resistant	resistant	resistant	resistant	No clear difference
Tim-1	resistant	resistant	resistant	resistant	No clear difference

* Returned first, before other depleted subpopulations

** Returned first, before other depleted lymphoid organs

When B cells were examined after a 24h culture period with LPS, anti-CD40 or left unstimulated, the reduced percentage of cells expressing the costimulatory molecules CD80 and CD86 in the B cell depleted mice (figure 5.12) may partially explain why B cell depletion leads to protection against type 1 diabetes. The percentages of B cells expressing these costimulatory proteins were lower in depleted mice even 12 weeks after the last injection, when all other markers studied were back to levels comparable to

the control group. On the other hand, when the function of B cells as APCs was assessed in >35 w.o. hCD20 NOD mice, there was no difference in the frequency of CD80 and CD86 between euglycaemic control and depleted and hyperglycaemic depleted mice. However, this finding does not remove the possibility that the reduction of B cells expressing CD80 or CD86 earlier, during the depletion, modulated the system when B cells functioning as APCs were more important for the onset of the disease. In a primate model of multiple sclerosis, it was demonstrated that anti-CD20 administration led to an environment in the lymphoid organs less favourable for T cell homing to the brain, with the remaining B cells expressing less costimulatory molecules (Kap et al. 2014). Moreover, transgenic mice with CD80/CD86$^{-/-}$ B cells were resistant to the induction of arthritis, in a similar way to mice lacking B cells (O'Neill et al. 2007).

Although showing the data in percentage/proportion demonstrated the difference between susceptible and resistant B cell subpopulations, it is important to note that a study of the absolute numbers would also contribute for the analysis. It would show the absolute level of depletion of each subpopulation and allow comparison of numbers of cells between the subpopulations in control and depleted mice. Therefore, the analysis of absolute numbers would ideally also be performed.

Lastly, the production of cytokines by remaining and repopulated B cells was analysed. During depletion, the production of IL-10 was compromised, probably as a result of depleted marginal zone cells and CD1d^{hi} B cells. The percentages of TGF-β^{+} and IL-6^{+} B cells was very low, but higher in depleted mice. When the spleen was repopulated, the frequency of B cells producing IL-10 returned to similar levels compared to the control. The percentages of TGF-β and IL-6 were similar too, 12 weeks after the last injection.

Indeed, when B cell depletion was analysed in transgenic hCD20 NOD mice expressing only specific TCRs for a peptide from chromogranin A (BDC 2.5 Tg mice), these CD4 T cells were more aggressive *in vitro* during the period when the B cells were depleted. BDC2.5 T cells from treated mice also caused accelarated diabetes when transferred to NOD.scid mice, compared to the control group. Nevertheless, in the BDC 2.5 Tg/hCD20 NOD model, the returning B cells were more suppressive (Xiang et al. 2012). Our findings that IL-10-producing B cells are depleted during anti-CD20

treatment is in agreement with previous observations that T cells are not well regulated during depletion.

B cell depletion enhances Treg functions after repopulation (Hu et al. 2007; Olalekan et al. 2015). However, here we were not able to demonstrate higher frequencies of B cells producing anti-inflammatory cytokines in the spleen of 2H7 treated mice or that B cells from these mice were more regulatory, after repopulation, in an experimental system testing DC activation of insulin-specific CD8 T cells. Nevertheless, our results do not exclude the possibility that B cell regulation of CD8 T cell function may not be as efficient as regulation of CD4 T cell function.

Future work in progress for this project includes the use of anti-CD20 to deplete B cells in 12-15 w.o. hCD20 NOD. The aim is to determine the effect of B cell depletion in a later stage of type 1 diabetes development.

In another part of this project, being developed by Joanne Boldison, the effect of B cell depletion on the insulitis of hCD20 NOD mice is being studied. Early results suggest that B cell depletion also caused the reduction of T cells in the pancreas infiltration.

Finally, the depletion of B cells (that affects MLNs and PPs, as observed in this chapter) could modulate the quality of the gut microbiota, which would then modulate the immune system differently. This is also under investigation, results of which are not yet available.

In conclusion, the use of anti-hCD20 to deplete B cells in hCD20 NOD mice led to the alteration of subpopulation proportions in the lymphoid organs. The treatment also delayed and reduced the incidence of type 1 diabetes. Our studies did not identify an association between this protection and IL-10 producing B cells, but suggested a role for the reduction of costimulatory proteins in remaining B cells during depletion and the early stages of repopulation.

6. Discussion

The main aim of this thesis was to study regulatory B cells in type 1 diabetes, using the NOD mouse model. A number of studies were carried out using different approaches. We demonstrated, in Chapter 3, that naturally protected NOD mice (more than 35 weeks old that had not developed diabetes) had similar frequencies of B cells producing the pro-inflammatory cytokine IL-6 and the regulatory cytokine TGF-β, when compared to diabetic NOD mice. However, those mice that did not show signs of hyperglycaemia had higher baseline percentages of IL-10-producing B cells than diabetic mice and age-matched congenic $B6^{g7}$ mice, the control strain (not diabetes-prone), and responded more to stimuli that increased the frequency of IL-10-producing cells, including LPS.

Moreover, evaluating their regulatory potential in Chapter 4, B cells from protected NOD mice led to less degranulation of CD8 T cells and reduced production of IL-12p70 by DCs, when compared to diabetic mice. Another interesting finding was that LPS-stimulated B cells had greater suppressive effects compared to unstimulated B cells, even when B cells were from diabetic mice.

When investigating the role of regulatory B cells on the protection conferred by transient B cell depletion, we observed, as shown previously, that mice that had been B cell-depleted developed a lower incidence of diabetes. Nevertheless, IL-10-producing B cells were susceptible to depletion, similar to other B cell populations and the repopulated B cells had similar regulatory potential, when interacting with CD8 T cells and DCs, to those found in the non-depleted mice.

Based on the idea that regulatory B cells need inflammation to produce IL-10 (Rosser et al. 2014; Menon et al. 2016), it is difficult to determine whether the increased frequency of $CD19^{+}IL\text{-}10^{+}$ cells seen in protected NOD mice is a cause or consequence of protection. Did the higher percentage of IL-10-producing B cells lead to protection from diabetes or were they increased as a result of inflammation that was then kept under control by other regulatory cells? Unfortunately, it is not possible to follow splenic B cell production of IL-10 over time to examine the fate of mice at an intermediate age, and follow those mice longitudinally until they became diabetic or became part of the protected pool of NOD mice. At the time that these 13-17 w.o. mice were evaluated in chapter 3, they could have become either diabetic or been protected. In one study in

humans, although the total number of B cells in peripheral blood did not change in patients with type 1 diabetes, compared to healthy controls, they also had fewer B10 cells (Deng et al. 2016). Thus, investigating the percentage of IL-10-producing B cells during type 1 diabetes development in patients, from the time that they develop islet-autoantibodies to the first signs of disease as well as "slow progressors", who develop islet-autoantibodies but who do not develop diabetes, might explain whether these regulatory cells are the cause or consequence of protection.

The observations made in relation to regulatory B cells in these studies raised questions to direct the future of this line of research. An interesting finding in chapter 3 was the variation caused by different stimulants in B cells from diabetic mice: B cells were able to respond, producing IL-10, to LPS and CpG (although less than in protected mice); but when stimulated with anti-CD40, the percentage was close to zero. With this in mind, as the IL-10 response by B cells from the diabetic was less compared to the protected older mice, it would be of importance to activate B cells with different stimulants and test their effects on dendritic cells and CD8 T cells. Our hypothesis is that the difference in suppression between B cells from protected and diabetic NOD mice after anti-CD40 stimulation would be even greater, while CpG-stimulated B cells would produce similar outcomes to those which was observed with LPS. Another important combination of stimulants to be tested would be aIgM and anti-CD40. The stimulation of naïve B cells by both of these together is known to generate germinal centre B cells and, further, plasma cells, but not regulatory B cells (Yanaba et al. 2009; Vinuesa et al. 2010).

The relevance of these stimulants *in vivo* should also be taken into consideration. The importance of CD40 stimulation in NOD mice is easily tracked back to the interaction with T cells. As discussed in chapter 3, in patients with SLE, the unresponsiveness of B cells to anti-CD40 was due to a problem in STAT3 signalling, not downregulation of the co-stimulatory molecule on the surface of B cells (Blair et al. 2010). Further investigation in patients with type 1 diabetes and NOD mice could give insights into the relation between impairment in CD40 signalling and the development of disease.

However, the role of LPS or CpG in a model for type 1 diabetes is more difficult to explain. The concept of lymphocytes producing regulatory cytokines after bacterial/viral encounter is not new. The "Old Friends" theory postulates that the immune system

suppresses responses against some types of microbes because they evolved together with humans and needed to be tolerated. Thus, infections or symbiotic interactions with certain bacteria or helminths are associated with protection against autoimmune diseases, allergy and asthma in humans (Rook 2012). One of the mechanisms proposed for tolerating these microbes is the induction of regulatory T and B cells, which would provide a more suppressive environment and regulate autoimmune diseases better (Correale et al. 2008; Zaccone et al. 2009).

For B cells specifically, studies have shown that they produce IL-10 during *Salmonella* infection, for example, in a Myd88-dependent manner (Neves et al. 2010). Although TLR ligands activate effector cells, they may also activate regulatory type cells, as shown in T cells (Sutmuller et al. 2006); when expressed in B cells, these receptors seem to also control the extension of inflammatory responses, by the secretion of regulatory cytokines. Moreover, B cells are also known to produce IL-35 (another regulatory cytokine) during bacterial infection, limiting the immune system efficacy (Shen et al. 2014).

The importance of gut microbiota modulating immune responses has also been a recent subject of study that ties together bacteria and autoimmunity. The quality of fecal bacteria was shown to be different in islet-autoantibody positive children when compared to controls (de Goffau et al. 2013). It has been suggested that an unbalanced ratio of *Bacteroides* and *Firmicutes*, favouring the former, might lead to susceptibility to type 1 diabetes (Davis-Richardson and Triplett 2015; Hu et al. 2015). Among other mechanisms, this could suggest that perhaps the ability of B cells from diabetic mice to produce IL-10, when activating TLRs, is impaired by the reduced expression of these receptors or by the absence of the "right" bacteria to activate the regulatory response.

It is broadly agreed that IL-10-producing B cells are mainly found within the $CD1d^{hi}CD5^{+}$ subpopulation, after LPS stimulation (Yanaba et al. 2008). However, the studies discussed above demonstrated that, upon infection, $CD19^{+}CD138^{+}$ B cells are the subset responsible for regulatory cytokine production (Shen et al. 2014). In our experiments, the lack of one unified marker for Bregs was the reason why B cells were not sorted before the set-up in chapter 4. Choosing one subset would not have allowed study of the regulatory function of B cells as a whole, especially for IL-10 independent mechanisms.

Despite the observation that the levels of IL-10 were significantly increased with the addition of B cells to the cultures containing CD8 T cells and DCs in chapter 4, IL-10-independent mechanisms could also be responsible for the regulation.

The first possible alternative to IL-10 could be TGF-β. Although, in chapter 4, we were not able to detect this cytokine intracellularly by flow cytometry or secreted in the supernatant, by ELISA, the possibility that membrane bound TGF-β could have been part of the response should not be discarded, as its function inducing CD8 T cell anergy was described by (Parekh et al. 2003). Interestingly, in our experiments, IL-10-producing B cells and TGF-β-producing B cells were not the exact same cells, but expressed the same putative regulatory markers, i.e., they showed low percentages of IL-10/TGF-β double positive B cells (shown as Figures A3 and A4 in the Appendix). Understanding the signalling pathways behind this "choice" of producing one cytokine or the other might reveal some important details about regulatory B cells.

Another cytokine-independent regulatory mechanism could be by cell-cell contact, through upregulation of suppressive surface markers. As a mechanism used for evasion, *Salmonella* infected B cells, for example, upregulate the expression of PD-1L (Programmed death-1 ligand – a molecule from the CD28/CTLA-4 family); this molecule can suppress CD8 T cell activity (Lopez-Medina et al. 2015). In humans, stimulation of B cells by CpG-DNA upregulated the expression of PD-1L as well (Kubo et al. 2012). The addition of PD-1 and PD-1L to the flow cytometric panel would help to evaluate if that is the case in our model.

Furthermore the upregulation of the markers Fas-FasL, receptors for the induction of apoptosis, could have also been responsible for the suppression observed in our experiments. Indeed, there was a significantly lower percentage of viable CD8 T cells in cultures where LPS-stimulated B cells from NOD mice were added, which was attributed to TGF-β-producing B cells previously in the literature (Tian et al. 2001).

It will also be important to evaluate more closely the effect of LPS-stimulated B cells on dendritic cells. Examples of how B cells might regulate DCs may include downregulation of co-stimulatory molecules and induction of apoptosis.

Transwell assays, isolating B cells from directly interacting with T cells and DCs, would highlight how much of the results were due to regulatory cytokines versus the importance of cell-cell contact. However, it is also important to note that cell-cell

contact could also result in cytokine production. CD8 T cells, for example, could be binding to B cells through CD40-CD40L, promoting more IL-10 production by LPS-stimulated B cells. The main findings and questions for future investigations based on the results in chapters 3 and 4 are illustrated in Figure 6.1.

As we did not demonstrate an increase in splenic IL-10-producing B cells in hCD20 NOD mice treated with anti-CD20, the IL-10 independent mechanisms described previously may also be relevant for the protection conferred by transient B cell depletion, as well as the reduced co-stimulatory molecules CD80 and CD86 on repopulating B cells.

One important observation in respect of these anti-CD20 experiments was the resistance by B-1 cells to depletion. Although we did not evaluate how the depletion affected peritoneal B cells (comprising mostly B-1 cells, but also some B2 cells), studies done by others have shown that 1) they are resistant to depletion (Hamaguchi et al. 2005) and 2) these peritoneal B-1 cells are able to produce greater levels of IL-10 (Maseda et al. 2013). Thus, the idea that after depletion of other B cells, these cells were more able to regulate the immune responses should not be ruled out.

The modifications in the immune system caused by the temporary absence of B cells should also be considered. Xiang and colleagues showed that, during B depletion, BDC2.5 CD4 T cells were more aggressive than in age-matched non-treated mice. However, they also showed that the returning B cell population were able to increase the population of Foxp3+ Treg cells in a cell-cell contact manner ($CD5^+$ B cells were shown to be responsible for the increase in regulatory properties) (Xiang et al. 2012).

If T cells become more inflammatory during the depletion but yet the incidence of the disease decreases, B cell depletion could regulate the immune system in a manner other than a direct effect on T cells. Indeed, one study showed that B cell depletion also expanded a population of myeloid-derived suppressor cells (MDSCs – $Gr1^+CD11b^+$), known for reducing T cell responses in autoimmune diseases and transplantation. These $Gr1^+$ cells are IL-10-producing cells (Hu et al. 2012). Thus, despite anti-CD20 treatment not increasing splenic IL-10-producing B cells, there may be effects on induction of other regulatory populations, including regulatory T cells and $Gr1^+$ cells.

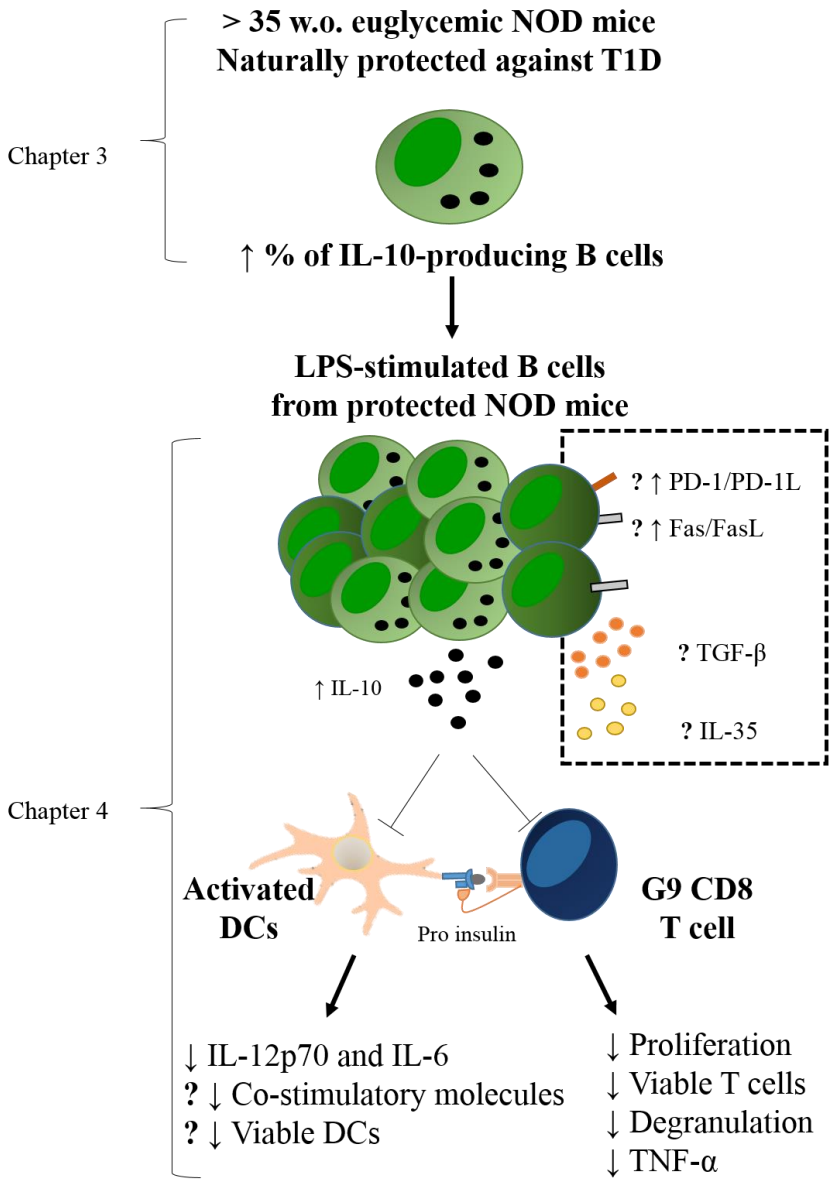

Figure 6.1 Diagram of the main findings and the possible mechanisms for the suppression seen in chapter 4. Results in chapter 3 demonstrated that the frequency of B cells producing IL-10 was higher in > 35 w.o. naturally protected NOD mice, when compared to diabetic NOD mice. In chapter 4, we showed that when LPS-stimulated B cells from these protected NOD mice were added to the culture with dendritic cells and antigen-specific CD8 T cells, they were able to suppress the activity of CD8 T cells and DCs (the main findings are listed below the cells). These results could be associated with the higher levels of IL-10 secreted by LPS-stimulated B cells. Alternatively, some IL-10-independent mechanisms for this suppression are listed in the panel shown with the dashed-line border and include: Secretion of TGF-β and IL-35 and the upregulation of suppressor receptors.

Finally, the outcome of anti-CD20 treatment should also be studied in the population of immune cells infiltrating the pancreatic islets. As discussed previously, B cells play many roles in the maintenance of insulitis, as APCs (Noorchashm et al. 1999) and/or enhancing CD8 T cell survival (Brodie et al. 2008). And although the majority of studies investigating islet infiltration were performed in experimental models, B cells were also detected in human pancreatic islet inflammation (In't Veld 2014). Thus, B cell depletion could also interfere locally with the β-cell destruction and the evaluation of anti-CD20 effect on pancreatic infiltration is currently ongoing in our lab.

Taken all together, these results showed the possible involvement of regulatory B cells as one of the mechanisms by which naturally protected NOD mice do not develop type 1 diabetes. On the other hand, as no difference were found after repopulation following B cell depletion therapy, they are unlikely to be as important for the protection that is induced by anti-CD20 treatment. Thus, although we set out to test the hypothesis that regulatory B cells may increase following B cell depletion, this does not seem to be the mechanism of protection. However depletion of the B cells, which allows other populations of cells including regulatory T cells and Gr 1 cells to expand, may then be acting indirectly with other immune cells with more efficacy (Figure 6.2).

As in the machinery of a clock, the immune responses that interact causing the development of type 1 diabetes have to be seen in their entirety, taking every gear as an important piece and, the function of each cell, being dependent on another cell. What we have demonstrated here was that there is one “gear” component of regulatory B cells in the immune system and, when working efficiently, its role may be to induce other regulatory mechanisms to prevent type 1 diabetes in NOD mice. However, a reduction or absence of regulatory B cell activity would allow effector cells to continue their islet destruction. Future work will be required to determine if this regulatory B cell component can be boosted to help to prevent type 1 diabetes.

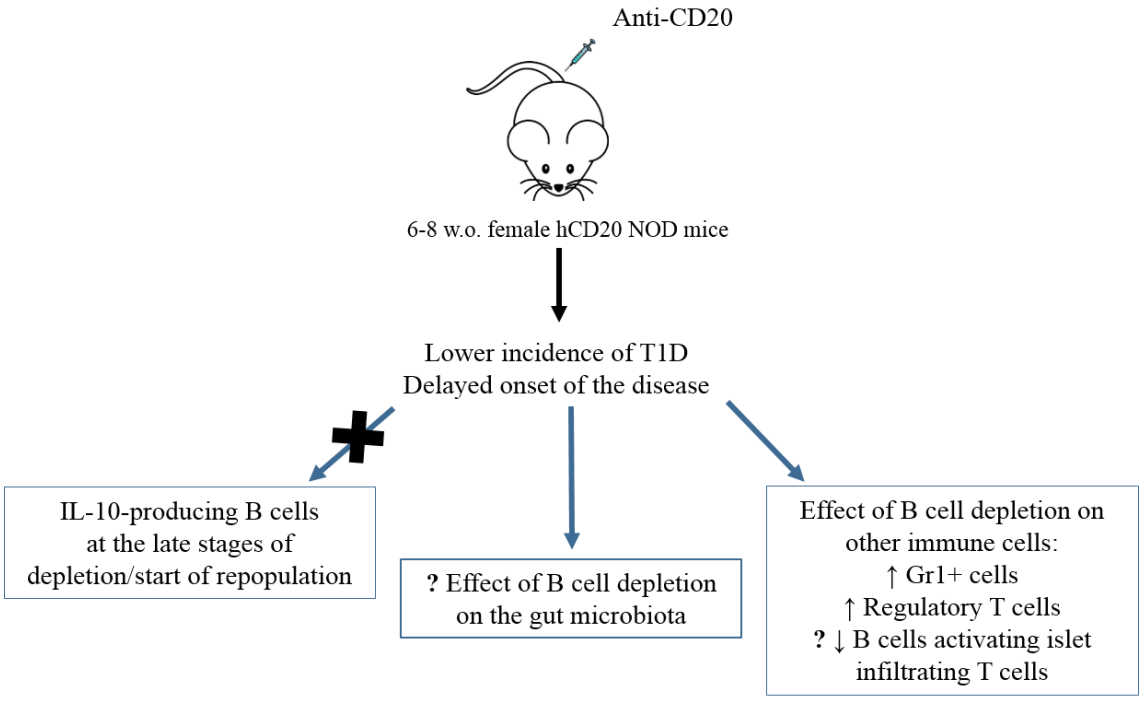

Figure 6.2 Diagram illustrating the main findings of chapter 5 and some possible effects of B cell depletion by anti-CD20 treatment. In agreement with data from the literature, the administration of anti-CD20 to young NOD mice led to delayed onset of type 1 diabetes and reduced incidence. Our aim was to investigate whether IL-10-producing B cells were modulating this protection. Because these cells were susceptible to depletion, it is unlikely that they were functioning to directly influence type 1 diabetes during the depletion period. However, other mechanisms were described in the literature and they have shown the effect of B cell depletion on other immune cells. How anti-CD20 treatment affects pancreatic islet-infiltrating cells and the gut microbiota are two questions for future work.

7. Appendix

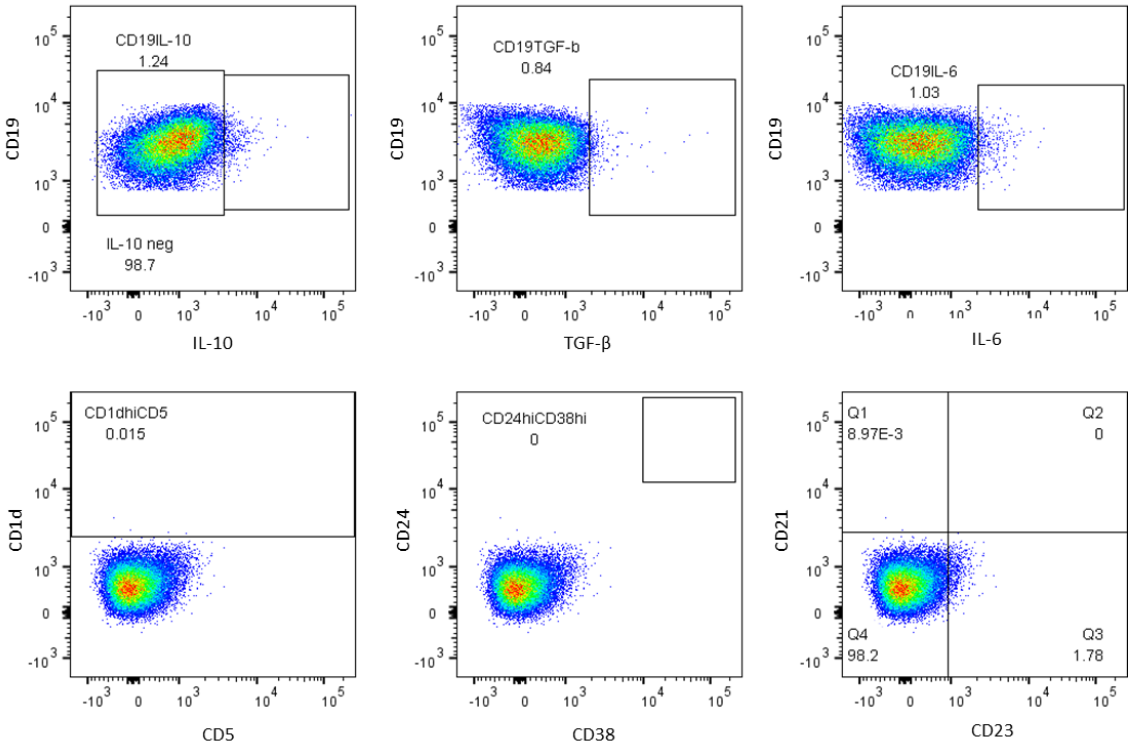

Figure A1 FMO and isotype controls for chapter 3. These flow cytometric gates are the negative control for the gating strategy showed in Figures 3.2 and 3.16. Methods were described previously.

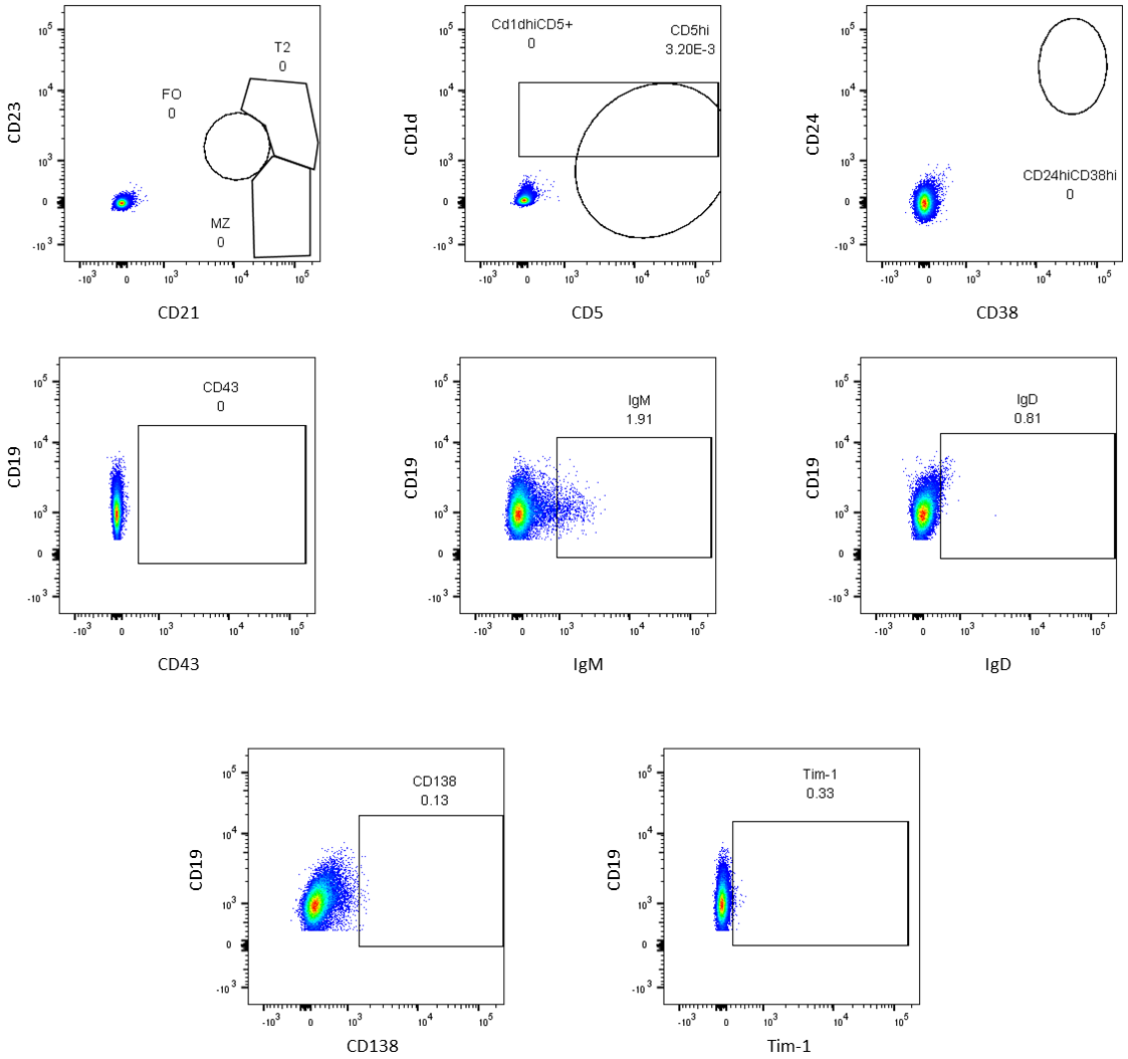

Figure A2 FMO and isotype controls for chapter 5. These flow cytometric gates are the negative control for the gating strategy showed in Figures 5.2. Methods were described previously.

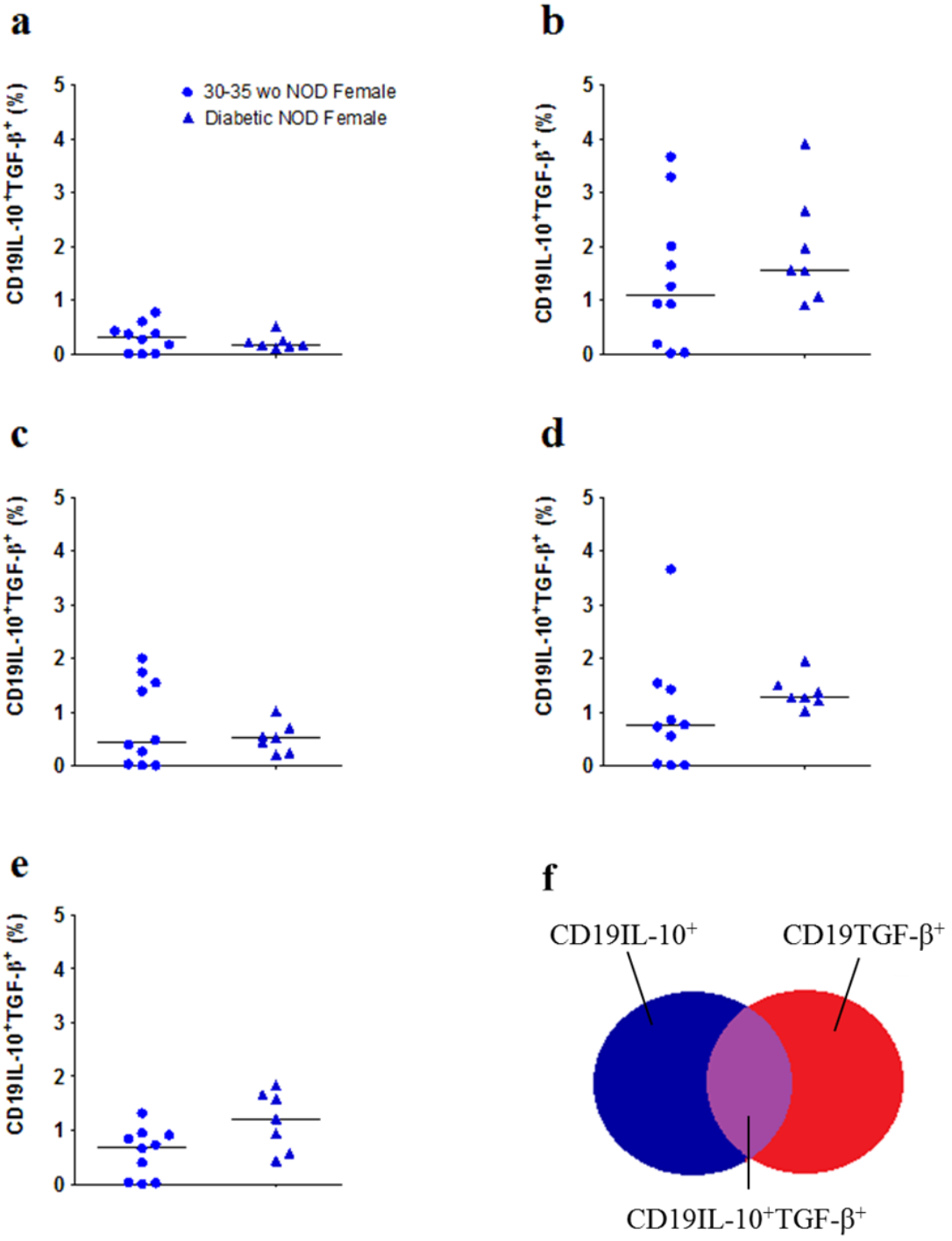

Figure A3 Percentage of B cells (CD19) double positive for IL-10$^+$ and TGF-β$^+$. Spleens from female NOD mice were collected, erythrocytes were lysed and removed and spleen cells were cultured for 24h unstimulated (a) or stimulated with LPS (b), anti-CD40 (c), CpG (d) or anti-CD40/CpG (e); PMA, ionomycin and monensin were added for the last 3 hours and then cells were stained for extracellular markers and intracellular IL-10 and TGF-β. The percentages of double positives were calculated using Flow Jo analysis software, by Boolean Gate, as the percentage of CD19$^+$IL-10$^+$ and CD19$^+$TGF-β$^+$ that overlap. Each symbol represents an individual mouse and a median bar is shown. The explanatory diagram is shown in (f).

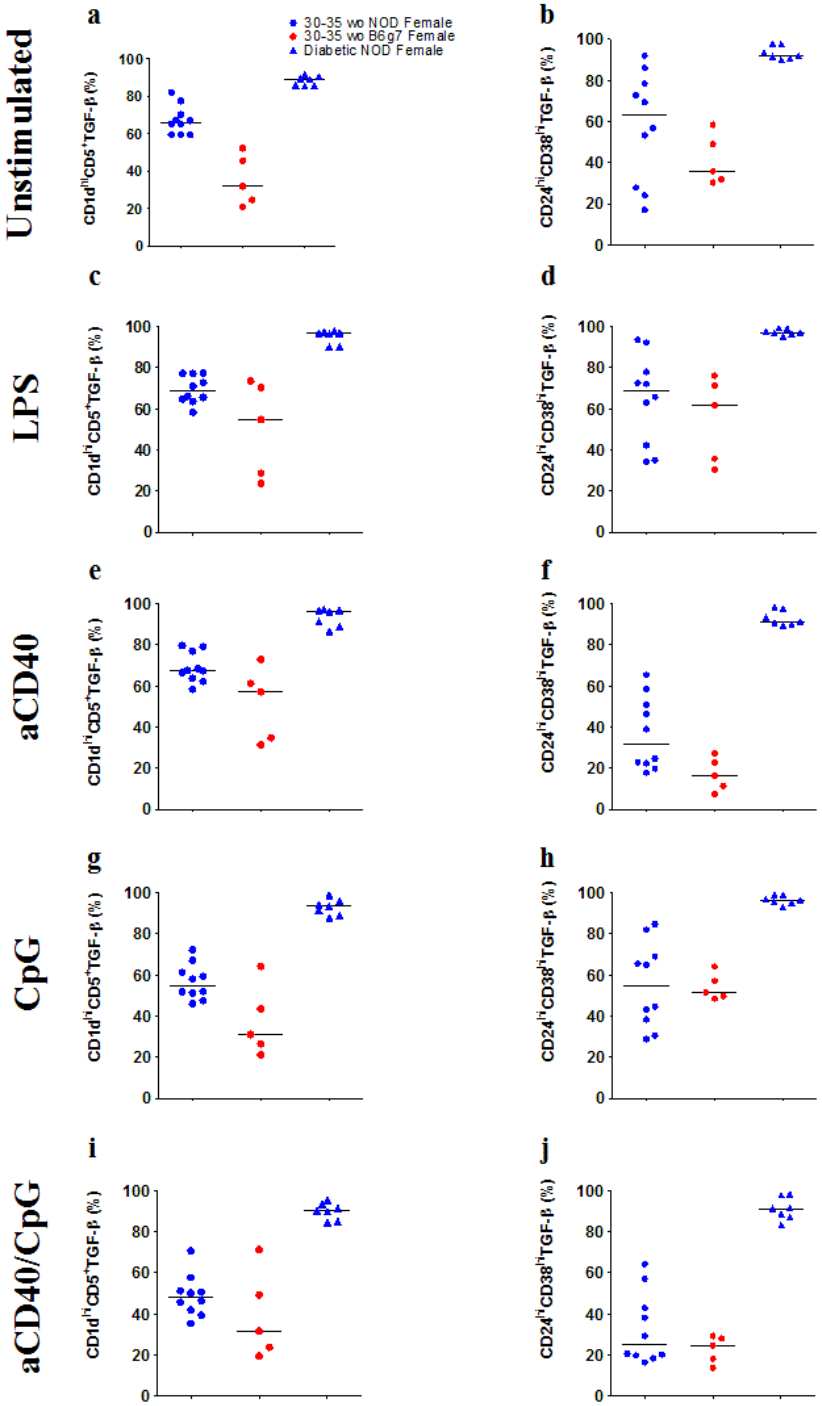

Figure A4 Frequency of regulatory markers expression in TGF-β-producing B cells. Spleens from 30-35 w.o. female NOD and $B6^{g7}$ mice, as well as diabetic female NOD mice, were collected, erythrocytes were lysed and removed and spleen cells were cultured for 24h unstimulated (a-b) or stimulated with LPS (c-d), anti-CD40 (e-f), CpG (g-h) or anti-CD40/CpG (i-j); PMA, ionomycin and monensin were added for the last 3 hours and then cells were stained for extracellular markers and intracellular cytokines. Samples were examined by flow cytometry. Frequencies of $CD1d^{hi}CD5^{+}$ expression in $CD19^{+}TGF\text{-}\beta^{+}$ cells are shown in (a,c,e,g and i) and frequencies of $CD24^{hi}CD38^{+}$ expression in $CD19^{+}TGF\text{-}\beta^{+}$ cells are shown in (b,d,f,h and j). Each symbol represents an individual mouse and a median bar is shown.

8. References

Ahuja, A. and Anderson, S. M. and Khalil, A. and Shlomchik, M. J. 2008. Maintenance of the plasma cell pool is independent of memory B cells. *Proc Natl Acad Sci U S A* 105(12), pp. 4802-4807.

Ahuja, A. and Shupe, J. and Dunn, R. and Kashgarian, M. and Kehry, M. R. and Shlomchik, M. J. 2007. Depletion of B cells in murine lupus: efficacy and resistance. *J Immunol* 179(5), pp. 3351-3361.

Akdis, M. and Aab, A. and Altunbulakli, C. and Azkur, K. and Costa, R. A. and Crameri, R. and Duan, S. and Eiwegger, T. and Eljaszewicz, A. and Ferstl, R. and Frei, R. and Garbani, M. and Globinska, A. and Hess, L. and Huitema, C. and Kubo, T. and Komlosi, Z. and Konieczna, P. and Kovacs, N. and Kucuksezer, U. C. and Meyer, N. and Morita, H. and Olzhausen, J. and O'Mahony, L. and Pezer, M. and Prati, M. and Rebane, A. and Rhyner, C. and Rinaldi, A. and Sokolowska, M. and Stanic, B. and Sugita, K. and Treis, A. and van de Veen, W. and Wanke, K. and Wawrzyniak, M. and Wawrzyniak, P. and Wirz, O. F. and Zakzuk, J. S. and Akdis, C. A. 2016. Interleukins (from IL-1 to IL-38), interferons, transforming growth factor beta, and TNF-alpha: Receptors, functions, and roles in diseases. *J Allergy Clin Immunol* 138, pp. 984-1010.

Alkanani, A. K. and Hara, N. and Gottlieb, P. A. and Ir, D. and Robertson, C. E. and Wagner, B. D. and Frank, D. N. and Zipris, D. 2015. Alterations in Intestinal Microbiota Correlate With Susceptibility to Type 1 Diabetes. *Diabetes* 64, pp. 3510-3520.

Allman, D. and Pillai, S. 2008. Peripheral B cell subsets. *Curr Opin Immunol* 20(2), pp. 149-157.

Almqvist, N. and Martensson, I. L. 2012. The pre-B cell receptor; selecting for or against autoreactivity. *Scand J Immunol* 76(3), pp. 256-262.

Amrani, A. and Verdaguer, J. and Anderson, B. and Utsugi, T. and Bou, S. and Santamaria, P. 1999. Perforin-independent beta-cell destruction by diabetogenic CD8(+) T lymphocytes in transgenic nonobese diabetic mice. *J Clin Invest* 103(8), pp. 1201-1209.

Anderson, M. S. and Bluestone, J. A. 2005. The NOD mouse: a model of immune dysregulation. *Annu Rev Immunol* 23, pp. 447-485.

Andre, I. and Gonzalez, A. and Wang, B. and Katz, J. and Benoist, C. and Mathis, D. 1996. Checkpoints in the progression of autoimmune disease: lessons from diabetes models. *Proc Natl Acad Sci U S A* 93(6), pp. 2260-2263.

Atkinson, M. A. and Eisenbarth, G. S. 2001. Type 1 diabetes: new perspectives on disease pathogenesis and treatment. *Lancet* 358, pp. 221-229.

Atkinson, M. A. and Eisenbarth, G. S. and Michels, A. W. 2014. Type 1 diabetes. *Lancet* 383(9911), pp. 69-82.

Atkinson, M. A. and Leiter, E. H. 1999. The NOD mouse model of type 1 diabetes: as good as it gets? *Nat Med* 5(6), pp. 601-604.

Attanavanich, K. and Kearney, J. F. 2004. Marginal zone, but not follicular B cells, are potent activators of naive CD4 T cells. *J Immunol* 172(2), pp. 803-811.

Baekkeskov, S. and Aanstoot, H. J. and Christgau, S. and Reetz, A. and Solimena, M. and Cascalho, M. and Folli, F. and Richter-Olesen, H. and De Camilli, P. 1990. Identification of the 64K autoantigen in insulin-dependent diabetes as the GABA-synthesizing enzyme glutamic acid decarboxylase. *Nature* 347(6289), pp. 151-156.

Bao, Y. and Cao, X. 2014. The immune potential and immunopathology of cytokine-producing B cell subsets: a comprehensive review. *J Autoimmun* 55, pp. 10-23.

Bao, Y. and Han, Y. and Chen, Z. and Xu, S. and Cao, X. 2011. IFN-alpha-producing PDCA-1+ Siglec-H- B cells mediate innate immune defense by activating NK cells. *Eur J Immunol* 41(3), pp. 657-668.

Barr, T. A. and Shen, P. and Brown, S. and Lampropoulou, V. and Roch, T. and Lawrie, S. and Fan, B. and O'Connor, R. A. and Anderton, S. M. and Bar-Or, A. and Fillatreau, S. and Gray, D. 2012. B cell depletion therapy ameliorates autoimmune disease through ablation of IL-6-producing B cells. *J Exp Med* 209(5), pp. 1001-1010.

Barrett, J. C. and Clayton, D. G. and Concannon, P. and Akolkar, B. and Cooper, J. D. and Erlich, H. A. and Julier, C. and Morahan, G. and Nerup, J. and Nierras, C. and Plagnol, V. and Pociot, F. and Schuilenburg, H. and Smyth, D. J. and Stevens, H. and Todd, J. A. and Walker, N. M. and Rich, S. S. 2009. Genome-wide association study and meta-analysis find that over 40 loci affect risk of type 1 diabetes. *Nat Genet* 41(6), pp. 703-707.

Baumgarth, N. 2011. The double life of a B-1 cell: self-reactivity selects for protective effector functions. *Nat Rev Immunol* 11, pp. 34-46.

Baxter, A. G. and Cooke, A. 1993. Complement lytic activity has no role in the pathogenesis of autoimmune diabetes in NOD mice. *Diabetes* 42(11), pp. 1574-1578.

Bennett, S. T. and Lucassen, A. M. and Gough, S. C. and Powell, E. E. and Undlien, D. E. and Pritchard, L. E. and Merriman, M. E. and Kawaguchi, Y. and Dronsfield, M. J. and Pociot, F. and et al. 1995. Susceptibility to human type 1 diabetes at IDDM2 is determined by tandem repeat variation at the insulin gene minisatellite locus. *Nat Genet* 9(3), pp. 284-292.

Betts, M. R. and Brenchley, J. M. and Price, D. A. and De Rosa, S. C. and Douek, D. C. and Roederer, M. and Koup, R. A. 2003. Sensitive and viable identification of antigen-specific CD8+ T cells by a flow cytometric assay for degranulation. *J Immunol Methods* 281, pp. 65-78.

Blair, P. A. and Chavez-Rueda, K. A. and Evans, J. G. and Shlomchik, M. J. and Eddaoudi, A. and Isenberg, D. A. and Ehrenstein, M. R. and Mauri, C. 2009. Selective targeting of B cells with agonistic anti-CD40 is an efficacious strategy for the generation of induced regulatory T2-like B cells and for the suppression of lupus in MRL/lpr mice. *J Immunol* 182(6), pp. 3492-3502.

Blair, P. A. and Norena, L. Y. and Flores-Borja, F. and Rawlings, D. J. and Isenberg, D. A. and Ehrenstein, M. R. and Mauri, C. 2010. CD19(+)CD24(hi)CD38(hi) B cells exhibit regulatory capacity in healthy individuals but are functionally impaired in systemic Lupus Erythematosus patients. *Immunity* 32(1), pp. 129-140.

Boes, M. and Prodeus, A. P. and Schmidt, T. and Carroll, M. C. and Chen, J. 1998. A critical role of natural immunoglobulin M in immediate defense against systemic bacterial infection. *J Exp Med* 188(12), pp. 2381-2386.

Boes, M. and Schmidt, T. and Linkemann, K. and Beaudette, B. C. and Marshak-Rothstein, A. and Chen, J. 2000. Accelerated development of IgG autoantibodies and autoimmune disease in the absence of secreted IgM. *Proc Natl Acad Sci U S A* 97(3), pp. 1184-1189.

Brink, R. 2007. Germinal-center B cells in the zone. *Immunity 26*, pp. 552-554.

Brodie, G. M. and Wallberg, M. and Santamaria, P. and Wong, F. S. and Green, E. A. 2008. B-cells promote intra-islet CD8+ cytotoxic T-cell survival to enhance type 1 diabetes. *Diabetes* 57, pp. 909-917.

Candon, S. and Perez-Arroyo, A. and Marquet, C. and Valette, F. and Foray, A. P. and Pelletier, B. and Milani, C. and Ventura, M. and Bach, J. F. and Chatenoud, L. 2015. Antibiotics in early life alter the gut microbiome and increase disease incidence in a spontaneous mouse model of autoimmune insulin-dependent diabetes. *PLoS One* 10(5), p. e0125448.

Castano, L. and Eisenbarth, G. S. 1990. Type-I diabetes: a chronic autoimmune disease of human, mouse, and rat. *Annu Rev Immunol* 8, pp. 647-679.

Cerutti, A. and Cols, M. and Puga, I. 2013. Marginal zone B cells: virtues of innate-like antibody-producing lymphocytes. *Nat Rev Immunol* 13(2), pp. 118-132.

Chamberlain, N. and Massad, C. and Oe, T. and Cantaert, T. and Herold, K. C. and Meffre, E. 2016. Rituximab does not reset defective early B cell tolerance checkpoints. *J Clin Invest* 126(1), pp. 282-287.

Chan, A. C. and Carter, P. J. 2010. Therapeutic antibodies for autoimmunity and inflammation. *Nat Rev Immunol* 10, pp. 301-316.

Chaudhry, M. S. and Karadimitris, A. 2014. Role and regulation of CD1d in normal and pathological B cells. *J Immunol* 193(10), pp. 4761-4768.

Christianson, S. W. and Shultz, L. D. and Leiter, E. H. 1993. Adoptive transfer of diabetes into immunodeficient NOD-scid/scid mice. Relative contributions of CD4+ and CD8+ T-cells from diabetic versus prediabetic NOD.NON-Thy-1a donors. *Diabetes* 42(1), pp. 44-55.

Cohen, M. D. and Keystone, E. 2015. Rituximab for Rheumatoid Arthritis. *Rheumatol Ther* 2(2), pp. 99-111.

Constant, S. L. 1999. B lymphocytes as antigen-presenting cells for CD4+ T cell priming in vivo. *J Immunol* 162(10), pp. 5695-5703.

Cooke, A. 2009. Review series on helminths, immune modulation and the hygiene hypothesis: how might infection modulate the onset of type 1 diabetes? *Immunology* 126(1), pp. 12-17.

Correale, J. and Farez, M. and Razzitte, G. 2008. Helminth infections associated with multiple sclerosis induce regulatory B cells. *Ann Neurol* 64(2), pp. 187-199.

Cross, A. H. and Stark, J. L. and Lauber, J. and Ramsbottom, M. J. and Lyons, J. A. 2006. Rituximab reduces B cells and T cells in cerebrospinal fluid of multiple sclerosis patients. *J Neuroimmunol* 180(1-2), pp. 63-70.

D'Alise, A. M. and Auyeung, V. and Feuerer, M. and Nishio, J. and Fontenot, J. and Benoist, C. and Mathis, D. 2008. The defect in T-cell regulation in NOD mice is an effect on the T-cell effectors. *Proc Natl Acad Sci U S A* 105(50), pp. 19857-19862.

Daifotis, A. G. and Koenig, S. and Chatenoud, L. and Herold, K. C. 2013. Anti-CD3 clinical trials in type 1 diabetes mellitus. *Clin Immunol* 149, pp. 268-278.

Davis-Richardson, A. G. and Triplett, E. W. 2015. A model for the role of gut bacteria in the development of autoimmunity for type 1 diabetes. *Diabetologia* 58(7), pp. 1386-1393.

de Goffau, M. C. and Luopajarvi, K. and Knip, M. and Ilonen, J. and Ruohtula, T. and Harkonen, T. and Orivuori, L. and Hakala, S. and Welling, G. W. and Harmsen, H. J. and Vaarala, O. 2013. Fecal microbiota composition differs between children with beta-cell autoimmunity and those without. *Diabetes* 62(4), pp. 1238-1244.

de Jersey, J. and Snelgrove, S. L. and Palmer, S. E. and Teteris, S. A. and Mullbacher, A. and Miller, J. F. and Slattery, R. M. 2007. Beta cells cannot directly prime diabetogenic CD8 T cells in nonobese diabetic mice. *Proc Natl Acad Sci U S A* 104(4), pp. 1295-1300.

De Smedt, T. and Van Mechelen, M. and De Becker, G. and Urbain, J. and Leo, O. and Moser, M. 1997. Effect of interleukin-10 on dendritic cell maturation and function. *Eur J Immunol* 27(5), pp. 1229-1235.

Deng, C. and Xiang, Y. and Tan, T. and Ren, Z. and Cao, C. and Huang, G. and Wen, L. and Zhou, Z. 2016. Altered Peripheral B-Lymphocyte Subsets in Type 1 Diabetes and Latent Autoimmune Diabetes in Adults. *Diabetes Care* 39(3), pp. 434-440.

DiLillo, D. J. and Hamaguchi, Y. and Ueda, Y. and Yang, K. and Uchida, J. and Haas, K. M. and Kelsoe, G. and Tedder, T. F. 2008. Maintenance of long-lived plasma cells and serological memory despite mature and memory B cell depletion during CD20 immunotherapy in mice.*J Immunol*. Vol. 180. United States, pp. 361-371.

Ding, Q. and Yeung, M. and Camirand, G. and Zeng, Q. and Akiba, H. and Yagita, H. and Chalasani, G. and Sayegh, M. H. and Najafian, N. and Rothstein, D. M. 2011. Regulatory B

cells are identified by expression of TIM-1 and can be induced through TIM-1 ligation to promote tolerance in mice. *J Clin Invest* 121(9), pp. 3645-3656.

Du, J. and Wang, H. and Zhong, C. and Peng, B. and Zhang, M. and Li, B. and Hou, S. and Guo, Y. and Ding, J. 2008. Crystal structure of chimeric antibody C2H7 Fab in complex with a CD20 peptide. *Mol Immunol* 45(10), pp. 2861-2868.

Edwards, J. C. and Cambridge, G. 2001. Sustained improvement in rheumatoid arthritis following a protocol designed to deplete B lymphocytes. *Rheumatology (Oxford)* 40(2), pp. 205-211.

Eisenbarth, G. S. 1986. Type I diabetes mellitus. A chronic autoimmune disease. *N Engl J Med* 314(21), pp. 1360-1368.

Erlich, H. and Valdes, A. M. and Noble, J. and Carlson, J. A. and Varney, M. and Concannon, P. and Mychaleckyj, J. C. and Todd, J. A. and Bonella, P. and Fear, A. L. and Lavant, E. and Louey, A. and Moonsamy, P. 2008. HLA DR-DQ haplotypes and genotypes and type 1 diabetes risk: analysis of the type 1 diabetes genetics consortium families. *Diabetes* 57(4), pp. 1084-1092.

Estella, E. and McKenzie, M. D. and Catterall, T. and Sutton, V. R. and Bird, P. I. and Trapani, J. A. and Kay, T. W. and Thomas, H. E. 2006. Granzyme B-mediated death of pancreatic beta-cells requires the proapoptotic BH3-only molecule bid. *Diabetes* 55, pp. 2212-2219.

Evans, J. G. and Chavez-Rueda, K. A. and Eddaoudi, A. and Meyer-Bahlburg, A. and Rawlings, D. J. and Ehrenstein, M. R. and Mauri, C. 2007. Novel suppressive function of transitional 2 B cells in experimental arthritis. *J Immunol* 178(12), pp. 7868-7878.

Fagraeus, A. 1948. The plasma cellular reaction and its relation to the formation of antibodies in vitro. *J Immunol* 58(1), pp. 1-13.

Fillatreau, S. and Sweenie, C. H. and McGeachy, M. J. and Gray, D. and Anderton, S. M. 2002. B cells regulate autoimmunity by provision of IL-10. *Nat Immunol* 3, pp. 944-950.

Fiorina, P. and Vergani, A. and Dada, S. and Jurewicz, M. and Wong, M. and Law, K. and Wu, E. and Tian, Z. and Abdi, R. and Guleria, I. and Rodig, S. and Dunussi-Joannopoulos, K. and Bluestone, J. and Sayegh, M. H. 2008. Targeting CD22 reprograms B-cells and reverses autoimmune diabetes. *Diabetes* 57(11), pp. 3013-3024.

French, M. B. and Allison, J. and Cram, D. S. and Thomas, H. E. and Dempsey-Collier, M. and Silva, A. and Georgiou, H. M. and Kay, T. W. and Harrison, L. C. and Lew, A. M. 1997. Transgenic expression of mouse proinsulin II prevents diabetes in nonobese diabetic mice. *Diabetes* 46(1), pp. 34-39.

Frommer, F. and Waisman, A. 2010. B cells participate in thymic negative selection of murine auto-reactive CD4+ T cells. *PLoS One* 5(10), p. e15372.

Gantner, F. and Hermann, P. and Nakashima, K. and Matsukawa, S. and Sakai, K. and Bacon, K. B. 2003. CD40-dependent and -independent activation of human tonsil B cells by CpG oligodeoxynucleotides. *Eur J Immunol* 33(6), pp. 1576-1585.

Gatto, D. and Brink, R. 2010. The germinal center reaction. *J Allergy Clin Immunol* 126, pp. 898-907.

Genestier, L. and Taillardet, M. and Mondiere, P. and Gheit, H. and Bella, C. and Defrance, T. 2007. TLR agonists selectively promote terminal plasma cell differentiation of B cell subsets specialized in thymus-independent responses. *J Immunol* 178, pp. 7779-7786.

Gies, V. and Guffroy, A. and Danion, F. and Billaud, P. and Keime, C. and Fauny, J. D. and Susini, S. and Soley, A. and Martin, T. and Pasquali, J. L. and Gros, F. and Andre-Schmutz, I. and Soulas-Sprauel, P. and Korganow, A. S. 2017. B cells differentiate in human thymus and express AIRE. *J Allergy Clin Immunol* 139, pp. 1049-1052 e1012.

Giltiay, N. V. and Chappell, C. P. and Clark, E. A. 2012. B-cell selection and the development of autoantibodies. *Arthritis Res Ther* 14 (4), p. S1.

Golay, J. T. and Clark, E. A. and Beverley, P. C. 1985. The CD20 (Bp35) antigen is involved in activation of B cells from the G0 to the G1 phase of the cell cycle. *J Immunol* 135(6), pp. 3795-3801.

Gong, Q. and Ou, Q. and Ye, S. and Lee, W. P. and Cornelius, J. and Diehl, L. and Lin, W. Y. and Hu, Z. and Lu, Y. and Chen, Y. and Wu, Y. and Meng, Y. G. and Gribling, P. and Lin, Z. and Nguyen, K. and Tran, T. and Zhang, Y. and Rosen, H. and Martin, F. and Chan, A. C. 2005. Importance of cellular microenvironment and circulatory dynamics in B cell immunotherapy. *J Immunol* 174, pp. 817-826.

Gopal, A. K. and Press, O. W. 1999. Clinical applications of anti-CD20 antibodies. *J Lab Clin Med* 134, pp. 445-450.

Gulden, E. and Ihira, M. and Ohashi, A. and Reinbeck, A. L. and Freudenberg, M. A. and Kolb, H. and Burkart, V. 2013. Toll-like receptor 4 deficiency accelerates the development of insulin-deficient diabetes in non-obese diabetic mice. *PLoS One* 8(9), p. e75385.

Gutcher, I. and Donkor, M. K. and Ma, Q. and Rudensky, A. Y. and Flavell, R. A. and Li, M. O. 2011. Autocrine transforming growth factor-beta1 promotes in vivo Th17 cell differentiation. *Immunity* 34(3), pp. 396-408.

Hamaguchi, Y. and Uchida, J. and Cain, D. W. and Venturi, G. M. and Poe, J. C. and Haas, K. M. and Tedder, T. F. 2005. The peritoneal cavity provides a protective niche for B1 and conventional B lymphocytes during anti-CD20 immunotherapy in mice. *J Immunol* 174, pp. 4389-4399.

Harbers, S. O. and Crocker, A. and Catalano, G. and D'Agati, V. and Jung, S. and Desai, D. D. and Clynes, R. 2007. Antibody-enhanced cross-presentation of self antigen breaks T cell tolerance. *J Clin Invest* 117(5), pp. 1361-1369.

Hardy, R. R. 2006. B-1 B cell development. *J Immunol 1*77, pp. 2749-2754.

Harris, D. P. and Haynes, L. and Sayles, P. C. and Duso, D. K. and Eaton, S. M. and Lepak, N. M. and Johnson, L. L. and Swain, S. L. and Lund, F. E. 2000. Reciprocal regulation of polarized cytokine production by effector B and T cells. *Nat Immunol* 1(6), pp. 475-482.

Hayakawa, K. and Hardy, R. R. and Herzenberg, L. A. 1985. Progenitors for Ly-1 B cells are distinct from progenitors for other B cells. *J Exp Med* 161(6), pp. 1554-1568.

Hayakawa, K. and Hardy, R. R. and Parks, D. R. and Herzenberg, L. A. 1983. The "Ly-1 B" cell subpopulation in normal immunodefective, and autoimmune mice. *J Exp Med* 157(1), pp. 202-218.

Hayakawa, K. and Hardy, R. R. and Stall, A. M. and Herzenberg, L. A. 1986. Immunoglobulin-bearing B cells reconstitute and maintain the murine Ly-1 B cell lineage. *Eur J Immunol* 16(10), pp. 1313-1316.

Hofmann, S. R. and Rosen-Wolff, A. and Tsokos, G. C. and Hedrich, C. M. 2012. Biological properties and regulation of IL-10 related cytokines and their contribution to autoimmune disease and tissue injury. *Clin Immunol* 143, pp. 116-127.

Hu, C. and Du, W. and Zhang, X. and Wong, F. S. and Wen, L. 2012. The role of Gr1+ cells after anti-CD20 treatment in type 1 diabetes in nonobese diabetic mice. *J Immunol* 188(1), pp. 294-301.

Hu, C. Y. and Rodriguez-Pinto, D. and Du, W. and Ahuja, A. and Henegariu, O. and Wong, F. S. and Shlomchik, M. J. and Wen, L. 2007. Treatment with CD20-specific antibody prevents and reverses autoimmune diabetes in mice. *J Clin Invest* 117(12), pp. 3857-3867.

Hu, Y. and Peng, J. and Tai, N. and Hu, C. and Zhang, X. and Wong, F. S. and Wen, L. 2015. Maternal Antibiotic Treatment Protects Offspring from Diabetes Development in Nonobese Diabetic Mice by Generation of Tolerogenic APCs. *J Immunol* 195(9), pp. 4176-4184.

Hussain, S. and Delovitch, T. L. 2005. Dysregulated B7-1 and B7-2 expression on nonobese diabetic mouse B cells is associated with increased T cell costimulation and the development of insulitis. *J Immunol* 174(2), pp. 680-687.

In't Veld, P. 2014. Insulitis in human type 1 diabetes: a comparison between patients and animal models. *Semin Immunopathol* 36(5), pp. 569-579.

Iwata, Y. and Matsushita, T. and Horikawa, M. and Dilillo, D. J. and Yanaba, K. and Venturi, G. M. and Szabolcs, P. M. and Bernstein, S. H. and Magro, C. M. and Williams, A. D. and Hall, R. P. and St Clair, E. W. and Tedder, T. F. 2011. Characterization of a rare IL-10-competent B-cell subset in humans that parallels mouse regulatory B10 cells. *Blood* 117(2), pp. 530-541.

Joffre, O. P. and Segura, E. and Savina, A. and Amigorena, S. 2012. Cross-presentation by dendritic cells. *Nat Rev Immunol* 12, pp. 557-569.

Johnson, P. W. and Glennie, M. J. 2001. Rituximab: mechanisms and applications. *Br J Cancer* 85(11), pp. 1619-1623.

Jun, H. S. and Yoon, J. W. 2003. A new look at viruses in type 1 diabetes. *Diabetes Metab Res Rev* 19(1), pp. 8-31.

Kap, Y. S. and van Driel, N. and Laman, J. D. and Tak, P. P. and t Hart, B. A. 2014. CD20+ B cell depletion alters T cell homing. *J Immunol* 192, pp. 4242-4253.

Kendall, P. L. and Case, J. B. and Sullivan, A. M. and Holderness, J. S. and Wells, K. S. and Liu, E. and Thomas, J. W. 2013. Tolerant anti-insulin B cells are effective APCs. *J Immunol* 190(6), pp. 2519-2526.

Kinnunen, T. and Chamberlain, N. and Morbach, H. and Choi, J. and Kim, S. and Craft, J. and Mayer, L. and Cancrini, C. and Passerini, L. and Bacchetta, R. and Ochs, H. D. and Torgerson, T. R. and Meffre, E. 2013. Accumulation of peripheral autoreactive B cells in the absence of functional human regulatory T cells. *Blood* 121(9), pp. 1595-1603.

Kitano, M. and Moriyama, S. and Ando, Y. and Hikida, M. and Mori, Y. and Kurosaki, T. and Okada, T. 2011. Bcl6 protein expression shapes pre-germinal center B cell dynamics and follicular helper T cell heterogeneity. *Immunity* 34, pp. 961-972.

Kleffel, S. and Vergani, A. and Tezza, S. and Ben Nasr, M. and Niewczas, M. A. and Wong, S. and Bassi, R. and D'Addio, F. and Schatton, T. and Abdi, R. and Atkinson, M. and Sayegh, M. H. and Wen, L. and Wasserfall, C. H. and O'Connor, K. C. and Fiorina, P. 2014. Interleukin-10+ Regulatory B Cells Arise Within Antigen-Experienced CD40+ B Cells to Maintain Tolerance to Islet Autoantigens. *Diabetes* 64(1), pp 158-71

Klein, U. and Dalla-Favera, R. 2008. Germinal centres: role in B-cell physiology and malignancy. *Nat Rev Immunol* 8, pp. 22-33.

Kubo, S. and Yamada, T. and Osawa, Y. and Ito, Y. and Narita, N. and Fujieda, S. 2012. Cytosine-phosphate-guanosine-DNA induces CD274 expression in human B cells and suppresses T helper type 2 cytokine production in pollen antigen-stimulated CD4-positive cells. *Clin Exp Immunol* 169(1), pp. 1-9.

Kuhn, C. and Besancon, A. and Lemoine, S. and You, S. and Marquet, C. and Candon, S. and Chatenoud, L. 2016. Regulatory mechanisms of immune tolerance in type 1 diabetes and their failures. *J Autoimmun* 71, pp. 69-77.

Kuppers, R. 2003. B cells under influence: transformation of B cells by Epstein-Barr virus. *Nat Rev Immunol* 3, pp. 801-812.

Kurts, C. and Heath, W. R. and Carbone, F. R. and Allison, J. and Miller, J. F. and Kosaka, H. 1996. Constitutive class I-restricted exogenous presentation of self antigens in vivo. *J Exp Med* 184(3), pp. 923-930.

Laitinen, O. H. and Honkanen, H. and Pakkanen, O. and Oikarinen, S. and Hankaniemi, M. M. and Huhtala, H. and Ruokoranta, T. and Lecouturier, V. and Andre, P. and Harju, R. and Virtanen, S. M. and Lehtonen, J. and Almond, J. W. and Simell, T. and Simell, O. and Ilonen, J. and Veijola, R. and Knip, M. and Hyoty, H. 2014. Coxsackievirus B1 is associated with induction of beta-cell autoimmunity that portends type 1 diabetes. *Diabetes* 63, pp. 446-455.

Lanzavecchia, A. 1985. Antigen-specific interaction between T and B cells. *Nature* 314(6011), pp. 537-539.

Leandro, M. J. and Edwards, J. C. and Cambridge, G. and Ehrenstein, M. R. and Isenberg, D. A. 2002. An open study of B lymphocyte depletion in systemic lupus erythematosus. *Arthritis Rheum* 46(10), pp. 2673-2677.

Leete, P. and Willcox, A. and Krogvold, L. and Dahl-Jorgensen, K. and Foulis, A. K. and Richardson, S. J. and Morgan, N. G. 2016. Differential Insulitic Profiles Determine the Extent of beta-Cell Destruction and the Age at Onset of Type 1 Diabetes. *Diabetes* 65, pp. 1362-1369.

Lennon, G. P. and Bettini, M. and Burton, A. R. and Vincent, E. and Arnold, P. Y. and Santamaria, P. and Vignali, D. A. 2009. T cell islet accumulation in type 1 diabetes is a tightly regulated, cell-autonomous event. *Immunity* 31(4), pp. 643-653.

Lieberman, S. M. and Evans, A. M. and Han, B. and Takaki, T. and Vinnitskaya, Y. and Caldwell, J. A. and Serreze, D. V. and Shabanowitz, J. and Hunt, D. F. and Nathenson, S. G. and Santamaria, P. and DiLorenzo, T. P. 2003. Identification of the beta cell antigen targeted by a prevalent population of pathogenic CD8+ T cells in autoimmune diabetes. *Proc Natl Acad Sci U S A* 100(14), pp. 8384-8388.

Lim, T. S. and Goh, J. K. and Mortellaro, A. and Lim, C. T. and Hammerling, G. J. and Ricciardi-Castagnoli, P. 2012. CD80 and CD86 differentially regulate mechanical interactions of T-cells with antigen-presenting dendritic cells and B-cells. *PLoS One* 7(9), p. e45185.

Lopez-Medina, M. and Perez-Lopez, A. and Alpuche-Aranda, C. and Ortiz-Navarrete, V. 2015. Salmonella induces PD-L1 expression in B cells. *Immunol Lett* 167, pp. 131-140.

Ludwig-Portugall, I. and Hamilton-Williams, E. E. and Gottschalk, C. and Kurts, C. 2008. Cutting edge: CD25+ regulatory T cells prevent expansion and induce apoptosis of B cells specific for tissue autoantigens. *J Immunol* 181, pp. 4447-4451.

Maloney, D. G. and Grillo-Lopez, A. J. and White, C. A. and Bodkin, D. and Schilder, R. J. and Neidhart, J. A. and Janakiraman, N. and Foon, K. A. and Liles, T. M. and Dallaire, B. K. and Wey, K. and Royston, I. and Davis, T. and Levy, R. 1997. IDEC-C2B8 (Rituximab) anti-CD20 monoclonal antibody therapy in patients with relapsed low-grade non-Hodgkin's lymphoma. *Blood* 90(6), pp. 2188-2195.

Marino, E. and Batten, M. and Groom, J. and Walters, S. and Liuwantara, D. and Mackay, F. and Grey, S. T. 2008. Marginal-zone B-cells of nonobese diabetic mice expand with diabetes onset, invade the pancreatic lymph nodes, and present autoantigen to diabetogenic T-cells. *Diabetes* 57, pp. 395-404.

Marino, E. and Tan, B. and Binge, L. and Mackay, C. R. and Grey, S. T. 2012. B-cell cross-presentation of autologous antigen precipitates diabetes. *Diabetes* 61(11), pp. 2893-2905.

Maseda, D. and Candando, K. M. and Smith, S. H. and Kalampokis, I. and Weaver, C. T. and Plevy, S. E. and Poe, J. C. and Tedder, T. F. 2013. Peritoneal cavity regulatory B cells (B10 cells) modulate IFN-gamma+CD4+ T cell numbers during colitis development in mice. *J Immunol* 191(5), pp. 2780-2795.

Matsumoto, M. and Baba, A. and Yokota, T. and Nishikawa, H. and Ohkawa, Y. and Kayama, H. and Kallies, A. and Nutt, S. L. and Sakaguchi, S. and Takeda, K. and Kurosaki, T. and Baba, Y. 2014. Interleukin-10-producing plasmablasts exert regulatory function in autoimmune inflammation. *Immunity* 41, pp. 1040-1051.

Matsumoto, M. and Yagi, H. and Kunimoto, K. and Kawaguchi, J. and Makino, S. and Harada, M. 1993. Transfer of autoimmune diabetes from diabetic NOD mice to NOD athymic nude mice: the roles of T cell subsets in the pathogenesis. *Cell Immunol* 148, pp. 189-197.

Matsushita, T. and Horikawa, M. and Iwata, Y. and Tedder, T. F. 2010. Regulatory B cells (B10 cells) and regulatory T cells have independent roles in controlling experimental autoimmune encephalomyelitis initiation and late-phase immunopathogenesis. *J Immunol* 185(4), pp. 2240-2252.

Maurer, M. and von Stebut, E. 2004. Macrophage inflammatory protein-1. *Int J Biochem Cell Biol* 36, pp. 1882-1886.

Mauri, C. and Gray, D. and Mushtaq, N. and Londei, M. 2003. Prevention of arthritis by interleukin 10-producing B cells. *J Exp Med* 197(4), pp. 489-501.

McDonald, K. G. and McDonough, J. S. and Newberry, R. D. 2005. Adaptive immune responses are dispensable for isolated lymphoid follicle formation: antigen-naive, lymphotoxin-sufficient B lymphocytes drive the formation of mature isolated lymphoid follicles. *J Immunol* 174, pp. 5720-5728.

Meffre, E. and Wardemann, H. 2008. B-cell tolerance checkpoints in health and autoimmunity. *Curr Opin Immunol* 20(6), pp. 632-638.

Melchers, F. 2005. The pre-B-cell receptor: selector of fitting immunoglobulin heavy chains for the B-cell repertoire. *Nat Rev Immunol* 5, pp. 578-584.

Menon, M. and Blair, P. A. and Isenberg, D. A. and Mauri, C. 2016. A Regulatory Feedback between Plasmacytoid Dendritic Cells and Regulatory B Cells Is Aberrant in Systemic Lupus Erythematosus. *Immunity* 44(3), pp. 683-697.

Mion, F. and Tonon, S. and Toffoletto, B. and Cesselli, D. and Pucillo, C. E. and Vitale, G. 2014. IL-10 production by B cells is differentially regulated by immune-mediated and infectious stimuli and requires p38 activation. *Mol Immunol* 62(2), pp. 266-276.

Mizoguchi, A. and Mizoguchi, E. and Takedatsu, H. and Blumberg, R. S. and Bhan, A. K. 2002. Chronic intestinal inflammatory condition generates IL-10-producing regulatory B cell subset characterized by CD1d upregulation. *Immunity* 16, pp. 219-230.

Mohr, S. B. and Garland, C. F. and Gorham, E. D. and Garland, F. C. 2008. The association between ultraviolet B irradiance, vitamin D status and incidence rates of type 1 diabetes in 51 regions worldwide. *Diabetologia* 51(8), pp. 1391-1398.

Mok, C. C. 2015. Current role of rituximab in systemic lupus erythematosus. *Int J Rheum Dis* 18(2), pp. 154-163.

Nagata, M. and Santamaria, P. and Kawamura, T. and Utsugi, T. and Yoon, J. W. 1994. Evidence for the role of CD8+ cytotoxic T cells in the destruction of pancreatic beta-cells in nonobese diabetic mice. *J Immunol* 152(4), pp. 2042-2050.

Nera, K. P. and Kohonen, P. and Narvi, E. and Peippo, A. and Mustonen, L. and Terho, P. and Koskela, K. and Buerstedde, J. M. and Lassila, O. 2006. Loss of Pax5 promotes plasma cell differentiation. *Immunity* 24, pp. 283-293.

Neves, P. and Lampropoulou, V. and Calderon-Gomez, E. and Roch, T. and Stervbo, U. and Shen, P. and Kuhl, A. A. and Loddenkemper, C. and Haury, M. and Nedospasov, S. A. and Kaufmann, S. H. and Steinhoff, U. and Calado, D. P. and Fillatreau, S. 2010. Signaling via the MyD88 adaptor protein in B cells suppresses protective immunity during Salmonella typhimurium infection. *Immunity* 33, pp. 777-790.

Nikolic, T. and Geutskens, S. B. and van Rooijen, N. and Drexhage, H. A. and Leenen, P. J. 2005. Dendritic cells and macrophages are essential for the retention of lymphocytes in (peri)-insulitis of the nonobese diabetic mouse: a phagocyte depletion study.*Lab Invest*. Vol. 85. United States, pp. 487-501.

Noorchashm, H. and Lieu, Y. K. and Noorchashm, N. and Rostami, S. Y. and Greeley, S. A. and Schlachterman, A. and Song, H. K. and Noto, L. E. and Jevnikar, A. M. and Barker, C. F. and Naji, A. 1999. I-Ag7-mediated antigen presentation by B lymphocytes is critical in overcoming a checkpoint in T cell tolerance to islet beta cells of nonobese diabetic mice. *J Immunol* 163, pp. 743-750.

Noorchashm, H. and Noorchashm, N. and Kern, J. and Rostami, S. Y. and Barker, C. F. and Naji, A. 1997. B-cells are required for the initiation of insulitis and sialitis in nonobese diabetic mice. *Diabetes* 46(6), pp. 941-946.

Nutt, S. L. and Hodgkin, P. D. and Tarlinton, D. M. and Corcoran, L. M. 2015. The generation of antibody-secreting plasma cells. *Nat Rev Immunol* 15, pp. 160-171.

O'Garra, A. and Howard, M. 1992. IL-10 production by CD5 B cells. *Ann N Y Acad Sci* 651, pp. 182-199.

O'Neill, S. K. and Cao, Y. and Hamel, K. M. and Doodes, P. D. and Hutas, G. and Finnegan, A. 2007. Expression of CD80/86 on B cells is essential for autoreactive T cell activation and the development of arthritis. *J Immunol* 179, pp. 5109-5116.

Okada, T. and Cyster, J. G. 2006. B cell migration and interactions in the early phase of antibody responses. *Curr Opin Immunol* 18(3), pp. 278-285.

Olalekan, S. A. and Cao, Y. and Hamel, K. M. and Finnegan, A. 2015. B cells expressing IFN-gamma suppress Treg-cell differentiation and promote autoimmune experimental arthritis. *Eur J Immunol* 45(4), pp. 988-998.

Palmer, J. P. and Asplin, C. M. and Clemons, P. and Lyen, K. and Tatpati, O. and Raghu, P. K. and Paquette, T. L. 1983. Insulin antibodies in insulin-dependent diabetics before insulin treatment. *Science* 222(4630), pp. 1337-1339.

Parekh, V. V. and Prasad, D. V. and Banerjee, P. P. and Joshi, B. N. and Kumar, A. and Mishra, G. C. 2003. B cells activated by lipopolysaccharide, but not by anti-Ig and anti-CD40 antibody, induce anergy in CD8+ T cells: role of TGF-beta 1. *J Immunol* 170(12), pp. 5897-5911.

Patterson, C. C. and Dahlquist, G. G. and Gyurus, E. and Green, A. and Soltesz, G. 2009. Incidence trends for childhood type 1 diabetes in Europe during 1989-2003 and predicted new cases 2005-20: a multicentre prospective registration study. *Lancet* 373(9680), pp. 2027-2033.

Pearson, J. A. and Wong, F. S. and Wen, L. 2016. The importance of the Non Obese Diabetic (NOD) mouse model in autoimmune diabetes. *J Autoimmun* 66, pp. 76-88.

Pelanda, R. and Torres, R. M. 2012. Central B-cell tolerance: where selection begins. *Cold Spring Harb Perspect Biol* 4(4), p. a007146.

Peng, Y. and Laouar, Y. and Li, M. O. and Green, E. A. and Flavell, R. A. 2004. TGF-beta regulates in vivo expansion of Foxp3-expressing CD4+CD25+ regulatory T cells responsible for protection against diabetes. *Proc Natl Acad Sci U S A* 101(13), pp. 4572-4577.

Perera, J. and Meng, L. and Meng, F. and Huang, H. 2013. Autoreactive thymic B cells are efficient antigen-presenting cells of cognate self-antigens for T cell negative selection. *Proc Natl Acad Sci U S A* 110(42), pp. 17011-17016.

Pescovitz, M. D. and Greenbaum, C. J. and Bundy, B. and Becker, D. J. and Gitelman, S. E. and Goland, R. and Gottlieb, P. A. and Marks, J. B. and Moran, A. and Raskin, P. and Rodriguez, H. and Schatz, D. A. and Wherrett, D. K. and Wilson, D. M. and Krischer, J. P. and Skyler, J. S. 2014. B-lymphocyte depletion with rituximab and beta-cell function: two-year results. *Diabetes Care* 37(2), pp. 453-459.

Pescovitz, M. D. and Greenbaum, C. J. and Krause-Steinrauf, H. and Becker, D. J. and Gitelman, S. E. and Goland, R. and Gottlieb, P. A. and Marks, J. B. and McGee, P. F. and Moran, A. M. and Raskin, P. and Rodriguez, H. and Schatz, D. A. and Wherrett, D. and Wilson, D. M. and Lachin, J. M. and Skyler, J. S. 2009. Rituximab, B-lymphocyte depletion, and preservation of beta-cell function. *N Engl J Med* 361, pp. 2143-2152.

Pieper, K. and Grimbacher, B. and Eibel, H. 2013. B-cell biology and development. *J Allergy Clin Immunol* 131(4), pp. 959-971.

Pillai, S. and Cariappa, A. 2009. The follicular versus marginal zone B lymphocyte cell fate decision. *Nat Rev Immunol* 9(11), pp. 767-777.

Pone, E. J. and Zhang, J. and Mai, T. and White, C. A. and Li, G. and Sakakura, J. K. and Patel, P. J. and Al-Qahtani, A. and Zan, H. and Xu, Z. and Casali, P. 2012. BCR-signalling synergizes with TLR-signalling for induction of AID and immunoglobulin class-switching through the non-canonical NF-kappaB pathway. *Nat Commun* 3, p. 767.

Ramos-Perez, W. D. and Fang, V. and Escalante-Alcalde, D. and Cammer, M. and Schwab, S. R. 2015. A map of the distribution of sphingosine 1-phosphate in the spleen. *Nat Immunol* 16(12), pp. 1245-1252.

Reff, M. E. and Carner, K. and Chambers, K. S. and Chinn, P. C. and Leonard, J. E. and Raab, R. and Newman, R. A. and Hanna, N. and Anderson, D. R. 1994. Depletion of B cells in vivo by a chimeric mouse human monoclonal antibody to CD20. *Blood* 83(2), pp. 435-445.

Richardson, S. J. and Willcox, A. and Bone, A. J. and Morgan, N. G. and Foulis, A. K. 2011. Immunopathology of the human pancreas in type-I diabetes. *Semin Immunopathol* 33(1), pp. 9-21.

Ridgway, W. M. and Fasso, M. and Fathman, C. G. 1999. A new look at MHC and autoimmune disease. *Science* 284(5415), pp. 749, 751.

Rivera, A. and Chen, C. C. and Ron, N. and Dougherty, J. P. and Ron, Y. 2001. Role of B cells as antigen-presenting cells in vivo revisited: antigen-specific B cells are essential for T cell expansion in lymph nodes and for systemic T cell responses to low antigen concentrations. *Int Immunol* 13(12), pp. 1583-1593.

Rolf, J. and Motta, V. and Duarte, N. and Lundholm, M. and Berntman, E. and Bergman, M. L. and Sorokin, L. and Cardell, S. L. and Holmberg, D. 2005. The enlarged population of marginal zone/CD1d(high) B lymphocytes in nonobese diabetic mice maps to diabetes susceptibility region Idd11. *J Immunol* 174, pp. 4821-4827.

Ronet, C. and Hauyon-La Torre, Y. and Revaz-Breton, M. and Mastelic, B. and Tacchini-Cottier, F. and Louis, J. and Launois, P. 2010. Regulatory B cells shape the development of Th2 immune responses in BALB/c mice infected with Leishmania major through IL-10 production. *J Immunol* 184, pp. 886-894.

Rook, G. A. 2012. Hygiene hypothesis and autoimmune diseases. *Clin Rev Allergy Immunol* 42(1), pp. 5-15.

Rosenspire, A. J. and Chen, K. 2015. Anergic B Cells: Precarious On-Call Warriors at the Nexus of Autoimmunity and False-Flagged Pathogens. *Front Immunol* 6, p. 580.

Rosser, E. C. and Mauri, C. 2015. Regulatory B cells: origin, phenotype, and function. *Immunity* 42, pp. 607-612.

Rosser, E. C. and Oleinika, K. and Tonon, S. and Doyle, R. and Bosma, A. and Carter, N. A. and Harris, K. A. and Jones, S. A. and Klein, N. and Mauri, C. 2014. Regulatory B cells are induced by gut microbiota-driven interleukin-1beta and interleukin-6 production. *Nat Med* 20(11), pp. 1334-1339.

Rothstein, T. L. and Quach, T. D. 2015. The human counterpart of mouse B-1 cells. *Ann N Y Acad Sci* 1362, pp. 143-152.

Ryan, G. A. and Wang, C. J. and Chamberlain, J. L. and Attridge, K. and Schmidt, E. M. and Kenefeck, R. and Clough, L. E. and Dunussi-Joannopoulos, K. and Toellner, K. M. and Walker, L. S. 2010. B1 cells promote pancreas infiltration by autoreactive T cells. *J Immunol* 185(5), pp. 2800-2807.

Salinas, G. F. and Braza, F. and Brouard, S. and Tak, P. P. and Baeten, D. 2013. The role of B lymphocytes in the progression from autoimmunity to autoimmune disease. *Clin Immunol* 146(1), pp. 34-45.

Savinov, A. Y. and Tcherepanov, A. and Green, E. A. and Flavell, R. A. and Chervonsky, A. V. 2003. Contribution of Fas to diabetes development. *Proc Natl Acad Sci U S A* 100(2), pp. 628-632.

Serreze, D. V. and Fleming, S. A. and Chapman, H. D. and Richard, S. D. and Leiter, E. H. and Tisch, R. M. 1998. B lymphocytes are critical antigen-presenting cells for the initiation of T cell-mediated autoimmune diabetes in nonobese diabetic mice. *J Immunol* 161(8), pp. 3912-3918.

Serreze, D. V. and Leiter, E. H. and Christianson, G. J. and Greiner, D. and Roopenian, D. C. 1994. Major histocompatibility complex class I-deficient NOD-B2mnull mice are diabetes and insulitis resistant. *Diabetes* 43(3), pp. 505-509.

Shahaf, G. and Zisman-Rozen, S. and Benhamou, D. and Melamed, D. and Mehr, R. 2016. B Cell Development in the Bone Marrow Is Regulated by Homeostatic Feedback Exerted by Mature B Cells. *Front Immunol* 7, p. 77.

Shapiro-Shelef, M. and Calame, K. 2005. Regulation of plasma-cell development. *Nat Rev Immunol* 5, pp. 230-242.

Shen, P. and Fillatreau, S. 2015. Antibody-independent functions of B cells: a focus on cytokines. *Nat Rev Immunol* 15, pp. 441-451.

Shen, P. and Roch, T. and Lampropoulou, V. and O'Connor, R. A. and Stervbo, U. and Hilgenberg, E. and Ries, S. and Dang, V. D. and Jaimes, Y. and Daridon, C. and Li, R. and Jouneau, L. and Boudinot, P. and Wilantri, S. and Sakwa, I. and Miyazaki, Y. and Leech, M. D. and McPherson, R. C. and Wirtz, S. and Neurath, M. and Hoehlig, K. and Meinl, E. and Grutzkau, A. and Grun, J. R. and Horn, K. and Kuhl, A. A. and Dorner, T. and Bar-Or, A. and Kaufmann, S. H. and Anderton, S. M. and Fillatreau, S. 2014. IL-35-producing B cells are critical regulators of immunity during autoimmune and infectious diseases. *Nature* 507(7492), pp. 366-370.

Silva, D. G. and Daley, S. R. and Hogan, J. and Lee, S. K. and Teh, C. E. and Hu, D. Y. and Lam, K. P. and Goodnow, C. C. and Vinuesa, C. G. 2011. Anti-islet autoantibodies trigger autoimmune diabetes in the presence of an increased frequency of islet-reactive CD4 T cells. *Diabetes* 60(8), pp. 2102-2111.

Silveira, P. A. and Dombrowsky, J. and Johnson, E. and Chapman, H. D. and Nemazee, D. and Serreze, D. V. 2004. B cell selection defects underlie the development of diabetogenic APCs in nonobese diabetic mice. *J Immunol* 172(8), pp. 5086-5094.

Smith, M. J. and Packard, T. A. and O'Neill, S. K. and Henry Dunand, C. J. and Huang, M. and Fitzgerald-Miller, L. and Stowell, D. and Hinman, R. M. and Wilson, P. C. and Gottlieb, P. A. and Cambier, J. C. 2015. Loss of anergic B cells in prediabetic and new-onset type 1 diabetic patients. *Diabetes* 64(5), pp. 1703-1712.

Solimena, M. and Dirkx, R., Jr. and Hermel, J. M. and Pleasic-Williams, S. and Shapiro, J. A. and Caron, L. and Rabin, D. U. 1996. ICA 512, an autoantigen of type I diabetes, is an intrinsic membrane protein of neurosecretory granules. *Embo j* 15(9), pp. 2102-2114.

Sun, C. M. and Deriaud, E. and Leclerc, C. and Lo-Man, R. 2005. Upon TLR9 signaling, CD5+ B cells control the IL-12-dependent Th1-priming capacity of neonatal DCs. *Immunity* 22, pp. 467-477.

Sutmuller, R. P. and den Brok, M. H. and Kramer, M. and Bennink, E. J. and Toonen, L. W. and Kullberg, B. J. and Joosten, L. A. and Akira, S. and Netea, M. G. and Adema, G. J. 2006. Toll-like receptor 2 controls expansion and function of regulatory T cells. *J Clin Invest* 116(2), pp. 485-494.

Tai, N. and Peng, J. and Liu, F. and Gulden, E. and Hu, Y. and Zhang, X. and Chen, L. and Wong, F. S. and Wen, L. 2016. Microbial antigen mimics activate diabetogenic CD8 T cells in NOD mice. *J Exp Med* 213(10), pp. 2129-2146.

Tai, N. and Wong, F. S. and Wen, L. 2013. TLR9 deficiency promotes CD73 expression in T cells and diabetes protection in nonobese diabetic mice. *J Immunol* 191(6), pp. 2926-2937.

Tang, Q. and Adams, J. Y. and Penaranda, C. and Melli, K. and Piaggio, E. and Sgouroudis, E. and Piccirillo, C. A. and Salomon, B. L. and Bluestone, J. A. 2008. Central role of defective interleukin-2 production in the triggering of islet autoimmune destruction. *Immunity* 28(5), pp. 687-697.

Tedder, T. F. and Engel, P. 1994. CD20: a regulator of cell-cycle progression of B lymphocytes. *Immunol Today* 15, pp. 450-454.

Thayer, T. C. and Pearson, J. A. and De Leenheer, E. and Hanna, S. J. and Boldison, J. and Davies, J. and Tsui, A. and Ahmed, S. and Easton, P. and Siew, L. K. and Wen, L. and Wong, F. S. 2016. Peripheral Proinsulin Expression Controls Low-Avidity Proinsulin-Reactive CD8 T Cells in Type 1 Diabetes. *Diabetes* 65, pp. 3429-3439.

Thayer, T. C. and Wilson, B. S. and Mathews, C. E. 2010. Use of NOD Mice to Understand Human Type 1 Diabetes. *Endocrinol Metab Clin North Am* 39(3), pp. 541-561.

Tian, J. and Zekzer, D. and Hanssen, L. and Lu, Y. and Olcott, A. and Kaufman, D. L. 2001. Lipopolysaccharide-activated B cells down-regulate Th1 immunity and prevent autoimmune diabetes in nonobese diabetic mice. *J Immunol* 167(2), pp. 1081-1089.

Tiselius, A. and Kabat, E. A. 1938. Electrophoresis Of Immune Serum. *Science* 87, pp. 416-417.

van Belle, T. L. and Coppieters, K. T. and von Herrath, M. G. 2011. Type 1 diabetes: etiology, immunology, and therapeutic strategies. *Physiol Rev* 91(1), pp. 79-118.

van de Veen, W. and Stanic, B. and Wirz, O. F. and Jansen, K. and Globinska, A. and Akdis, M. 2016. Role of regulatory B cells in immune tolerance to allergens and beyond. *J Allergy Clin Immunol* 138, pp. 654-665.

Vasquez, A. C. and Feili-Hariri, M. and Tan, R. J. and Morel, P. A. 2004. Qualitative and quantitative abnormalities in splenic dendritic cell populations in NOD mice. *Clin Exp Immunol* 135(2), pp. 209-218.

Velupillai, P. and Garcea, R. L. and Benjamin, T. L. 2006. Polyoma virus-like particles elicit polarized cytokine responses in APCs from tumor-susceptible and -resistant mice. *J Immunol* 176, pp. 1148-1153.

Verdaguer, J. and Schmidt, D. and Amrani, A. and Anderson, B. and Averill, N. and Santamaria, P. 1997. Spontaneous autoimmune diabetes in monoclonal T cell nonobese diabetic mice. *J Exp Med* 186(10), pp. 1663-1676.

Vinay, D. S. and Kim, C. H. and Chang, K. H. and Kwon, B. S. 2010. PDCA expression by B lymphocytes reveals important functional attributes.*J Immunol* 184, pp. 807-815.

Vinuesa, C. G. and Linterman, M. A. and Goodnow, C. C. and Randall, K. L. 2010. T cells and follicular dendritic cells in germinal center B-cell formation and selection. *Immunol Rev* 237, pp. 72-89.

Visperas, A. and Vignali, D. A. 2016. Are Regulatory T Cells Defective in Type 1 Diabetes and Can We Fix Them? *J Immunol* 19, pp. 3762-3770.

Vomund, A. N. and Zinselmeyer, B. H. and Hughes, J. and Calderon, B. and Valderrama, C. and Ferris, S. T. and Wan, X. and Kanekura, K. and Carrero, J. A. and Urano, F. and Unanue, E. R. 2015. Beta cells transfer vesicles containing insulin to phagocytes for presentation to T cells. *Proc Natl Acad Sci U S A* 112, pp. E5496-5502.

von Herrath, M. and Sanda, S. and Herold, K. 2007. Type 1 diabetes as a relapsing-remitting disease? *Nat Rev Immunol* 7, pp. 988-994.

Wang, R. X. and Yu, C. R. and Dambuza, I. M. and Mahdi, R. M. and Dolinska, M. B. and Sergeev, Y. V. and Wingfield, P. T. and Kim, S. H. and Egwuagu, C. E. 2014. Interleukin-35 induces regulatory B cells that suppress autoimmune disease. *Nat Med* 20(6), pp. 633-641.

Wang, W. W. and Yuan, X. L. and Chen, H. and Xie, G. H. and Ma, Y. H. and Zheng, Y. X. and Zhou, Y. L. and Shen, L. S. 2015. CD19+CD24hiCD38hiBregs involved in downregulate helper T cells and upregulate regulatory T cells in gastric cancer. *Oncotarget* 6, pp. 33486-33499.

Wardemann, H. and Yurasov, S. and Schaefer, A. and Young, J. W. and Meffre, E. and Nussenzweig, M. C. 2003. Predominant autoantibody production by early human B cell precursors. *Science* 301(5638), pp. 1374-1377.

Wells, S. M. and Kantor, A. B. and Stall, A. M. 1994. CD43 (S7) expression identifies peripheral B cell subsets. *J Immunol* 153(12), pp. 5503-5515.

Wenzlau, J. M. and Juhl, K. and Yu, L. and Moua, O. and Sarkar, S. A. and Gottlieb, P. and Rewers, M. and Eisenbarth, G. S. and Jensen, J. and Davidson, H. W. and Hutton, J. C. 2007. The cation efflux transporter ZnT8 (Slc30A8) is a major autoantigen in human type 1 diabetes. *Proc Natl Acad Sci U S A* 104(43), pp. 17040-17045.

Wicker, L. S. and Leiter, E. H. and Todd, J. A. and Renjilian, R. J. and Peterson, E. and Fischer, P. A. and Podolin, P. L. and Zijlstra, M. and Jaenisch, R. and Peterson, L. B. 1994. Beta 2-microglobulin-deficient NOD mice do not develop insulitis or diabetes. *Diabetes* 43(3), pp. 500-504.

Willcox, A. and Richardson, S. J. and Bone, A. J. and Foulis, A. K. and Morgan, N. G. 2009. Analysis of islet inflammation in human type 1 diabetes. *Clin Exp Immunol* 155(2), pp. 173-181.

Wong, F. S. and Karttunen, J. and Dumont, C. and Wen, L. and Visintin, I. and Pilip, I. M. and Shastri, N. and Pamer, E. G. and Janeway, C. A., Jr. 1999. Identification of an MHC class I-restricted autoantigen in type 1 diabetes by screening an organ-specific cDNA library. *Nat Med* 5(9), pp. 1026-1031.

Wong, F. S. and Siew, L. K. and Scott, G. and Thomas, I. J. and Chapman, S. and Viret, C. and Wen, L. 2009. Activation of insulin-reactive CD8 T-cells for development of autoimmune diabetes. *Diabetes* 58(5), pp. 1156-1164.

Wong, F. S. and Visintin, I. and Wen, L. and Flavell, R. A. and Janeway, C. A., Jr. 1996. CD8 T cell clones from young nonobese diabetic (NOD) islets can transfer rapid onset of diabetes in NOD mice in the absence of CD4 cells. *J Exp Med* 183(1), pp. 67-76.

Wong, F. S. and Wen, L. and Tang, M. and Ramanathan, M. and Visintin, I. and Daugherty, J. and Hannum, L. G. and Janeway, C. A., Jr. and Shlomchik, M. J. 2004. Investigation of the role of B-cells in type 1 diabetes in the NOD mouse. *Diabetes* 53(10), pp. 2581-2587.

World Health Organization, W. H. O. 2014. *Diabetes fact sheet nº312 - Updated November/2014* [Online]. Available at: http://www.who.int/mediacentre/factsheets/fs312/en/ [Accessed: 30/09/2014].

Xiang, Y. and Peng, J. and Tai, N. and Hu, C. and Zhou, Z. and Wong, F. S. and Wen, L. 2012. The dual effects of B cell depletion on antigen-specific T cells in BDC2.5NOD mice. *J Immunol* 188(10), pp. 4747-4758.

Xiao, S. and Brooks, C. R. and Sobel, R. A. and Kuchroo, V. K. 2015. Tim-1 is essential for induction and maintenance of IL-10 in regulatory B cells and their regulation of tissue inflammation. *J Immunol* 194(4), pp. 1602-1608.

Yanaba, K. and Bouaziz, J. D. and Haas, K. M. and Poe, J. C. and Fujimoto, M. and Tedder, T. F. 2008. A regulatory B cell subset with a unique CD1dhiCD5+ phenotype controls T cell-dependent inflammatory responses. *Immunity* 28, pp. 639-650.

Yanaba, K. and Bouaziz, J. D. and Matsushita, T. and Tsubata, T. and Tedder, T. F. 2009. The development and function of regulatory B cells expressing IL-10 (B10 cells) requires antigen receptor diversity and TLR signals. *J Immunol* 182(12), pp. 7459-7472.

Yoon, J. W. and Onodera, T. and Notkins, A. L. 1978. Virus-induced diabetes mellitus. XV. Beta cell damage and insulin-dependent hyperglycemia in mice infected with coxsackie virus B4. *J Exp Med* 148(4), pp. 1068-1080.

Yoshizaki, A. and Miyagaki, T. and DiLillo, D. J. and Matsushita, T. and Horikawa, M. and Kountikov, E. I. and Spolski, R. and Poe, J. C. and Leonard, W. J. and Tedder, T. F. 2012. Regulatory B cells control T-cell autoimmunity through IL-21-dependent cognate interactions. *Nature* 491(7423), pp. 264-268.

Young, E. F. and Hess, P. R. and Arnold, L. W. and Tisch, R. and Frelinger, J. A. 2009. Islet lymphocyte subsets in male and female NOD mice are qualitatively similar but quantitatively distinct. *Autoimmunity* 42(8), pp. 678-691.

Yui, M. A. and Muralidharan, K. and Moreno-Altamirano, B. and Perrin, G. and Chestnut, K. and Wakeland, E. K. 1996. Production of congenic mouse strains carrying NOD-derived diabetogenic genetic intervals: an approach for the genetic dissection of complex traits. *Mamm Genome* 7(5), pp. 331-334.

Yurkovetskiy, L. and Burrows, M. and Khan, A. A. and Graham, L. and Volchkov, P. and Becker, L. and Antonopoulos, D. and Umesaki, Y. and Chervonsky, A. V. 2013. Gender bias in autoimmunity is influenced by microbiota. *Immunity* 39(2), pp. 400-412.

Zaccone, P. and Burton, O. and Miller, N. and Jones, F. M. and Dunne, D. W. and Cooke, A. 2009. Schistosoma mansoni egg antigens induce Treg that participate in diabetes prevention in NOD mice. *Eur J Immunol* 39(4), pp. 1098-1107.

Zekavat, G. and Rostami, S. Y. and Badkerhanian, A. and Parsons, R. F. and Koeberlein, B. and Yu, M. and Ward, C. D. and Migone, T. S. and Yu, L. and Eisenbarth, G. S. and Cancro, M. P. and Naji, A. and Noorchashm, H. 2008. In vivo BLyS/BAFF neutralization ameliorates islet-directed autoimmunity in nonobese diabetic mice. *J Immunol* 181(11), pp. 8133-8144.